# *IN VITRO* INVESTIGATION OF THE INFLUENCE OF NANO-CELLULOSE ON FOOD DIGESTION AND NUTRIENT ABSORPTION

by

LINGLING LIU

(Under the Direction of FANBIN KONG)

## ABSTRACT

Nanocellulose (NC) has become a topic of increasing interest due to its potential applications and special characteristics, including its rheological and structural properties (specifically viscous property and large specific surface area). The objective of this research was to investigate the influence of three types of nanocellulose (nano-fibrillated cellulose (also called cellulose nanofibrils (CNF)), TEMPO (2,2,6,6-tetramethylpiperidine-1-oxyl radical) oxidized CNF (TEMPO-CNF) & nano-crystalline cellulose (also called cellulose nanocrystals (CNC))) on food digestion and nutrient absorption as well as its behavior during gastrointestinal digestion using a simulated static *in vitro* digestion model. It was found that all three types of nanocellulose exerted hypoglycemic potential, delayed lipid digestion and free amino nitrogen (FAN) absorption at high NC concentrations. The viscosity was observed to play a major role in the effects of all three types of NC on food (starch, lipid and protein) digestion and nutrient absorption. Specifically, the addition of higher concentrations of NC (corresponding to higher viscosity) resulted in lower initial digestion rates, even though the final amount of digestion products released were almost the same with 4% (w/w) CNC as an exception (which resulted in significantly lower amounts of FAN

released). Nanocellulose at higher concentrations (0.5~1% (w/w) CNF, 0.36% (w/w) TEMPO-CNF and 2~4% (w/w) CNC) was found to significantly retard nutrient absorption, especially glucose and FAN diffusion. Furthermore, compared to cellulose, CNF had higher glucose and cholesterol adsorption capacity as well as bile acid retardation effects. Interactions can also occur between NC and food products. TEMPO-CNF and CNC bound with whey protein isolate (WPI) at the initial and gastric phase, resulted in changes in mean particle size and viscosity. Three types of NC showed different behaviors during digestion. In particular, CNF and cellulose were morphologically stable during the digestion, while TEMPO-CNF became aggregated and CNC formed hydrogels at the gastric phase. This study indicates that all three types of nanocellulose are advantageous than cellulose in the gastrointestinal (GI) tract in terms of increasing digesta viscosity, delaying food digestion and nutrient absorption, and has potential to be used in the development of functional foods to control nutrient absorption and promote satiety.

INDEX WORDS: Nanocellulose, cellulose nano-fibrils, TEMPO-oxidized cellulose nano-fibrils, cellulose nanocrystals, viscosity, *in vitro* digestion, nutrient absorption

# *IN VITRO* INVESTIGATION OF THE INFLUENCE OF NANO-CELLULOSE ON FOOD DIGESTION AND NUTRIENT ABSORPTION

by

LINGLING LIU

BS, Southwest University, 2011

MS, China Agricultural University, 2013

A Dissertation Submitted to the Graduate Faculty of The University of Georgia in Partial Fulfillment of the Requirements for the Degree

DOCTOR OF PHILOSOPHY

ATHENS, GEORGIA

2018

*IN VITRO* INVESTIGATION OF THE INFLUENCE OF NANO-CELLULOSE ON FOOD DIGESTION AND NUTRIENT ABSORPTION

by

LINGLING LIU

| | |
|---|---|
| Major Professor: | Fanbin Kong |
| Committee: | William L. Kerr |
| | Derek R Dee |
| | Suraj Sharma |

Electronic Version Approved:

Suzanne Barbour
Dean of the Graduate School
The University of Georgia
December 2018

# DEDICATION

To my caring family and my beloved significant other who love me, supported me and encouraged me along the journey.

ACKNOWLEDGEMENTS

First and foremost, I would like to express my thanks and sincere gratitude to my major professor, Dr. Fanbin Kong, who has given me this opportunity to work on this project. Completion of this PhD would not be possible without Dr. Kong's help and support. I appreciate all the patience and time he has spent with me throughout the challenges I encountered in my research. I would also like to thank all of my committee members (Dr. William L Kerr, Dr. Derek R Dee and Dr. Suraj Sharma) for their guidance and advice. Dr. Kerr has been a mentor and role model, both in academic and career development. The encouragement and advice from Dr. Kerr have helped me grow both as a research scientist and as an individual. Dr. Dee has given me a lot of personal advice in navigating through the academic world. His creativity and personal experiences have been an inspiration to me. I also would like to thank Dr. Sharma who has supported me from the beginnings of my graduate program with his advice and help, especially in my research. He has been very generous with sharing ideas and resources which aided me in my progress.

Finally, I would also like to acknowledge and express my thanks to some of the professors and staff in the department. I would like to thank Dr. Singh and Dr. Harrison for their suggestions and guidance on my PhD journal. I also like to express my thanks to Dr. Hung, Dr. Cannon, Dr. Zhao, Dr. Park, Dr. Ortega, Lisa, Karen, Jessica, Carl, Taryn, Daniel, Daoyuan, Jye-yin and Xi for their help and friendship. I also like to express my special appreciation to previous and current labmates in Dr. Kong's lab for their help and support: Floi, Duc, Samet, Luna, Damla, Nakia, Jiannan, Jin, Dr. Liu, Himanshu, etc.

Lastly, I like to express my thanks to my family and friends who have continuously supported me along this journey, no matter how difficult it was. Completion of this PhD would not be possible without all of the people who stood by my side and supported me along the way.

Thank you all so much!

TABLE OF CONTENTS

LIST OF TABLES

Page

LIST OF FIGURES

Page

# CHAPTER 1

# INTRODUCTION

Nanocellulose (NC) is defined as nano-scaled cellulosic materials with at least one dimension less than 100 nm. Through mechanical shearing, acid/enzymatic hydrolysis of cellulose materials or biosynthesis, NC hydrogels can be obtained (Anderson et al., 2014; Khosravi-Darani, Koller, Akramzadeh, & Mortazavian, 2016; Li et al., 2012; Lu et al., 2013; Liu, Li, Xie, & Deng, 2017). This hydrogel may resemble gelling properties similar to dietary fiber. NC has larger specific surface area when compared with cellulose. It also shows negligible toxicity. There is currently no evidence of any serious safety issues associated with nanocellulose (Lin & Dufresne, 2014). Due to its viscous property, large specific surface area, negligible toxicity, low density, biodegradability, and biocompatibility, nanocellulose has been applied in a number of fields, including textile, pharmaceutics, cosmetics, and packaging (Ioelovich & Figovsky, 2008; Jorfi & Foster, 2015; Kolakovic, Laaksonen, Peltonen, Laukkanen, & Hirvonen, 2012; Lin & Dufresne, 2014; Minko et al., 2016; Sun et al., 2018).

As a nanoscale fiber, it has become of interest to investigate if nanocellulose possesses similar effects as dietary fiber towards food digestion and nutrient absorption. Dietary fibers are a continuing topic of interest in the past several decades, due to its beneficial effects towards human health. Dietary fibers can lower plasma glucose levels, thus reducing the risks of type 2 diabetes (Nichols, Hillier, & Brown, 2008). Other benefits include increasing digesta viscosity, prolonging transit time in the gastrointestinal (GI) tract, as well as promoting satiation, and satiety. In addition,

Dietary fibers can affect food digestion and nutrient absorption, which are related to their effects on reducing the risks of hyperlipidemia, hypertension, other coronary heart diseases, and some cancers (Tiwari & Cummins, 2011). So far there is little research available regarding the potential effects of nanocellulose on food digestion and nutrient absorption as well as the behavior of NC in the gastro-intestinal (GI) tract. Thus, the objectives of this study were to investigate the behavior of NC during simulated gastrointestinal digestion, including its impact on food digestion and nutrient absorption.

### 1.1. Significance of the study

Nanotechnology has continuously been applied in the food industry in order to improve taste, nutritional value, monitor food quality, and extend shelf-life (Wang, Du, Song, & Chen, 2013). Nanomaterials can enter the human gastrointestinal tract as a food ingredient or as a contaminant. Thus, it is essential to understand the behavior of NC in the GI tract as well as their effects on food digestion and nutrient absorption.

This study investigates the effects of three types of nanocellulose on food digestion and nutrient absorption. The nanocellulose materials used in this study include nano-fibrillated cellulose (NFC, also called cellulose nano-fibrils (CNF)), TEMPO (2,2,6,6-tetramethylpiperidine-1-oxyl radical) oxidized CNF (TEMPO-CNF), and nano-crystalline cellulose (NCC, also called cellulose nano-crystals (CNC)). An *in vitro* digestion model was used to understand the mechanisms involved, aside from all the other advantages over *in vivo* models, including low cost, time efficiency, and reproducibility. As a comprehensive study, NC behavior during each digestion phase, its interactions with different food components, and their corresponding mechanisms were all investigated. Findings from this study show potential applications of NC in future food or beverage products to help regulate food digestion and nutrient absorption.

## 1.2. Objectives

The overall goal of this study was to investigate the behavior of nanocellulose (CNF, TEMPO-CNF and CNC) during gastrointestinal digestion using simulated digestion models, including its impact on food digestion and nutrient absorption. Specifically, the study can be divided into three categories:

(a) Investigate the influence of NC on starch digestion and glucose absorption

(b) Examine the influence of NC on *in vitro* digestion of lipid emulsions

(c) Investigate the influence of NC on *in vitro* digestion of protein

## 1.3 Outline

This dissertation includes three research chapters. The first focuses on investigating the influence of nanocellulose (CNF, TEMPO-CNF and CNC) on starch digestion and nutrient absorption. Specifically, the effects of CNF on digestive enzyme (α-amylase and α-glucosidase) activities, the interaction between CNF and glucose (including glucose adsorption capacity of CNF and its effects on glucose diffusion), the effects of CNF on glucose diffusion during starch hydrolysis, the effects of nanocellulose (CNF, TEMPO-CNF and CNC) on starch *in vitro* digestion, and glucose absorption were investigated. The second research chapter focuses on determining the effects of CNF on lipase activity, the interactions of CNF with cholesterol and bile salts, as well as the effects of nanocellulose (CNF, TEMPO-CNF and CNC) on *in vitro* digestion of lipid emulsions. Finally, the third research chapter investigates the influence of three types of nanocellulose on *in vitro* digestion of whey protein isolate (WPI) as well as their effects on free amino nitrogen diffusion.

## 1.4 References

Ioelovich, M., & Figovsky, O. (2008). Nano-cellulose as promising biocarrier. *Advanced Materials Research* (Vol. 47, pp. 1286-1289): Trans Tech Publ.

Jorfi, M., & Foster, E. J. (2015). Recent advances in nanocellulose for biomedical applications. *Journal of Applied Polymer Science*, 132(14).

Khosravi-Darani, K., Koller, M., Akramzadeh, N., & Mortazavian, A. M. (2016). Bacterial nanocellulose: biosynthesis and medical application. *Biointerface Research in Applied Chemistry*, 6(5), 1511-1516.

Kolakovic, R., Laaksonen, T., Peltonen, L., Laukkanen, A., & Hirvonen, J. (2012). Spray-dried nanofibrillar cellulose microparticles for sustained drug release. *International journal of pharmaceutics*, 430(1-2), 47-55.

Lin, N., & Dufresne, A. (2014). Nanocellulose in biomedicine: Current status and future prospect. *European Polymer Journal*, 59, 302-325.

Minko, S., Sharma, S., Hardin, I., Luzinov, I., Daubenmire, S. W., Zakharchenko, A., . . . Kim, Y. S. (2016). Textile dyeing using nanocellulosic fibers. Google Patents.

Nichols, G. A., Hillier, T. A., & Brown, J. B. (2008). Normal fasting plasma glucose and risk of type 2 diabetes diagnosis. *The American Journal of Medicine*, 121(6), 519-524.

Sun, X., Wu, Q., Zhang, X., Ren, S., Lei, T., Li, W., . . . Zhang, Q. (2018). Nanocellulose films with combined cellulose nanofibers and nanocrystals: tailored thermal, optical and mechanical properties. *Cellulose*, 25(2), 1103-1115.

Tiwari, U., & Cummins, E. (2011). *Functional and physicochemical properties of legume fibers*. In *Pulse Foods: Processing, Quality and Nutraceutical Applications* (pp. 121-156). London Burlington, MA: Academic Press

Wang, H., Du, L.-J., Song, Z.-M., & Chen, X.-X. (2013). Progress in the characterization and safety evaluation of engineered inorganic nanomaterials in food. *Nanomedicine*, 8(12), 2007-2025.

# CHAPTER 2

# LITERATURE REVIEW

## 2.1 Nanocellulose

### 2.1.1 Sources, preparation and characterization of nanocellulose

Cellulose is commonly considered as one of the most important, sustainable and abundantly found materials. The production of cellulose is estimated to be between $10^{11}$ and $10^{12}$ tons per year (Klemm, Philpp, Heinze, Heinze, & Wagenknecht, 1998). Sources of cellulose can come from plants (including leaf, seed, bast, fruit, and stalk), marine animals (tunicates), bacteria, and amoeba (protozoa) (Jorfi & Foster, 2015). The content and physicochemical properties of cellulose vary in different sources. As an example, the cellulose contents of unprocessed fiber in wood and plant sources are 40-50% and 60-70%, respectively. Wood fibers also have lower crystallinity (55-70%) than plant fibers (90-95%) (Madsen & Gamstedt, 2013).

Nanocellulose is a subcategory of cellulose that has at least one dimension in nanoscale (1~100 nm). They can be prepared via chemical treatments (acid hydrolysis) (Liu, Li, Xie, & Deng, 2017), mechanical shearing methods (Li et al., 2012; Lu et al., 2013), enzymatic methods (Anderson et al., 2014) and biosynthesis (bacteria nanocellulose) (Khosravi-Darani, Koller, Akramzadeh, & Mortazavian, 2016). Nanocellulose can be mainly divided into three types which include nano-fibrillated cellulose, nano-crystalline cellulose and bacterial cellulose (BC). Nano-fibrillated cellulose (NFC), also called cellulose nano-fibrils (CNF), has a width of 20~50 nm and a length of up to several hundred microns. Nano-crystalline cellulose (NCC), also known as cellulose nano-crystals (CNC), has a width of ~ 5 nm and a length of 150~200 nm. CNC is usually

made from sulfuric acid hydrolysis of nano/micro-fibrillated cellulose, microcrystalline cellulose (i.e., micro-scale cellulose crystals), or raw cellulose (Liu, Li, Xie, & Deng, 2017). Different from CNF and CNC, bacterial cellulose (BC) is usually biosynthesized from bacteria in high purities, and in web-shaped network structure with diameters of 20-100 nm (Lin & Dufresne, 2014).

Substantial energy consumption is required for the manufacturing of CNF. As an example, the energy required for the production of micro-fibrillated cellulose (MFC) from bleached kraft and sulfite pulp were 12,000~70,000 and 27,000 KWh/t, respectively (Klemm et al., 2011). However, this can be significantly reduced by incorporating pretreatments to the material. According to Tejado, Alam, Antal, Yang, & van de Ven (2012), less disintegration energy is required for cellulose fibrils with higher carboxyl groups. In particular, only 500 and 1500 KWh/t were required for carboxymethylated kraft pulp (DS = 0.1) and enzymatic treated/refined sulfite pulp (Klemm et al., 2011). The pretreatments involved in order to reduce the energy consumption during the nanofibril isolation process include enzymatic hydrolysis, TEMPO-mediated oxidation, carboxymethylation, grafting, cationization and phosphorylation (Mertaniemi, 2017).

Isogai, Saito, & Isogai (2011) have developed a way of introducing charged carboxylate groups to cellulosic materials without changing original cellulose crystallinity or width by using TEMPO (2,2,6,6-tetramethylpiperidine-1-oxyl radical)-mediated oxidation. Specifically, the primary hydroxyl groups at C6 of the cellulose molecules were oxidized and significant amounts of carboxylate groups were formed. TEMPO (2,2,6,6-tetramethylpiperidine-1-oxyl radical) oxidized CNF (TEMPO-CNF) carries negative surface charge with a width of ~20 nm and length up to 2 μm (Isogai, Saito, & Fukuzumi, 2011). TEMPO-CNF possesses high yields of fibrillation and transparency (Serra et al., 2017). Furthermore, TEMPO oxidation could reduce 24% ~ 54% energy reduction for fibrillation of cellulose (Hubbe et al., 2017).

Large-scale production of nanocellulose has been commercially available, especially in Europe and North America (Lin & Dufresne, 2014). The price of unmodified CNF is low, but TEMPO-CNF or CNC is usually more expensive. According to the price listed on the University of Maine process development center website, the cost of CNF is $50 per 1 pound (dry weight); cost of TEMPO-oxidized CNF is $330 per 100 grams (dry weight), while the cost of CNC is $250 per 1 pound (dry weight). Even though TEMPO oxidation process reduces the number of passes of CNF through high pressure homogenizers or microfluidizers, the high cost of the reactant and manufacturing process surpasses the savings on the energy consumption cost (Serra et al., 2017).

NC has been characterized with a variety of techniques. For examples, specific surface area characterization of NC can be performed by X-ray scattering or small-angle X-ray scattering, dimensions/aspect ratio/appearance determination by particle size analyzer, scanning electron microscopy (SEM), transmission electron microscopy (TEM) or atomic force microscopy (AFM), while crystallinity determination by X-ray diffraction, surface charge test by conductometric titration or zeta potential measurement and rheology determination by rheometer (Ioelovich, 2017). Examples of microscopic images of nanocellulose are shown in Fig. 2.1. Characteristics of nanocellulose include large specific surface area, lightweight, negligible toxicity, viscous property, biodegradability and biocompatibility (Lin & Dufresne, 2014). Materials incorporated with nanocellulose have great tensile strength and high thermal stability (Klemm et al., 2011; Nasir, Hashim, Sulaiman, & Asim, 2017). Among all the rheological characteristics of NC, viscosity is one of the most important properties. Typically, NC shows concentration and time dependent shear-thinning behavior ( Hubbe et al., 2017; Lasseuguette, Roux, & Nishiyama, 2008; Shafiei-Sabet, Hamad, & Hatzikiriakos, 2012). NC suspension is pseudo-plastic and exhibits gelling

behavior under some conditions (e.g., high concentrations) or liquid-like behavior under others (e.g., low concentrations).

There are several factors that influence the rheological measurement of NC, including intrinsic factors (nanocellulose concentration, surface charge, size and aspect ratios), extrinsic factors (temperature, moisture, pH and ionic strength) as well as measurement conditions (geometry (probe type and surface roughness), gap and shear rate) (Nechyporchuk, Belgacem, & Pignon, 2016). Specifically, intrinsic viscosity (defined as a measure of a solute's contribution to the viscosity) of NC suspension is a function of its aspect ratio (Tanaka, Saito, Hondo, & Isogai, 2015). Higher viscosity of NC can be achieved when the aspect ratio is high which enables more flexibility and entanglement. CNF possesses long and rigid network which renders its solid-like viscoelastic behavior due to the entanglement of the fibrils (Li et al., 2015). Compared with CNF, during the production of CNC, the highly entangled, long and rigid network was broken down upon acid hydrolysis, which decreased its viscoelastic properties (Li et al., 2015). At the same NC concentration, it was found that CNF possesses higher strength and modulus than CNC due to their high entanglement and large aspect ratio (Xu et al., 2013). However, compared with CNF, TEMPO-CNF was shown to have higher viscosity due to the increased fibril individualization and stronger network formation after TEMPO oxidation (Bettaieb et al., 2015).

Due to the slight or high surface charges present on different types of NC, electrostatic repulsion and van der Waals attraction can exist between nanocellulose fibrils upon the adjustment of pH or the addition of electrolytes (e.g., salt) (Karppinen et al., 2012). The increased ionic strength reduces the electrostatic repulsion effect and favors the hydrogen bonding between fibrils which results in larger flocs or aggregates formation (Saarikoski, Saarinen, Salmela, & Seppälä,

2012). Moreover, de-swelling or phase separation may occur at high ionic strength and low pH conditions for carboxylated nanocellulose (Mendoza, Batchelor, Tabor, & Garnier, 2018).

So far, several rheometers and various geometries have been used to study the rheological behavior of nanocellulose. Specifically, shear viscosity, which is a measure of the fluid's resistance to gradual deformation by shear, has been widely studied for NC. Different geometries have been used include parallel-plate, cone-plate, serrated Couette (or cylinder-cup) as well as vane-cup geometry (Agoda-Tandjawa et al., 2010; Dimic-Misic, Gane, & Paltakari, 2013; Nechyporchuk, Belgacem, & Pignon, 2015; Winuprasith & Suphantharika, 2013). CNF was shown to have wall-slip problems during rheological measurement when using parallel-plate or cone-plate, while this effect was reduced when using serrated Couette or vane-cup rheometers (Hubbe et al., 2017; Nechyporchuk, Belgacem, & Pignon, 2016). The wall-slip problem tends to be more influential in measurements with lower geometry gap since larger floc size formed at lower gaps (Nechyporchuk, Belgacem, & Pignon, 2016). However, the nano-fibril flocs tended to split at high shear rates (Nechyporchuk, Belgacem, & Pignon, 2016). For TEMPO-CNF or CNC, parallel-plate, cone-plate, Couette or vane geometries have been used for the rheological measurement (Chau et al., 2015; Moberg et al., 2017; Mohtaschemi et al., 2014; Saarinen, Lille, & Seppälä, 2009; Xu, Atrens, & Stokes, 2017). Even though TEMPO-oxidized CNF suspension was non-flocculated, it was shown that structural changes in TEMPO-CNF could occur after certain high shear rate (e.g., 30-40 $s^{-1}$) (Lasseuguette et al., 2008). Similarly, CNC also showed different rheological responses at different shear rate ranges (Xu et al., 2017).

2.1.2 Safety and applications of nanocellulose

The safety of NC has been extensively discussed in several review papers (Dourado, Gama, & Rodrigues, 2017; Lin & Dufresne, 2014; Roman, 2015; Seabra, Bernardes, Fávaro, Paula, &

Durán, 2017). Overall, there is no evidence of any serious safety issues associated with NC, either in the genetic level, cellular level or in *in vivo* animal trials (Lin & Dufresne, 2014). Specifically, research showed that unmodified or carboxymethylated/ hydroxypropyltrimethylammonium-modified CNFs did not exert cytotoxic effects when exposed to human dermal fibroblasts, lung MRC-5 cells and immune cells (THP-1 macrophage cells) (Lopes, Sanchez-Martinez, Strømme, & Ferraz, 2017). Unmodified CNF at a dose of 250~500 ug/mL showed pro-inflammatory effects while surface modified CNF did not. Moreover, CNF did not cause significant differences in the production of reactive oxygen species (ROS) and THP-1 macrophages did not uptake CNF materials (Lopes, Sanchez-Martinez, Strømme, & Ferraz, 2017). CNC has no oral or dermal toxicity, though it shows some pulmonary and cytotoxicity effects (Roman, 2015). Inhalation of certain amounts of nanocellulose, especially CNC, may cause pulmonary inflammation (Lin & Dufresne, 2014). Bacteria cellulose was shown to be safe in the biomedical applications, and it did not cause inflammatory reactions or irritation to eyes or dermal tissues (Dourado et al., 2017). TEMPO-oxidized bacteria cellulose was shown to be safe in the application for tissue engineering, and bring new functional groups to the scaffolds (Luo et al., 2013).

Due to the special characteristics of NC, it has been widely applied in several fields, including pharmaceutics, cosmetics, textile and packaging. Thin films made with the incorporation of CNC and CNF showed better thermal stability, thermal expansion behavior, optical properties and more uniform strength than conventional porous polymer battery separator film (Sun et al., 2018). CNF films functionalized with luminescent silver nanoclusters, mediated by poly(methacrylic acid), have been shown to exhibit fluorescence and antibacterial activity (Díez et al., 2011). Moreover, NC has been shown to be able to work as a drug carrier and maintain sustained drug release due to the formation of tight fiber network and limited diffusion (Kolakovic,

Laaksonen, Peltonen, Laukkanen, & Hirvonen, 2012). Drug loaded CNF microparticles can be produced by spray drying or wet granulation method (Kolakovic et al., 2011). So far, several model drugs have been successfully studied, including nystatin (Tade, More, Chatap, Patil, & Deshmukh, 2018), ibuprofen, indomethacin, metoprolol tartrate, verapamil hydrochloride, nadolol, ibuprofen, atenolol (Kolakovic et al., 2012) and lidocaine (Trovatti et al., 2011).

Bacterial nanocellulose (BNC) has been used as a topical material in wound healing. Some BNC-based materials are commercially available, including XCell, Bioprocess, and Biofill. Research has shown the benefits of using BNC-based materials over conventional wound healing materials, that is, biocompatible, faster tissue regeneration, lower inflammatory response and better healing effects (Jorfi & Foster, 2015). Moreover, nanocellulose based biomaterials have been widely developed and applied for soft-tissue implants and cartilage replacements, due to its biocompatibility, hydrophilicity, great tensile mechanical properties, durability, non-degradability, long-term chemical stability and interconnected porosity (Jorfi & Foster, 2015). NC is also a promising material for bone tissue engineering. Bionanocomposites comprising of BNC possess biocompatibility, three-dimensional (3D) network, low cytotoxicity and high porosity as well as great mechanical properties (Jorfi & Foster, 2015).

NC has been shown to have higher binding forces with dyes than conventional fibers, which improves the dying efficiency, reduces waste and is more environmentally friendly (Minko et al., 2016). A dyed nanocellulose suspension or gel can be easily made by adding wood pulp fibers and dye to the homogenizer, then applied to fabric or textile materials followed by drying (Minko et al., 2016). Moreover, NC is shown to be active as a biocarrier, in cosmetics and remedies for skin care. Specifically, bioactive nanocellulose can clean skin pores since it can open and penetrate through the skin strata due to its nanosized (Ioelovich & Figovsky, 2008). Bacterial

cellulose (BC) has been successfully applied as cosmetic facial masks (Ludwicka et al., 2017). Aside from all the applications that have been mentioned, nanocellulose can also be used for lipid emulsion stabilizers (Gestranius, Stenius, Kontturi, Sjöblom, & Tammelin, 2017) and antimicrobial agent carriers (Jebali et al., 2013).

**2.2 Effects of nanocellulose and dietary fiber on food digestion and nutrient absorption**

So far, there are limited studies on the effect of nanocellulose on food digestion and nutrient absorption. Since nanocellulose is a nanoscale fiber, it may behave similar to other fibers used in the diet. In this section, a review of publications on the effects of nanocellulose and dietary fibers on food digestion and nutrient absorption is given. Specifically, a summary of the effects of nanocellulose and cellulose on digestive enzyme activities was shown in Table 2.1, and a summary of the effects of them on nutrient absorption and fecal microflora was shown in Table 2.2.

Dietary fiber (DF) is defined as carbohydrate polymers (with ten or more monomeric units) that are not hydrolyzed by endogenous enzymes in the human small intestine (Kendall, Esfahani, & Jenkins, 2010). Although dietary fibers are indigestible, they play an imperative role in the human diet and significantly contribute to human health. It has been reported that a high-fiber diet can improve gastrointestinal health, glucose tolerance, insulin response, satiety, and weight loss. It has also been known to reduce hyperlipidemia, hypertension, other coronary heart disease risks and some cancers (Tiwari & Cummins, 2011).

Dietary fibers have been shown to exert metabolic effects on food digestion and nutrient absorption. The presence of dietary fibers prolongs transit time in the GI tract, promotes satiation, and improves satiety. Dietary fibers (DF) can increase digestive viscosity, delay gastric emptying and slow down digestion as well as nutrient transport. DF can also influence the growth of gut microbiota and stimulate production of short-chain fatty acids that are beneficial for glucose and

lipid metabolism (Giacco, Costabile, & Riccardi, 2016). Furthermore, an increased intake of DF has been shown to result in increased excretion of some compounds (like bile acid) as well as increased fecal wet weight, fecal dry matter and energy content of feces (B.O. Schneeman, 1998; Southgate, 1982). Certain dietary fibers are capable of binding other polar molecules and ions (including minerals) (Cui & Roberts, 2009). In addition, dietary fibers have been shown to be effective at adsorbing hydrophobic carcinogens (Ferguson, Roberton, Watson, Kestell, & Harris, 1993; Harris, Roberton, Hollands, & Ferguson, 1991; Harris, Triggs, Roberton, Watson, & Ferguson, 1996) as well as enhancing fecal excretion of some toxic substances (e.g., dioxin isomers) (Aozasa, Ohta, Nakao, Miyata, & Nomura, 2001).

The metabolic effects of dietary fibers to some extent depend on the physicochemical properties of fiber (water-holding capacity, bile absorption and cation exchange capacity), its interaction with other nutrients, and possibly other gastrointestinal factors (Munoz, 1982). Physicochemical properties of DF include water-holding capacity (or hydration property), fat-binding capacity, viscosity, chelating capacity, and organic compound adsorptive property (Adams, Sello, Qin, Che, & Han, 2018; Cui & Roberts, 2009). These properties are highly influenced by fiber type (solubility or fermentability), size, aspect ratio, porosity and surface charge (Cui & Roberts, 2009). Water-holding capacity and viscosity are two important properties of DF that are associated with the physiological functions of DF in the upper GI tract (Tiwari & Cummins, 2011). The chelating capacity of fiber seems to be related with the number of free carboxyl groups and the uronic acid contents (Cui & Roberts, 2009). The susceptibility of fibers to bacteria fermentation in the colon is associated with their chemical structure (Tiwari & Cummins, 2011). In addition, both soluble and insoluble fibers can increase stool frequency but

through different mechanisms. Specifically, soluble fibers can increase the stool bulk and weight while insoluble fiber accelerates intestinal transit time (Eswaran, Muir, & Chey, 2013).

2.2.1 Effects of nanocellulose and dietary fiber on digestive enzyme activities

Overall, the results of nanocellulose and DF on digestive enzyme activities have been varied among studies, as shown in Table 2.1. So far, very few studies have been carried out on the effects of NC on digestive enzyme activities. Among the limited studies, Ji, et al., (2018) found that 0.28% CNC addition decreased α-amylase activity by 28% and glucoamylase by 10~15%. Based on Fourier-transform infrared spectroscopy (FTIR) and circular dichroism (CD) spectroscopy studies, the authors found that CNC induced secondary structural changes in α-amylase and glucoamylase. Specifically, weak non-covalent interactions (including hydrogen bonding) were thought to be responsible for the binding between CNC and digestive enzymes (α-amylase and glucoamylase) (Ji, et al., 2018). Similarly, Dhital, Gidley, & Warren (2015) found that α-cellulose could reduce α-amylase activity by 48% at a cellulose to starch (w/w) ratio of 5:1. However, *in vivo* studies showed that cellulose did not cause significant differences in enzyme (α-amylase, lipase, trypsin and chymotrypsin) activities nor pancreatic secretion rates (BO Schneeman, Forman, & Gallaher, 1983; Barbara Olds Schneeman, 1979). In addition, cellulose was reported to show no changes to the activity of sucrose, lactase, maltase, and thymidine kinase though it increased peptidase activity (Schneeman & Gallaher, 2001).

The differences in the effects of fibers on enzyme activities among studies are due to the differences in fiber purity, sources, concentration, test conditions, and methodologies used. It was shown that high purity fiber had more distinct effects than natural fiber. For example, acid detergent fiber, which was absent of hemicelluloses, was shown to have stronger inhibition than dietary fiber that contained hemicellulose, cellulose and lignin (Amarowicz, Korczakowska, &

Smoczyńska, 1988). In addition, the effects of different fiber components towards enzyme activities were dependent on their structure (Amarowicz et al., 1988). For example, the lipase inhibition effect by alginate was shown to relate to the amount of guluronate and mannuronate (Wilcox, Brownlee, Richardson, Dettmar, & Pearson, 2014). Specifically, alginates with high guluronate content have been shown to possess greater lipase inhibition than high mannuronate (Wilcox et al., 2014). Furthermore, test conditions have also been shown to be contributors. Specifically, it was observed that a more pronounced effect of fiber on digestive enzyme activity occurred when dissolving enzymes in intestinal juices than in buffers (Isaksson, Lundquist, & Ihse, 1982). This was thought to be associated with the higher viscosity of intestinal juices than buffers. Moreover, Schneeman and Gallaher (2001) showed that even though digestive enzyme activities were inhibited by various fibers based on *in vitro* data, no differences in the total amount of measurable digestive enzyme activity were observed in rats.

Mechanisms of the effects of fiber on digestive enzyme activities include reducing the contact between enzyme and substrate as well as the electrostatic interaction of fiber with amphoteric part of enzyme (Amarowicz et al., 1988; Hasik & Bartnikowska, 1987). The physical adsorption of enzyme solution on the fiber matrix has also been proposed as a mechanism where fibers result in decreased enzyme activities (Schneeman, 1978). An *in vitro* study by Schneeman (1978) showed that a wide range of inhibitions were due to the adsorption of enzymes on the fiber matrix. Alfalfa and rice bran showing inhibition on trypsin activity in addition to Solka Floc and xylan showing inhibition on chymotrypsin activity; were only a few examples that Schneeman had observed in his studies. A few years following this study, Dunaif & Schneeman (1981) also showed wheat bran and oat bran inhibited both amylase and chymotrypsin activity, while alfalfa inhibited trypsin and chymotrypsin activity.

The effects of a certain dietary fiber may have varying behaviors towards different digestive enzymes. For example, alginate was shown to inhibit lipase and pepsin activity but not trypsin (Chater, Wilcox, Brownlee, & Pearson, 2015). Alginate is a negatively charge polysaccharide, and it does not bind with negatively charged trypsin at pH 7. However, for pepsin at pH 2, alginate would interact with pepsin through hydrophobic interactions since the carboxyl group of alginate is mostly not dissociated (Chater et al., 2015; Kumar & Chauhan, 2010). Fibers with carboxyl groups have been shown to inhibit lipase activity since carboxyl groups affect the protonation of active serine residue of lipase (Chater et al., 2015; Kumar & Chauhan, 2010). Furthermore, pectin, which was shown to significantly increase amylase and chymotrypsin activity *in vitro* (Dunaif and Schneeman, 1981), was found to reduce lipase activity *in vivo* (Isaksson, Lundquist, Åkesson, & Ihse, 1984). It was also reported that higher methoxylated (corresponding to lower carboxylated) pectin had less inhibition effect on lipase activity than lower methoxylated pectin (Isaksson, Lundquist and Ihse, 1982).

2.2.2 Effects of nanocellulose and dietary fiber on starch digestion and glucose absorption

Carbohydrates are a major source of energy intake in the human diet, with starch being the main component in the digestible ones. Starch, composing of a-amylose and a-amylopectin, can be categorized into rapidly digested starch (RDS), slowly digested starch (SDS) and resistant starch (RS) according to their resistance to digestion (Englyst, Kingman, & Cummings, 1992). Digestion of starch starts from salivary α-amylase where the main products contain maltose, maltotriose and dextrins. In the stomach, the excretion of acid (HCl) brings down the pH at which starch hydrolysis can occur, and the α-amylase activity is inhibited. In the intestine, α-amylase activity resumes while further digestion of starch and its products is rendered by the brush border enzymes, including maltase-glucoamylase as well as sucrase-isomaltase (Diaz-Sotomayor et al.,

2013; Warren, Zhang, Waltzer, Gidley, & Dhital, 2015), followed by glucose absorption in the small intestine.

Dietary fibers have been shown to be effective at reducing postprandial blood glucose levels, especially viscous dietary fiber. Even though it has been shown that purified insoluble fibers had little or no effects on postprandial glucose levels (Jenkins, Kendall, Axelsen, Augustin, & Vuksan, 2000), it is the total amount dietary fiber (instead of soluble fiber) and uronic acid content in insoluble fibers that were found to be significantly related to the glycemic index of the diet (Wolever, 1990), in which the effect of food on blood glucose levels are related to. Dietary fibers can reduce postprandial glucose levels via several mechanisms, which includes inhibiting digestive enzyme activities, hindering glucose diffusion by increasing system viscosity, and decreasing available glucose concentration by adsorbing glucose (Ahmed, Sairam, & Urooj, 2011; Moron, Melito, & Tovar, 1989; Ou, Kwok, Li, & Fu, 2001). Even though insoluble fibers are not very effective at increasing digesta viscosity, they may bind with digestive enzymes and reduce available glucose levels due to their adsorption capacity. As an example, insoluble fiber-rich fractions (including insoluble dietary fibers, alcohol- and water-insoluble solids) isolated from citrus peels were shown to effectively adsorb glucose, retard glucose diffusion, and inhibit α-amylase activity *in vitro* (Chau, Huang, & Lee, 2003).

Similar to the effects of dietary fiber on starch digestion and glucose absorption, studies on nanocellulose also showed alike findings. According to Nsor-Atindana et al. (2018), the addition of CNC to whey protein isolate-starch system prior to heating at 70°C led to increased digesta viscosity as well as decreased glucose release and glucose diffusion. Moreover, this effect was more substantial in CNC with larger aspect ratios. Similarly, Ji et al., 2018 carried out a study by

mixing CNC and starch prior to the gelatinization process, and found that 0.2% CNC addition reduced starch digestibility.

Dietary fibers can hamper starch hydrolysis through physical interaction, inhibiting digestive enzyme activities, or increased viscosity. The interactions between starch and gums, including the electrostatic interaction between cationic starch and anionic gums, as well as the interaction between starch and non-ionic gums, have been shown to influence starch digestibility. Specifically, the former leads to instant aggregations, while the latter form sheet structures loosely wrapping around starch granules (Aylward, 2018). In particular, anionic gums (e.g., xanthan gum) were found to form a protective layer completely wrapping outside starch granules, while non-ionic gums (e.g., guar gum) formed loosely folded layers outside starch granules and were less effective at preventing starch hydrolysis during *in vitro* digestion (Aylward, 2018; Chaisawang & Suphantharika, 2006). In an *in vivo* study where wheat bread containing guar gum was fed to pigs, galactomannan was found to coat starch granules, which limit α-amylase access (Grundy et al., 2016). Furthermore, it was observed that both soluble and insoluble dietary fibers exerted inhibition on α-amylase activity. Enzyme-resistant starch (RS), carboxymethyl cellulose (CMC), guar gum and xanthan gum all decreased α-amylase activity since the amount of glucose produced was much less than that of control (Ou et al., 2001). In addition, apple pectin and CMC sodium salt were found to inhibit α-amylase activity *in vitro* (Ikeda & Kusano, 1983). For some fibers (acid-treated rice bran insoluble fiber), amylase-fiber complex was formed, as shown by fluorescence spectroscopy, which inhibited α-amylase activity (Qi et al., 2016).

Dietary fibers can influence glucose diffusion via the increased viscosity and glucose adsorption capacity of fibers. The effects of increased viscosity induced by fiber were shown to cause delayed glucose diffusion (Qi et al., 2016). High viscosity oat gums caused 79~96% changes

in plasma glucose levels and insulin responses, while low viscosity oat gum (after acid hydrolysis treatment) was shown to be less effective (Wood et al., 1994). However, the resistance of fiber against viscosity decrease during digestion may be different. Among all the gums tested by Fabek, Messerschmidt, Brulport, & Goff (2014), xanthan gum (XG) was shown to be more resilient against viscosity decrease during *in vitro* digestion than other fibers ((locust bean gum (LBG), guar gum (GG), fenugreek gum, flaxseed gum, and soy-soluble polysaccharide)) tested. The resistance of each polysaccharide against pH change and dilution effect during digestion was thought to depend on the polysaccharide concentration, its surface charge as well as conformation (Fabek et al., 2014). For some polysaccharides, like LBG, pH and digestive enzymes did not cause much influence on their structure and thus, there were no effects on viscosity during digestion. However, dilution due to digestive juice addition resulted in a large reduction in LBG viscosity (Fabek et al., 2014). For other polysaccharides, such as high viscosity guar gum and xanthan gum, pH caused significant reductions in viscosity during digestion (Fabek et al., 2014).

Both soluble and insoluble dietary fibers exert glucose adsorption capacity. The amount of glucose adsorbed by fibers was shown to have a positive linear relationship with the glucose input concentration before reaching saturation (Liu et al., 2018). For example, the amount of glucose bound by RS, CMC, guar gum, and xanthan gum were 48, 28, 49, and 26 μmol/g respectively, at a 5 mM glucose input concentration. At a 100 mM glucose input concentration, the amount of glucose bound for them increased to 414, 418, 538, and 432 μmol/g respectively (Ou et al., 2001). In addition, cellulose, insoluble dietary fiber, alcohol-insoluble solids, and water-insoluble solids prepared from citrus peels were shown to possess glucose adsorption capacity as well, with a glucose adsorption capacity of 19, 23, 20, and 19 mmol/g respectively, at a 200 mM glucose input concentration (Chau et al., 2003). Furthermore, oats, barley, and psyllium husk as well as rice bran

insoluble fiber had been shown to exhibit glucose adsorption capacity (Ahmed et al., 2011; Qi et al., 2016). The glucose adsorption capacity of insoluble fibers increased with increasing porosity and specific surface area of fiber (Qi et al., 2016). The amount of glucose adsorbed by acid-alkaline treated rice bran insoluble fiber was 2-3 folds higher than that of untreated material, where the former had larger porosity and specific surface area (Qi et al., 2016).

Furthermore, it was found that the frequency of fiber usage also made a difference in terms of its effect on starch digestion and glucose absorption. In particular, chronic fiber (cellulose/pectin) supplementation caused significantly lower serum glucose levels in rats compared to acute supplementation of fiber (10% cellulose or 5% pectin) (Schwartz & Levine, 1980). It was also postulated that the effect of acute dietary fiber ingestion on glucose homeostasis may be due to the increased viscosity and delayed gastric emptying, while chronic fiber supplementation caused adaptive changes in rat intestine (Schwartz & Levine, 1980).

2.2.3 Effects of nanocellulose and dietary fiber on lipid digestion and absorption

A negligible extent of lipolysis occurs by the action of lingual lipase in the mouth (Capuano, 2017). However, a small extent (6-16%) of lipolysis occurs in the stomach via gastric lipase (Armand et al., 1994; Armand et al., 1996), followed by further hydrolysis in the small intestine via pancreatic lipase-colipase, phospholipase $A_2$, and cholesterol esterase (Capuano, 2017). Lipid digestion products, including free fatty acids and monoacylglycerols, are incorporated together with cholesterol and bile acids into mixed micelles and unilamellar vesicles which are absorbed by the epithelial cells through pinocytosis (Capuano, 2017). Short chain fatty acids can also be produced in the colon after fermentation of dietary fiber by bacteria (Capuano, 2017).

Dietary fiber consumption has been shown to result in lower serum triglyceride and cholesterol levels as well as increased excretion of lipids, cholesterols, and bile acid contents in

feces. The above-mentioned effect of dietary fiber is related to lower incidence of cardiovascular disease and is thus considered to be beneficial for human health (McRae, 2017). Vegetable juices (containing fibers) reduced lipid digestion *in vitro* by inhibiting lipase activity, decreasing cholesterol solubility, and binding with bile acids (Trisat, Wong-on, Lapphanichayakool, Tiyaboonchai, & Limpeanchob, 2017). An *in vivo* study in hamsters showed that the addition of 5% insoluble fiber-rich fractions from a plant seed to diets was effective at decreasing serum triglyceride, serum cholesterol, liver cholesterol levels as well as increasing the amount of lipids, cholesterol, and bile acids in feces, fecal bulk, and moisture content (Chau & Huang, 2005).

Several mechanisms have been known regarding the effects of dietary fibers (especially viscous soluble dietary fibers) on inhibiting lipid digestion and absorption. Dietary fibers can reduce triglyceride hydrolysis via reducing lipid emulsification, inhibition on lipase activity or increased viscosity. However, they can also reduce/delay absorption of lipid digestion products as well as lymphatic secretion of lipids, via binding with lipids, cholesterols, and bile acids to reduce their incorporation in micelles and vesicles, altering mucosal morphology, increased viscosity or ion binding effect (Lairon, 1997; Venema, Minekus, & Havenaar, 2004; Zhang, Zhang, Zhang, Decker, & McClements, 2015). Among the limited studies of the effects of nanocellulose on lipid digestion, though the main food type is protein-stabilized lipid emulsions, similar mechanisms were elucidated. According to DeLoid et al. (2018), addition of 0.75% (w/w) nanocellulose (CNF or CNC) could significantly reduce hydrolysis of triglycerides in four types of “fatty” food (including heavy cream, coconut oil, mayonnaise and corn oil). Two mechanisms were proposed: 1) NC caused lipid droplet coalescence/flocculation via bridging effect which reduced the effective surface area for lipase access; 2) NC could sequester bile salt which resulted in less interfacial displacement and solubilization of lipid digestion products. Similarly, according to Sarkar et al.

(2018), CNC could sequester bile salt and bind with protein-coated lipid droplets via bridging effects. Specifically, the former restricted interfacial displacement and solubilization of lipid digestion products, while the latter reduced the available surface area for lipase access.

Viscous polysaccharides can decrease triglyceride hydrolysis in the stomach and small intestine *in vitro* by increasing lipid droplets/micelle size, which causes a reduction in the available surface area for lipase access (Pasquier, Armand, Castelain, et al., 1996; Pasquier, Armand, Guillon, et al., 1996). *In vitro* and *in vivo* studies by Lairon (1997) also showed the effects of viscous polysaccharides on lipid emulsification and hydrolysis. Moreover, cereal soluble dietary fibers were shown to inhibit lipolysis mainly due to the increased lipid droplet size via flocculation rather than the increased viscosity (Zhai, Gunness, & Gidley, 2016).

Certain dietary fibers have been shown to inhibit activities of enzymes that are related to lipid digestion and cholesterol synthesis. Alginate was shown to exhibit substantial lipase inhibition effect even though it was incorporated into a bread or applying cooking process to the alginate-enriched bread (Houghton et al., 2015). Some vegetable juices (e.g., sweet basil juice) were effective at inhibiting pancreatic lipase with an $IC_{50}$ of 1.5 mg/mL, while others (e.g., leafbush juice) could inhibit 94% cholesterol esterase activity at a concentration of 2 mg/mL (Trisat et al., 2017). Furthermore, a variety of dietary fibers are able to increase digesta viscosity which restricted the contact between lipid substrates and lipase, as well as decrease lipid digestion rates due to their ion binding effect. In particular, the addition of high levels of pectin inhibited lipid digestion due to the calcium binding effect and increased viscosity that restricted lipase access (Silva, Morita, & Boleli, 2013; Zhang et al., 2015).

Soluble fibers (including pectin, gums and some hemicellulose) as well as some insoluble fibers (including lignin and modified chitosan) may affect the absorption of lipid digestion

products by adsorption or interaction with fatty acids, cholesterol, and bile acids in the GI tract (Gropper & Smith, 2012). It was shown that the amounts of cholesterol, lipids or bile acids bound by fibers are not available for forming micelles, which meant that they are not available for absorption (Gropper & Smith, 2012). Certain fiber sources (including chitosan) are able to bind with bile acids and phospholipids both *in vitro and in vivo* (Ebihara & Schneeman, 1989; Vahouny, Tombes, Cassidy, Kritchevsky, & Gallo, 1980). It was also reported that guar gum or konjac mannan could reduce the intestinal absorption of cholesterol and triglyceride in rats (Ebihara & Schneeman, 1989). According to Vahouny et al. (1980), guar gum could bind 20-83% of micelle components, while lignin, alfalfa, wheat bran, and cellulose bound progressively less. However, conflicted findings have been reported in literature. One *in vivo* study showed that the addition of cellulose could reduce the appearance of cholesterol after 4 hr (Vahouny et al., 1988), but another *in vivo* study showed that the addition of large quantities of plant cell wall materials (derived from corn, beans, bran, pectin and purified cellulose) did not change plasma cholesterol, bile acid, and steroid levels though decreased intestinal transit time and increased stool bulk were observed (Raymond et al., 1977).

Several mechanisms have been proposed regarding the effects of fibers on lowered serum cholesterol levels. According to Gropper & Smith (2012), the proposed mechanism that is the most widely accepted is the adsorption or interaction capacity of fiber that increased excretion of bile acids and cholesterol. In this mechanism, decreased hepatic cholesterol levels facilitate the removal of serum low-density lipoprotein cholesterol while decreased bile acid levels also necessitate the synthesis of new bile acids from cholesterol. Another commonly accepted mechanism ascribes to the effect of fibers on shifting the bile acid production from cholic acid to chenodeoxycholic acid, which consequently inhibit an enzyme that regulates cholesterol

biosynthesis. The final mechanism mentioned by Gropper & Smith (2012), is suggested to be due to the product inhibition effect on fatty acid/cholesterol synthesis by the short-chain fatty acids which is generated by fermentation of dietary fibers. In addition, Mackie, Bajka, & Rigby (2016) have proposed a mechanism that suggests the reduced absorption of cholesterol due to the entanglement between fiber and intestinal mucus. It was shown that dietary fiber can interact with intestinal mucus and form a layer that significantly hampers transport of lipid digestion products. Viscous fibers, including guar gum, pectin, oat bran and psyllium, have been shown to be hypocholesterolemic *in vivo* (Brown, Rosner, Willett, & Sacks, 1999). However, insoluble fibers (like cellulose or brans) are shown not to be hypocholesterolemic in a male clinical study (Kritchevsky, 1987). It was shown that hemicellulose from rice bran was able to bind cholesterol and bile acid, but cellulose, lignin and insoluble fiber fractions from rice bran show very poor binding (Hu & Yu, 2013). Furthermore, some dietary fibers are shown to lower plasma cholesterol levels due to their binding with bile acids and reducing bile recirculation (Ebihara & Schneeman, 1989).

Dietary fibers have also been shown to cause increased excretion of bile acids *in vivo* (Story & Furumoto, 1990), since bile acids that are bound by fibers are not reabsorbed or re-circulated, but instead are excreted in feces (Gropper & Smith, 2012). Increased fecal lipid excretion was also shown in ileostomized humans with fiber supplemented diets (Lairon, 1997). The interaction between dietary fiber and bile acids was shown to partly depend on the hydrophobicity of the bile acids (Schneeman, 1998). Lignin isolated from olive stones showed substantial bile acid binding capacity, especially cholic acids (Rodríguez-Gutiérrez, Rubio-Senent, Lama-Muñoz, García, & Fernández-Bolaños, 2014; Story & Kritchevsky, 1976).

2.2.4 Effects of nanocellulose and dietary fibers on protein digestion and nitrogen absorption

Protein is also a major component in the human diet. Following its ingestion, protein digestion starts at the gastric phase where pepsin action generates a mixture of large polypeptides, small oligopeptides and some free amino acids. In the duodenum, the increase in pH results in deactivated pepsin, but activated endopeptidases (trypsin, chymotrypsin and elastase) as well as exopeptidases (carboxypeptidases A and B) cleave peptide bonds which then generates free amino acids and oligopeptides (2-6 amino acids) (Erickson & Kim, 1990). Different mechanisms exist in the transport of free amino acids and peptides. Specifically, the transport of free amino acids is via group (amino acid) specific active transport systems (Silk, Grimble, & Rees, 1985). Oligopeptides (including dipeptides and tripeptides) uptake is independent of free amino acids. Most of the absorbed intact peptides get hydrolyzed intracellularly into free amino acids followed by exporting to the blood, though very few intact peptides can directly enter into the blood (Erickson & Kim, 1990).

Summaries of the effects of NC and dietary fiber on protein *in vitro* and *in vivo* digestion as well as nitrogen utilization are shown in Table 2.3 and 2.4, respectively. So far, there are limited studies regarding the effects of NC on protein digestion and nitrogen utilization. The study carried out by Sarkar et al. (2017) showed that 3 wt% CNC could reduce the rate and extent of protein digestion at the gastric phase, based on sodium dodecyl sulfate polyacrylamide gel electrophoresis (SDS-PAGE) results. The efficacy of NC on protein digestion is similar to that exerted by dietary fiber. In general, viscous soluble fibers tend to decrease protein digestibility as well as increase pancreatic-bile excretion and fecal nitrogen content, while non-viscous insoluble fibers, seem to be less effective at decreasing protein digestion though they can still cause increased fecal nitrogen content. For example, highly viscous polysaccharides (sodium alginate, locust bean gum, guar and

xanthan gum) were shown to increase pancreatic-bile secretion while insoluble polysaccharides did not show such an effect (Ikegami et al., 1990). Soluble dietary fibers in dry beans were shown to significantly reduce protein digestibility and increase fecal nitrogen content in rats, while insoluble dietary fibers did not show any effects (Hughes, Acevedo, Bressani, & Swanson, 1996). Similarly, soluble dietary fibers in algae and mushroom were shown to result in lower (9.4% less) apparent protein digestibility than that of insoluble dietary fibers at the same concentration in rats (Horie, Sugase, & Horie, 1995). Even though *in vivo* studies in rats showed that increased cellulose contents in diets resulted in lower apparent protein digestibility (Hove & King, 1979), studies of incorporating cellulose (10 g or 30 g/day) to human diets showed that cellulose did not cause any differences in protein apparent digestibility or fecal nitrogen output (Mickelsen et al., 1979; Slavin & Marlett, 1980).

Soluble and insoluble DF increase fecal bulk excretion and fecal nitrogen excretion via different mechanisms. Specifically, the former was due to increased excretion of microbial nitrogen while the latter was due to the increased excretion of fiber bound protein (Eggum, 1995). Proteins or protein digestion products that are not absorbed in the small intestine are transported to the large intestine where they are used as nitrogen sources for bacteria growth. Furthermore, indigestible DF can also be used as energy sources for bacteria growth, leading to increased bacterial nitrogen in fecal samples (Eggum, 1995).

Dietary fibers can reduce protein digestibility via several mechanisms, including inhibiting protease activity, binding with protein substrate, interaction with protein digestion products as well as increased digesta viscosity. Specifically, dietary fibers have been shown to inhibit protease activity both *in vitro* and *in vivo* (Harmuth-Hoene & Schwerdtfeger, 1979; Ikeda & Kusano, 1983). For example, some fibers (including xylan, apple pectin, or buckwheat hemicellulose) were found

to inhibit trypsin activity *in vitro*, and some (including xylan, sodium alginate, and yeast mannan) inhibited α-chymotrypsin activity *in vitro*, while others (e.g., apple pectin) caused inhibition in pepsin activity *in vitro* (Ikeda & Kusano, 1983). Partially inhibited apparent trypsin activity was found upon the addition of 10% (w/w) carrageenan in the rat diets, as reported by Harmuth-Hoene & Schwerdtfeger (1979). In addition, lignin could inhibit isolated trypsin and chymotrypsin activity, which further affects *in vitro* protein digestion (Hansen, 1986).

The effects of pectin and xylan towards inhibition of trypsin activity was due to their binding with the protein substrate (Ikeda & Kusano, 1983). Cationic polysaccharides (e.g., chitosan) can bind with protein (e.g., WPI) via electrostatic interaction at or close to neutral pH (e.g., pH 6.5) (Liu, Gao, & Yuan, 2015), while anionic polysaccharides (e.g., xanthan gum, alginate, carrageenan) can form aggregates with proteins during gastric digestion (Borreani, Llorca, Larrea, & Hernando, 2016). For neutral polysaccharides, including holo-cellulose (containing cellulose and semi-cellulose) and guar gum as well as locust bean gum, slightly or negligible inhibition was observed towards casein digestion (Acton, Breyer, & Satterlee, 1982). At the gastric pH, electrostatic attraction between positively charged protein and anionic fiber dominates even though non-electrostatic interaction (including hydrogen bonding) may also exist and play a role in the complexes formed between protein and polysaccharides (Mouécoucou, Villaume, Sanchez, & Méjean, 2004b). Electrostatic interaction was reported to occur between positively charged WPI and negatively charged anionic NC at the gastric phase (Sarkar et al., 2017). The interaction between CNC and WPI was reported to involve van der Waals forces, hydrogen bonding and capillary forces (Sarkar et al., 2018). It was reported by David-Birman, Mackie, & Lesmes (2013) that pectin, alginate and carrageenan influenced the proteolysis of bovine lactoferrin nano-particles due to the formation of protein-fiber core-shell structure. According to Acton et al. (1982), gum

ghatti (an anionic soluble fiber) inhibited casein *in vitro* digestion due to the matrix restriction effect and the digestion products only contained small MW peptides. However, pectin substantially inhibited casein *in vitro* digestion due to its ionic interference effects towards enzyme and/or substrate and the digestion products only contained large MW peptides.

Dietary fibers were also found to interact with protein digestion products. According to Mouécoucou, Villaume, Sanchez, & Méjean (2004a), gum arabic and xylan reduced PPI hydrolysis via interaction with some proteins and high molecular weight (MW) peptides. LM pectin on the other hand did not impact PPI hydrolysis but affected nitrogen diffusion via interaction with protein hydrolysis products (low MW peptides and amino acids). This was supported by the phenomena that fiber significantly reduced protein digestibility when using a dialysis membrane with molecular weight cut-offs (MWCO) of 1 KDa while no significant effects were observed with MWCO of 8 KDa (Mouécoucou et al., 2004b).

There are several factors that influence the testing efficacy of dietary fibers on protein digestion and nitrogen utilization, including fiber (sources, purity and surface charge), protein-fiber ratios, test conditions and methodologies. For example, it was found that fiber in natural sources (e.g., food fiber) show different physiological effects as purified fiber on protein digestion and fiber fermentation (Eggum, 1995). In addition, as shown in a review article by Gallaher & Schneeman (1986), purified fibers negatively affected protein digestion in rats while no effects were observed in humans (Eggum, 1995). Lower protein digestibility was observed with higher amount of natural DF sources adding to the diets of rats (Eggum, 1995), while 30% cellulose did not show any effects on protein digestibility (Eggum, 1973). The ratio of fiber to protein also played a role. Specifically, it has been reported by Liu et al. (2018) and Sarkar et al. (2018) that CNC can bind with WPI or BSA at pH 3 and there exists an optimum ratio for the binding between

CNC and protein (WPI/BSA). A much denser network surround WPI interface at higher CNC concentrations (e.g., 3 wt%) than lower (e.g., 1 wt%) was reported by Sarkar et al. (2017). As shown by Sarkar et al. (2017), based on SDS-PAGE patterns, 3 wt% CNC could cause 60% intact protein bands remaining after gastric digestion, and 3 wt% CNC was more capable at reducing WPI digestibility than 1 wt% CNC. Moreover, it was shown by Zhang & Vardhanabhuti (2014) that intragastric gel formation between WPI and pectin only occurs at certain ratios. Specifically, lower pectin concentrations (e.g., 0.25%) did not form intragastric gels with WPI while higher pectin concentrations (e.g., 1%) did. Similarly, Huang (2017) and Hu et al. (2017) showed that the attraction between SPI and alginate, xanthan gum or carrageenan at the gastric environment increased with higher fiber concentrations, due to more protein-fiber interaction and stronger network formation at high fiber concentrations. According to Huang (2017), the digestibility of intragastric gel between protein and fiber is governed by the interaction strength of the gel, with weaker gels more easily digested due to less susceptible sites for pepsin digestion.

### 2.2.5 Effects of nanocellulose and dietary fiber on mineral absorption

Dietary fibers are shown to impair mineral absorption in the small intestine due to their binding and/or sequestering effects (Staffolo, Bevilacqua, Rodríguez, & Albertengo, 2012). However, in the large intestine, this negative effect is offset by the fermentation of fibers and reabsorption of liberated minerals (Baye, Guyot, & Mouquet-Rivier, 2017). No clear conclusions can yet be drawn regarding the effects of dietary fibers on mineral absorption, due to conflicted findings from *in vitro* and *in vivo* studies (Ghodrat, Yaghobfar, Ebrahimnezhad, Shahryar, & Ghorbani, 2015). As an example, sugar beet fiber has been shown to reduce calcium bioavailability *in vitro* (Weber, Kohlhepp, Idouraine, & Ochoa, 1993), but it was shown to improve calcium balance in humans (Coudray et al., 1997).

The mechanisms of dietary fibers in reduced bioavailability of minerals include shortened transit times (reduced time for mineral absorption), chelation of minerals by fibers, influence on active and passive transport of minerals as well as dilution of intestinal content and fecal bulking effect (Harland, 1989). On the other hand, the mechanism of some soluble fibers (including pectin and short-chain fructo-oligosaccharide) on enhancing mineral absorption may be due to the effect of fermentation products generated. Specifically, the production of short-chain fatty acid may trigger proliferation of epithelial cells which increase the surface area for mineral absorption. In addition, the production of osmotically active sugars may favor the passive absorption or production of weak organic acids that enhance mineral absorption (Baye et al., 2017).

Comparisons among the studies of dietary fibers on mineral absorption are difficult due to their various differences, including the fiber itself (source, type and content), experimental conditions (pH, concentration), testing methodologies (e.g., sensitivity of detection methods), and other interfering factors (e.g., co-existence of phytate, polyphenols) (Baye et al., 2017; Idouraine, Khan, & Weber, 1996; Rossander, Sandberg, & Sandström, 1992). On one hand, fiber type is important in mineral binding since different fibers possess different number of binding sites and affinity for minerals (Plait & Clydesdale, 1987). Guar gum in particular has the highest binding affinity with iron when compared to lignin, cellulose, and methoxy pectin. Lignin is shown to have higher binding affinity with iron than copper or zinc (Plait & Clydesdale, 1987). In addition, the calcium binding capacity of 18 fibers varied from 480 μg/g (the lowest) by cellulose to 20137 μg/g (the highest) by orange fiber (Weber et al., 1993). The maximum copper adsorption on TEMPO-CNF was 135 mg/g., which was ten-fold larger than that observed in native CNF (Sehaqui et al., 2014; Liu et al., 2015). The silver ion removal capacity of CNC was 34.4 mg/g, which was larger than that of CNF (Liu, 2015). Moreover, it was also found that regardless of surface functionality

of nanocellulose, the metal ion selectivity was Ag(I) > Fe(III) > Cu(II) (Liu et al., 2015). On the other hand, pH has been argued to be the most important factor that influences mineral binding, since the binding was more favorable at or close to neutral pH (e.g., pH 6.8) than acidic pH (Thompson & Weber, 1979). It was suggested that pH influences the dissociation of the phosphate ester of phytic acid and carboxyl ester of uronic acids, with fewer binding sites available in the undissociated groups at low pH (Luccia & Kunkel, 2002). The adsorption process of copper ions to TEMPO-CNF was reported to relate to pH and carboxylate content (Sehaqui et al., 2014). In addition, it was shown that the metal ion uptake by the aldehyde-modified CNCs (aCNCs, containing carboxylate groups) was mainly governed by the electrostatic interactions between the metal ions and the acidic groups on CNC (Alizadehgiashi et al., 2018). Furthermore, competitive interactions among minerals may also affect their binding with fibers (Luccia & Kunkel, 2002). Lastly, some processing treatments may influence the mineral binding capacity of fibers as well. For example, extrusion processing of oat, wheat and rice brans did not decrease their binding capacity with copper divalent ions ($Cu^{2+}$), but caused increase in their binding capacity in calcium divalent ions ($Ca^{2+}$) and zinc divalent ions ($Zn^{2+}$) (Gualberto, Bergman, & Weber, 1997).

The human body may be able to adjust to reduced mineral bioavailability due to the presence of fibers by increasing mineral absorption (Gordon, 1990; Kelsay, 1987). A moderate intake of non-digestible dietary fibers (20~25 g/day) have not been shown to cause mineral shortage. In addition, deficiency or excess intake of dietary fibers have not been shown to cause any mineral related pathologies as well (Gordon, 1990). It was also shown that the intake of dietary fibers did not seem to affect mineral balances unless higher fiber intakes and lower mineral intakes were maintained (Kelsay, 1987). Nevertheless, even though vegetarian diets result in lower iron and zinc absorption, adverse health effects have not been demonstrated. Instead, moderately lower

iron stores may reduce the risk of chronic diseases (Hunt, 2003). The addition of pure fiber to human diet has shown no effects on mineral absorption which indicates that pure fiber is relatively inert (Rossander et al., 1992).

**2.3 References**


Acton, J., Breyer, L., & Satterlee, L. (1982). Effect of dietary fiber constituents on the in vitro digestibility of casein. *Journal of food science,* 47(2), 556-560.

Adams, S., Sello, C. T., Qin, G.-X., Che, D., & Han, R. (2018). Does Dietary Fiber Affect the Levels of Nutritional Components after Feed Formulation? *Fibers,* 6(2), 29.

Agoda-Tandjawa, G., Durand, S., Berot, S., Blassel, C., Gaillard, C., Garnier, C., & Doublier, J.-L. (2010). Rheological characterization of microfibrillated cellulose suspensions after freezing. *Carbohydrate Polymers,* 80(3), 677-686.

Ahmed, F., Sairam, S., & Urooj, A. (2011). In vitro hypoglycemic effects of selected dietary fiber sources. *Journal of food science & technology,* 48(3), 285-289.

Alizadehgiashi, M., Khuu, N., Khabibullin, A., Henry, A., Tebbe, M., Suzuki, T., & Kumacheva, E. (2018). Nanocolloidal Hydrogel for Heavy Metal Scavenging. *ACS nano*, *12*(8), 8160-8168.

Amarowicz, R., Korczakowska, B., & Smoczyńska, K. (1988). Effect of fiber from buckwheat on the In vitro enzymatic digestion of protein. *Food/Nahrung,* 32(10), 1005-1006.

Anderson, S. R., Esposito, D., Gillette, W., Zhu, J., Baxa, U., & Mcneil, S. E. (2014). Enzymatic preparation of nanocrystalline and microcrystalline cellulose. *TAPPI JOURNAL,* 13(5), 35-42.

Andrade, D. R. M., Mendonça, M. H., Helm, C. V., Magalhães, W. L., de Muniz, G. I. B., & Kestur, S. G. (2015). Assessment of nano cellulose from peach palm residue as potential food additive: part II: preliminary studies. *Journal of food science and technology*, *52*(9), 5641-5650.

Aozasa, O., Ohta, S., Nakao, T., Miyata, H., & Nomura, T. (2001). Enhancement in fecal excretion of dioxin isomer in mice by several dietary fibers. *Chemosphere,* 45(2), 195-200.

Armand, M., Borel, P., Dubois, C., Senft, M., Peyrot, J., Salducci, J., . . . Lairon, D. (1994). Characterization of emulsions and lipolysis of dietary lipids in the human stomach. *American Journal of Physiology-Gastrointestinal and Liver Physiology,* 266(3), G372-G381.

Armand, M., Borel, P., Pasquier, B., Dubois, C., Senft, M., Andre, M., . . . Lairon, D. (1996). Physicochemical characteristics of emulsions during fat digestion in human stomach and duodenum. *American Journal of Physiology-Gastrointestinal and Liver Physiology,* 271(1), G172-G183.

Aylward, D. (2018). Investigating the Attenuation of Starch Hydrolysis by Synergistic Interaction of Xanthan and Guar Gum Fortification during In Vitro Digestion.

Baye, K., Guyot, J.-P., & Mouquet-Rivier, C. (2017). The unresolved role of dietary fibers on mineral absorption. *Critical reviews in food science & nutrition,* 57(5), 949-957.

Bettaieb, F., Nechyporchuk, O., Khiari, R., Mhenni, M. F., Dufresne, A., & Belgacem, M. N. (2015). Effect of the oxidation treatment on the production of cellulose nanofiber suspensions from Posidonia oceanica: the rheological aspect. *Carbohydrate Polymers,* 134, 664-672.

Borreani, J., Llorca, E., Larrea, V., & Hernando, I. (2016). Adding neutral or anionic hydrocolloids to dairy proteins under in vitro gastric digestion conditions. *Food Hydrocolloids,* 57, 169-177.

Brown, L., Rosner, B., Willett, W. W., & Sacks, F. M. (1999). Cholesterol-lowering effects of dietary fiber: a meta-analysis. *The American journal of clinical nutrition,* 69(1), 30-42.

Cao, B., Zhang, X., Guo, Y., Karasawa, Y., & Kumao, T. (2003). Effects of dietary cellulose levels on growth, nitrogen utilization, retention time of diets in digestive tract and caecal microflora of chickens. *Asian Australasian Journal of Animal Sciences,* 16(6), 863-866.

Capuano, E. (2017). The behavior of dietary fiber in the gastrointestinal tract determines its physiological effect. *Critical reviews in food science and nutrition,* 57(16), 3543-3564.

Chaisawang, M., & Suphantharika, M. (2006). Pasting and rheological properties of native and anionic tapioca starches as modified by guar gum and xanthan gum. *Food Hydrocolloids,* 20(5), 641-649.

Chater, P. I., Wilcox, M. D., Brownlee, I. A., & Pearson, J. P. (2015). Alginate as a protease inhibitor in vitro and in a model gut system; selective inhibition of pepsin but not trypsin. *Carbohydrate Polymers,* 131, 142-151.

Chau, C.-F., Chen, C.-H., & Wang, Y.-T. (2004). Effects of a novel pomace fiber on lipid and cholesterol metabolism in the hamster. *Nutrition Research,* 24(5), 337-345.

Chau, C.-F., Huang, Y.-L., & Lee, M.-H. (2003). In vitro hypoglycemic effects of different insoluble fiber-rich fractions prepared from the peel of Citrus sinensis L. cv. Liucheng. *Journal of Agricultural & Food Chemistry,* 51(22), 6623-6626.

Chau, C. F., & Huang, Y. L. (2005). Effects of the insoluble fiber derived from Passiflora edulis seed on plasma and hepatic lipids and fecal output. *Molecular nutrition & food research,* 49(8), 786-790.

Chau, M., Sriskandha, S. E., Pichugin, D., Thérien-Aubin, H. l., Nykypanchuk, D., Chauve, G. g., . . . Kumacheva, E. (2015). Ion-mediated gelation of aqueous suspensions of cellulose nanocrystals. *Biomacromolecules,* 16(8), 2455-2462.

Coudray, C., Bellanger, J., Castiglia-Delavaud, C., Remesy, C., Vermorel, M., & Rayssignuier, Y. (1997). Effect of soluble or partly soluble dietary fibres supplementation on absorption and balance of calcium, magnesium, iron and zinc in healthy young men. *European journal of clinical nutrition,* 51(6), 375.

Cui, S. W., & Roberts, K. T. (2009). *Dietary fiber: fulfilling the promise of added-value formulations*. In *Modern biopolymer science* (pp. 399-448): Elsevier

David-Birman, T., Mackie, A., & Lesmes, U. (2013). Impact of dietary fibers on the properties and proteolytic digestibility of lactoferrin nano-particles. *Food Hydrocolloids,* 31(1), 33-41.

DeLoid, G. M., Sohal, I. S., Lorente, L. R., Molina, R. M., Pyrgiotakis, G., Stevanovic, A., . . . Bousfield, D. W. (2018). Reducing Intestinal Digestion and Absorption of Fat Using a Nature-Derived Biopolymer: Interference of Triglyceride Hydrolysis by Nanocellulose. *ACS nano*, 12 (7), 6469–6479.

Dhital, S., Gidley, M. J., & Warren, F. J. (2015). Inhibition of α-amylase activity by cellulose: Kinetic analysis and nutritional implications. *Carbohydrate Polymers,* 123, 305-312.

Diaz-Sotomayor, M., Quezada-Calvillo, R., Avery, S. E., Chacko, S. K., Yan, L.-k., Lin, A. H.-M., . . . Nichols, B. L. (2013). Maltase-glucoamylase modulates gluconeogenesis and sucrase-isomaltase dominates starch digestion glucogenesis. *Journal of pediatric gastroenterology & nutrition,* 57(6), 704-712.

Díez, I., Eronen, P., Österberg, M., Linder, M. B., Ikkala, O., & Ras, R. H. (2011). Functionalization of nanofibrillated cellulose with silver nanoclusters: fluorescence and antibacterial activity. *Macromolecular bioscience,* 11(9), 1185-1191.

Dimic-Misic, K., Gane, P., & Paltakari, J. (2013). Micro-and nanofibrillated cellulose as a rheology modifier additive in CMC-containing pigment-coating formulations. *Industrial & Engineering Chemistry Research,* 52(45), 16066-16083.

Dourado, F., Gama, M., & Rodrigues, A. C. (2017). A Review on the toxicology and dietetic role of bacterial cellulose. *Toxicology reports*.

Dunaif, G., & Schneeman, B. (1981). The effect of dietary fiber on human pancreatic enzyme activity in vitro. *The American journal of clinical nutrition,* 34(6), 1034-1035.

Dutta, S. K., & Hlasko, J. (1985). Dietary fiber in pancreatic disease: effect of high fiber diet on fat malabsorption in pancreatic insufficiency and in vitro study of the interaction of dietary fiber with pancreatic enzymes. *The American journal of clinical nutrition,* 41(3), 517-525.

Ebihara, K., & Schneeman, B. O. (1989). Interaction of bile acids, phospholipids, cholesterol and triglyceride with dietary fibers in the small intestine of rats. *The Journal of nutrition,* 119(8), 1100-1106.

Eggum, B. (1973). Study of certain factors influencing protein utilization in rats and pigs.

Eggum, B. (1995). The influence of dietary fibre on protein digestion and utilization in monogastrics. *Archiv für Tierernaehrung,* 48(1-2), 89-95.

Englyst, H. N., Kingman, S., & Cummings, J. (1992). Classification and measurement of nutritionally important starch fractions. *European journal of clinical nutrition,* 46, S33-50.

Erickson, R. H., & Kim, Y. S. (1990). Digestion and absorption of dietary protein. *Annual review of medicine,* 41(1), 133-139.

Eswaran, S., Muir, J., & Chey, W. D. (2013). Fiber and functional gastrointestinal disorders. *The American journal of gastroenterology,* 108(5), 718.

Fabek, H., Messerschmidt, S., Brulport, V., & Goff, H. D. (2014). The effect of in vitro digestive processes on the viscosity of dietary fibres and their influence on glucose diffusion. *Food Hydrocolloids,* 35, 718-726.

Ferguson, L. R., Roberton, A. M., Watson, M. E., Kestell, P., & Harris, P. J. (1993). The adsorption of a range of dietary carcinogens by α-cellulose, a model insoluble dietary fiber. *Mutation Research/Genetic Toxicology,* 319(4), 257-266.

Gallaher, D., & Schneeman, B. O. (1986). Intestinal interaction of bile acids, phospholipids, dietary fibers, and cholestyramine. *American Journal of Physiology-Gastrointestinal & Liver Physiology,* 250(4), G420-G426.

Gestranius, M., Stenius, P., Kontturi, E., Sjöblom, J., & Tammelin, T. (2017). Phase behaviour and droplet size of oil-in-water Pickering emulsions stabilised with plant-derived nanocellulosic materials. *Colloids & Surfaces A: Physicochemical & Engineering Aspects,* 519, 60-70.

Ghodrat, A., Yaghobfar, A., Ebrahimnezhad, Y., Shahryar, H. A., & Ghorbani, A. (2015). In vitro Binding Capacity of Wheat and Barley for Mn, Zn, Cu and Fe. *International Journal of Life Sciences,* 9(6), 56-60.

Giacco, R., Costabile, G., & Riccardi, G. (2016). Metabolic effects of dietary carbohydrates: The importance of food digestion. *Food Research International,* 88, 336-341.

Gordon, D. T. (1990). *Total dietary fiber and mineral absorption*. In *Dietary Fiber* (pp. 105-128): Springer

Gropper, S. S., & Smith, J. L. (2012). *Advanced nutrition and human metabolism*: Cengage Learning.

Grundy, M. M.-L., Edwards, C. H., Mackie, A. R., Gidley, M. J., Butterworth, P. J., & Ellis, P. R. (2016). Re-evaluation of the mechanisms of dietary fibre and implications for macronutrient bioaccessibility, digestion and postprandial metabolism. *British Journal of Nutrition,* 116(5), 816-833.

Gualberto, D., Bergman, C., & Weber, C. (1997). Mineral binding capacity of dephytinized insoluble fiber from extruded wheat, oat and rice brans. *Plant foods for human nutrition,* 51(4), 295-310.

Hansen, W. E. (1986). Effect of dietary fiber on proteolytic pancreatic enzymes in vitro. *International Journal of Pancreatology,* 1(5-6), 341-351.

Harland, B. F. (1989). Dietary fibre and mineral bioavailability. *Nutrition research reviews,* 2(1), 133-147.

Harmuth-Hoene, A.-E., & Schwerdtfeger, E. (1979). Effect of indigestible polysaccharides on protein digestibility and nitrogen retention in growing rats. *Annals of Nutrition & Metabolism,* 23(5), 399-407.

Harris, P. J., Roberton, A. M., Hollands, H. J., & Ferguson, L. R. (1991). Adsorption of a hydrophobic mutagen to dietary fibre from the skin and flesh of potato tubers. *Mutation Research/Genetic Toxicology,* 260(2), 203-213.

Harris, P. J., Triggs, C. M., Roberton, A. M., Watson, M. E., & Ferguson, L. R. (1996). The adsorption of heterocyclic aromatic amines by model dietary fibres with contrasting compositions. *Chemico-biological interactions,* 100(1), 13-25.

Hasik, J., & Bartnikowska, E. (1987). Wbkno roilinne w iywieniu czlowieka. *PZWL, Warszawa*.

Horie, Y., Sugase, K., & Horie, K. (1995). Physiological differences of soluble and insoluble dietary fibre fractions of brown algae and mushrooms in pepsin activity in vitro and protein digestibility. *Asia Pac J Clin Nutr,* 4(2), 251-255.

Houghton, D., Wilcox, M. D., Chater, P. I., Brownlee, I. A., Seal, C. J., & Pearson, J. P. (2015). Biological activity of alginate and its effect on pancreatic lipase inhibition as a potential treatment for obesity. *Food Hydrocolloids,* 49, 18-24.

Hove, E. L., & King, S. (1979). Effects of pectin and cellulose on growth, feed efficiency, and protein utilization, and their contribution to energy requirement and cecal VFA in rats. *The Journal of nutrition,* 109(7), 1274-1278.

Hu, B., Chen, Q., Cai, Q., Fan, Y., Wilde, P. J., Rong, Z., & Zeng, X. (2017). Gelation of soybean protein and polysaccharides delays digestion. *Food Chemistry,* 221, 1598-1605.

Hu, G., & Yu, W. (2013). Binding of cholesterol and bile acid to hemicelluloses from rice bran. *International journal of food sciences & nutrition,* 64(4), 461-466.

Huang, Z. (2017). Intragastric gelation of mixed soy protein isolate and alginate as well as its effect on postprandial glucose response and satiety. University of Missouri--Columbia.

Hubbe, M. A., Tayeb, P., Joyce, M., Tyagi, P., Kehoe, M., Dimic-Misic, K., & Pal, L. (2017). Rheology of nanocellulose-rich aqueous suspensions: a review. *BioResources,* 12(4), 9556-9661.

Hughes, J. S., Acevedo, E., Bressani, R., & Swanson, B. G. (1996). Effects of dietary fiber and tannins on protein utilization in dry beans (Phaseolus vulgaris). *Food Research International,* 29(3-4), 331-338.

Hunt, J. R. (2003). Bioavailability of iron, zinc, and other trace minerals from vegetarian diets. *The American journal of clinical nutrition,* 78(3), 633S-639S.

Idouraine, A., Khan, M., & Weber, C. (1996). In vitro binding capacity of wheat bran, rice bran, and oat fiber for Ca, Mg, Cu, and Zn alone and in different combinations. *Journal of Agricultural & Food Chemistry,* 44(8), 2067-2072.

Ikeda, K., & Kusano, T. (1983). In vitro inhibition of digestive enzymes by indigestible polysaccharides. *Cereal Chem,* 60(4), 260-263.

Ikegami, S., Tsuchihashi, F., Harada, H., Tsuchihashi, N., Nishide, E., & Innami, S. (1990). Effect of viscous indigestible polysaccharides on pancreatic-biliary secretion and digestive organs in rats. *The Journal of nutrition,* 120(4), 353-360.

Ioelovich, M. (2017). Characterization of various kinds of nanocellulose. In I. A. Kargarzadeh, S. Thomas, A. Dufresne. (Ed.), *Handbook of Nanocellulose and Cellulose Nanocomposites* (pp. 51-100): John Wiley & Sons

Ioelovich, M., & Figovsky, O. (2008). Nano-cellulose as promising biocarrier. *Advanced Materials Research* (Vol. 47, pp. 1286-1289): Trans Tech Publ.

Isaksson, G., Lundquist, I., Åkesson, B., & Ihse, I. (1984). Effects of pectin and wheat bran on intraluminal pancreatic enzyme activities and on fat absorption as examined with the triolein breath test in patients with pancreatic insufficiency. *Scandinavian journal of gastroenterology,* 19(4), 467-472.

Isaksson, G., Lundquist, I., & Ihse, I. (1982). In vitro inhibition of pancreatic enzyme activities by dietary fiber. *Digestion,* 24(1), 54-59.

Ismail-Beigi, F., Reinhold, J. G., Faraji, B., & Abadi, P. (1977). Effects of cellulose added to diets of low and high fiber content upon the metabolism of calcium, magnesium, zinc and phosphorus by man. *The Journal of nutrition,* 107(4), 510-518.

Isogai, A., Saito, T., & Fukuzumi, H. (2011). TEMPO-oxidized cellulose nanofibers. *nanoscale,* 3(1), 71-85.

Isogai, T., Saito, T., & Isogai, A. (2011). Wood cellulose nanofibrils prepared by TEMPO electro-mediated oxidation. *Cellulose,* 18(2), 421-431.

Jebali, A., Hekmatimoghaddam, S., Behzadi, A., Rezapor, I., Mohammadi, B. H., Jasemizad, T., . . . Soltani, M. (2013). Antimicrobial activity of nanocellulose conjugated with allicin and lysozyme. *Cellulose,* 20(6), 2897-2907.

Jenkins, D. J., Kendall, C. W., Axelsen, M., Augustin, L. S., & Vuksan, V. (2000). Viscous and nonviscous fibres, nonabsorbable and low glycaemic index carbohydrates, blood lipids and coronary heart disease. *Current opinion in lipidology,* 11(1), 49-56.

Ji, N., Liu, C., Li, M., Sun, Q., & Xiong, L. (2018). Interaction of cellulose nanocrystals and amylase: Its influence on enzyme activity and resistant starch content. *Food chemistry,* 245, 481-487.

Jorfi, M., & Foster, E. J. (2015). Recent advances in nanocellulose for biomedical applications. *Journal of Applied Polymer Science,* 132(14).

Karppinen, A., Saarinen, T., Salmela, J., Laukkanen, A., Nuopponen, M., & Seppälä, J. (2012). Flocculation of microfibrillated cellulose in shear flow. *Cellulose,* 19(6), 1807-1819.

Keim, K., & Kies, C. (1979). Effects of dietary fiber on nutritional status of weanling mice. *Cereal Chemistry*.

Kelsay, J. L. (1987). Effects of fiber, phytic acid, and oxalic acid in the diet on mineral bioavailability. *American Journal of Gastroenterology,* 82(10).

Kendall, C. W., Esfahani, A., & Jenkins, D. J. (2010). The link between dietary fibre and human health. *Food Hydrocolloids,* 24(1), 42-48.

Keys, A., Grande, F., & Anderson, J. T. (1961). Fiber and pectin in the diet and serum cholesterol concentration in man. *Proceedings of the Society for Experimental Biology & Medicine,* 106(3), 555-558.

Khosravi-Darani, K., Koller, M., Akramzadeh, N., & Mortazavian, A. M. (2016). Bacterial nanocellulose: biosynthesis and medical application. *Biointerface Research in Applied Chemistry,* 6(5), 1511-1516.

Klemm, D., Kramer, F., Moritz, S., Lindström, T., Ankerfors, M., Gray, D., & Dorris, A. (2011). Nanocelluloses: a new family of nature-based materials. *Angewandte Chemie International Edition,* 50(24), 5438-5466.

Klemm, D., Philpp, B., Heinze, T., Heinze, U., & Wagenknecht, W. (1998). *Comprehensive cellulose chemistry. Volume 1: Fundamentals and analytical methods*: Wiley-VCH Verlag GmbH.

Kolakovic, R., Laaksonen, T., Peltonen, L., Laukkanen, A., & Hirvonen, J. (2012). Spray-dried nanofibrillar cellulose microparticles for sustained drug release. *International journal of pharmaceutics,* 430(1-2), 47-55.

Kolakovic, R., Peltonen, L., Laaksonen, T., Putkisto, K., Laukkanen, A., & Hirvonen, J. (2011). Spray-dried cellulose nanofibers as novel tablet excipient. *Aaps Pharmscitech,* 12(4), 1366-1373.

Kritchevsky, D. (1987). Dietary fibre and lipid metabolism. *Int J Obes.,* 11 Suppl 1:33-43.

Kumar, A., & Chauhan, G. S. (2010). Extraction and characterization of pectin from apple pomace and its evaluation as lipase (steapsin) inhibitor. *Carbohydrate Polymers,* 82(2), 454-459.

Lairon, D. (1997). *Soluble fibers and dietary lipids*. In *Dietary fiber in health and disease* (pp. 99-108): Springer

Lasseuguette, E., Roux, D., & Nishiyama, Y. (2008). Rheological properties of microfibrillar suspension of TEMPO-oxidized pulp. *Cellulose,* 15(3), 425-433.

Li, J., Wei, X., Wang, Q., Chen, J., Chang, G., Kong, L., . . . Liu, Y. (2012). Homogeneous isolation of nanocellulose from sugarcane bagasse by high pressure homogenization. *Carbohydrate Polymers,* 90(4), 1609-1613.

Li, M.-C., Wu, Q., Song, K., Lee, S., Qing, Y., & Wu, Y. (2015). Cellulose nanoparticles: structure–morphology–rheology relationships. *ACS Sustainable Chemistry & Engineering,* 3(5), 821-832.

Lin, N., & Dufresne, A. (2014). Nanocellulose in biomedicine: Current status and future prospect. *European Polymer Journal,* 59, 302-325.

Liu, F., Gao, Y., & Yuan, F. (2015). Effects of chitosan addition on in vitro digestibility of protein-coated lipid droplets. *Journal of Dispersion Science & Technology,* 36(11), 1556-1563.

Liu, P. (2015). Adsorption behavior of heavy metal ions from aqueous medium on nanocellulose (Doctoral dissertation, Luleå tekniska universitet).

Liu, Z., Li, X., Xie, W., & Deng, H. (2017). Extraction, isolation and characterization of nanocrystalline cellulose from industrial kelp (Laminaria japonica) waste. *Carbohydrate Polymers,* 173, 353-359.

Liu, F., Zheng, J., Huang, C.-H., Tang, C.-H., & Ou, S.-Y. (2018). Pickering high internal phase emulsions stabilized by protein-covered cellulose nanocrystals. *Food Hydrocolloids,* 82, 96-105.

Lopes, V. R., Sanchez-Martinez, C., Strømme, M., & Ferraz, N. (2017). In vitro biological responses to nanofibrillated cellulose by human dermal, lung and immune cells: surface chemistry aspect. *Particle and fibre toxicology,* 14(1), 1.

Lu, Z., Fan, L., Zheng, H., Lu, Q., Liao, Y., & Huang, B. (2013). Preparation, characterization and optimization of nanocellulose whiskers by simultaneously ultrasonic wave and microwave assisted. *Bioresource technology,* 146, 82-88.

Luccia, B. H., & Kunkel, M. E. (2002). In vitro availability of calcium from sources of cellulose, methylcellulose, and psyllium. *Food Chemistry,* 77(2), 139-146.

Ludwicka, K., Jedrzejczak-Krzepkowska, M., Kubiak, K., Kolodziejczyk, M., Pankiewicz, T., & Bielecki, S. (2017). *Medical and cosmetic applications of bacterial nanocellulose*. In *Bacterial Nanocellulose* (pp. 145-165): Elsevier

Luo, H., Xiong, G., Hu, D., Ren, K., Yao, F., Zhu, Y., . . . Wan, Y. (2013). Characterization of TEMPO-oxidized bacterial cellulose scaffolds for tissue engineering applications. *Materials Chemistry & Physics,* 143(1), 373-379.

Mackie, A., Bajka, B., & Rigby, N. (2016). *Dietary Fibre: More than a Prebiotic*. In *Gums and Stabilisers for the Food Industry 18* (pp. 227-234)

Madsen, B., & Gamstedt, E. K. (2013). Wood versus plant fibers: similarities and differences in composite applications. *Advances in Materials Science & Engineering,* 2013.

McRae, M. P. (2017). Dietary fiber is beneficial for the prevention of cardiovascular disease: an umbrella review of meta-analyses. *Journal of chiropractic medicine,* 16(4), 289-299.

Mendoza, L., Batchelor, W., Tabor, R. F., & Garnier, G. (2018). Gelation mechanism of cellulose nanofibre gels: A colloids and interfacial perspective. *Journal of colloid & interface science,* 509, 39-46.

Mertaniemi, H. (2017). Studies on nanocellulose-Functional microparticles, threads, and aerogels of cellulose nanofibrils (Doctoral dissertation). Aalto University.

Mickelsen, O., Makdani, D., Cotton, R. H., Titcomb, S. T., Colmey, J. C., & Gatty, R. (1979). Effects of a high fiber bread diet on weight loss in college-age males. *The American journal of clinical nutrition,* 32(8), 1703-1709.

Minko, S., Sharma, S., Hardin, I., Luzinov, I., Daubenmire, S. W., Zakharchenko, A., . . . Kim, Y. S. (2016). Textile dyeing using nanocellulosic fibers. Google Patents.

Moberg, T., Sahlin, K., Yao, K., Geng, S., Westman, G., Zhou, Q., . . . Rigdahl, M. (2017). Rheological properties of nanocellulose suspensions: effects of fibril/particle dimensions and surface characteristics. *Cellulose,* 24(6), 2499-2510.

Mohtaschemi, M., Dimic-Misic, K., Puisto, A., Korhonen, M., Maloney, T., Paltakari, J., & Alava, M. J. (2014). Rheological characterization of fibrillated cellulose suspensions via bucket vane viscometer. *Cellulose,* 21(3), 1305-1312.

Moron, D., Melito, C., & Tovar, J. (1989). Effect of indigestible residue from foodstuffs on trypsin and pancreatic α-amylase activity in vitro. *Journal of the Science of Food & Agriculture,* 47(2), 171-179.

Mouécoucou, J., Villaume, C., Sanchez, C., & Méjean, L. (2004a). Effects of gum arabic, low methoxy pectin and xylan on in vitro digestibility of peanut protein. *Food Research International,* 37(8), 777-783.

Mouécoucou, J., Villaume, C., Sanchez, C., & Méjean, L. (2004b). β-Lactoglobulin/polysaccharide interactions during in vitro gastric and pancreatic hydrolysis assessed in dialysis bags of different molecular weight cut-offs. *Biochimica et Biophysica Acta -General Subjects,* 1670(2), 105-112.

Mousavi, S. M., Afra, E., Tajvidi, M., Bousfield, D., & Dehghani-Firouzabadi, M. (2017). Cellulose nanofiber/carboxymethyl cellulose blends as an efficient coating to improve the structure and barrier properties of paperboard. *Cellulose,* 24(7), 3001-3014.

Munoz, J. M. (1982). *Interactions of dietary fiber and nutrients*. In *Dietary Fiber in Health and Disease* (pp. 85-89): Springer

Nasir, M., Hashim, R., Sulaiman, O., & Asim, M. (2017). *Nanocellulose: Preparation methods and applications*. In *Cellulose-Reinforced Nanofibre Composites* (pp. 261-276): Elsevier.

Nechyporchuk, O., Belgacem, M. N., & Pignon, F. (2015). Concentration effect of TEMPO-oxidized nanofibrillated cellulose aqueous suspensions on the flow instabilities and small-angle X-ray scattering structural characterization. *Cellulose,* 22(4), 2197-2210.

Nechyporchuk, O., Belgacem, M. N., & Pignon, F. d. r. (2016). Current progress in rheology of cellulose nanofibril suspensions. *Biomacromolecules,* 17(7), 2311-2320.

Nsor-Atindana, J., Goff, H. D., Liu, W., Chen, M., & Zhong, F. (2018). The resilience of nanocrystalline cellulose viscosity to simulated digestive processes and its influence on glucose diffusion. *Carbohydrate polymers*, *200*, 436-445.

Ou, S., Kwok, K.-c., Li, Y., & Fu, L. (2001). In vitro study of possible role of dietary fiber in lowering postprandial serum glucose. *Journal of Agricultural & Food Chemistry,* 49(2), 1026-1029.

Pasquier, B., Armand, M., Castelain, C., Guillon, F., Borel, P., LAFONT, H., & LAIRON, D. (1996). Emulsification and lipolysis of triacylglycerols are altered by viscous soluble dietary fibres in acidic gastric medium in vitro. *Biochemical Journal,* 314(1), 269-275.

Pasquier, B., Armand, M., Guillon, F., Castelain, C., Borel, P., Barry, J.-L., . . . Lairon, D. (1996). Viscous soluble dietary fibers alter emulsification and lipolysis of triacylglycerols in duodenal medium in vitro. *Journal of Nutritional Biochemistry,* 7(5), 293-302.

Peng, Y., Gardner, D. J., Han, Y., Cai, Z., & Tshabalala, M. A. (2013). Influence of drying method on the surface energy of cellulose nanofibrils determined by inverse gas chromatography. *Journal of colloid and interface science,* 405, 85-95.

Plait, S. R., & Clydesdale, F. M. (1987). Mineral binding characteristics of lignin, guar gum, cellulose, pectin and neutral detergent fiber under simulated duodenal pH conditions. *Journal of food science,* 52(5), 1414-1419.

Qi, J., Li, Y., Masamba, K. G., Shoemaker, C. F., Zhong, F., Majeed, H., & Ma, J. (2016). The effect of chemical treatment on the in vitro hypoglycemic properties of rice bran insoluble dietary fiber. *Food Hydrocolloids,* 52, 699-706.

Raymond, T. L., Connor, W. E., Lin, D. S., Warner, S., Fry, M. M., & Connor, S. L. (1977). The interaction of dietary fibers and cholesterol upon the plasma lipids and lipoproteins, sterol balance, and bowel function in human subjects. *The Journal of clinical investigation,* 60(6), 1429-1437.

Rodríguez-Gutiérrez, G., Rubio-Senent, F. t., Lama-Muñoz, A., García, A. n., & Fernández-Bolaños, J. (2014). Properties of lignin, cellulose, and hemicelluloses isolated from olive cake and olive stones: Binding of water, oil, bile acids, and glucose. *Journal of Agricultural & Food Chemistry,* 62(36), 8973-8981.

Roman, M. (2015). Toxicity of cellulose nanocrystals: a review. *Industrial Biotechnology,* 11(1), 25-33.

Rossander, L., Sandberg, A.-S., & Sandström, B. (1992). *The influence of dietary fibre on mineral absorption and utilisation*. In *Dietary fibre—a component of food* (pp. 197-216): Springer

Saarikoski, E., Saarinen, T., Salmela, J., & Seppälä, J. (2012). Flocculated flow of microfibrillated cellulose water suspensions: an imaging approach for characterisation of rheological behaviour. *Cellulose,* 19(3), 647-659.

Saarinen, T., Lille, M., & Seppälä, J. (2009). Technical aspects on rheological characterization of microfibrillar cellulose water suspensions. *Annu Trans Nord Rheol Soc,* 17, 121-128.

Saito, Y. (1992). Effects of Dietary Fiber and Protein Levels on Protein Digestion by Rats. *Nippon Nogeikagaku Kaishi,* 66, 1481-1481.

Sarkar, A., Li, H., Cray, D., & Boxall, S. (2018). Composite whey protein–cellulose nanocrystals at oil-water interface: Towards delaying lipid digestion. *Food Hydrocolloids,* 77, 436-444.

Sarkar, A., Zhang, S., Murray, B., Russell, J. A., & Boxal, S. (2017). Modulating in vitro gastric digestion of emulsions using composite whey protein-cellulose nanocrystal interfaces. *Colloids & Surfaces B: Biointerfaces,* 158, 137-146.

Schneeman, B. (1978). Effect of plant fiber on lipase, trypsin and chymotrypsin activity. *Journal of food science,* 43(2), 634-635.

Schneeman, B., Forman, L., & Gallaher, D. (1983). Pancreatic and intestinal enzyme activity in rats fed various fiber sources. *Proc. of Intl. Symp. On Dietary Fiber*: Royal Society of New Zealand Bulletin 20.

Schneeman, B. O., & Gallaher, D. (1980). Changes in small intestinal digestive enzyme activity and bile acids with dietary cellulose in rats. *The Journal of nutrition,* 110(3), 584-590.

Schneeman, B., & Gallaher, D. (2001). *Effects of dietary fiber on digestive enzymes*. In S. G. A. (Ed.), *CRC Handbook of dietary fiber in human nutrition*. United States: CRC press LLC

Schneeman, B. O. (1979). Acute pancreatic and biliary response to protein, cellulose, and pectin [rats]. *Nutrition Reports International*.

Schneeman, B. O. (1998). Dietary fiber and gastrointestinal function. *Nutrition Research,* 18(4), 625-632.

Schwartz, S. E., & Levine, G. D. (1980). Effects of dietary fiber on intestinal glucose absorption and glucose tolerance in rats. *Gastroenterology,* 79(5), 833-836.

Seabra, A. B., Bernardes, J. S., Fávaro, W. J., Paula, A. J., & Durán, N. (2017). Cellulose nanocrystals as carriers in medicine and their toxicities: A review. *Carbohydrate Polymers*.

Sehaqui, H., de Larraya, U. P., Liu, P., Pfenninger, N., Mathew, A. P., Zimmermann, T., & Tingaut, P. (2014). Enhancing adsorption of heavy metal ions onto biobased nanofibers from waste pulp residues for application in wastewater treatment. *Cellulose*, *21*(4), 2831-2844.

Serra, A., González, I., Oliver-Ortega, H., Tarrès, Q., Delgado-Aguilar, M., & Mutjé, P. (2017). Reducing the Amount of Catalyst in TEMPO-Oxidized Cellulose Nanofibers: Effect on Properties and Cost. *Polymers,* 9(11), 557.

Shafiei-Sabet, S., Hamad, W. Y., & Hatzikiriakos, S. G. (2012). Rheology of nanocrystalline cellulose aqueous suspensions. *Langmuir,* 28(49), 17124-17133.

Silk, D., Grimble, G., & Rees, R. (1985). Protein digestion and amino acid and peptide absorption. *Proceedings of the Nutrition Society,* 44(1), 63-72.

Silva, V. K., Morita, V. d. S., & Boleli, I. C. (2013). Effect of pectin extracted from citrus pulp on digesta characteristics and nutrient digestibility in broilers chickens. *Revista Brasileira de Zootecnia,* 42(8), 575-583.

Slavin, J. L., & Marlett, J. A. (1980). Effect of refined cellulose on apparent energy, fat and nitrogen digestibilities. *The Journal of nutrition,* 110(10), 2020-2026.

Southgate, D. A. T. (1982). *Digestion and absorption of nutrients*. In *Dietary Fiber in Health and Disease* (pp. 45-52). US: Springer

Staffolo, M. D., Bevilacqua, A. E., Rodríguez, M. S., & Albertengo, L. (2012). *Dietary fiber and availability of nutrients: a case study on yoghurt as a food model*. In *The complex world of polysaccharides*: InTech

Story, J. A., & Furumoto, E. J. (1990). *Dietary fiber and bile acid metabolism*. In *Dietary fiber* (pp. 365-374): Springer

Story, J. A., & Kritchevsky, D. (1976). Comparison of the binding of various bile acids and bile salts in vitro by several types of fiber. *The Journal of nutrition,* 106(9), 1292-1294.

Sun, X., Wu, Q., Zhang, X., Ren, S., Lei, T., Li, W., . . . Zhang, Q. (2018). Nanocellulose films with combined cellulose nanofibers and nanocrystals: tailored thermal, optical and mechanical properties. *Cellulose,* 25(2), 1103-1115.

Tade, R. S., More, M. P., Chatap, V. K., Patil, P. O., & Deshmukh, P. K. (2018). Fabrication and In vitro drug release characteristics of magnetic nanocellulose fiber composites for efficient delivery of nystatin. *Materials Research Express,* 5(11), 116102.

Tanaka, R., Saito, T., Hondo, H., & Isogai, A. (2015). Influence of flexibility and dimensions of nanocelluloses on the flow properties of their aqueous dispersions. *Biomacromolecules,* 16(7), 2127-2131.

Tejado, A., Alam, M. N., Antal, M., Yang, H., & van de Ven, T. G. (2012). Energy requirements for the disintegration of cellulose fibers into cellulose nanofibers. *Cellulose,* 19(3), 831-842.

Thompson, S., & Weber, C. (1979). Influence of pH on the binding of copper, zinc and iron in six fiber sources. *Journal of food science,* 44(3), 752-754.

Tiwari, U., & Cummins, E. (2011). *Functional and physicochemical properties of legume fibers*. In *Pulse Foods: Processing, Quality and Nutraceutical Applications* (pp. 121-156). London Burlington, MA: Academic Press

Trisat, K., Wong-on, M., Lapphanichayakool, P., Tiyaboonchai, W., & Limpeanchob, N. (2017). Vegetable Juices and Fibers Reduce Lipid Digestion or Absorption by Inhibiting Pancreatic Lipase, Cholesterol Solubility and Bile Acid Binding. *International Journal of Vegetable Science,* 23(3), 260-269.

Trovatti, E., Silva, N. H., Duarte, I. F., Rosado, C. F., Almeida, I. F., Costa, P., . . . Neto, C. P. (2011). Biocellulose membranes as supports for dermal release of lidocaine. *Biomacromolecules,* 12(11), 4162-4168.

Vahouny, G., Satchithanandam, S., Chen, I., Tepper, S., Kritchevsky, D., Lightfoot, F., & Cassidy, M. (1988). Dietary fiber and intestinal adaptation: effects on lipid absorption and lymphatic transport in the rat. *The American journal of clinical nutrition,* 47(2), 201-206.

Vahouny, G. V., Tombes, R., Cassidy, M. M., Kritchevsky, D., & Gallo, L. L. (1980). Dietary fibers: V. Binding of bile salts, phospholipids and cholesterol from mixed micelles by bile acid sequestrants and dietary fibers. *Lipids,* 15(12), 1012-1018.

Venema, K., Minekus, M., & Havenaar, R. (2004). *Advanced in vitro models of the gastrointestinal tract—novel tools to study functionality of dietary fibres*. In N.-G. A. J.W. van der Kamp, J. Miller Jones and G. Schaafsma (Ed.), *Dietary Fibre: Bio-active Carbohydrates for Food and Feed* (pp. 99-112): Wageningen Academic Publishers

Warren, F. J., Zhang, B., Waltzer, G., Gidley, M. J., & Dhital, S. (2015). The interplay of α-amylase and amyloglucosidase activities on the digestion of starch in in vitro enzymic systems. *Carbohydrate Polymers,* 117, 192-200.

Weber, C. W., Kohlhepp, E. A., Idouraine, A., & Ochoa, L. J. (1993). Binding capacity of 18 fiber sources for calcium. *Journal of agricultural food chemistry,* 41(11), 1931-1935.

Wilcox, M. D., Brownlee, I. A., Richardson, J. C., Dettmar, P. W., & Pearson, J. P. (2014). The modulation of pancreatic lipase activity by alginates. *Food Chemistry,* 146, 479-484.

Winuprasith, T., & Suphantharika, M. (2013). Microfibrillated cellulose from mangosteen (Garcinia mangostana L.) rind: Preparation, characterization, and evaluation as an emulsion stabilizer. *Food Hydrocolloids,* 32(2), 383-394.

Wolever, T. (1990). Relationship between dietary fiber content and composition in foods and the glycemic index. *The American journal of clinical nutrition,* 51(1), 72-75.

Wood, P. J., Braaten, J. T., Scott, F. W., Riedel, K. D., Wolynetz, M. S., & Collins, M. W. (1994). Effect of dose and modification of viscous properties of oat gum on plasma glucose and insulin following an oral glucose load. *British Journal of Nutrition,* 72(5), 731-743.

Xu, X., Liu, F., Jiang, L., Zhu, J., Haagenson, D., & Wiesenborn, D. P. (2013). Cellulose nanocrystals vs. cellulose nanofibrils: a comparative study on their microstructures and effects as polymer reinforcing agents. *ACS applied materials & interfaces,* 5(8), 2999-3009.

Xu, Y., Atrens, A. D., & Stokes, J. R. (2017). Rheology and microstructure of aqueous suspensions of nanocrystalline cellulose rods. *Journal of colloid & interface science,* 496, 130-140.

Zhai, H., Gunness, P., & Gidley, M. J. (2016). Effects of cereal soluble dietary fibres on hydrolysis of p-nitrophenyl laurate by pancreatin. *Food & function,* 7(8), 3382-3389.

Zhang, S., Zhang, Z., & Vardhanabhuti, B. (2014). Effect of charge density of polysaccharides on self-assembled intragastric gelation of whey protein/polysaccharide under simulated gastric conditions. *Food & function,* 5(8), 1829-1838.

Zhang, R., Zhang, Z., Zhang, H., Decker, E. A., & McClements, D. J. (2015). Influence of emulsifier type on gastrointestinal fate of oil-in-water emulsions containing anionic dietary fiber (pectin). *Food Hydrocolloids,* 45, 175-185.

Zhang, S., & Vardhanabhuti, B. (2014). Intragastric gelation of whey protein–pectin alters the digestibility of whey protein during in vitro pepsin digestion. *Food & function,* 5(1), 102-110.

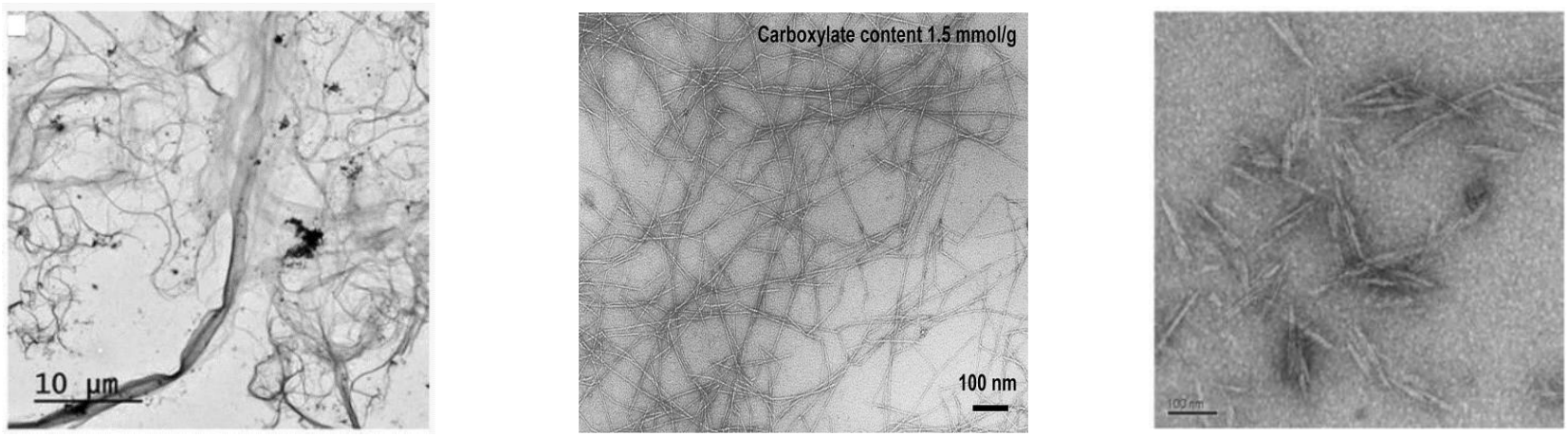


Fig 2.1 TEM images of (a) nano-fibrillated cellulose (NFC/CNF) (Figure is adapted from Mousavi, Afra, Tajvidi, Bousfield, & Dehghani-Firouzabadi (2017) with permission from Springer Nature); (b) TEMPO (2,2,6,6-tetramethylpiperidine-1-oxyl radical) oxidized CNF (TEMPO-CNF) (Figure is reproduced from Isogai, Saito, & Fukuzumi (2011) with permission from RSC Pub) and (c) nano-crystalline cellulose (NCC/CNC) (Figure is reproduced from Peng, Gardner, Han, Cai, & Tshabalala (2013) with permission from Elsevier).

Table 2.1 Effects of nanocellulose and cellulose on digestive enzyme activities

| Fiber | Fiber concentration (w/w) | Test | α-amylase | α-glucosidase/ glucoamylase | Lipase | Trypsin | Chymotrypsin | Pepsin | Reaction conditions | Reference |
|---|---|---|---|---|---|---|---|---|---|---|
| Solka Floc (85-99.5% cellulose and up to 15% hemicellulose) | 5% | *In vitro* | | | ↓ (90%) | ↓ (12%) | ↓ (22%) | | 37° C for 5 min, then filtered | Schneeman, 1978 |
| Solka-Floc | 20% | *In vivo* | ↓ (25%~50%) | | ↓ (< 10%) | ↓ (25%~50%) | ↓ (25%~50%) | | | Schneeman and Gallaher, 1980 |
| Solka-Floc | 5% | *In vitro* | ↓ (79.6%) | | ↓ (95.4%) | ↓ (44.7%) | ↓ (47.1%) | | 37° C for 5 min, and then centrifuged at 3000 *g* for 10 min at 0°C | Dunaif and Schneeman, 1981 |
| Cellulose (99%) | 1% | *In vitro* | ↓ (21%) | | ↑ | ↓ (9%) | ↓ (43%) | ↓ (19%) | 37° C for 10 min | Ikeda and Kusano, 1983 |
| Purified cellulose (99.5%) | 1.50% | *In vitro* | No reduction | | ↓ (< 10%) | No reduction | | | 37° C for 60 min at 150 rpm, then centrifuged at 1000 *g* for 10 min; for trypsin, filtration and | Dutta and Hlasko,1985 |

| | | | | | | | |
|---|---|---|---|---|---|---|---|
| | | | | | | second wash applied | |
| Alpha-cellulose | cellulose/starch 5:1 | *In vitro* | ↓(~48%) | | | 37 ◦C, 350 rpm stirring, 5 hr | Dhital, Gidley and Warren, 2015 |
| Nano-crystalline cellulose (CNC) | 0.28% | *In vitro* | ↓(~28%) | ↓(10~15%, glucoamylase) | | Mixing CNC and starch prior to the gelatinization process, 10 min at 40 °C, no centrifugation afterwards | Ji et al., 2018 |

Note: "↓" represents decrease.

Table 2.2 Effects of nanocellulose and cellulose on nutrient absorption and fecal microflora

| Nanocellulose/Cellulose dose | Test | Glucose | Cholesterol, phospholipid and bile acid | Protein digestibility | Minerals | Fecal microflora | Reference |
|---|---|---|---|---|---|---|---|
| Cellulose | *In vitro* | | No effect (bile acid) | | | | Story and Kritchevsky, 1976 |
| Cellulose (8 mg/mL) | *In vitro* | | 4.7%~7.5% cholesterol, 0.5%~1.3% phsopholipid and 1.4%~3.5% bile acid Binding | | | | Vahouny et al., 1980 |
| Cellulose | *In vitro* | | | | 480 µg/g calcium binding (the lowest) | | Weber et al., 1993 |
| Cellulose | *In vitro* | 19 mmol/g Binding | | | | | Chau et al., 2003 |
| Cellulose | *In vitro* | | Very poor binding in cholesterol and bile acid | | | | Hu & Yu, 2013 |
| Nano-fibrillated cellulose (7%~21%) | *In vivo* (Rat) | No effect | No effect | | No effect | | Andrade et al., 2015 |
| Cellulose | *In vivo* (Rat) | | ↓ (serum cholesterol) | | | | Vahouny et al., 1988 |

| | | | | | | |
|---|---|---|---|---|---|---|
| Cellulose (20%) | *In vivo* (Rat) | | | ↓ | | Hove & King, 1979 |
| Cellulose (30%) | *In vivo* (Rat) | | | No effect | | Eggum, 1973 |
| Cellulose | *In vivo* (Rat) | ↓ | | | | Schwartz and Levine, 1980 |
| Cellulose (5%) | *In vivo* (Hamsters) | | ↓(17%)* (serum cholesterol) | | | Chau et al., 2004 |
| Cellulose (10%) | *In vivo* (Chicken) | | | ↓ (*) in nitrogen utilization | ↑ (*) | Cao et al., 2003 |
| Cellulose | *In vivo* (Male) | | No effect (serum cholesterol) | | | Kritchevsky, 1987 |
| Cellulose (10 or 30 g/d) | *In vivo* (Human) | | | No effect | | Mickelsen et al., 1979; Slavin & Marlett, 1980 |
| Cellulose (10~21 g/d) | *In vivo* (Human) | | | | ↓ | Ismail-Beigi et al., 1977 |
| Cellulose | *In vivo* (Human) | | No effect on serum cholesterol, but slightly increase in feces | | | Keys, Grande and Anderson, 1961 |

Note: "↓" represents decrease, while * represents significantly.

Table 2.3 Effects of nanocellulose and dietary fiber on protein *in vitro* digestion

| Fiber | Fiber characteristics | Fiber level (w/w) | Substrate | Effect on protein digestibility | Mechanism | Reference |
|---|---|---|---|---|---|---|
| Gum ghatti | Highly branched with low (3%) glucuronic acid residues | Fiber/casein ratio 0~1 | Casein | Inhibit | Matrix restriction | Acton, Breyer, & Satterlee, 1982 |
| Pectin | Slightly branched galacturonic acid-containing polysaccharide | Fiber/casein ratio 0~1 | Casein | Substantially inhibit | Ionic interferences (negatively charged acidic residues (in pH 6-8 range) of pectin interfere/complex with enzyme/substrate) | Acton, Breyer, & Satterlee, 1982 |
| Holocellulose (containing cellulose and semi-cellulose) | | Fiber/casein ratio 0~1 | Casein | Slightly inhibit | | Acton, Breyer, & Satterlee, 1982 |
| Guar and locust bean gum | Neutral and predominant linear galactomannans | Fiber/casein ratio 0~1 | Casein | Negligible | | Acton, Breyer, & Satterlee, 1982 |
| Lignin | Hydrophobic and rich in aromatic units | Fiber to protein ratio 0.96:1 | Casein | Significantly inhibit (5%) | | Acton, Breyer, & Satterlee, 1982 |
| Gum arabic | Polyanionic with pIs of around 3, | 10% | peanut protein isolate (PPI) | Significant reduction of N diffusion at a MWCO of 1 KDa | Interaction with some proteins and high MW peptides | Mouécoucou, Villaume, Sanchez, & Méjean, 2004 |

| | | | | | | |
|---|---|---|---|---|---|---|
| | composing of uronic acids | | | but not with a MWCO of 8 KDa | | |
| Xylan | A low MW linear oligomer composed of xylose | 20% | PPI | Significant reduction of N diffusion at a MWCO of 1 KDa but not with a MWCO of 8 Kda | Interaction with some proteins and high MW peptides | Mouécoucou, Villaume, Sanchez, & Méjean, 2004 |
| Low methoxy pectin | Polyanionic with pIs of around 3, composing of uronic acids | 10%~50% | PPI | Did not reduce protein hydrolysis but significant reduction of N diffusion with a MWCO of 1 KDa (at 10%LM pectin) or 8 KDa (at 50% LM pectin) | Interaction with low MW peptides and amino acids | Mouécoucou, Villaume, Sanchez, & Méjean, 2004 |
| Guar gum | Neutral charge | 2% or lower | whey protein isolate (WPI) | No effect | | Zhang, Zhang, & Vardhanabhuti, 2014 |
| Xanthan gum and carrageenan | Medium negative and highly negative charge with carboxyl groups, respectively | | WPI | No effect at 2% or lower fiber concentration, but significantly reduced protein digestion rate at fiber concentration higher than 2% | Intragastric gelation due to the cross-linking between oppositely charged protein and polysaccharides | Zhang, Zhang, & Vardhanabhuti, 2014 |

| | | | | | | |
|---|---|---|---|---|---|---|
| Konjac glucomannan (KGM) | Uncharged | 0.50% | Milk, whey proteins and calcium caseinate (10%) | Slight effect on the proteolysis patterns | KGM is uncharged and the aggregate formed between protein and KGM could be easily dissociated during gastric digestion | Borreani, Llorca, Larrea, & Hernando, 2016 |
| Alginate | Negatively charged | 0.55% | Milk, whey proteins and calcium caseinate (10%) | Significantly slowed down protein digestion rate with less digestion products observed | Cluster formation between alginate and protein which could not be dissociated during gastric digestion | Borreani, Llorca, Larrea, & Hernando, 2016 |
| Nano-crystalline cellulose (CNC) | Negatively charged | 1~3% | WPI (1%) | Reduced protein digestion (60% intact interfacial protein remained after gastric digestion) | Electrostatic attraction between CNC and WPI at pH 3 as well as increased viscosity | Sarkar et al., 2017 |

Table 2.4 Effects of dietary fiber on protein *in vivo* digestion

| Subject | Fiber type | Fiber level (w/w) | Effects on protein digestibility or nitrogen utilization | Reference |
|---|---|---|---|---|
| Weanling rats | Soluble and insoluble fiber from dry beans (Phaseolus vulgaris) | Varied (0.5%~14%) | Soluble dietary fiber (DF) significantly increased fecal nitrogen losses and reduced protein digestibility, while insoluble DF had no effect on either fecal nitrogen loss or protein digestibility | Hughes, Acevedo, Bressani, & Swanson, 1996 |
| Rats | Guar gum (GG) or cellulose | 4%~20% cellulose and 5% guar gum | At a diet containing 18% casein, 5% GG or 20% cellulose caused significantly lower apparent protein digestibility; but at a 40% casein diet, little effects shown by fiber | Saito, 1992 |
| Chicken (2-month old male) | Cellulose | 0, 3.5% and 10% in diets with isolated soybean protein and amino acids | 10% cellulose addition showed lower body weight gain and nitrogen utilization and retention time of the diet in the digestive tract, but higher total microflora counts in the caecal contents | Cao et al., 2003 |
| Weanling mice | Cellulose | 5, 10 or 15% in a semi-purified casein basal diet | Decreased protein efficiency, nitrogen (N) balance, and apparent protein digestibility, but increased faecal N excretion | Keim & Kies, 1979 |
| Weanling mice | Hemicellulose and lignin | 5, 10 or 15% in a semi-purified casein basal diet | Decreased protein efficiency, N balance, and apparent protein digestibility, but increased Urinary N and faecal N excretion | Keim & Kies, 1979 |
| Weanling mice | Cellulose | 0~20% | Decreased apparent protein digestibility, but no effect on the biological value of the protein | Hove & King, 1979 |
| Young women (n=7) | Cellulose | 10g cellulose/day to the diet | No effect on apparent digestibility of protein | Slavin & Marlett, 1980 |
| College males | Cellulose | 30.2g cellulose/day to the diets | No effect on faecal N output | Mickelsen et al., 1979 |
| Rats | Gum guar, carob bean gum and sodium alginate | 10% | Apparent protein digestibility was significantly decreased; urinary N excretion was reduced, thus compensating for increased fecal N losses by these animals | Harmuth-Hoene & Schwerdtfeger, 1979 |

| | | | | |
|---|---|---|---|---|
| Rats | Agar-agar | 10% | Apparent protein digestibility was significantly decreased; N retention was significantly lower | Harmuth-Hoene & Schwerdtfeger, 1979 |
| Rats | Carrageenan | 10% | Apparent protein digestibility was significantly decreased; N retention was significantly lower; inhibited trypsin activity | Harmuth-Hoene & Schwerdtfeger, 1979 |

# CHAPTER 3

# INFLUENCE OF NANOCELLULOSE ON STARCH DIGESTION AND GLUCOSE ABSORPTION[1]

[1] Liu, L., Kerr, W. L., Kong, F., Dee, D. R., & Lin, M. (2018). Influence of nano-fibrillated cellulose (NFC) on starch digestion and glucose absorption. *Carbohydrate polymers*, *196*, 146-153. Adapted here with permission of the publisher.

**Abstract**

Nano-cellulose (NC) is of interest in several fields due to its unique physical properties derived from its nanoscale dimensions. NC has potential use in food systems as a dietary fiber that increases viscosity and limit diffusion flux of glucose. This study focused on the effects of added NC on solution viscosity, starch digestion and glucose adsorption. Three types of nanocellulose, namely nano-fibrilated cellulose (NFC, also called cellulose nano-fibrils (CNF)), TEMPO (2,2,6,6-tetramethylpiperidine-1-oxyl radical) oxidized cellulose nano-fibrils (TEMPO-CNF), and nano-crystalline cellulose (NCC, also called cellulose nano-crystals (CNC)), were studied. Results showed that CNF did not affect α-amylase and α-glucosidase activity, but significantly retarded glucose diffusion flux, delayed amylolysis and reduced the amount of glucose released during *in vitro* digestion of starch. Specifically, 1% (w/w) CNF retarded ~ 26.6% of glucose released during the amylolysis process. The greatly increased viscosity of CNF at concentrations > 0.5% was thought to be the main mechanism for its potential hypoglycemic effects. CNF suspensions also had higher glucose adsorption capacity than those containing cellulose. In addition, CNF bound 35.6% of the glucose when the initial glucose level was within the range of 5–200 mM. TEMPO-CNF or CNC did not show any significant effects on the amount of glucose release, but both anionic NC at high concentrations caused significant reductions in the amount of glucose diffusion flux, especially at 0.36% TEMPO-CNF and 2~4% CNC. These results suggest that NC may be useful for building viscosity in food products and serving to inhibit glucose absorption *in vivo* in starch-containing products.

**Keywords:** Nano-fibrillated cellulose; cellulose; *in vitro* digestion; glucose diffusion; viscosity

## 3.1 Introduction

Dietary fiber can provide many health benefits including reducing the risk of hypertension, cancer, stroke, obesity, coronary heart disease, certain gastrointestinal diseases, and diabetes. Among the beneficial effects of dietary fiber, its capability in lowering plasma glucose levels and thus the risks of type 2 diabetes is one of the most intriguing aspects (Nichols, Hillier, & Brown, 2008). Several studies have shown the ability of soluble and insoluble dietary fiber to retard starch digestion and glucose absorption (Fabek, Messerschmidt, Brulport, & Goff, 2014; Qi et al., 2016). Three main mechanisms have been elucidated for this phenomenon (Chau, Huang, & Lee, 2003; Ou, Kwok, Li, & Fu, 2001). First, soluble and insoluble fibers increase the viscosity of liquids in the digestive system and thus retard the diffusion of glucose in the intestinal lumen. Second, glucose molecules may bind with the large molecules in dietary fiber that hinders movement and transport of glucose in the intestine. Finally, dietary fiber may inhibit the activity of α-amylase enzymes that convert starch to glucose.

Nano-cellulose (NC), as the name suggests, is a cellulosic material composed of nano-sized fibrils/crystals. It has high aspect (length to width) ratios with longitudinal dimensions ranging anywhere between tens of nanometers to several micrometers and lateral dimensions in the range of 5–20 nm. NC has a variety of unique properties when compared to other food fiber sources (Jorfi & Foster, 2015). It forms relatively viscous solutions at low concentrations and can form gels under the right conditions. Suspensions of NC are biodegradable and have no cytotoxic effects. Incorporation of NC in materials can increase tensile strength and thermal stability. However, little research has been done with regards to potential metabolic effects when NC is used as a dietary fiber source in the human diet.

Although considered as an insoluble fiber, NC differs from cellulose in that it forms higher viscosity solutions and can also form gels. Thus, it is of interest to investigate whether NC solutions have unique properties that influence starch digestion and glucose absorption. The aim of this study was to determine if NC can limit the production or absorption of glucose in an *in vitro* model of the human digestion system, and to investigate the mechanisms behind any such activity. More specifically, this research examined the effects of CNF on α-amylase and α-glucosidase activity, glucose diffusion, glucose adsorption capacity, and the effects of three types of NC on *in vitro* digestion of starch. To our knowledge, this is the first systematic study on the potential hypoglycemic effects of NC via *in vitro* studies. As NC is derived from the same sources as cellulose and its derivatives that are more commonly used in foods, the same analyses were done on cellulose. These results are meaningful for the potential development and application of NC into food products.

## 3.2 Materials and methods

### 3.2.1. Materials

Nanofibrillated cellulose (3% (w/w)) was obtained from the Process Development Center at the University of Maine (Orono, ME). CNF was produced from bleached softwood kraft pulp via an ultrafine grinder (Masuko MKZB15-50J supermass colloider) which creates a high shear zone to liberate nanocellulose. CNF produced has a nominal width of 50 nm and length of up to several hundred microns. Samples of TEMPO-based cellulose nano-fibrils (1.1 wt% in water, 1.5 mmol-COONa/g dry CNF) and cellulose nanocrystals (10.8 wt% in water, 0.94 wt% sulfur on dry CNC, sodium form) were both obtained from the USDA's Forest Products Laboratory. The nominal sizes of TEMPO-CNF and CNC materials were: TEMPO-CNF (~ 20 nm width and length up to 2 μm); CNC (~ 5 nm width and 150 nm length). Argo corn starch (100% pure) was purchased

from a local market while all other materials used were purchased from Sigma-Aldrich Chemical Co. (St. Louis, MO) or Fisher Scientific (Pittsburgh, PA).

3.2.2. Effect of fiber on α-amylase and α-glucosidase activity

The effects of fiber on the activity of α-amylase was determined according to Dhital, Gidley, and Warren (2015) with modifications. Specifically, porcine pancreatic α-amylase (A3176, Sigma) was dis-solved in 100 mM of sodium phosphate buffer (PBS) containing 6.7 mM sodium chloride (pH 6.9). Gelatinized corn starch of 7.5% (w/v) was prepared by dissolving corn starch in PBS in an Erlenmeyer flask and boiling it for 5 min with continuous stirring to ensure homogeneity, followed by cooling at room temperature with continuous stirring as well. *In vitro* hydrolysis was carried out in a total reaction volume of 100 mL, with 0.02 unit α-amylase per mg of corn starch in the presence of 0, 0.01%, 0.1%, 0.4% and 1% (w/w) CNF at 37 °C in a shaking water bath (Model 290400S, Boekel Scientific, USA) at 100 rpm. In a similar experiment, 2% cellulose (C6288, Sigma) was studied in comparison. Aliquots of 1 mL were taken at time intervals (2.5–240 min) and 0.5 mL 0.3 M $Na_2CO_3$ was added to terminate the reaction. This was followed by centrifugation at 5000g for 2 min (AccuSpin Micro 17, ThermoFisher Scientific, Germany) to remove any suspended materials. The amount of reducing sugar in the supernatant was analyzed by a dinitrosalicylic acid (DNS) assay (Sigma-Aldrich, 2017) with glucose as a standard, and results were reported as amount of glucose equivalent produced in μmol.

A modified version of the method by Flores, Singh, Kerr, Pegg, and Kong (2013) was used to determine the effects of CNF and cellulose on α-glucosidase activity. In the original method, type I α-glucosidase from Saccharomyces cerevisiae (G5003, Sigma) was used with a substrate of p-nitrophenyl-α-D-glucopyranoside (pNPG) dissolved in 100 mM PBS (pH 6.9). In the revised method, the reaction was performed in a total volume of 10 mL, with 0.23 unit α-glucosidase per

mmol of pNPG in the presence of 0, 0.01%, 0.1%, 0.4% and 1% (w/w) CNF at 37 °C while shaking at 100 rpm. Aliquots of 100 μL were taken at time intervals (5–300 min), with 400 μL 1 M $Na_2CO_3$ added to terminate the reaction, followed by centrifugation at 5000g for 2 min. The product concentration in the supernatant was determined by the absorbance reading at 400 nm. A similar experiment was conducted with the addition of 2% cellulose as a comparison.

3.2.3. Effect of fiber on glucose diffusion

A modified form of the method of Ou et al. (2001) was used to study the effects of CNF and cellulose fiber on glucose diffusion. In a total volume of 25 mL, 100 mM glucose in the presence of 0, 0.01%, 0.1%, 0.5%, 1% and 2% (w/w) CNF was dialyzed in tubing with a cutoff molecular weight (MWCO) of 12,000–14,000 Da (Spectra/Por 4 RC Dialysis Membrane Tubing, Spectrum Medical Industries, Inc.) against 200 mL of deionized water at 37 °C. Tests with shaking at 100 rpm were conducted as well as tests without shaking. The glucose content in the dialysate was determined by using the K-GLUHK glucose assay kit (Megazyme International Ireland, Bray, Ireland). Glucose diffusion into the dialysate was measured as:

$$\%\ Glucose = 100\ \frac{Glucose\ in\ the\ dialysate}{Original\ glucose\ level} \quad (1)$$

Glucose dialysis retardation index (GDRI) of fiber was also calculated by:

$$GDRI = 100\ (1 - \frac{Glucose\ content\ with\ fiber\ addition}{Glucose\ content\ of\ control}) \quad (2)$$

3.2.4. Rheological measurements of fiber solutions

The viscosity of suspensions containing CNF, cellulose and glucose were measured using a Discovery HR-2 rheometer (TA instruments, Newcastle, DE) equipped with a 4-blade rotor vane 42 mm in length and 28 mm in diameter. Viscous properties of the fluid samples were measured at 37 °C using a flow ramp test over a shear rate range of 1–100 $s^{-1}$. The rate was increased over a 180 s period with a sampling interval of 1 s/pt. The viscosity of intestinal digesta containing

TEMPO-CNF or CNC was determined under similar conditions as described above, with exception that a pre-shear at 40 $s^{-1}$ for 2 min. was performed before the flow ramp test.

3.2.5. Glucose adsorption capacity of fiber

The glucose adsorption capacity of the CNF or cellulose fibers was determined utilizing a modified version of the Ou et al. (2001) method. Specifically, the equivalent of 1 g CNF or cellulose (d.b.) was mixed well with 100 mL of glucose solution (5–200 mM) and incubated at 37 °C for 6 h, followed by centrifugation at 4000g for 20 min. The glucose con-tent in the supernatant was measured using the glucose assay kit and the amount of glucose adsorbed on the fiber sample was calculated as:

$$\text{Glucose adsorbed} = \frac{C_0 \times V_0 - C_1 \times V_1}{m} \quad (3)$$

where $C_o$ is the original glucose content (mM), $C_1$ is the glucose con-centration in the supernatant (mM), $V_o$ is the original volume (mL), $V_1$ is the supernatant volume (mL), and m is the fiber mass (g).

3.2.6. Effect of fiber on *in vitro* amylolysis kinetics

The effects of CNF or cellulose fibers on α-amylase activity were determined according to Ou et al. (2001) with modifications. Up to 7.5% (w/v) gelatinized corn starch and α-amylase solutions were pre-pared as previously described. The starch-α-amylase-fiber system was comprised of 1% corn starch, 0.4% α-amylase, and specific concentrations of CNF (0, 0.01%, 0.1%, 0.4%, 1% and 2% (w/w)) and buffer. Cellulose with a concentration of 2% (w/w) was studied in a similar experiment as a comparison. The mixture with a volume of 25 mL was dialyzed in tubing against 200 mL of DI water at 37 °C in a shaking water bath with a speed of 100 rpm. Aliquots of 1 mL were taken from the dialysate at time intervals (10–300 min). The amount of glucose equivalent in the dialysate was measured by the DNS assay.

3.2.7. Effect of fiber on the *in vitro* digestion of starch

*In vitro* digestion of starch with and without the presence of fiber was studied using a modified version of the method of Flores, Singh, Kerr, Pegg, and Kong (2014). Specifically, 25 mL of 0.6% (w/w) or 3% (w/w) fiber (cellulose or CNF) solution was added to 5 g of 5% (w/v) corn starch and mixed well before the experiment. A control test was also conducted without the addition of fiber. The digestion trial was carried out in a shaking water bath (100 rpm, 37 °C) via salivary digestion (5 min, pH 6.8 ± 0.2), gastric digestion (2 h, pH 3.0 ± 0.1) and intestinal digestion (2 h, pH 7.0 ± 0.1). To study the effects of fiber on starch digestion and glucose absorption separately, the *in vitro* digestion was conducted both with and without dialysis tubing. In the former, intestinal digestion was performed by placing digesta inside dialysis tubing against 0.1 M PBS (pH 7.4) (inside and outside volume ratio of 1:6.25). Aliquots (200 μL) were collected followed by the inactivation of enzymes at 95 °C for 5 min. Subsequently, the samples were centrifuged at 6000g for 5 min after which the amount of glucose in the supernatant was determined by the glucose assay kit. During the intestinal digestion phase, the final concentrations after addition of 0.6% (w/w) and 3% (w/w) fiber (CNF/cellulose) solution resulted in 0.22% (w/w) and 1.1% (w/w) fiber solution respectively. Thus results were reported as the amount of glucose produced at 0.22% or 1.1% (w/w) fiber addition.

*In vitro* digestion of starch with and without the presence of TEMPO-CNF or CNC was studied using similar procedures as above. The initial 25 mL of fiber solution contained several concentrations of TEMPO-CNF (0.13%, 0.26% and 0.95% (w/w)) or CNC (0.26%, 2.64%, 5.28% and 10.56% (w/w)). A control experiment was also performed without the addition of fiber. During the digestion experiment with dialysis, the digesta was placed inside dialysis tubing against 0.1 M PBS (pH 7.4) (inside and outside volume ratio of 1:12.5). For digesta containing TEMPO-CNF,

300 µl aliquots were taken at time intervals and 150 µl 0.3 M sodium carbonate ($Na_2CO_3$) was added to terminate the reaction. For digesta containing CNC, 300 µl aliquots were taken followed by inactivation of enzyme at 95 °C for 5 min. The sample aliquots were then centrifuged and analyzed as above. At the intestinal phase, the final fiber concentrations were TEMPO-CNF (0.05%, 0.1% and 0.36% (w/w)) or CNC (0.1%, 1%, 2% and 4% (w/w)). Results were reported as the amount of glucose produced at these final nanocellulose concentrations.

3.2.8. Data analysis

All measurements were done in triplicate and the results analyzed by Duncan's multiple comparison tests using the SAS/STAT statistical software (SAS Institute Inc., Cary, NC) with $p = 0.05$. All the fittings in the graphs were performed by Origin data analysis and graphing software.

**3.3 Results and discussion**

3.3.1. Effect of fiber on the activity of α-amylase and α-glucosidase

Fig 3.1(a) shows that glucose equivalent was produced steadily from the starch and reached a steady value over the 240 min period. In most cases, glucose equivalent levels were no different in the CNF or control solutions, with the exception that glucose equivalent levels were slightly lower in samples containing 0.4% (w/w) CNF. In any event, the effect of CNF on α-amylase activity may be considered negligible. Furthermore, glucose equivalent production in samples containing 2% cellulose was no different than that in the control.

The effects of dietary fiber on α-amylase and other enzymes have been widely studied. However, results have varied depending on the fiber sources, concentration, purity and test conditions. For example, rats fed a diet including 20 wt% of purified cellulose (Solka-Floc) had greater total weight in the intestinal contents and decreased enzyme activity (including α-amylase) when compared to the control (Schneeman & Gallaher, 1980). In an *in vitro* study, Dunaif and

Schneeman (1981) found that 5% Solka-Floc inhibited 79.6% of α-amylase activity. However, *in vitro* studies by Dutta and Hlasko (1985) showed that addition of 1.5% purified cellulose produced no changes in α-amylase activity.

Alpha-amylase is found primarily in saliva and pancreatic juice and hydrolyzes starch into maltose and other dextrins. In contrast, α-glucosidase resides mostly in the small intestine and hydrolyzes the end-groups of starch to produce glucose. As the mechanisms of these enzymes are different, studies were also conducted on the activity of α-glucosidase in the presence of CNF or cellulose (Fig 3.1b). As found with α-amylase, the activity of α-glucosidase was no different when CNF was added than in the control. However, when 2% (w/w) cellulose was present there was a slight but significant ($p < 0.05$) reduction in glucose equivalent production particularly during the initial 20–60 min.

Both α-amylase and α-glucosidase act upon α(1 → 4) bonds of carbohydrates, thus one might expect similar influence of fiber on their activities. While not observed here in our results, some studies have found that fiber may decrease digestive enzyme activity by presenting diffusional barriers to the contact of the enzyme with the substrate, while polar or ionic sites on the fiber may allow electrostatic interactions with the amphoteric part of enzymes (Amarowicz, Korczakowska, Smoczyńska, 1988; Hasik & Bartnikowska, 1987). The presence of inhibitors in the unpurified insoluble fiber may also be a reason for the decreased α-amylase activity in the presence of citrus peel (Chau et al., 2003) or rice bran (Qi et al., 2016) fiber.

Studies on enzyme activity (Fig 3.1) suggest that binding was not prevalent between α-amylase or α-glucosidase active sites and CNF or cellulose, or at least that any binding between the enzymes and fiber did not cause a change in enzymatic activity. The fact that neither CNF or cellulose produced significant effects on enzymatic activity may be due to the low surface charge,

or relatively low concentrations of the fibers tested. Both CNF and cellulose used in this study were un-modified, and thus expected to carry few charges in the many hydroxyl groups. Furthermore, the concentration of fiber tested in this study was limited (up to 1% (w/w) for CNF), and this may not have exerted a high enough viscosity to hinder the contact between α-amylase and starch. CNF at higher concentrations (up to 2% (w/w)) was also studied but it was too viscous for aliquots to be collected. It should also be noted that the mixing required by the chemical assays may negate any influence that fiber viscosity exerts on enzymatic activity. For example, Dhital, Dolan, Stokes, and Gidley (2014) studied the effects of various levels of shear mixing on enzymatic activity in the presence of cereal fibers. They found that higher mixing rates significantly increased the rate of amylolytic starch digestion and mass transfer of glucose. However, further studies are needed to determine if this phenomenon influences *in vivo* processes.

3.3.2. Effect of fiber on glucose diffusion

The effect of CNF and cellulose on glucose diffusion is shown in Fig 3.2, which shows that the amount of glucose diffusing into the dialysate was dependent upon both time and concentration. The percentage of glucose in the dialysate was approximately an exponential function of the dialysis time, with the greatest change in the first 60 min. These results are similar to those observed by Qi et al. (2016), who studied the effect of rice bran insoluble dietary fiber on glucose diffusion. After 300 min, a steady-state glucose level was reached in all samples for both this study and that of Qi et al. (2016). This is in agreement with Ou et al. (2001) who studied glucose diffusion in the presence of dietary fiber over 12 hr and reported that maximum glucose levels were reached after 300 min.

Fig 3.2(a) and (b) shows that the addition of higher concentrations of CNF resulted in reduced glucose diffusion. With the addition of 2% (w/w) cellulose or 0.01% (w/w) CNF, no

significant difference was observed in glucose diffusion as compared with that of the control either with or without applied shaking. The addition of 0.1% (w/w) CNF only resulted in a significant decrease when no shaking was applied. With a 0.5%–2% (w/w) CNF, however, significant differences in glucose diffusion were observed both with and without applied shaking.

The initial diffusion rate of glucose was calculated based on the slope of the linear region (0–60 min) of the curves from Fig 3.2(a) and (b). The initial diffusion rate of glucose (D) was found to be exponentially dependent on the CNF concentration (C):

$$D = D_0 + Ae^{R_0 C} \quad (4)$$

A plot of the initial glucose diffusion rate and CNF concentration is shown in Fig 3.2(c) and the fitting parameters are presented in Table 3.1. In general, greater CNF concentrations led to lower rates of diffusion. When the solutions were not stirred, rates with 0% (w/w) CNF were 19.3 μmol/min and reached a steady value of ~8 μmol/min at concentrations > 0.5% (w/w) CNF. When stirring was applied, diffusion rates diminished steadily from 22.4 μmol/min to 9.5 μmol/min as the concentration was increased from 0 to 2% (w/w) CNF. Similar trends have been observed by Srichamroen and Chavasit (2011), who found that increasing the con-centration of malva nut gum resulted in decreased glucose diffusion rates.

The glucose dialysis retardation index (GDRI), which has been used as an indicator of the retardation effect of fiber on glucose absorption in jejunum (Adiotomre, Eastwood, Edwards, & Brydon, 1990), was also calculated to compare the results with other studies (data not shown). Specifically, with addition of 2% (w/w) CNF, the maximum GDRI was 50% for both with and without shaking, which was higher than that of reported values for insoluble fiber-rich fractions (GDRI 22%–31.4%) prepared from citrus peel (Chau et al., 2003) or wheat bran (GDRI 29.2%; Ahmed, Sairam, and Urooj (2011)).

At a dialysis time of 300 min in the shaken samples, the GDRI increased from 11.36% to 27.70% as CNF concentration increased from 0.5% to 2% (w/w). The relatively high GDRI associated with higher concentrations of CNF may be due to several factors. According to Ou et al. (2001), the apparent glucose diffusion in fiber-containing suspensions is affected by the solution viscosity and the amount of glucose adsorbed by the fiber. To better understand the mechanisms behind reduced glucose diffusion caused by CNF, both viscosity and glucose adsorption studies were performed and the results are shown in later sections.

As seen in Fig 3.2, there were significant differences between glucose diffusion with and without shaking. Adiotomre et al. (1990) suggested that studies with stirring or mixing are better able to simulate the intestinal movement that occurs *in vivo*. Increasing shear through mixing accelerated the rate of glucose diffusion, as shown in Fig 3.2(c). The effects of shaking on glucose diffusion were also reported by Dhital et al. (2014). These results showed that even with the convective movement in the intestine, CNF may still be able to exert its retardation effect on glucose diffusion.

### 3.3.3 Rheological measurement of fiber

The viscosity of mixtures containing glucose and different concentrations of CNF or cellulose are shown as a function of shear rate in Fig 3.3(a). All solutions showed shear-thinning behavior, and shear-thinning has been observed in modified and unmodified suspensions of CNF (Pahimanolis et al., 2011). In general, the viscosity of 2% (w/w) cellulose solutions was lower, and more shear thinning, than solutions containing more than 0.5% (w/w) CNF. This difference may be related to particle structure and size, which determines the hydration properties (including viscosity) of dietary fiber (López et al., 1996).

Shear rates between 10 $s^{-1}$ and 100 $s^{-1}$ have been reported to occur during digestion, and shear rates towards the lower end were found in the intestinal brush border (Fabek et al., 2014; Steffe, 1996). Thus, the viscosity at two shear rates (15 $s^{-1}$ and 30 $s^{-1}$) were chosen for com-parison among the samples (Fig 3.3b). Viscosity (η) as a function of CNF concentration was best fit by a cubic function, that is:

$$\eta = a + bC + cC^2 + dC^3 \quad (5)$$

The fitting parameters (*a*,*b*,*c*,*d*) are shown in Table 3.2. This relationship applied to the viscosity both at 15 $s^{-1}$ and 30 $s^{-1}$. The Flory Huggins' viscosity model has been used to show cubic dependence on polymer concentration, for example in solutions of hydrolyzed polyacrylamide (Choi, Jeong, & Lee, 2014). For suspensions with non-cohesive particles, several models have been used to correlate suspension viscosity and solid particle concentration (Zhu, Wang, & Peng, 2017). The choices of these models depend on the concentration of solid particles in complex disperse systems, ranging from dilute monodisperse fluids to highly concentrated systems.

At a shear rate of 15 $s^{-1}$, viscosity (in Pa s) decreases in the order of 2% (w/w) CNF > 1% CNF > 0.5% CNF > 2% (w/w) Cellulose > 0.1% CNF > 0.01% CNF ≈ control. Thus with 2% (w/w) and 0.5% (w/w) CNF addition, the viscosity of the solution increased ~1835- and 55- fold, respectively. The viscosity of 2% (w/w) CNF at 10 $s^{-1}$ (5.5 ± 0.4 Pa s) was slightly higher than that reported for untreated rice bran insoluble dietary fiber but lower than sulfuric acid modified rice bran insoluble fibers (Qi et al., 2016). At 50 $s^{-1}$, the viscosity of 2% (w/w) CNF (1.2 ± 0.1 Pa s) was higher than 1% (w/w) guar gum (GG), 1% (w/w) locust bean gum (LBG) and 1% (w/w) xanthan gum (XG), but lower than 2% (w/w) GG, 2% (w/w) LBG and 4% (w/w) XG (Fabek et al., 2014).

When combining the results of Fig 3.2(c) with Fig 3.3(b), it is apparent that the decreased initial diffusion rate by higher concentrations of CNF addition is due to the increased viscosity. In order to further understand the relationship between initial diffusion rate and sample viscosity, a plot of initial diffusion rate of glucose and viscosity of CNF solution (e.g., at 15 $s^{-1}$) was generated, as shown in Fig 3.3(c). This shows that the initial diffusion rate of glucose (data from Fig 3.2) was an exponential function of the CNF solution viscosity at 15 $s^{-1}$, with the fitting parameters presented in Table 3.3. At a given viscosity, the diffusion rate in shaken samples was higher than that without shaking. The results also showed that the viscosity of solutions containing fiber played an important role in delaying glucose diffusion. This agrees with the findings of Ou et al. (2001), Srichamroen and Chavasit (2011) and Qi et al. (2016). The mechanism by which viscous polysaccharides inhibit absorption of nutrients was attributed to the increase in the thickness of an unstirred water layer (UWL) adjacent to the intestinal membrane. However, the thickness of the UWL also depends on the rate of mixing (Thomson & Dietschy, 1984), as higher shear counters the effects of increased viscosity (Dhital et al., 2014).

### 3.3.4 Glucose adsorption capacity of fiber

The glucose adsorption capacity of CNF is shown as a function of glucose concentration in Fig 3.4. A linear relationship ($y_b = a \cdot c_{gl}$) was found between glucose adsorption capacity of the fiber ($y_b$) and the glucose concentration ($c_{gl}$). Similar trends have been observed for fiber-rich fractions from citrus peel (Chau et al., 2003) and insoluble rice-bran flour (Qi et al., 2016). The linear relationship suggests that glucose adsorption has not reached saturation, as a plateau is usually evident when saturation is reached. A study by Ou et al. (2001) showed that the amount of glucose bound by fibers (carboxymethyl cellulose (CMC), XG and GG) were similar at glucose

concentrations of 50 mM (324–478 μmol/g) and 100 mM (413–555 μmol/g), which suggested saturation was nearly reached for the fiber tested.

As seen in Fig 3.4, CNF binds with more glucose than does cellulose. Specifically, the slope of CNF and cellulose were 33 and 9 (μmol/g/ mM), respectively. Additionally, at 200 mM glucose concentration, the average glucose adsorption capacity of CNF (7.12 mmol/g) was around three times of that of cellulose (2.56 mmol/g). It was calculated (based on the amount of glcuose bound versus the total amount of input glucose) that CNF binds 35.6% of glucose added while cellulose binds only 12.8% of glucose. However, the glucose adsorption capacity of CNF at a glucose concentration of 200 mM was lower than that of insoluble dietary fiber from citrus peel (Chau et al., 2003). For a glucose concentration of 100 mM, the adsorption capacity of CNF was lower than that of wheat bran (Ahmed et al., 2011), but higher than those of the dietary fibers tested by Ou et al. (2001), including CMC, GG and XG.

Even at a relatively low glucose concentration of 5 mM, CNF can still bind with glucose (∼16 μmol/g), which indicates that CNF may help maintain low glucose levels in the gastrointestinal tract (Qi et al., 2016). Ou et al. (2001) found that the glucose adsorption capacity could not be determined for some fibers if the glucose concentration is lower than 5 mM, thus this concentration range was not tested in this study. Further *in vivo* studies will provide more evidence on the hypoglycemic effects of CNF.

3.3.5 Effect of fiber on in vitro amylolysis kinetics

The above studies focused on determining the effects of fiber on enzyme activity and glucose diffusion flux separately. The influence of fiber on *in vitro* amylolysis kinetics was also studied to understand the combined effects (Fig 3.5). The addition of 2% (w/w) CNF resulted in the lowest amount of glucose equivalent in the dialysate. For 0.1% (w/w) CNF or 2% (w/w)

cellulose addition, no significant differences were observed in the amount of glucose equivalent diffused into the dialysate when compared to that of the control. However, addition of 0.5% (w/w) CNF and above significantly reduced the glucose equivalent content in the dialysate (Fig 3.5).

In the first 60 min glucose equivalent uptake in the dialysate was linear (Fig 3.5b), and the average initial amylolysis velocity (μmol/min) decreased in the order: control (6.18) ≈ 0.1% (w/w) CNF > 2% Cellulose (5.97) > 0.5% CNF (4.79) > 1% CNF (4.60) > 2% CNF (3.19). An exponential function was fitted to a plot of amylolysis velocity against CNF concentration (Fig 3.5c), and the fitting parameters shown in Table 3.4. The relationship was like that observed in Figs. 2(c) and 3(c) where the initial glucose diffusion rate decreased exponentially with CNF concentration or viscosity of the CNF solution. At 360 min, the final amount of glucose in the dialysate with 1%–2% CNF addition was 71.4%–73.4% of the control; that is, 1%–2% CNF retarded 26.6%–28.6% of glucose equivalent released during the amylolysis process. This was similar to the retardation effects of CNF on glucose diffusion with shaking applied (21.6%–27.6%), as presented in Fig 3.2. Similar effects of CNF on amylolysis and glucose diffusion suggests that the effects on amylolysis is mainly due to high viscosity. The effects of increased viscosity on delaying glucose uptake has been reported in other papers (Qi et al., 2016; Srichamroen & Chavasit, 2011). Additionally, Nishimune et al. (1991) showed that the glycemic index (GI) of food can be estimated from an empirical equation based on the amount of total dietary fiber present, and that higher dietary fiber amount is related to lower GI values.

3.3.6 Effect of fiber on the in vitro digestion of starch

Previous studies have shown that a more pronounced effect of fiber on digestive enzyme activities was observed when dissolving the enzymes in intestinal juice rather than in buffers alone (Isaksson, Lundquist, & Ihse, 1982; Schneeman & Gallaher, 2001). This was thought to be

associated with the composition and properties of intestinal components. To better simulate the effect of fiber on starch digestion in the gastrointestinal tract, a static *in vitro* digestion trial was carried out as it mimics the physicochemical changes that occur during digestion and is simple, reproducible, rapid and cost-effective (Donhowe & Kong, 2014).

During salivary digestion, α-amylase can hydrolyze starch. However, due to the short residing time (5 min), the amount of glucose produced among the samples were very small (< 10 μmol). During the gastric digestion, the activity of α-amylase was inhibited due to the low pH. During intestinal digestion, α-amylase activity was re-activated and starch hydrolysis continued due to both α-amylase and pancreatin action. Results from Fig 3.6(a) and (b) show that with the addition of 1.1% (w/w) CNF, the lowest amount of glucose was released under both situations after 2 h of intestinal digestion. The amount of glucose produced with 1.1% (w/w) CNF or 1.1% (w/w) cellulose was significantly different than that of the control, 0.22% (w/w) CNF and 0.22% (w/w) cellulose (Fig 3.6(a)). The amount of glucose diffused was the lowest with the addition of 1.1% (w/w) CNF, followed by that with 0.22% (w/w) CNF (Fig 3.6(b)). Both concentrations of CNF resulted in significantly different glucose content than that of other groups. The differing amounts of glucose produced and diffusion rates, as affected by fiber addition, indicate that the diffusion process may take a longer time (more than 2 hr) to reach equilibrium. In addition, the effects of CNF addition on glucose diffusion may be more significant than its effect on glucose production when compared to the control.

Considering the results from Fig 3.6 and those from the above studies, it is suggested that the addition of high concentrations of CNF (1.1% (w/w) in this case) can potentially exert its hypoglycemic effects, including de-laying glucose diffusion, even in the presence of a complex digestive environment (with digestive juices and rotational mixing). Overall, the results from Fig

3.6 show that the addition of 1.1% (w/w) CNF can significantly inhibit starch *in vitro* digestion, which is attributed to the increased viscosity of the digesta. This finding agrees with that of Takahashi, Karita, Ogawa, and Goto (2005), who found that ingestion of crystalline cellulose decreased post-infusion plasma glucose concentration in rats due to the increased viscosity. In addition, Dhital et al. (2014) showed that starch *in vitro* hydrolysis and glucose diffusion were reduced at increased viscosity after addition of beta-glucan from barleys or oats.

In a nutshell, CNF exerts hypoglycemic potential due to its effect on the retardation of glucose diffusion, delayed amylolysis, and reduced glucose released during static *in vitro* digestion. The highly viscous properties of CNF, especially at concentrations higher than 0.5%, seem to be the major contributing factor for its hypoglycemic effect. However, other mechanisms may also contribute to the effects of CNF on starch digestion and glucose absorption, including possible interaction between CNF and gelatinized starch gel. It was reported that starch can adhere to cellulose fiber due to their similar chemical structure, polarity, and hydrophilic properties (Hanna & Xu, 2009). Further study is necessary to fully understand the interaction between CNF and starch and its influences on the hypoglycemic effects of CNF.

3.3.7 Effects of fiber types and concentrations on starch digestion and glucose absorption

Above studies have shown that the effects of CNF on starch digestion and glucose absorption was mainly due to high viscosity achieved at high fiber concentration. Thus when investigating the effects of TEMPO-CNF and CNC on starch digestion and glucose absorption, only viscous properties as well as the amount of glucose release/diffusion flux were measured. The results of the amount of glucose release with TEMPO-CNF or CNC addition were shown in Fig 3.7(a) and 3.8(a), while the amount of glucose diffusion flux for both was plotted in Fig 3.7(b) and 3.8(b). In addition, the intestinal viscosity of digesta containing various concentrations of TEMPO-

CNF or CNC were shown in Fig 3.9, with a trend shown between initial glucose diffusion rate and digesta viscosity.

Results from Fig 3.7(a) and Fig 3.8(a) showed that the addition of TEMPO-CNF or CNC at any concentration tested did not show significant differences on the amount of glucose released, though a lower initial glucose release rate was observed with the presence of higher NC (TEMPO-CNF/CNC) concentration. Results from Fig 3.7(b) and 3.8(b) showed that 0.36% (w/w) TEMPO-CNF or 2~4% (w/w) CNC addition caused significantly lower amount of glucose diffused out. In addition, 0.1~0.36% (w/w) TEMPO-CNF and 1~4% (w/w) CNC addition resulted in lower initial glucose diffusion rate, as shown in the inserted figure of Fig 3.7(b) and 3.8(b). As shown in Fig 3.9, the viscosity of digesta containing TEMPO-CNF and CNC increased with higher nanocellulose concentration, which is similar to the trends observed in Fig 3.3(b). Moreover, the initial glucose diffusion rate is also shown to decrease with increasing viscosity of digesta that contain the two anionic nanocellulose, as similar to the trends observed in Fig 3.3(c).

**3.4 Conclusion**

The results from this study suggest that addition of all three types of NC to diets might decrease available blood glucose levels. From *in vitro* studies, CNF was shown to bind with glucose, delay glucose diffusion, delay amylolysis and inhibit starch *in vitro* digestion. The high viscosity of CNF at concentrations > 0.5% (w/w) was likely the main reason associated with its hypoglycemic potential. However, addition of up to 1% (w/w) CNF had no significant effects towards α-amylase and α-glucosidase activity. TEMPO-CNF or CNC did not show any significant effects on the amount of glucose release, but both anionic NC at high concentrations caused significant reductions in the amount of glucose diffusion flux, especially at 0.36% (w/w) TEMPO-CNF and 2~4% (w/w) CNC. Overall, this study lays a foundation for future investigations of the

potential metabolic effects of NC and possible incorporation of NC into food or supplements as a zero-calorie fiber for reducing post-prandial serum glucose levels. Further studies should be performed, including *in vivo* studies of the effect of NC on starch digestion and glucose absorption to validate these results.

### 3.5 Acknowledgement

This work was supported by the USDA National Institute of Food and Agriculture [grant no. 2016-67021-24994/project accession no. 1009090].

### 3.6 References

Adiotomre, J., Eastwood, M. A., Edwards, C., & Brydon, W. G. (1990). Dietary fiber: in vitro methods that anticipate nutrition and metabolic activity in humans. *The American Journal of Clinical Nutrition,* 52(1), 128-134.

Ahmed, F., Sairam, S., & Urooj, A. (2011). In vitro hypoglycemic effects of selected dietary fiber sources. *Journal of Food Science and Technology,* 48(3), 285-289.

Amarowicz, R., Korczakowska, B., & Smoczyńska, K. (1988). Effect of fiber from buckwheat on the In vitro enzymatic digestion of protein. *Molecular Nutrition & Food Research,* 32(10), 1005-1006.

Chau, C.-F., Huang, Y.-L., & Lee, M.-H. (2003). In vitro hypoglycemic effects of different insoluble fiber-rich fractions prepared from the peel of Citrus sinensis L. cv. Liucheng. *Journal of Agricultural and Food Chemistry,* 51(22), 6623-6626.

Choi, B., Jeong, M. S., & Lee, K. S. (2014). Temperature-dependent viscosity model of HPAM polymer through high-temperature reservoirs. *Polymer Degradation and Stability,* 110, 225-231.

Dhital, S., Dolan, G., Stokes, J. R., & Gidley, M. J. (2014). Enzymatic hydrolysis of starch in the presence of cereal soluble fibre polysaccharides. *Food & Function,* 5(3), 579-586.

Dhital, S., Gidley, M. J., & Warren, F. J. (2015). Inhibition of α-amylase activity by cellulose: Kinetic analysis and nutritional implications. *Carbohydrate Polymers,* 123, 305-312.

Donhowe, E. G., & Kong, F. (2014). Beta-carotene: digestion, microencapsulation, and in vitro bioavailability. *Food and Bioprocess Technology,* 7(2), 338-354.

Dunaif, G., & Schneeman, B. (1981). The effect of dietary fiber on human pancreatic enzyme activity in vitro. *The American Journal of Clinical Nutrition,* 34(6), 1034-1035.

Dutta, S. K., & Hlasko, J. (1985). Dietary fiber in pancreatic disease: effect of high fiber diet on fat malabsorption in pancreatic insufficiency and in vitro study of the interaction of dietary fiber with pancreatic enzymes. *The American Journal of Clinical Nutrition,* 41(3), 517-525.

Fabek, H., Messerschmidt, S., Brulport, V., & Goff, H. D. (2014). The effect of in vitro digestive processes on the viscosity of dietary fibres and their influence on glucose diffusion. *Food Hydrocolloids,* 35, 718-726.

Flores, F. P., Singh, R. K., Kerr, W. L., Pegg, R. B., & Kong, F. (2013). Antioxidant and enzyme inhibitory activities of blueberry anthocyanins prepared using different solvents. *Journal of Agricultural and Food Chemistry,* 61(18), 4441-4447.

Flores, F. P., Singh, R. K., Kerr, W. L., Pegg, R. B., & Kong, F. (2014). Total phenolics content and antioxidant capacities of microencapsulated blueberry anthocyanins during in vitro digestion. *Food Chemistry,* 153, 272-278.

Hanna, M. A., & Xu, Y. (2009). Starch–Fiber Composites. In L. Yu, *Biodegradable Polymer Blends and Composites from Renewable Resources* (pp. 349-366). Hoboken: John Wiley & Sons

Hasik, J., & Bartnikowska, E. (1987). *Włókno roślinne w żywieniu człowieka*. Warszawa: PZWL.

Isaksson, G., Lundquist, I., & Ihse, I. (1982). Effect of dietary fiber on pancreatic enzyme activity in vitro. *Gastroenterology,* 82(5), 918-924.

Jorfi, M., & Foster, E. J. (2015). Recent advances in nanocellulose for biomedical applications. *Journal of Applied Polymer Science,* 132(14), 41719.

López, G., Ros, G., Rincón, F., Periago, M., Martinez, M., & Ortuno, J. (1996). Relationship between physical and hydration properties of soluble and insoluble fiber of artichoke. *Journal of Agricultural and Food Chemistry,* 44(9), 2773-2778.

Nichols, G. A., Hillier, T. A., & Brown, J. B. (2008). Normal fasting plasma glucose and risk of type 2 diabetes diagnosis. *The American Journal of Medicine,* 121(6), 519-524.

Nishimune, T., Yakushiji, T., Sumimoto, T., Taguchi, S., Konishi, Y., Nakahara, S., Kunita, N. (1991). Glycemic response and fiber content of some foods. *The American Journal of Clinical Nutrition*, 54(2), 414-419.

Ou, S., Kwok, K.-c., Li, Y., & Fu, L. (2001). In vitro study of possible role of dietary fiber in lowering postprandial serum glucose. *Journal of Agricultural and Food Chemistry,* 49(2), 1026-1029.

Pahimanolis, N., Hippi, U., Johansson, L.-S., Saarinen, T., Houbenov, N., Ruokolainen, J., & Seppälä, J. (2011). Surface functionalization of nanofibrillated cellulose using click-chemistry approach in aqueous media. *Cellulose*, 18(5), 1201.

Qi, J., Li, Y., Masamba, K. G., Shoemaker, C. F., Zhong, F., Majeed, H., & Ma, J. (2016). The effect of chemical treatment on the in vitro hypoglycemic properties of rice bran insoluble dietary fiber. *Food Hydrocolloids,* 52, 699-706.

Schneeman, B. O., & Gallaher, D. (1980). Changes in small intestinal digestive enzyme activity and bile acids with dietary cellulose in rats. *The Journal of Nutrition,* 110(3), 584-590.

Schneeman, B. O., & Gallaher, D. (2001). Effects of dietary fiber on digestive enzymes. In G. A. Spiller (Ed.), *CRC Handbook of dietary fiber in human nutrition* (pp. 277-283). Boca Raton: CRC Press.

Sigma-Aldrich (2017). Enzymatic assay of α-amylase (EC 3.2.1.1). http://www.sigmaaldrich.com/technical-documents/protocols/biology/enzymatic-assay-of-a-amylase.html. (Accessed 4 May 2017).

Srichamroen, A., & Chavasit, V. (2011). In vitro retardation of glucose diffusion with gum extracted from malva nut seeds produced in Thailand. *Food Chemistry,* 127(2), 455-460.

Steffe, J. F. (1996). *Rheological methods in food process engineering*. East Lansing: Freeman Press.

Takahashi, T., Karita, S., Ogawa, N., & Goto, M. (2005). Crystalline cellulose reduces plasma glucose concentrations and stimulates water absorption by increasing the digesta viscosity in rats. *The Journal of Nutrition*, 135(10), 2405-2410.

Thomson, A., & Dietschy, J. (1984). The role of the unstirred water layer in intestinal permeation. In T. Z. Csáky (Ed.). *Pharmacology of intestinal permeation II* (pp. 165– 269). Springer-Verlag Berlin Heidelberg.

Zhu, Z., Wang, H., & Peng, D. (2017). Dependence of Sediment Suspension Viscosity on Solid Concentration: A Simple General Equation. *Water*, 9(7), 474.

Table 3.1. Exponential fittings ($y = y_0 + A \times e^{R_0 x}$) for curves of initial diffusion rate versus CNF concentration as shown in Fig 3.2(c).

| Fitting parameters | No shaking | With shaking at 100 rpm |
|---|---|---|
| $y_0$ | 8.02 | 9.26 |
| A | 11.3 | 13.8 |
| $R_0$ | -1015 | -197 |
| Adj. $R^2$ | 0.9994 | 0.9756 |

Table 3.2. Cubic fittings ( $y = a + bx + cx^2 + dx^3$ ) for curves of viscosity versus CNF concentrations as shown in Fig 3.3(b).

| Fitting parameters | At 15 $s^{-1}$ shear rate | At 30 $s^{-1}$ shear rate |
|---|---|---|
| a | 0.0019 | 0.0014 |
| b | 0.88 | 0.95 |
| c | 2755 | 1422 |
| d | 313,910 | 142,580 |
| Adj. $R^2$ | 0.9998 | 0.9999 |

Table 3.3. Exponential fittings ($y = y_0 + A \times e^{R_0 x}$) for curves of initial diffusion rate versus viscosity at 15 $s^{-1}$ shear rate as shown in Fig 3.3(c).

| Fitting parameters | No shaking | With shaking at 100 rpm |
|---|---|---|
| $y_0$ | 8.08 | 10.4 |
| A | 18.2 | 12.6 |
| $R_0$ | -251 | -10.4 |
| Adj. $R^2$ | 0.9919 | 0.9723 |

Table 3.4. Exponential fittings ($y = y_0 + A \times e^{R_0 x}$) for curves of initial amylolysis velocity versus CNF concentration as shown in Fig 3.5(c).

| Fitting parameters | Values |
|---|---|
| $y_0$ | 2.67 |
| A | 3.58 |
| $R_0$ | -0.94 |
| Adj. $R^2$ | 0.9478 |

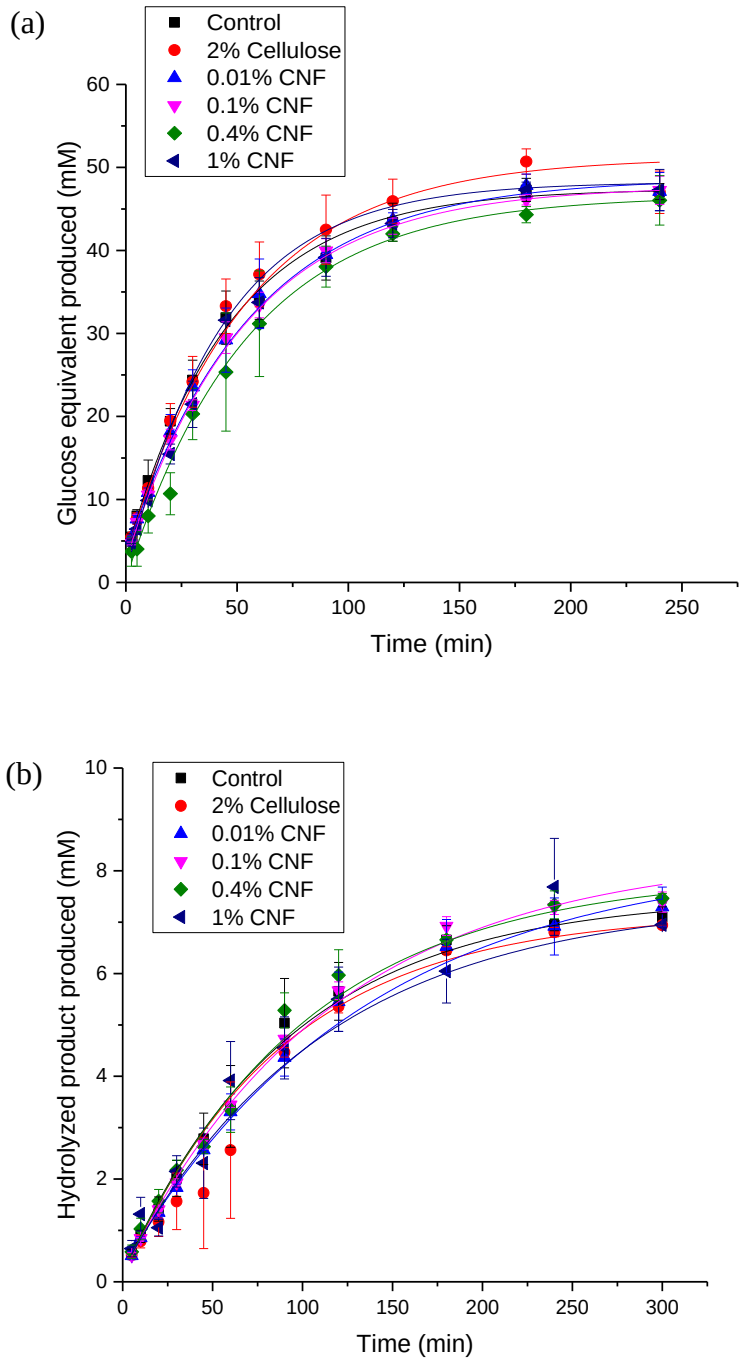


Fig 3.1. Effect of CNF or cellulose fiber on enzyme activity: (a) α-amylase activity measured by glucose equivalent produced and (b) and α-glucosidase activity measured by hydrolyzed product produced over time.

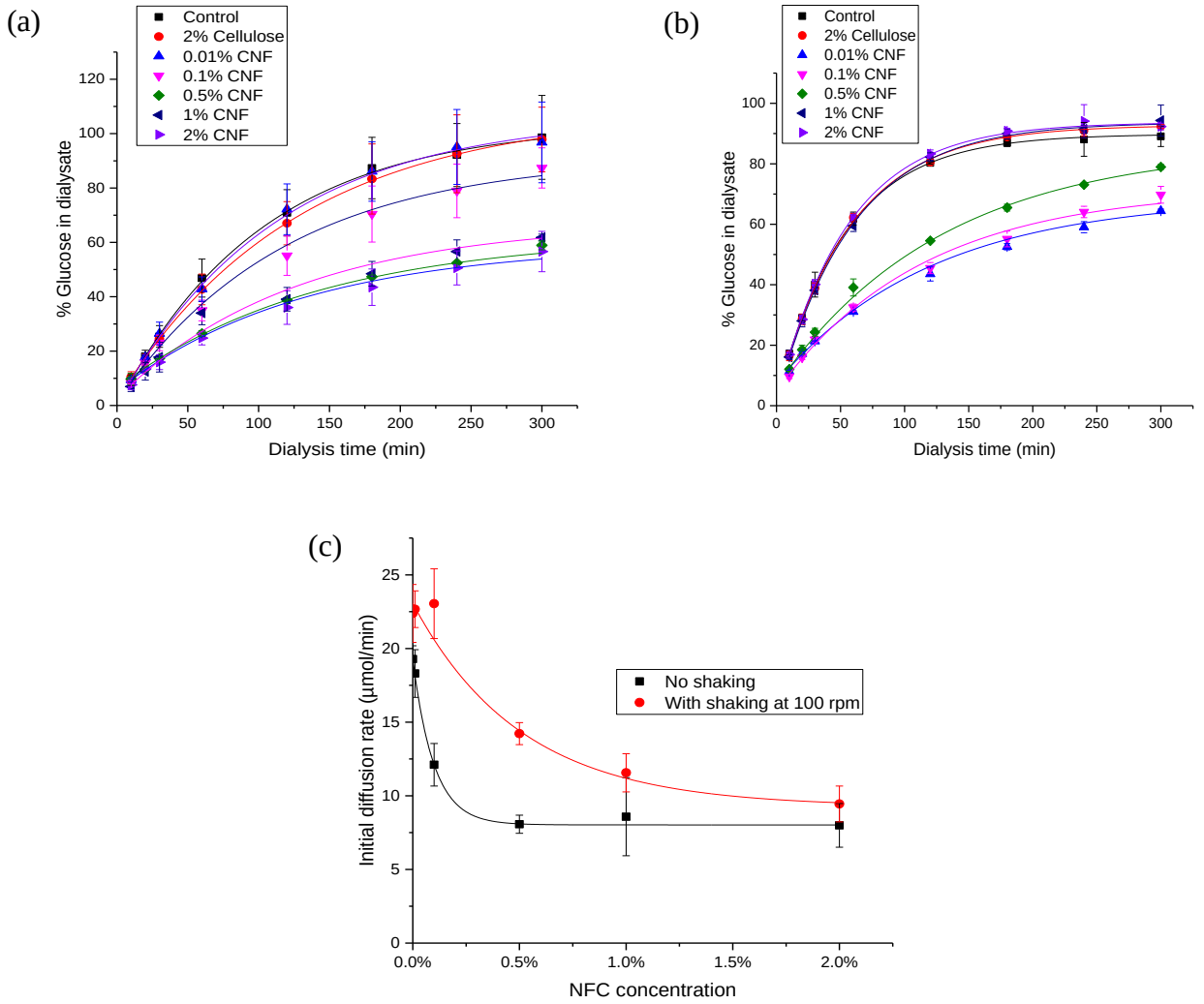


Fig 3.2. Effect of fiber on diffusion flux of glucose. (a) % glucose diffused into dialysate with no shaking; (b) % glucose diffused into dialysate with shaking at 100 rpm; (c) Initial diffusion rate versus CNF concentration.

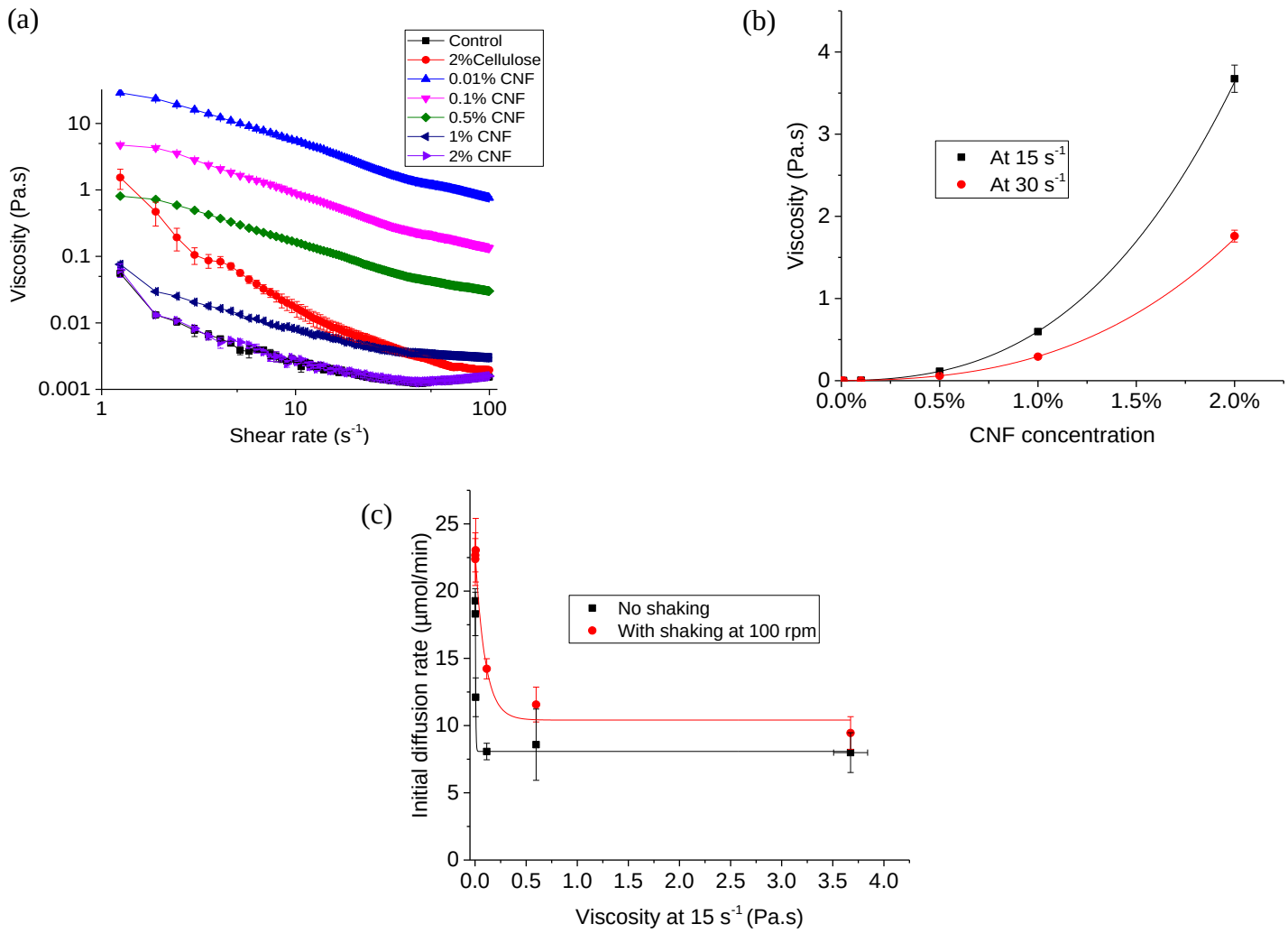


Fig 3.3. Viscosity of CNF and cellulose solutions and its relationship with initial diffusion rate. (a) Viscosity as a function of shear rates; (b) Viscosity as a function of concentration at select shear rates (15 and 30 $s^{-1}$); (c) Glucose diffusion rate versus viscosity at 15 $s^{-1}$.

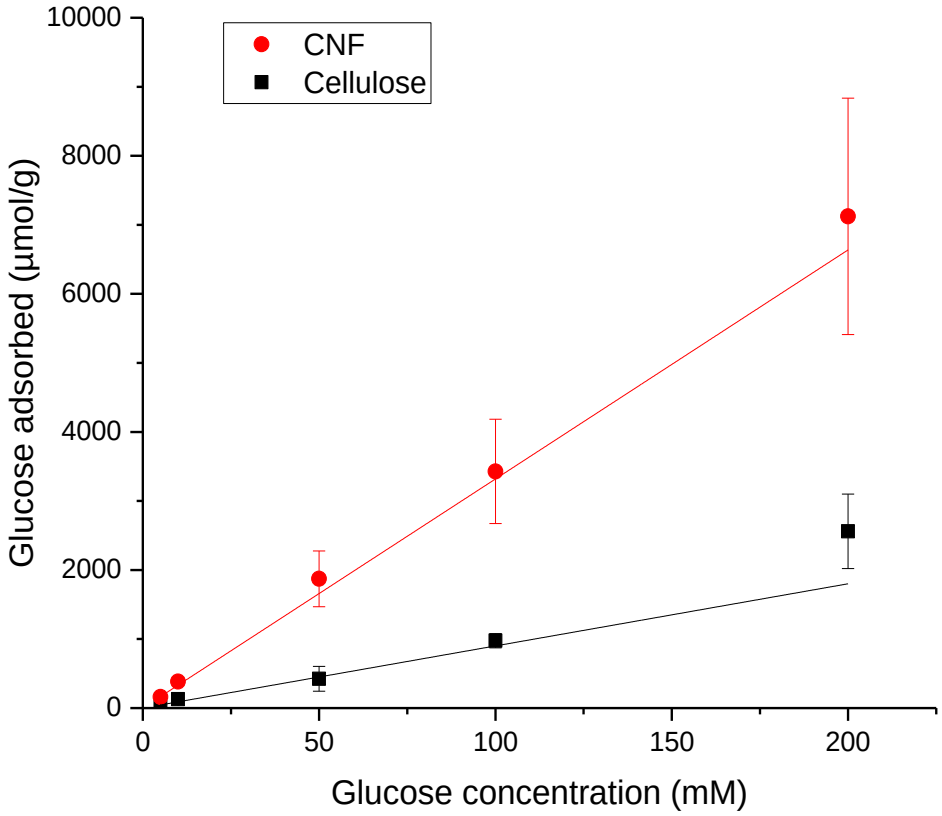


Fig 3.4. Glucose adsorption capacity of CNF or cellulose fiber as a function of glucose concentration.

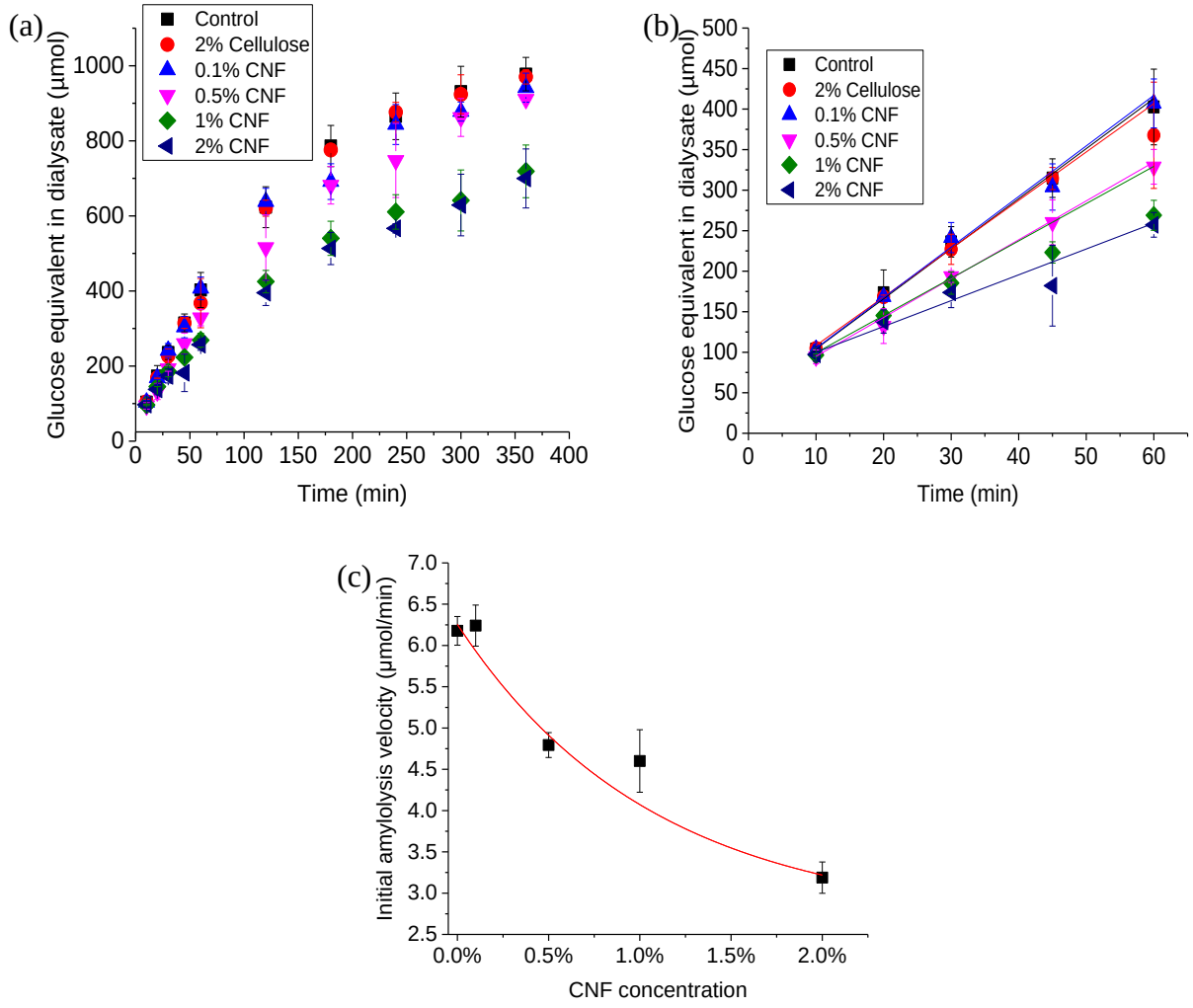


Fig 3.5. Effect of CNF or cellulose fiber on diffusion flux of glucose equivalent into dialysate during starch hydrolysis. (a) Glucose equivalent concentration in dialysate over time; (b) Initial progress curves of starch hydrolysis in the presence of fiber; (c) Plot of initial amylolysis velocity against CNF concentration.

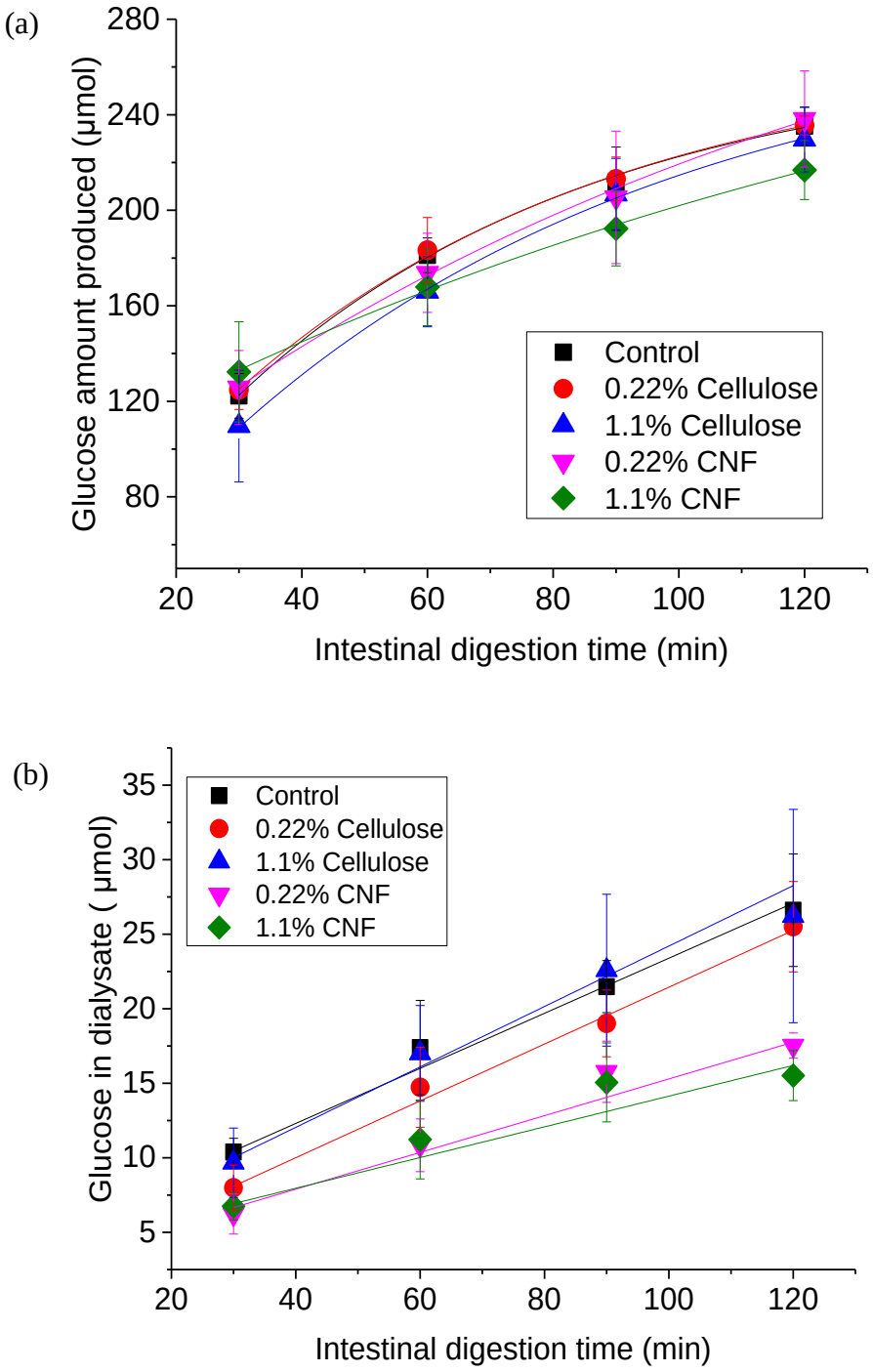


Fig 3.6. Effect of fiber on static *in vitro* digestion of corn starch. (a) Progress curves of amount of glucose produced during intestinal digestion; (b) Progress curves of amount of glucose in dialysate during intestinal digestion.

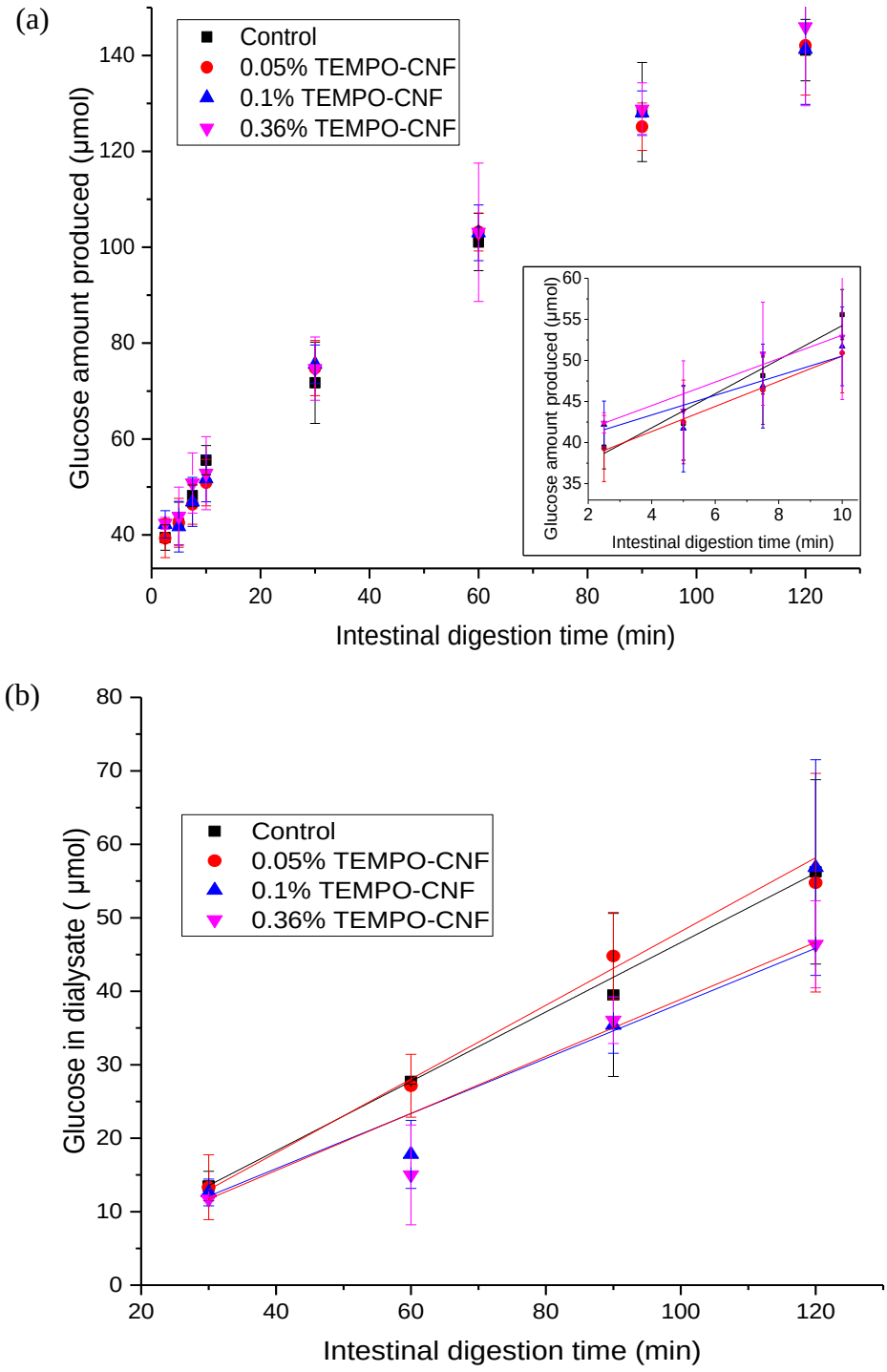


Fig 3.7. Effect of TEMPO-CNF on static *in vitro* digestion of corn starch. (a) Progress curves of amount of glucose produced during intestinal digestion; (b) Progress curves of amount of glucose in dialysate during intestinal digestion.

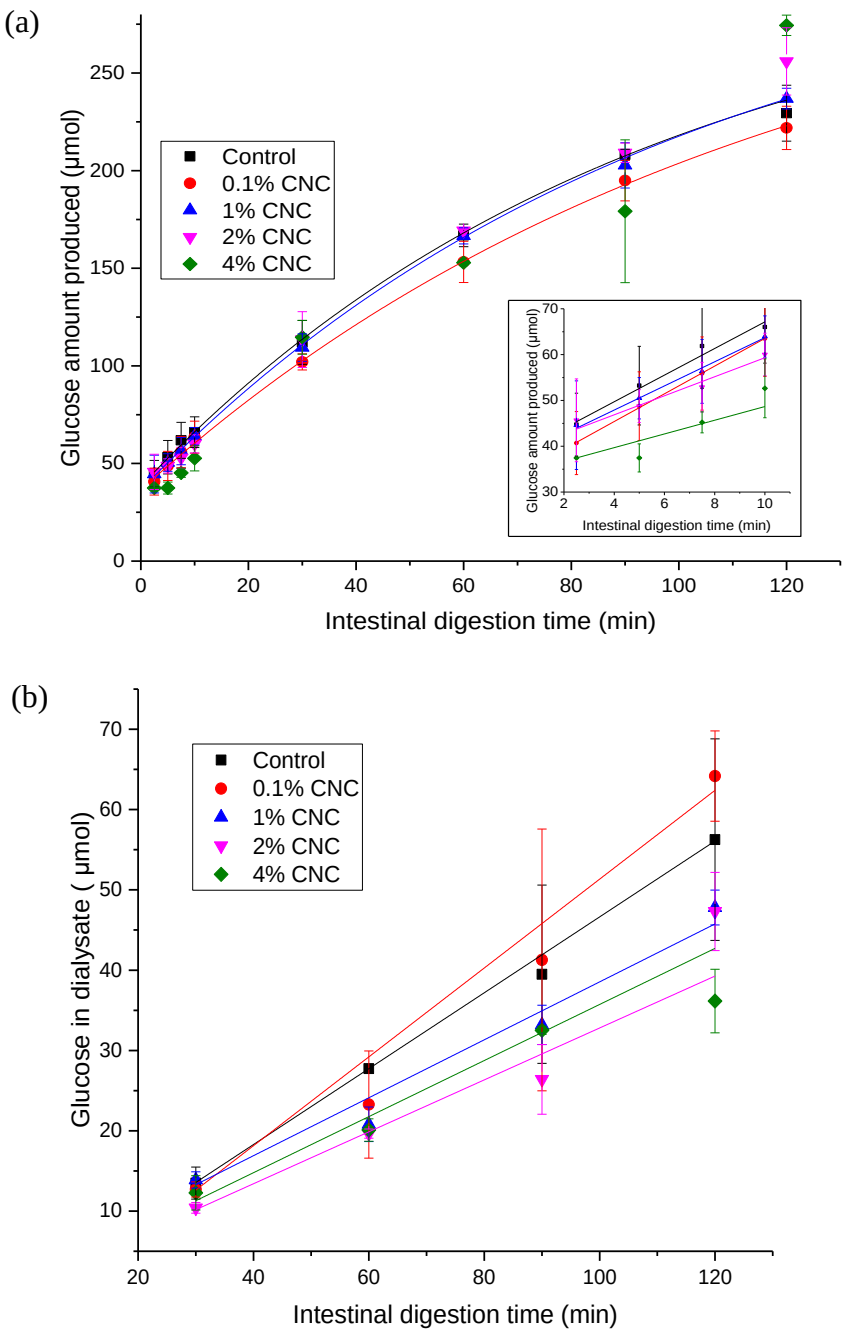


Fig 3.8. Effect of CNC on static *in vitro* digestion of corn starch. (a) Progress curves of amount of glucose produced during intestinal digestion; (b) Progress curves of amount of glucose in dialysate during intestinal digestion.

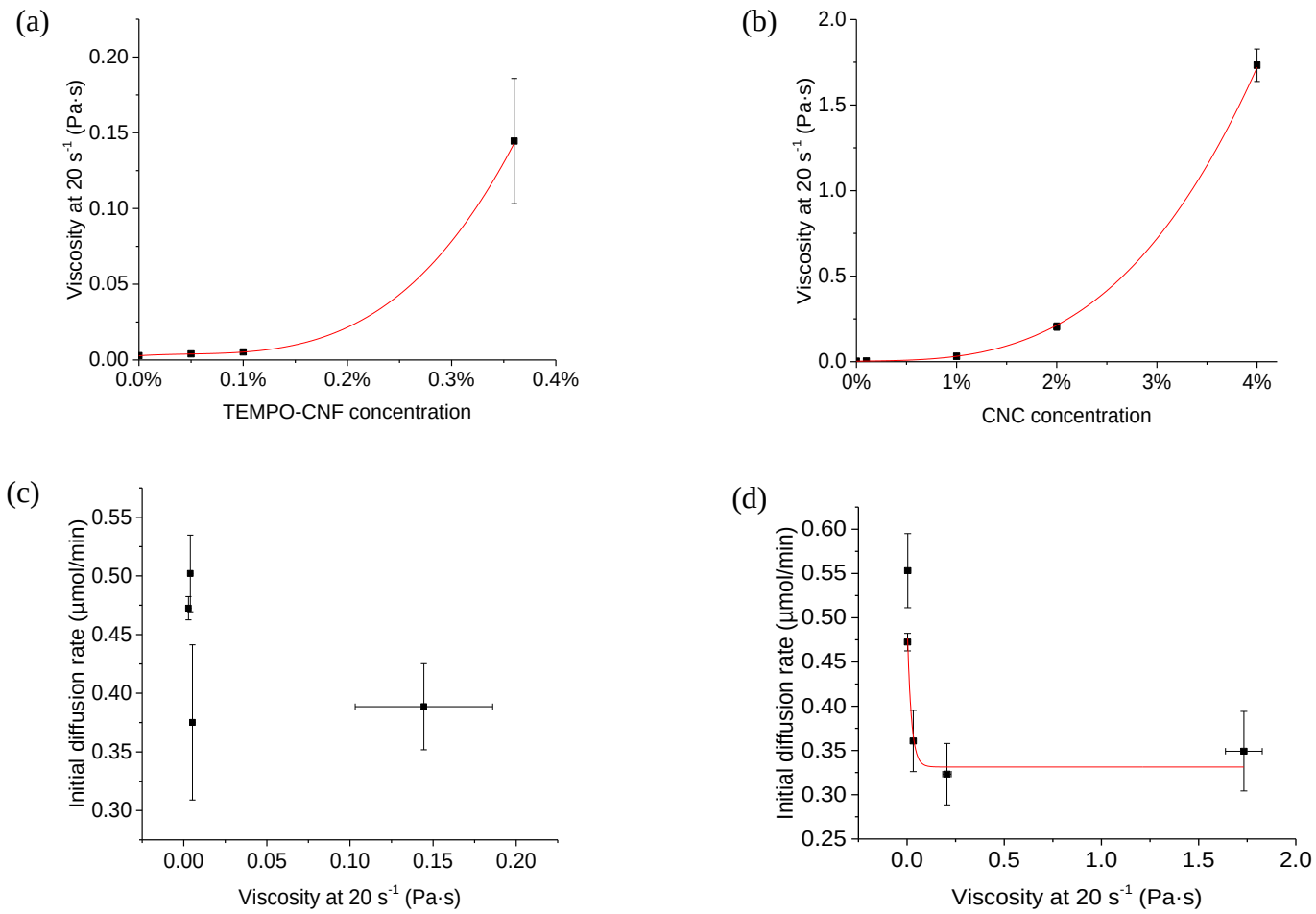


Fig 3.9. Viscosity of intestinal digesta containing TEMPO-CNF/CNC and its relationship with nanocellulose concentrations or initial glucose diffusion rate. Viscosity of digesta containing (a) TEMPO-CNF (b) CNC as a function of nanocellulose concentration; initial glucose diffusion rate of digesta containing (c) TEMPO-CNF (d) CNC versus viscosity at 20 $s^{-1}$.

# CHAPTER 4

# INFLUENCE OF NANOCELLULOSE ON *IN VITRO* DIGESTION OF LIPID EMULSIONS[2]

[2] Liu L, Kerr W L, Kong F. Characterization of lipid emulsions during *in vitro* digestion in the presence of three types of nanocellulose. Submitted to *Food Research International*, 11/13/2018.

**Abstract:**

Nanocellulose has been a topic of significant interest and many studies have focused on using it for the design of stable oil-in-water emulsions. In this study, the effects of CNF on lipase activity, cholesterol adsorption capacity, micellar solubility of cholesterol as well as bile acid diffusion were studied with conventional cellulose as a comparison. Moreover, the influences of three types of nanocellulose (CNF, TEMPO-CNF and CNC) on the gastrointestinal fate of Tween 80 stabilized lipid emulsions were investigated. The changes in physicochemical characteristics (including particle size, microstructure, viscosity and zeta potential) of the emulsions containing nanocellulose/cellulose as well as the amount of free fatty acid (FFA) released were studied and compared among different types and concentrations of fiber as well as digestion phases. Results showed that CNF significantly reduced lipase activity and showed greater bile acid retardation effect as well as slightly higher cholesterol adsorption capacity than cellulose. But CNF did not affect micellar solubility of cholesterol. In addition, all three types of nanocellulose at high concentrations (1% CNF, 0.25~0.36% TEMPO-CNF or 2~3% CNC) delayed initial *in vitro* digestion of emulsions, though the final lipolysis extent was nearly the same amongst all (47~55%). The behavior of each type of nanocellulose differed during each digestion phase. Specifically, CNC was found to increase viscosity of gastric digesta, TEMPO-CNF showed aggregation after gastric digestion while CNF had no morphological changes during gastrointestinal digestion. Results from this study indicated that all three types of nanocellulose are advantageous over cellulose in terms of increasing digesta viscosity and delaying initial lipid digestion. Nanocellulose also showed potential benefits in promoting satiation and improving satiety.

**Keywords**: Cellulose nano-fibrils; TEMPO-oxidized cellulose nano-fibrils; cellulose nanocrystals; viscosity; fluorescence

## 4.1 Introduction

Lipids are important components to the human diet and there has been growing interest in methods to control their digestibility and bioavailability. One approach has been to develop foods in which the lipids are consumed along with dietary fiber. A number of studies have shown that certain dietary fiber have hypolipidemic effects and can cause a reduction of serum cholesterol levels (Sugano, Ikeda, Imaizumi, & Lu, 1990; Mackie, Bajka, & Rigby, 2016). Several mechanisms have been proffered on how fiber affects the fate of lipid emulsions during gastrointestinal digestion. Research suggests that fiber may inhibit lipase activity; promote lipid flocculation; bind with lipid droplets, calcium ions or bile salts; and may alter mixing and mass transport processes (Zhang, Zhang, Zhang, Decker, & McClements, 2015).

In addition to conventional fibers, which are divided into soluble and insoluble fibers based on their solubility and gelling behaviors, a new type of cellulosic material called nanocellulose (NC) has garnered significant interest due to its unique properties. Though categorized as an insoluble fiber, NC behaves as a gel under certain conditions. It has been shown to be non-toxic for humans, compatible for use with biological tissues, and biodegradable in the environment (Lin & Dufresne, 2014). NC can be categorized as cellulose nanofibrils (CNF), cellulose nanocrystals (CNC) or bacteria cellulose based on how it is produced. CNF, with nanoscale diameter but micron-sized length, is often generated by mechanical disintegration of cellulosic materials. A variety of chemical treatments, such as TEMPO (2, 2, 6, 6-tetramethylpiperidine-1-oxyl radical) oxidation, have been applied to reduce the energy required to disintegrate CNF and increase fibril individualization (Mertaniemi, 2017). TEMPO oxidation converts primary hydroxyl groups of cellulose into carboxylate groups under mild conditions. TEMPO oxidized CNF (TEMPO-CNF) carries negative surface charge and can form stable colloidal suspensions due to electrostatic

repulsions (Maloney, 2015). CNC, on the other hand, is often generated via acid hydrolysis and thus has high crystallinity, shorter length and diameter but high negative surface charge. As with TEMPO-CNF, CNC forms more stable colloidal suspensions due to electrostatic repulsion. The pKa of CNC (associated with the sulfate half-ester group) was reported as 2.46. Thus CNC can be fully ionized at pH above 4.76 (Roman, 2015; Wang, Qian, & Roman, 2011).

A few studies have focused on designing Pickering emulsions using nanocellulose, and how it affects the stability and properties of those emulsions (Saelices and Capron, 2018). While there is increasing interest in using nanocellulose in foods, little research exists on its fate during digestion and its influence on the absorption of lipids and other nutrients. Among the limited studies available, the focus of their research is on the effects of nanocellulose on protein-stabilized lipid emulsions, where the effects at a large extent may be due to the changes of proteins rather than lipids (DeLoid, et al., 2018; Sarkar, Li, Cray, & Boxall, 2018; Sarkar et al., 2017). Thus the objective of this research was to study how nanocellulose might affect the digestion of lipids contained in oil-in-water emulsions stabilized by a non-ionic surfactant. This was carried out in an *in vitro* model simulating salivary, gastric and intestinal digestion phases. Different nanocellulose materials were tested including CNF, TEMPO-CNF and CNC, which varied in fibril length, diameter, surface charge and rheological properties. In addition, these were investigated at concentration ranges that would be realistic for food systems. Changes in physical dimensions (size) or aggregation states (isolated/flocculated/coalesced) of emulsion systems during gastrointestinal digestion were determined by particle size measurement, followed by examination of structural changes by confocal microscopy. Tendencies for the emulsions to be stabilized by electrostatic forces were assessed by measuring the surface charge (zeta-potential). To better understand how mass transport might influence digestibility, rheological properties were

measured. Finally, lipid digestion in the intestinal phase was assessed through titration of free fatty acids formed.

## 4.2 Materials and methods

### 4.2.1. Materials

Nano-fibrillated cellulose (also called cellulose nanofibrils (CNF), 3 wt%) was purchased from the Process Development Center at the University of Maine (Orono, ME). Samples of TEMPO-based cellulose nano-fibrils (1.1 wt% in water, 1.5 mmol-COONa/g dry CNF) and nano-crystalline cellulose (also called cellulose nanocrystals (CNC), 10.8 wt% in water, 0.94 wt% sulfur on dry CNC, sodium form) were both obtained from the USDA's Forest Products Laboratory. The nominal sizes of the three nanocellulose materials were: CNF (~50 nm width and length up to several hundred microns); CNC (~ 5 nm width and 150 nm length); TEMPO-CNF (~ 20 nm width and length up to 2 μm). According to our test, the zeta potential of three nanomaterials dissolved in 1 mM PBS (pH 7.0) were: CNF (-21 ± 2 mV); TEMPO-CNF (-44 ± 2 mV); CNC (-23 ± 4 mV). Characterization of the nanomaterials has been widely studied in the literature (Jowkarderis & van de Ven, 2015; Moon, Schueneman, & Simonsen, 2016; Zhou et al., 2013) as well as on the manufacturers' website.

Crisco pure canola oil was obtained from a local grocery store. As stated by the manufacturer, the oil was comprised of 7% saturated, 64% monounsaturated, and 29% polyunsaturated fatty acids. Digestive components including α-amylase from porcine pancreas (A3176, 12 U/mg), pepsin from porcine gastric mucosa (P7000, 479 U/mg), bile extract porcine (B8631), lipase from porcine pancreas (Type II, L3126) and mucin from porcine stomach (Type II, M2378, bound sialic acid 0.4%) were purchased from Sigma-Aldrich Chemical Co. (St. Louis, MO). The lipase activity was 398 units/mg protein when using olive oil as the substrate (where

one unit will hydrolyze 1.0 microequivalent of fatty acid from olive oil). Tween 80 and other chemicals were purchased from either Fisher Scientific (Pittsburgh, PA) or Sigma-Aldrich.

4.2.2. Emulsion preparation

The aqueous phase of the emulsion was prepared by dissolving 1% Tween 80 (w/v) in 5 mM phosphate buffer (pH 7.0) solution and stirring to ensure complete dissolution. A stock emulsion was prepared by mixing 10% (w/v) canola oil with 90% (w/v) emulsifier solution, and blending at ~25,000 rpm with a PRO250 lab homogenizer (PRO Scientific Inc., Oxford, CT) for 2 min. The material was then passed 3 times through a valve homogenizer (15MR-8TA, Gaulin, Everett, MA) operating at 9,000 psi. The stock emulsion was stored at 4 °C with no light exposure.

4.2.3. Free fatty acid release during *in vitro* digestion of lipid emulsions

4.2.3.1 Initial phase

The initial emulsion systems included several concentrations of CNF (0.23%, 1.17% and 2.34% (w/w)); TEMPO-CNF (0.12%, 0.23%, 0.59% and 0.85% (w/w)); or CNC (0.23%, 1.17%, 2.35%, 4.70% and 7.04% (w/w)). In addition, 2.34% cellulose suspensions were studied to determine the differences between nanocellulose and conventional cellulose on lipid digestion. These concentrations were selected based on calculations of the final fiber concentration after intestinal digestion. Different concentrations of nanocellulose solution were prepared by diluting the stock nanocellulose with DI water. Specifically, 16 mL of each nanocellulose mixture were blended with the stock emulsion (4.5 g) to obtain a final concentration of 2.2% (w/w) canola oil. These were held at 37 °C in a shaking water bath (Model 290400S, Boekel Scientific, USA) prior to the *in vitro* digestion. A control sample was also prepared that contained no added fiber.

Lipid emulsions with nanocellulose or cellulose addition were passed through a static *in vitro* digestion model which consisted of salivary, gastric and intestinal digestion phases.

Specifically, salivary and gastric digestion were carried out according to Liu, Kerr, Kong, Dee, & Lin (2018), while intestinal digestion was performed according to Qin, Yang, Gao, Yao, & McClements (2016) with modifications. Aliquots (1 mL) from samples at the initial phase as well as after salivary, gastric and intestinal digestion phases were collected and used for analysis.

4.2.3.2 Salivary phase

Salivary digestion was initiated via the addition of 6 mL of 'salivary juice' to the initial emulsion system. The 'salivary juice' consisted of 0.1 wt% mucin and 0.2 wt% α-amylase in a buffered solution. The digesta pH was quickly adjusted to 6.8 ± 0.2, followed by incubation at 37°C with a shaking speed of 100 rpm for 5 min. Magnetic stirring was applied during the addition of 'salivary juice' in order to prevent mass accumulation within a small area of the emulsion systems.

4.2.3.3 Gastric phase

The process of gastric digestion was simulated following the salivary phase via the addition of 'gastric juice' (12 mL) composed of 0.5 wt% pepsin and 0.6 wt% mucin in buffered solution. The pH of digesta was then adjusted to 3.0 ± 0.1 and incubated for 2 h at 37°C (100 rpm). Magnetic stirring was applied during the addition of gastric juice as well.

4.2.3.4 Intestinal phase

Following the gastric phase, bile (54 mg/mL bile in 0.1 M PBS (pH 7)) and salt solution (0.25 M $CaCl_2$ and 3.75 M NaCl) were added to the emulsions with a volume of 4.5 mL and 1.925 mL, respectively, and the pH of the mixture was adjusted to 7.00. Lipase solution (24 mg/mL lipase in 5 mM PBS) was prepared and the pH adjusted to 7.0. The intestinal digestion phase was initiated by the addition of 3.2 mL lipase solution to the emulsion mixture and incubated at 37°C (100 rpm) for 2 hr.

During intestinal digestion, the amount of free fatty acid (FFA) produced was titrated with the addition of 0.5 M standardized sodium hydroxide (NaOH) while the pH of the digesta was kept at 7.0. The volume of NaOH needed to neutralize the FFA released was recorded over time and used to calculate the amount of FFA released during the digestion using the formula:

$$\%\text{FFA} = \frac{100 \times V_{N_aOH} \times C_{N_aOH} \times M_{Oil}}{W_{Oil} \times 2} \quad (1)$$

where $C_{N_aOH}$ is the concentration of NaOH used (g/mL), $V_{N_aOH}$ is the amount of NaOH added (mL), $M_{Oil}$ is the molecular weight of canola oil (876.6 g/mol) and $W_{Oil}$ is the mass of oil (g). It was assumed that each triacylglyceride molecule was hydrolyzed into 1 molecule of monoacylglyceride and 2 molecules of free fatty acid. Titration blanks were performed for samples without the addition of canola oil.

The final digesta contained 0.94 wt% oil, 10.4 mM $CaCl_2$, 159 mM NaCl, 1.6 mg/mL lipase and 5 mg/mL bile. Due to the addition of digestive juices, the final nanocellulose concentrations were lower than initial values. During intestinal digestion the corrected concentrations for each were: CNF (0.1%, 0.5% and 1% (w/w)), TEMPO-CNF (0.05%, 0.1%, 0.25% and 0.36% (w/w)), CNC (0.1%, 0.5%, 1%, 2% and 3% (w/w)) and cellulose (1% (w/w)). Results were reported with respect to the final concentration of each fiber.

4.2.4. Determination of particle size

The particle size distribution during each digestion phase was measured using a laser diffraction device (Mastersizer S, Malvern Instruments Ltd., Worcestershire, United Kingdom). The detection range was 0.05 ~ 900 μm with a beam length of 2.4 mm. Sample was added to the detection cell until the obscuration reached the detection range. A mixing rate of 2000 rpm was used inside the chamber to disperse the samples and ensure homogeneity. A polydisperse model and a standard-wet presentation were chosen for the analysis. A relative particle refractive index

of 1.15 was chosen as the refractive indexes of canola oil and nanocellulose/cellulose were 1.465 and 1.47~1.54, respectively, while the refractive index of water is 1.33. Alignment and background measurement were performed before measurement of each sample. Results of particle size were reported as distribution profiles (showing volume fraction (%) versus particle diameter (μm)). $D_{43}$ and volume percentage (%V) were calculated using an in-house MATLAB script (MATLAB R2018b).

4.2.5. Microstructural characterization

The microstructure of emulsion droplets and nanocellulose/cellulose during each digestion phase was characterized by a Zeiss LSM 710 confocal microscope system, using a Zeiss AXIO Observer Z1 inverted microscope stand with transmitted (HAL), UV (HBO) and laser illumination sources. A 63X (oil) objective lens was used to capture images. Solutions of the fluorescent dye Nile Red (0.1% (w/v) dissolved in absolute ethanol) and fluorescent brightener 28 (0.1% (w/v) dissolved in water) were prepared and used for staining of oil droplets and nanocellulose/cellulose, respectively. Control samples, as well as samples containing 1% cellulose, 0.1% CNF, 0.1% TEMPO-CNF and 0.1% CNC during each digestion phase were stained with the fluorescent dyes at a volume ratio of 200:1:1. The stained samples were vortexed for ~5 s to ensure homogeneous staining. A small aliquot of the stained samples (5 μl) was added to a glass slide and covered with a cover slip. The samples were illuminated at the excitation wavelengths of 543 nm and 405 nm corresponding to the Nile red and fluorescent brightener 28, respectively. The emission spectra were collected within 548~669 nm and 410~538 nm for both dyes, respectively. Images were analyzed with the instrument software ZEN 2.3 SP1.

4.2.6. Determination of surface charge (zeta potential)

The surface charge of suspensions containing emulsion droplets and/or macromolecules was measured by electrophoretic light scattering with a NanoBrook 90Plus Zeta instrument (NanoBrook 90Plus Zeta instrument, Brookhaven Instruments Corporation, New York, USA). Prior to analysis, samples were diluted with buffer solution to a concentration of 0.01% (w/v). Specifically, initial and salivary samples were diluted with 1 mM PBS (pH 7.0), while gastric and intestinal samples were diluted with 1 mM citric buffer (pH 3.0) and 0.01 mM PBS (pH 7.0), respectively. The choices of 0.01% (w/w) sample concentration for measurement depended on the ratio of sample and reference count rate as well as the opacity of the diluted samples. The choices of pH and ionic strength of buffer solution depended on the pH of digesta and the conductance of the samples. Measurements were performed at 25°C with 10 continuous runs and results were reported from the average values.

4.2.7 Rheological measurements

The viscosity of suspensions containing emulsion and fiber during each digestion phase was measured using a Discovery HR-2 rheometer (TA instruments, Newcastle, DE) equipped with a 4-blade rotor vane (42 mm in length and 28 mm in diameter). Viscous properties of the samples were measured at 37°C using a flow ramp test over a shear rate range of 1~100 $s^{-1}$. The rate was increased over a 180 s period with a sampling interval of 3 s/pt.

4.2.8 Effect of fiber on lipase activity

The effects of fiber on the activity of α-amylase was determined using a modified method based on McDougall, Kulkarni, & Stewart (2009). Specifically, lipase (10 mg/ml) was dissolved in 100 mM Tris–HCl buffer (pH 8.2). pNP laurate (0.08% W/V) as the substrate was prepared first by dissolving in 5 mM sodium acetate buffer (pH 5.0) containing 1%

Triton X-100. This was followed by heating in boiling water for 1 min. with stirring to aid dissolution, and then cooled to room temperature. The assay was carried out in a total reaction volume of 200 mL containing 40 mL enzyme solution, 80 mL pNP substrate, and different concentrations of CNF (0, 0.01%, 0.1%, 0.4% and 1% (w/w)) at 37 °C in a shaking water bath (Model 290400S, Boekel Scientific, USA). In a similar experiment, a concentration of 2% (w/w) cellulose was studied as a comparison. Aliquots of 1 mL were taken at time intervals (5–300 min), heated in a boiling water bath for 10 min to stop the reaction and centrifuged at 16000 rpm for 2.5 min (AccuSpin Micro 17, ThermoFisher Scientific, Germany). The absorbance of the supernatant was read at 400 nm against the blank and results were reported as the amount of hydrolyzed product produced.

4.2.9 Cholesterol adsorption capacity of fiber

A method based on Zhang, Huang, & Ou (2011) was used to determine the cholesterol adsorption capacity of fiber. Specifically, egg yolk was used as a model food that contains cholesterol. The yolk was whipped well and diluted with 9 volumes of DI water. The equivalent of 2 g CNF or cellulose (d.b.) was mixed well with 50 ml diluted egg yolk at 7.0 (mimicking intestinal pH conditions), respectively. The mixture was then shaken at 80 rpm for 2 hr at 37 °C, followed by centrifugation at 4000 *g* for 20 min. A control experiment was also performed without the addition of fiber.

The cholesterol in the supernatant was extracted and determined by using the modified method of Park (1999). Specifically, 5 ml of supernatant was added to a tube, followed by the addition of 3 ml 95% ethanol and 2 ml 50% KOH. The mixture was capped and thoroughly mixed. Subsequently, the tube was placed in a 60°C water bath for 15 min, followed by cooling to room temperature. 5 ml of hexane was added to the tube and mixed thoroughly, then 3 ml of DI water

was added, mixed, and the tube was set aside for several minutes until the upper hexane layer became clear. 1 mL (if using different volumes, calculate the dilution factor) of the hexane layer was added to a new tube, then the solvent was evaporated in a sealed vacuum oven at 40°C, then the cholesterol content in the tube was determined by the o-phthaladehyde (OPA) method (Park, 1999). Specifically, 4 mL of freshly prepared OPA reagent (0.5 mg/ml in glacial acetic acid) was added to the evaporated tube and mixed thoroughly, then after 10 min, 2 ml concentrated sulfuric acid was added to the tube wall, followed by immediately vortexing. Absorbance of the sample at 550 nm was read against a reagent blank after 20 min. of sulfuric acid addition. The cholesterol concentration in samples was read from a cholesterol standard curve and the adsorption capacity was calculated using the following formula:

$$\text{Cholesterol adsorption capacity} = (C_{control} - C_{fiber}) \times 10 \times \frac{50}{w} \qquad (1)$$

where $C_{control}$ and $C_{fiber}$ are the concentrations of cholesterol in the supernatant of the control and fiber groups, respectively; 10 is the dilution factor of the egg yolk; 50 is the adsorption volume and $w$ is the dry weight of fiber.

4.2.10 Effect of fibers on micellar solubility of cholesterol

The effect of CNF or cellulose on cholesterol solubility in micelles was determined based on a method by Liu, Zhang, & Xia (2008). Specifically, in a total volume of 2.5 mL, the fiber and micelle mixture containing 6.6 mM sodium taurocholate, 0.4 mM cholesterol, 1 mM oleic acid, 132 mM NaCl, and 15 mM PBS (pH 7.4) in the presence of series fiber concentrations (0%, 0.05%, 0.10%, 0.50%, 1% and 2% (w/w) CNF, or 2% (w/w) cellulose) was prepared by sonication. The mixture was then incubated in a shaking water bath at 100 rpm at 37°C for 2 h, followed by centrifugation at 17,000 $g$ for 20 min and the supernatant was collected. The amount of cholesterol in the supernatant was determined by the OPA method as described above.

4.2.11 Effects of fibers on retardation of bile acid diffusion

The effects of fibers on bile acid retardation was determined based on Adiotomre, Eastwood, Edwards, & Brydon (1990). Specifically, in a total volume of 6 mL, 4 mM taurocholic acid (T9034, Sigma) in the presence of 0, 0.05%, 0.1%, 0.5%, 1% and 2% (w/w) CNF was dialyzed in tubing with a molecular weight cutoff (MWCO) of 12,000–14,000 Da (Spectra/Por 4 RC Dialysis Membrane Tubing, Spectrum Laboratories, Los Angeles, CA) against 100 mL of 50 mM phosphate buffer (pH 7.0) containing 0.1% (w/v) sodium azide at 37 °C. A similar experiment was performed with a concentration of 2% cellulose as a comparison. The dialysis was performed for 8 h., with a 2 mL dialysate collected at 1, 2, 3, 4, 6, and 8 hours. The amount of taurocholic acid diffused out was determined by a total bile acids test kit (DZ042A-K01, Diazyme Laboratories, Inc., Poway, CA). The bile acid retardation index (BARI) was calculated by the following formula in order to effectively compare to other studies in literature.

$$BARI = 100(1 - \frac{Bile\ acid\ content\ in\ dialysate\ with\ fiber\ addition}{Bile\ acid\ content\ in\ dialysate\ of\ control}) \quad (2)$$

4.2.12. Statistical analysis

All the measurements were performed in triplicate and analyzed for significance ($p < 0.05$) using Duncan's multiple comparison tests with SAS/STAT software (SAS Institute Inc., Cary, NC). Regression models in the graphs were performed by data analysis and graphing software (OriginLab, Northhampton, MA).

**4.3 Results and discussion**

4.3.1 Particle size measurement of lipid emulsions with nanocellulose

The particle size distributions for each of the emulsion systems are shown in Fig 4.1, at each stage of digestion. Emulsions containing cellulose, CNF, or TEMPO-CNF had two major

peaks, including a peak corresponding to the smaller emulsion particles and the peaks of the fiber itself. Where appropriate, the peaks were analyzed separately to give a $d_{43,lo}$ associated with the smaller diameter population ($d < 3$ μm) and a $d_{43,hi}$ associated with the larger diameter population ($d > 3$ μm). In addition, the volume fraction was determined for each region and designated $\%V_{lo}$ and $\%V_{hi}$. The calculated results are shown in Table 4.1.

The control emulsion initially had a single peak characterized by a $d_{43}$ value of 0.554 μm, with 100% of the particles smaller than 3 μm. The control retained a single peak in the salivary phase with a $d_{43}$ of 0.576 μm. After addition of gastric juice, 3.44% of the control had size > 3 μm ($d_{43,hi}$ = 6.251 μm). The slight increase in size may be due to depletion flocculation caused by mucin, or the aggregation of lipid droplets due to weakened electrostatic repulsion at low pH and high ionic strength (Espinal-Ruiz, Restrepo-Sánchez, Narváez-Cuenca, & McClements, 2016; Zhang, et al., 2015). Specifically, the concentration of mucin in the gastric phase (1.81 mg/mL) was much higher than that in the salivary phase (0.19 mg/mL). A much greater increase in size was noticed with the addition of intestinal juice, as the $\%V_{hi}$ had increased to 81.2% with $d_{43,hi}$ = 40.3 μm. This may be due to the addition of bile salts, ion solution and higher pH (pH 7.0) used in this phase, since all these factors were shown to cause an increase in emulsion size (Chang & McClements, 2016). The addition of salt reduces electrostatic repulsion between droplets allowing lipid particles to approach and flocculate. Moreover, replacement of the surfactant from the droplet surface by bile salt can alter the interaction between droplets (Chang & McClements, 2016). An increase in size of Tween 80 stabilized emulsions after intestinal digestion was also observed by Chang, et al. (2016) as well as Espinal-Ruiz, et al. (2016).

When CNF was added to the emulsion, a second peak was observed with $d_{43,hi}$ ranging from 95 to 106 μm as concentration increased, and the $\%V_{hi}$ ranging from 76 to 95%. Similar

results were seen in the salivary and gastric phase. However, the addition of intestinal liquid caused the formation of larger particles. As noted above, even the control had 81.2% of particles > 3 μm in the intestinal phase. Thus, the loss of lower size particles in the CNF systems is likely due to changes in the emulsion itself.

With TEMPO-CNF a second peak was also observed with $d_{43,hi}$ ranging from 90 to 186 μm. However, the volume of particles in this peak ($\%V_{hi}$ ranging from 20.0 to 53.5%) was much less than that observed with CNF. Slight variations in the peak of TEMPO-CNF at different concentrations may be due to it being able to disperse more easily at lower concentrations, and forming gels at higher concentrations. Little change was observed with addition of salivary juice. Much greater changes were noted upon addition of gastric juice, in which case the $d_{43,hi}$ had increased to 208~383 μm and the $\%V_{hi}$ to 95~ 98%. It is found that TEMPO-CNF aggregates formed during gastric digestion. Other researchers have reported that aggregation or precipitation (in the form of heterogeneous clumps) of TEMPO-CNF occurred upon the addition of salt and lowering pH (pH < 3), resulting in phase separation (Mendoza, Batchelor, Tabor, & Garnier, 2018). This is likely due to reductions in electrostatic repulsion and occurrence of dimerization between carboxyl groups via H-bridges (Belitz, 2009; Maloney, 2015; Mendoza, et al., 2018). Similar phenomena have been reported for other polysaccharides with carboxyl groups including pectin, carboxymethyl cellulose and alginate (Belitz, 2009). No differences in particle size distribution were found between the gastric and intestinal phases for the TEMPO-CNF emulsions.

In contrast with the other fibers, the emulsions with CNC showed only one peak during the initial phase and the volume distribution profiles nearly overlap at any concentration of CNC tested. The $d_{43,lo}$ ranged from 0.553 to 0.612, and with 99.7~100% of the volume in the lower fraction. The size of CNC, as reported within 10~100 nm (Shafiei-Sabet, Hamad, & Hatzikiriakos,

2014; Xu, Atrens, & Stokes, 2017), is much smaller than that of the emulsion droplets, thus it seems reasonable that only one peak was found. The particle size profiles of emulsions containing nanocellulose in our study were similar to those reported by Saelices and Capron (2018). Moreover, microscopic images taken by those authors showed that CNC formed an armored layer around the outside of the oil droplets, which they attributed to the high adsorption energy. In comparison, they found that CNF formed interconnected lateral fibril networks, and TEMPO-CNF formed an entangled gel network.

No changes in particle size distribution were observed when CNC emulsions were taken to the salivary or gastric phases, with $\%V_{lo}$ of 96.9~99.9% and 95.6~96.4%, respectively. It should be noted that CNC has sulfate half-esters in the polysaccharide chains which make it very stable in strong acidic conditions (Belitz, 2009). More significant differences were noticed with the addition of intestinal juice, as a population with relatively large particles size was observed. The lower $d_{43,lo}$ ranged from 1.34 to 1.52 μm, and $d_{43,hi}$ from 70.4 μm to 82.4 μm. The $\%V_{hi}$ ranged from 77.5 to 90.3%, although this did not show a dependence on CNC concentration. While the control emulsion alone showed an increase in particle size, it also influenced the overall particle size distribution once various fibers were added. The particle size of emulsions with different concentrations of CNC was similar to that of control after intestinal digestion, suggesting that CNC did not have much influence on the size of Tween 80 stabilized lipid emulsions during gastrointestinal digestion.

Emulsions with 1% cellulose also had a bimodal particle size distribution with initial $d_{43,lo}$ and $d_{43,hi}$ of 0.745 and 66.7 μm, and with 84.4% of the particles larger than 3 μm. Little change in particle size was observed in the salivary or gastric phases. In the intestinal phase, more of the

lower size population was diminished with 92.2% of particles >3 μm. Again, changes of particle size in the intestinal phase are likely dominated by the changes in the emulsion itself.

4.3.2 Microstructural characterization of lipid emulsions with nanocellulose

The structure of the biopolymer network has been reported to influence lipid digestion (Wooster, et al., 2014). Specifically, lipid droplets may disperse in liquid, or embed within large particles or gels (McClements & Li, 2010). Thus insights into the microstructure of lipid droplets as well as the fiber during each digestion phase are important for the understanding of the transformation and interactions of fiber and the emulsions during the process.

Images by confocal microscopy are shown in Fig 4.2 for lipid emulsions containing 1% (w/w) cellulose or 0.1% (w/w) nanocellulose (CNF, TEMPO-CNF and CNC), where lipid droplets are shown as red and fiber as blue. For the control emulsion, the lipid droplets remained stable during salivary and gastric phase while flocculation and coalescence were observed after the intestinal phase (Fig 4.2 A1-A4). The fact that Tween 80 stabilized emulsions were stable during the salivary and gastric phase was also reported by Zhang, et al. (2015). After the digestion of lipid droplets in the intestinal phase, changes in microstructure of emulsions were expected as the surfactant surrounding lipid droplets were replaced by bile salts, lipase and digestion products. The complex mixtures developed during intestinal digestion were shown to include undigested lipid droplets, calcium soaps, micelles and biopolymer complexes (Espinal-Ruiz, et al., 2016). The increase in lipid droplet size after the intestinal phase (Fig 4.2 A4) corresponds to the particle size results in Fig 4.1. The differences between the size measured in Fig 4.1 and that shown in Fig 4.2 may be because some of the substances in the digesta (including bile salt) were not stained and did not show in the confocal images. In addition, the flocculation and coalescence phenomenon were

also observed in emulsions with nanocellulose (0.1% (w/w) CNF, TEMPO-CNF or CNC) after intestinal digestion (Fig 4.2 C4-E4).

For emulsions with 1% (w/w) cellulose or 0.1% (w/w) CNF, cellulose crystals and nanocellulose fibrils maintained their morphology during each digestion phase (Fig 4.2 B1-B4, C1-C4). The addition of 1% (w/w) cellulose or 0.1% (w/w) CNF did not show much effect on the state of lipid droplets, and no binding or entrapment was observed between cellulose/CNF and lipid droplets. This result agrees with Fig 4.1 which shows the insignificant effect of cellulose/CNF on lipid droplet size.

With the addition of 0.1% (w/w) TEMPO-CNF, some lipid droplets appeared to be entrapped inside the gel or attached to its surface during initial, salivary and gastric phases (Fig 4.2 D1-D3). TEMPO-CNF formed gel structures during all 4 phases. However, several discrete regions were observed during initial and salivary phases (Fig 4.2 D1-D2), while denser gels or aggregates were observed after gastric and intestinal phases (Fig 4.2 D3-D4). This corresponds to the particle size results in Fig 4.1 that indicated aggregation of TEMPO-CNF after gastric and intestinal digestion. Moreover, macroscopic observation of the digesta as shown in Fig S4.2 C2 also showed the aggregation and phase separation of TEMPO-CNF. In particular, following intestinal digestion, most lipid droplets seemed to distribute outside the gel structure, and the size of lipid droplets was similar to that of the control emulsion (Fig 4.2 A4). Similarly, a study of emulsions with added alginate showed that lipid droplets were excluded from the alginate-calcium gel during the intestinal digestion (Qin, et al., 2016). The gel structure of TEMPO-CNF was also observed in emulsions stabilized with the nanocellulose by Saelices and Capron (2018).

Emulsions with the addition of 0.1% (w/w) CNC have a different morphology during each digestion phase. During initial and salivary phases (Fig 4.2 E1-E2), the gel structure of CNC had

lipid droplets located both outside and on its surface. Following gastric digestion (Fig 4.2 E3), the condensed gel structure was replaced by networks of many discrete regions of CNC. This network structure remained even after intestinal digestion (Fig 4.2 E4), and most lipid droplets were attached to the CNC surface.

Based on the particle size results and microstructural images, it appears that all three types of nanocellulose (as well as cellulose) did not cause aggregation of lipid droplets. Both CNF and cellulose are non-ionic and do not interact strongly with lipid droplets or digestive components (including bile salt, enzymes, ions and FFA). In contrast, TEMPO-CNF and CNC are anionic fiber, thus electrostatic repulsion may exist between the anionic fiber and lipid droplets. Similar observations were stated by Qin, et al. (2016), who investigated the effects of alginate on the microstructure of Tween 80 stabilized emulsions.

4.3.3 Zeta-potential of lipid emulsions with nanocellulose

The surface charge of lipid emulsions, as measured by the zeta-potential (ζ), influences their stability during gastrointestinal digestion. However, the surface charge of the fiber is also related to emulsion stability, as is the pH and ionic strength of the digesta. In order to investigate the impact of different concentrations and types of fiber on the surface charge of lipid emulsions during digestion, zeta potential values were tested in all samples during each digestion phase. The results are reported in Fig 4.3.

Even though Tween 80 is a non-ionic surfactant, the control emulsions were found to carry a slightly negative charge. This may be due to free fatty acids or other impurities present in the oil or the preferential adsorption of hydroxyl ions from water (Espinal-Ruiz, et al., 2016). Similar phenomenon have been reported in other studies (Espinal-Ruiz, et al., 2016; Zhang, et al., 2015). Significant differences in ζ for the emulsions alone were found when comparing the different

digestion phases. Specifically, ζ was -15 mV for the initial, -22 mV for the salivary, -11 mV for the gastric and -54 mV for the intestinal phase. The slightly more negative charge in the emulsions during the salivary phase may be due to the presence of anionic mucin molecules, which has also been reported by Espinal-Ruiz, et al. (2016). However, ζ for the gastric phase was closer to zero. This may reflect the much lower pH and higher ionic strength in the gastric phase, both factors which tend to compress the electric double layer and reduce ζ. Once in the intestinal phase, ζ for the emulsions was significantly more negative. The pronouncedly increased negative charge may be due to the presence of numerous anionic species which included bile salt, FFA, and phospholipids (Espinal-Ruiz, et al., 2016). Addition of 1% (w/w) cellulose did not show any significant differences on the zeta-potential of emulsions during all phases of digestion.

Significant differences in zeta potential, as compared to control, were observed in the initial samples with 0.1~0.5% (w/w) CNF. Zeta potential values were not significantly different for CNF samples in the salivary phase. As with the control, CNF samples had ζ values closer to zero in the gastric phase. In the intestinal phase, ζ values were much more negative (-22 to -53 mV). Significant differences were observed in ζ values of 0.5~1% (w/w) CNF compared to that of control in the intestinal phase, which may indicate some interaction between CNF and other digestive components (including bile salt). Studies by DeLoid et al. (2018) showed that CNF could sequester bile salt, which is a property possessed by many dietary fibers (Vahouny, Tombes, Cassidy, Kritchevsky, & Gallo, 1980).

For samples with TEMPO-CNF there were no significant differences in ζ between control and any concentration of TEMPO-CNF during all digestion phases. But in general, samples with TEMPO-CNF had more negative ζ values at greater polymer concentration. TEMPO-CNF carries more negative surface charges than CNF as carboxylate groups have higher surface potential (-75

mV) than that of hydroxyl groups (-25 mV) (Mendoza, et al., 2018). However, this did not seem to result in any pronounced differences in ζ between CNF and TEMPO-CNF samples. Again, taking the digesta to the gastric phase resulted in a ζ much closer to zero, while more negative (-54 ~ -62 mV) after intestinal digestion. This suggests that the anionic nanocellulose did not adsorb to the anionic lipid surface due to the electrostatic repulsion. This is similar to the findings of Qin, et al. (2016) and Espinal-Ruiz, et al. (2016), who observed that the addition of alginate significantly increased the negative charge of emulsions and lower degrees of methoxylation (corresponding to more anionic carboxyl groups) resulted in more increased negative charge in Tween 80 stabilized emulsions.

Initial ζ values for CNC samples ranged from -17 to -26 mV, with samples at the highest concentration having the most negative value. Significant differences in ζ were observed in the initial samples with 3% CNC as compared to the control. As with TEMPO-CNF, this probably reflects the contribution of the anionic polymer to the overall surface charge. Zeta potential in the salivary stage were significantly lower than the initial phase for 0.1% ~ 1% CNC. In the gastric phase ζ had decreased to between -11 and -13 mV, and these values were no different than those for CNF or TEMPO-CNF samples in the gastric phase. As with the other fibers, CNC samples in the intestinal state had the most negative values ranging from -45 to -66 mV.

### 4.3.4 Rheological properties of lipid emulsions with nanocellulose

All samples containing cellulose or nanocellulose were shear-thinning within shear rates of 1 to 100 $s^{-1}$ (Fig S4.1 in supporting information). Shear-thinning behavior of nanocellulose suspensions has been reported by other researchers (Lasseuguette, Roux, & Nishiyama, 2008; Liu, et al., 2018; Shafiei-Sabet, Hamad, & Hatzikiriakos, 2012). This specific range was chosen as the

shear rate in the intestinal brush border has been reported to be in the lower range of 10~100 $s^{-1}$ (Fabek, Messerschmidt, Brulport, & Goff, 2014; Steffe, 1996).

An apparent viscosity at 20 $s^{-1}$ ($\eta_{20}$) was calculated and is shown in Fig 4.4 as a function of concentration. Note that Fig 4.4 reflects the actual concentration of fiber, that is it accounts for the increasing dilution as fluid is added at each digestion stage. The data were also fit by a power law model and the calculated parameters shown in Table 4.2. In some cases, the samples were fluid at low concentrations but showed signs of gelling at higher concentrations once a critical concentration was reached. It was shown that above the critical concentration, overlap of nanocellulose causes entanglement or network formation (Mendoza et al., 2018; Shafiei-Sabet et al., 2012). In those cases, the data were fit to separate power law equations above and below the critical concentration.

The viscosity of the control emulsion was relatively low ($\eta_{20}$ ~2 mPa·s in all the digestion phases). For 1% cellulose addition, the viscosity was significantly different than that of the control during all phases. All three types of nanocellulose-containing lipid emulsions showed greater viscosity at greater concentrations of nanocellulose (NC), which is expected as all of them contribute to the increased effective volume fraction of the dispersed phase. At the same concentration of NC (0.1 wt%), the viscosity of emulsions containing TEMPO-CNF (40 mPa·s) showed significantly higher viscosity than those containing CNF (14.4 mPa·s) or CNC (1.79 mPa·s). It was shown by Tanaka, Saito, Hondo, & Isogai (2015) that higher intrinsic viscosity of nanocellulose is realized with greater aspect ratios, as more flexibility and entanglements are enabled. TEMPO-CNF was shown to have higher viscosity than CNF due to increased fibril individualization and stronger network formation after TEMPO oxidation (Bettaieb, et al., 2015).

In contrast, CNC has much shorter fragments as it is produced through acid hydrolysis. Thus CNC tends to have more fluidity or less viscous at relatively low concentrations.

In the initial phase, samples with 0.23 to 2.34% CNF had a $\eta_{20}$ ranging from 14 to 3306 mPa·s, and were described by a single power law model with slope b = 2.34. At a specific concentration, the viscosity of the CNF solutions did not vary through the different phases of digestion, and the power law dependence decreased only slightly from 2.34 to 1.86. CNF is unmodified and carries only hydroxyl groups with slight surface charges, thus the effects of ionic strength and pH on its rheological properties were much smaller than on anionic nanocellulose (TEMPO-CNF and CNC).

For systems with TEMPO-CNF, the $\eta_{20}$ in the initial phase ranged from 12 to 4337 mPa·s over concentrations of 0.12 to 0.85% (w/w). In addition, the concentration dependence was described by a single power law index (b = 3.0). When compared at the same concentrations, values in the salivary phase were very similar to those in the initial phase. When placed in the gastric phase, TEMPO-CNF samples had significantly lower viscosity than those in the salivary phase at equivalent concentrations. In addition, a biphasic dependence on concentration was noticed. At c < 0.13% (w/w), the power law dependence was b = 0.92; at c > 0.13% (w/w), b = 3.16. Both ionic strength and pH determines the electrostatic interaction between nanocellulose, which can further dictate the gelation and colloidal stability of nanocellulose suspensions (Mendoza, et al., 2018). In the gastric phase, the pH of digesta was adjusted from 7.0 to 3.0 while the calculated ionic strength increased from 15 mM (salivary phase) to 53 mM (gastric phase). Gelation of TEMPO-CNF can occur at increased ionic strength and low pH due to the compression of the electrical double layer around TEMPO-CNF fibrils, resulting in deswelling of the fibrils and phase separation (Fukuzumi, Tanaka, Saito, & Isogai, 2014; Mendoza, et al., 2018). In the

intestinal phase, there was an even greater decrease in $\eta_{20}$ at equivalent concentrations, with a critical concentration at ~0.1%. Here, the power law index was 0.71 at c < 0.1% (w/w) and 2.02 at c > 0.1% (w/w). This may be a sign of even further phase separation at the even higher ionic strength (~226 mM) realized in the intestinal phase. Aside from the effects of pH and ionic strength, digestive components such as mucin may also influence the rheological properties of nanocellulose suspensions (Taylor, Pearson, Draget, Dettmar, & Smidsrød, 2005). As mucin is amphoteric and contains sialic acid, both electrostatic interactions and hydrogen bonding may occur between TEMPO-CNF/CNC and mucin (Menchicchi, et al., 2015).

Even greater differences in rheological properties in the four digestion stages were noticed for samples with CNC. Initially, the $\eta_{20}$ varied from 2 to 232 mPa·s over 0.23 to 1.17% (w/w) CNC. In addition, there was a pronounced critical concentration at ~1% (w/w) CNC, with a very flat response (b = 0.16) at c < 1% (w/w), and stronger concentration dependence (b = 1.29) at c > 1% (w/w). The concentration-dependent rheology in CNC is similar to that reported by Wu, et al. (2014) where the authors observed a critical concentration of 0.4 wt%. This was attributed to the formation of hydrogels at concentrations above the critical value. Viscosity in the salivary phase was similar to that of the initial phase, but had a somewhat lower concentration dependence (b = 0.71) at c > 0.9 % (w/w). In the gastric phase, the $\eta_{20}$ were significantly higher. For example, at 1% (w/w) CNC, $\eta_{20}$ was 2 mPa·s in the salivary phase and 147 mPa·s in the gastric phase. This is in contrast to the samples with CNF or TEMPO-CNF in which the $\eta_{20}$ values were less (at a specific concentration) in the gastric and intestinal phases. The increased CNC viscosity after gastric digestion was also observed in other studies (Nsor-Atindana, et al., 2018). According to Xu, et al. (2017), the influence of pH on CNC viscosity was negligible at high concentrations of CNC (e.g., 5 wt%) in the presence of high salt (0.1 M NaCl). Thus in our study, the increase in

viscosity of digesta in the gastric and intestinal phases is likely due to the increased ionic strength. The high ionic strength can compress the electric double layer and allow the CNC strands to interact. It has been reported that gelation in CNC can occur via van der Waals forces and hydrogen bonds (Bertsch, Isabettini, & Fischer, 2017; Xu, et al., 2017). Thus, the CNC systems in the gastric and intestinal phases had lower critical concentrations.

The differences in rheological properties of the emulsions systems containing CNF, TEMPO-CNF or CNC may also be discussed in terms of changes in the structural features (Fig 4.2). Thus, for samples containing CNF there was little change in morphological features and viscosity in each of the digestive states. For TEMPO-CNF, the decreased in viscosity after gastric digestion due to aggregates formation and phase separation corresponded to the particle size and microstructural results as shown in Fig. 1 and Fig. 2. Similar observations have been made for emulsions with added chitosan, in which the digesta viscosity decreased as the dense chitosan aggregates could not trap much water (Qin, et al., 2016). For samples with CNC, there were signs of gel formation in each digestion stage, but no indication of phase separation. Thus, the increased aggregation of CNC in the gastric and intestinal phases resulted in an increase in viscosity or greater gel-forming ability.

4.3.5 Free fatty acid release during *in vitro* digestion of lipid emulsions with nanocellulose

The influence of fiber on the rate and extent of lipid digestion is shown in Fig 4.5. The initial lipolysis rate and final lipolysis extent were also compared among the emulsions (Fig 4.6). The initial lipolysis rate was calculated based on the slope of the curves with the first few data points (0.5 ~ 1.5 min) in the inserted figures of Fig 4.5(a)-(c). The FFA released during digestion of all lipid emulsions followed a similar pattern. Specifically, the amount of FFA released

increased rapidly in the first few minutes and then increased gradually after 10 min until saturation was reached at around 120 min.

Significant differences were observed in the initial lipolysis rate for high concentrations of nanocellulose (1% (w/w) CNF, 0.25~0.36% (w/w) TEMPO-CNF and 2~3% (w/w) CNC). Nonetheless, the final lipolysis extent was very similar for all the emulsions, even though significant differences were observed for 1% (w/w) CNF and 2% CNC (w/w) addition. The effects of nanocellulose on initial lipolysis rate, but not on its final extent, showed that lipid digestion was slowed down but not prevented. This is similar to the results of Qin, et al. (2016), who reported on the effects of 0.1~0.2 wt% chitosan on the digestion of lipid emulsions. The decrease in lipolysis rates may be due to the substantial increase in viscosity at high fiber concentrations. This increase in viscosity or development of soft gel networks can alter the access and diffusion of lipase to lipid droplets. It has also been suggested that fiber inhibits lipid digestion by inhibiting mixing and mass transport processes (Zhang, et al., 2015). All fibers tested did not have much influence on the aggregation state of lipid droplets, as seen by the particle size and microstructural results presented in Fig. 1 and 2. Moreover, it appears that little if any binding exists between all fibers and lipid droplets, calcium ions or bile salts. The influence of fiber concentration on lipid digestion has been reported by Qin, et al. (2016) who found that low concentrations (0.1~0.2 wt%) of alginate did not influence initial lipolysis rates of lipid emulsions, while high concentrations of the two fibers caused significant reductions in the amount of FFA released.

CNF and cellulose did not have an impact on lipid digestion, which may be because both are non-ionic fiber that do not interact strongly with charged components in the digestive fluids. Similar observations were found with LBG, a neutral fiber, which did not influence the extent of lipolysis of protein-stabilized emulsions (Qin, et al., 2016). In the case of TEMPO-CNF, despite

the fact that gels were formed in the gastric phase, the dense gel resulted in its separation from the bulk liquid causing the viscosity to decrease instead, thus this did not totally prevent the access of lipase to the lipid droplets. Based on the microstructural images, even though TEMPO-CNF formed aggregates after gastric digestion, the lipid droplets were still exposed mostly outside of the aggregates. Thus the lipid droplets were still accessible to the lipase hydrolysis. In related research, Espinal-Ruiz, et al. (2016) proposed that low methoxylated pectin carried high amounts of negative surface charge and the electrostatic repulsion between pectin and lipid droplets resulted in an open structure for lipase access. In the case of CNC, even though it formed a hydrogel during gastric and intestinal digestion, the porous network (as seen in Fig 4.2) still allowed the access of lipase during intestinal digestion. This lack of effectiveness of negative charged nanocellulose to limit FFA release is similar to that of fucoidan, an anionic fiber which had no effect on the final digestion extent of Tween 80 stabilized emulsions (Chang, et al., 2016).

4.3.6 Effects of fiber on lipase activity

Results from Fig 4.7 showed that the lipolysis reaction in all samples steadily progressed and reached steady values after 300 min. A concentration of 1% (w/w) CNF addition resulted in the lowest amount of product produced over time. All concentrations of CNF addition showed significant differences to control, though no significant difference was observed between all concentrations of CNF. Cellulose addition did not cause any significant differences, which are similar to results reported by Lairon et al. (1985) (who observed that cellulose did not show marked effects on pancreatic lipase activity *in vitro*). However, other studies showed that Solka-Floc (containing 85-99.5% cellulose and up to 15% hemicellulose) or purified cellulose inhibited lipase activity *in vivo* or *in vitro* (Dunaif & Schneeman, 1981; Dutta & Hlasko, 1985; Schneeman, 1978; Schneeman & Gallaher, 1980). Slightly increased enzyme activity was even observed by Ikeda &

Kusano (1983). The varied findings among these studies were ascribed to the differences in fiber source, purity, fiber dosage, experimental conditions, and test methodologies.

Viscous fibers have been shown to decrease triglyceride hydrolysis in vitro by increasing lipid droplets size, resulting in less available area for lipase access (Lairon, 1997). Zhai, Gunness, & Gidley (2016) showed that the inhibition effect of soluble fibers on lipolysis was mainly due to the increased droplet size instead of increased viscosity. In addition, some dietary fibers showed lipase inhibition effects due to their interaction with lipase via polar or ionic sites of fiber (Chater, Wilcox, Brownlee, & Pearson, 2015). Since CNF is unmodified, and slightly charged due to the presence of large quantities of hydroxyl groups, it does not exhibit ionic interference effects or strong binding with enzymes. The mechanism of CNF addition on slightly reduced lipase activity can be related to the barriers and viscous effects exerted by CNF. Interactions between CNF and substrate/lipase may also occur, which hinders the interaction between substrate and lipase themselves. The significant effects of CNF on lipase but not on α-amylase or α-glucosidase may indicate some interaction between CNF and pNP laurate/lipase (Liu, Kerr, Kong, Dee, & Lin, 2018). Understanding of a more detailed mechanism would require further study.

4.3.7 Cholesterol adsorption capacity of fiber

Results from Table 4.3 showed that CNF had higher cholesterol adsorption capacity than cellulose. Specifically, CNF and cellulose could adsorb 99.99% and 84% of cholesterol, respectively which amounts to 8.5 and 7.1 mg cholesterol per gram dry weight of fiber. Results in this study were similar to those reported in other literature. As an example, Jin, Yu, Wang, Li, & Li (2017) showed that cellulose could adsorb 5~10 mg cholesterol per gram of fiber, which was much lower than that by water-soluble chitosan (50~65 mg/g). The amount of cholesterol adsorbed by dry grain legume seeds (including bean, lentil, pea and soybean) with a particle size of 1 mm

varied from 45%~96% (Górecka, Korczak, & Flaczyk, 2003). In addition, Zhang et al. (2011) showed that the cholesterol adsorption capacity of several fiber sources (including wheat bran, soybean hull, apple peel and mixed fiber) varied from 3.48 mg/g to 11.34 mg/g. Thus CNF showed slightly higher cholesterol adsorption capacity than that of soybean hull (7.4 mg/g) but lower than that of apple peel (11.34 mg/g) or water-soluble chitosan.

The cholesterol adsorption capacity of fibers was shown to be affected by the particle size, where smaller size correlated to larger specific surface area and more adsorption site. For example, 30% increase in cholesterol adsorption was observed in soybean when reducing the particle size from 1 mm to 0.2 mm (Górecka et al., 2003). Furthermore, the authors (Górecka et al., 2003) observed higher cholesterol adsorption capacity in other legume seeds (including bran, lentil, and pea) with smaller particle size. Thus the higher cholesterol adsorption capacity observed in CNF than cellulose may be related to its larger specific surface area and its gel trapping property.

4.3.8 Effect of fibers on micellar solubility of cholesterol

Results from Fig 4.8 showed that CNF or cellulose did not reduce the micellar solubility of cholesterol. Similarly, cellulose was found to show little affinity (~5%) for micellar lipid binding (Vahouny, Tombes, Cassidy, Kritchevsky, & Gallo, 1981). A number of *in vivo* studies showed that cellulose addition resulted in reduced serum cholesterol levels (Chau, Chen, & Wang, 2004), but some showed no effects (Kritchevsky, 1987). Studies by van Bennekum, Nguyen, Schulthess, Hauser, & Phillips (2005) showed that cellulose in the diet did not affect intestinal cholesterol absorption, though it was concluded by the authors that the cholesterol-lowering properties of insoluble fiber was due to its effect on satiation and satiety.

Viscous soluble fibers are often hypocholesterolemic since they reduce the micellar solubility of cholesterol (Brown, Rosner, Willett, & Sacks, 1999). For example, guar gum, pectin,

oat bran, and psyllium have been shown to be hypocholesterolemic *in vivo* (Brown et al., 1999). Thus our study showed that CNF is as inert as cellulose regarding its effect on micellar solubility of cholesterol. The results in Table 4.3 and Fig 4.8 may seem contradictory, but the test methodologies and the ratios of fiber to cholesterol were different. Moreover, in the cholesterol adsorption experiment, the cholesterol in the egg yolk is mainly in the form of low-density lipoprotein (Kuang, Yang, Zhang, Wang, & Chen, 2018) and some cholesterol may precipitate with proteins which may not be available for binding by the fibers. It seems that CNF could weakly adsorb some cholesterol via physical interaction or entrapment, but it did not influence the solubility/concentration of cholesterol in micelles. Thus CNF may not influence cholesterol absorption *in vivo*, though certain minute amount of cholesterol adsorption may occur, especially for cholesterol from egg yolk.

4.3.9 The effects of fibers on bile acid diffusion

The effect of fibers on bile acid diffusion flux is shown in Fig 4.9. A linear diffusion trend was observed in all samples. This is similar to that observed by Im & Yoon (2015), where a linear increase occurred in the amount of bile acid diffusion over a 8-hr time period. According to Han, Lee, & Rhee (2009), the dialysis time required for reaching equllibrium was more than 18 h. for control, which indicated that the simulation of bile acid transport via dialysis membrane was slow.

CNF at concentrations higher than 0.1% (w/w) caused significantly lower amount of bile acid diffusion than control. 2% CNF resulted in significantly lower diffusion rate than others. In particular, after 8 h, the percent bile acid diffusion in control was 8.0%, while it was 5.84% in samples containing 2% (w/w) CNF. The diffusion rate with an addition of 2% (w/w) CNF was 0.46 (percent bile acid per hr) while it was 0.68 in the control. The BARI of 2% (w/w) CNF at 8 hrs. was 27, while BARI of 0.1%~1% (w/w) CNF varied from 16.2~19.6. The bile acid retardation

index was shown to vary among fibers as well as diffusion time (Im & Yoon, 2015). According to Adiotomre et al. (1990), the BARI of wheat bran (coarse) was around 11%, and BARI in fibers can vary from 5.1% (Karaya, at 1 h diffusion time) to 41% (guar, at 1 h). For a diffusion time 8 hrs., the BARI of carboxymethyl cellulose (CMC) and pectin were 28 and 32, respectively. Thus the BARI of CNF was within the range studied. The BARI of 2% (w/w) CNF was close to that observed in CMC, but lower than pectin.

It was observed that 2% (w/w) cellulose did not show any significant effects on the bile acid diffusion, which is similar to the *in vivo* results from other literature where cellulose had slight or no effects on bile acid excretion (Eastwood, Kirkpatrick, Mitchell, Bone, & Hamilton, 1973; Gallaher & Schneeman, 1986). Studies have shown that bile acid reduction by fiber can cause hypocholesterolemic effects, since the reduced amount of bile acid available due to the excretion of bile acid bound by fiber will trigger further conversion of cholesterol to bile acid, which can then reduce the amount of cholesterol available. On the other hand, the reduced amount of bile acid will cause less micelle formation, which in turn decreases the amount of solubilized lipids and cholesterol. This will then result in a decreased absorption of lipids and cholesterol (Gallaher & Schneeman, 1986). Thus it is possible that CNF may exert hypocholesterolemic effects due to its effects on bile acid diffusion.

**4.4 Conclusions**

The results from this study suggest that three types of nanocellulose at high concentrations delayed the digestion of Tween 80 stabilized lipid emulsions due to increased viscosity, though the final extent of lipolysis was nearly the same amongst all samples. The addition of nanocellulose did not appear to influence the aggregation state of lipid emulsions. However, the types and concentrations of nanocellulose play a role in the physicochemical characteristics including

particle size, microstructure, viscosity and zeta potential of the emulsions during different digestion phases. It was noted that the increase in digesta viscosity is concentration-dependent. The differences in ionic strength, pH, and digestive components during each digestion phase have distinct effects on the behavior of lipid emulsions as well as the fate of nanocellulose. Specifically, lipid emulsions were stable during salivary and gastric digestion, but flocculation and coalescence of lipid droplets were observed in the intestinal phase. Furthermore, the behavior of each type of nanocellulose also differed during gastrointestinal digestion. No morphological changes were observed in cellulose and CNF during the entire digestion phase. However, gelation of TEMPO-CNF and CNC after gastric digestion was observed. TEMPO-CNF aggregates formed during gastric digestion but a decrease in viscosity was observed due to de-swelling and phase separation of TEMPO-CNF gels. Even though CNC gelation was also found during gastric digestion, the suspension was stable causing an increase in digesta viscosity. The effect of increased digesta viscosity with all three types of nanocellulose addition shows that there is a potential of incorporating them in developing functional foods as rheology modifiers as well as to delay lipid digestion and reduce further absorption. Further research should be performed, including *in vivo* studies regarding the effects of these three types of nanocellulose on digestion of lipid emulsions to validate these results. Moreover, CNF significantly reduced lipase activity and showed higher bile acid retardation effect when compared to cellulose. In addition, slightly higher cholesterol adsorption capacity was observed in CNF than cellulose, though CNF did not affect micellar solubility of cholesterol.

### 4.5 Acknowledgements

This work was supported by the USDA National Institute of Food and Agriculture [grant no. 2016-67021-24994].

## 4.6 Supporting Information

Viscosity of lipid emulsions with different concentrations of fiber as a function of shear rate (1~100 $s^{-1}$) after each *in vitro* digestion phase was shown in Fig S4.1.

## 4.7 References


Adiotomre, J., Eastwood, M. A., Edwards, C., & Brydon, W. G. (1990). Dietary fiber: in vitro methods that anticipate nutrition and metabolic activity in humans. *The American journal of clinical nutrition,* 52(1), 128-134.

Belitz, H. D., Grosch, W. and Schieberle, P. (2009). Carbohydrates. In *Food Chemistry* (4th ed. ed., pp. 296-309). Berlin, Germany: Springer.

Bertsch, P., Isabettini, S., & Fischer, P. (2017). Ion-Induced Hydrogel Formation and Nematic Ordering of Nanocrystalline Cellulose Suspensions. *Biomacromolecules, 18*(12), 4060-4066.

Bettaieb, F., Nechyporchuk, O., Khiari, R., Mhenni, M. F., Dufresne, A., & Belgacem, M. N. (2015). Effect of the oxidation treatment on the production of cellulose nanofiber suspensions from Posidonia oceanica: The rheological aspect. *Carbohydrate polymers, 134*, 664-672.

Brown, L., Rosner, B., Willett, W. W., & Sacks, F. M. (1999). Cholesterol-lowering effects of dietary fiber: a meta-analysis. *The American journal of clinical nutrition*, 69(1), 30-42.

Chang, Y., & McClements, D. J. (2016). Influence of emulsifier type on the in vitro digestion of fish oil-in-water emulsions in the presence of an anionic marine polysaccharide (fucoidan): Caseinate, whey protein, lecithin, or Tween 80. *Food Hydrocolloids, 61*, 92-101.

Chater, P. I., Wilcox, M. D., Brownlee, I. A., & Pearson, J. P. (2015). Alginate as a protease inhibitor in vitro and in a model gut system; selective inhibition of pepsin but not trypsin. *Carbohydrate polymers*, 131, 142-151.

Chau, C.-F., Chen, C.-H., & Wang, Y.-T. (2004). Effects of a novel pomace fiber on lipid and cholesterol metabolism in the hamster. *Nutrition Research,* 24(5), 337-345.

DeLoid, G. M., Sohal, I. S., Lorente, L. R., Molina, R. M., Pyrgiotakis, G., Stevanovic, A., . . . Bousfield, D. W. (2018). Reducing Intestinal Digestion and Absorption of Fat Using a Nature-Derived Biopolymer: Interference of Triglyceride Hydrolysis by Nanocellulose. *ACS nano*, 12 (7), 6469–6479.

Dunaif, G., & Schneeman, B. (1981). The effect of dietary fiber on human pancreatic enzyme activity in vitro. *The American journal of clinical nutrition,* 34(6), 1034-1035.

Dutta, S. K., & Hlasko, J. (1985). Dietary fiber in pancreatic disease: effect of high fiber diet on fat malabsorption in pancreatic insufficiency and in vitro study of the interaction of dietary fiber with pancreatic enzymes. *The American journal of clinical nutrition,* 41(3), 517-525.

Eastwood, M., Kirkpatrick, J., Mitchell, W., Bone, A., & Hamilton, T. (1973). Effects of dietary supplements of wheat bran and cellulose on faeces and bowel function. *Br Med J,* 4(5889), 392-394.

Espinal-Ruiz, M., Restrepo-Sánchez, L.-P., Narváez-Cuenca, C.-E., & McClements, D. J. (2016). Impact of pectin properties on lipid digestion under simulated gastrointestinal conditions: comparison of citrus and banana passion fruit (Passiflora tripartita var. mollissima) pectins. *Food Hydrocolloids, 52,* 329-342.

Fabek, H., Messerschmidt, S., Brulport, V., & Goff, H. D. (2014). The effect of in vitro digestive processes on the viscosity of dietary fibres and their influence on glucose diffusion. *Food Hydrocolloids, 35,* 718-726.

Fukuzumi, H., Tanaka, R., Saito, T., & Isogai, A. (2014). Dispersion stability and aggregation behavior of TEMPO-oxidized cellulose nanofibrils in water as a function of salt addition. *Cellulose, 21*(3), 1553-1559.

Gallaher, D., & Schneeman, B. O. (1986). Intestinal interaction of bile acids, phospholipids, dietary fibers, and cholestyramine. *American journal of physiology-Gastrointestinal and liver physiology,* 250(4), G420-G426.

Górecka, D., Korczak, J., & Flaczyk, E. (2003). Adsorption of bile acids and cholesterol by dry grain legume seeds. *Polish journal of food and nutrition sciences,* 12(1), 69-72.

Han, S.-H., Lee, S.-W., & Rhee, C. (2009). Effect of heat treatment of digestion-resistant fraction from soybean on retarding of bile acid transport in vitro. *Nutrition research and practice,* 3(2), 149-155.

Ikeda, K., & Kusano, T. (1983). In vitro inhibition of digestive enzymes by indigestible polysaccharides. *Cereal Chem,* 60(4), 260-263.

Im, H. J., & Yoon, K. Y. (2015). Production and Characterisation of Alcohol-Insoluble Dietary Fibre as a Potential Source for Functional Carbohydrates Produced by Enzymatic Depolymerisation of Buckwheat Hulls. *Czech Journal of Food Science,* 33(5), 449 – 457.

Jin, Q., Yu, H., Wang, X., Li, K., & Li, P. (2017). Effect of the molecular weight of water-soluble chitosan on its fat-/cholesterol-binding capacities and inhibitory activities to pancreatic lipase. *PeerJ,* 5, e3279.

Jowkarderis, L., & van de Ven, T. G. (2015). Mesh size analysis of cellulose nanofibril hydrogels using solute exclusion and PFG-NMR spectroscopy. *Soft matter*, *11*(47), 9201-9210.

Kritchevsky, D. (1987). Dietary fibre and lipid metabolism. *Int J Obes.*, 11 Suppl 1:33-43.

Kuang, H., Yang, F., Zhang, Y., Wang, T., & Chen, G. (2018). The Impact of Egg Nutrient Composition and Its Consumption on Cholesterol Homeostasis. *Cholesterol*, 1-22.

Lairon, D. (1997). *Soluble fibers and dietary lipids*. In *Dietary fiber in health and disease* (pp. 99-108): Springer

Lairon, D., Lafont, H., Vigne, J.-L., Nalbone, G., Léonardi, J., & Hauton, J. C. (1985). Effects of dietary fibers and cholestyramine on the activity of pancreatic lipase in vitro. *The American journal of clinical nutrition,* 42(4), 629-638.

Lasseuguette, E., Roux, D., & Nishiyama, Y. (2008). Rheological properties of microfibrillar suspension of TEMPO-oxidized pulp. *Cellulose, 15*(3), 425-433.

Liu, J., Zhang, J., & Xia, W. (2008). Hypocholesterolaemic effects of different chitosan samples in vitro and in vivo. *Food Chemistry,* 107(1), 419-425.

Liu, L., Kerr, W. L., Kong, F., Dee, D. R., & Lin, M. (2018). Influence of nano-fibrillated cellulose (NFC) on starch digestion and glucose absorption. *Carbohydrate polymers*, 196, 146-153.

Lin, N., & Dufresne, A. (2014). Nanocellulose in biomedicine: Current status and future prospect. *European Polymer Journal, 59*, 302-325.

Liu, L., Kerr, W. L., Kong, F., Dee, D. R., & Lin, M. (2018). Influence of Nano-Fibrillated Cellulose (NFC) on Starch Digestion and Glucose Absorption. *Carbohydrate polymers, 196*, 146-153.

Mackie, A., Bajka, B., & Rigby, N. (2016). *Dietary Fibre: More than a Prebiotic*. In *Gums and Stabilisers for the Food Industry 18* (pp. 227-234).

Maloney, T. C. (2015). Network swelling of TEMPO-oxidized nanocellulose. *Holzforschung, 69*(2), 207-213.

McClements, D. J., & Li, Y. (2010). Review of in vitro digestion models for rapid screening of emulsion-based systems. *Food & function, 1*(1), 32-59.

McDougall, G. J., Kulkarni, N. N., & Stewart, D. (2009). Berry polyphenols inhibit pancreatic lipase activity in vitro. *Food Chemistry,* 115(1), 193-199.

Menchicchi, B., Fuenzalida, J., Hensel, A., Swamy, M., David, L., Rochas, C., & Goycoolea, F. (2015). Biophysical analysis of the molecular interactions between polysaccharides and mucin. *Biomacromolecules, 16*(3), 924-935.

Mendoza, L., Batchelor, W., Tabor, R. F., & Garnier, G. (2018). Gelation mechanism of cellulose nanofibre gels: A colloids and interfacial perspective. *Journal of colloid and interface science, 509*, 39-46.

Mertaniemi, H. (2017). Studies on nanocellulose-Functional microparticles, threads, and aerogels of cellulose nanofibrils (Doctoral dissertation). Aalto University.

Moon, R. J., Schueneman, G. T., & Simonsen, J. (2016). Overview of cellulose nanomaterials, their capabilities and applications. *JOM, 68*(9), 2383-2394.

Nsor-Atindana, J., Goff, H. D., Liu, W., Chen, M., & Zhong, F. (2018). The resilience of nanocrystalline cellulose viscosity to simulated digestive processes and its influence on glucose diffusion. *Carbohydrate polymers*, *200*, 436-445.

Park, Y. (1999). Cholesterol contents of US and imported goat milk cheeses as quantified by different colorimetric methods. *Small Ruminant Research,* 32(1), 77-82.

Qin, D., Yang, X., Gao, S., Yao, J., & McClements, D. J. (2016). Influence of Hydrocolloids (Dietary Fibers) on Lipid Digestion of Protein-Stabilized Emulsions: Comparison of Neutral, Anionic, and Cationic Polysaccharides. *Journal of food science, 81*(7), C1636-C1645.

Roman, M. (2015). Toxicity of cellulose nanocrystals: a review. *Industrial Biotechnology, 11*(1), 25-33.

Saelices, C. J., Capron, I. (2018). Design of Pickering micro and nanoemulsions based on the structural characteristics of nanocelluloses. *Biomacromolecules, 19*, 460-469.

Sarkar, A., Li, H., Cray, D., & Boxall, S. (2018). Composite whey protein–cellulose nanocrystals at oil-water interface: Towards delaying lipid digestion. *Food Hydrocolloids,* 77, 436-444.

Sarkar, A., Zhang, S., Murray, B., Russell, J. A., & Boxal, S. (2017). Modulating in vitro gastric digestion of emulsions using composite whey protein-cellulose nanocrystal interfaces. *Colloids & Surfaces B: Biointerfaces,* 158, 137-146.

Schneeman, B. O. (1978). Effect of plant fiber on lipase, trypsin and chymotrypsin activity. *Journal of Food Science,* 43(2), 634-635.

Schneeman, B. O., & Gallaher, D. (1980). Changes in small intestinal digestive enzyme activity and bile acids with dietary cellulose in rats. *The Journal of nutrition,* 110(3), 584-590.

Shafiei-Sabet, S., Hamad, W., & Hatzikiriakos, S. (2014). Ionic strength effects on the microstructure and shear rheology of cellulose nanocrystal suspensions. *Cellulose, 21*(5), 3347-3359.

Shafiei-Sabet, S., Hamad, W. Y., & Hatzikiriakos, S. G. (2012). Rheology of nanocrystalline cellulose aqueous suspensions. *Langmuir, 28*(49), 17124-17133.

Steffe, J. F. (1996). *Rheological methods in food process engineering*. East Lansing: Freeman press.

Sugano, M., Ikeda, I., Imaizumi, K., & Lu, Y.-F. (1990). Dietary fiber and lipid absorption. In C. B. David Kritchevsky, James W. Anderson (Ed.), *Dietary Fiber: Chemistry, Physiology, and Health Effects* (pp. 137-156). New York: Springer.

Tanaka, R., Saito, T., Hondo, H., & Isogai, A. (2015). Influence of flexibility and dimensions of nanocelluloses on the flow properties of their aqueous dispersions. *Biomacromolecules, 16*(7), 2127-2131.

Taylor, C., Pearson, J. P., Draget, K. I., Dettmar, P. W., & Smidsrød, O. (2005). Rheological characterisation of mixed gels of mucin and alginate. *Carbohydrate polymers, 59*(2), 189-195.

Vahouny, G. V., Tombes, R., Cassidy, M. M., Kritchevsky, D., & Gallo, L. L. (1980). Dietary fibers: V. Binding of bile salts, phospholipids and cholesterol from mixed micelles by bile acid sequestrants and dietary fibers. *Lipids,* 15(12), 1012-1018.

Vahouny, G., Tombes, R., Cassidy, M., Kritchevsky, D., & Gallo, L. (1981). Dietary fibers VI: binding of fatty acids and monolein from mixed micelles containing bile salts and lecithin. *Proceedings of the Society for Experimental Biology and Medicine,* 166(1), 12-16.

van Bennekum, A. M., Nguyen, D. V., Schulthess, G., Hauser, H., & Phillips, M. C. (2005). Mechanisms of cholesterol-lowering effects of dietary insoluble fibres: relationships with intestinal and hepatic cholesterol parameters. *British Journal of Nutrition,* 94(3), 331-337.

Wang, H., Qian, C., & Roman, M. (2011). Effects of pH and salt concentration on the formation and properties of chitosan–cellulose nanocrystal polyelectrolyte–macroion complexes. *Biomacromolecules, 12*(10), 3708-3714.

Wooster, T. J., Day, L., Xu, M., Golding, M., Oiseth, S., Keogh, J., & Clifton, P. (2014). Impact of different biopolymer networks on the digestion of gastric structured emulsions. *Food Hydrocolloids, 36*, 102-114.

Wu, Q., Meng, Y., Wang, S., Li, Y., Fu, S., Ma, L., & Harper, D. (2014). Rheological behavior of cellulose nanocrystal suspension: influence of concentration and aspect ratio. *Journal of Applied Polymer Science, 131*(15), 40525.

Xu, Y., Atrens, A. D., & Stokes, J. R. (2017). Rheology and microstructure of aqueous suspensions of nanocrystalline cellulose rods. *Journal of colloid and interface science, 496*, 130-140.

Zhai, H., Gunness, P., & Gidley, M. J. (2016). Effects of cereal soluble dietary fibres on hydrolysis of p-nitrophenyl laurate by pancreatin. *Food & function*, 7(8), 3382-3389.

Zhang, N., Huang, C., & Ou, S. (2011). In vitro binding capacities of three dietary fibers and their mixture for four toxic elements, cholesterol, and bile acid. *Journal of hazardous materials*, 186(1), 236-239.

Zhang, R., Zhang, Z., Zhang, H., Decker, E. A., & McClements, D. J. (2015). Influence of emulsifier type on gastrointestinal fate of oil-in-water emulsions containing anionic dietary fiber (pectin). *Food Hydrocolloids, 45*, 175-185.

Zhou, Y., Fuentes-Hernandez, C., Khan, T. M., Liu, J. C., Hsu, J., Shim, J. W., ... & Kippelen, B. (2013). Recyclable organic solar cells on cellulose nanocrystal substrates. *Scientific reports, 3*, 1536.

Table 4.1. $D_{43}$ and volume percentage (%V) of peaks in particle size distribution of lipid emulsions after each digestion phase (as shown in Fig 4.1)

| Fiber | *Initial* | | | | *Salivary* | | | | *Gastric* | | | | *Intestinal* | | | |
|---|---|---|---|---|---|---|---|---|---|---|---|---|---|---|---|---|
| %wt | $d_{43}$ hi | $d_{43}$ lo | %V hi | %V lo | $d_{43}$ hi | $d_{43}$ lo | %V hi | %V lo | $d_{43}$ hi | $d_{43}$ lo | %V hi | %V lo | $d_{43}$ hi | $d_{43}$ lo | %V hi | %V lo |
| CNF | | | | | | | | | | | | | | | | |
| 0 | NP[a] | 0.554 | 0 | 100.0 | NP | 0.576 | 0.06 | 99.9 | 6.251 | 0.632 | 3.44 | 96.6 | 40.3 | 1.651 | 81.2 | 18.8 |
| 0.1 | 95.3 | 0.669 | 75.8 | 24.2 | 94.8 | 0.688 | 76.9 | 23.1 | 94.5 | 0.704 | 78.5 | 21.5 | 94.6 | 1.634 | 91.2 | 8.8 |
| 0.5 | 105.2 | 0.941 | 92.9 | 7.1 | 107.0 | 0.927 | 92.8 | 7.16 | 105.9 | 0.965 | 93.3 | 6.69 | 107.9 | 1.765 | 95.2 | 4.8 |
| 1 | 106.0 | 1.098 | 95.0 | 5.0 | 107.3 | 1.169 | 95.6 | 4.38 | 108.8 | 1.204 | 95.9 | 4.12 | 109.2 | 1.839 | 96.7 | 3.3 |
| TEMPO | | | | | | | | | | | | | | | | |
| 0 | NP | 0.554 | 0.0 | 100 | 3.60 | 0.576 | 0.064 | 99.9 | 6.250 | 0.632 | 3.45 | 96.6 | 40.3 | 1.651 | 81.2 | 18.8 |
| 0.05 | 145.1 | 0.573 | 20.0 | 80.0 | 139.8 | 0.567 | 27.7 | 72.3 | 208.1 | 0.592 | 96.2 | 3.78 | 118.9 | 1.530 | 92.5 | 7.5 |
| 0.10 | 148.6 | 0.618 | 40.5 | 59.6 | 137.4 | 0.608 | 57.7 | 42.3 | 298.4 | 0.644 | 97.7 | 2.31 | 171.4 | 1.298 | 97.1 | 2.9 |
| 0.25 | 89.6 | 1.016 | 41.7 | 58.3 | 172.6 | 1.064 | 58.7 | 41.3 | 380.8 | 0.978 | 95.9 | 4.09 | 274.4 | 1.296 | 98.4 | 1.6 |
| 0.36 | 185.7 | 1.133 | 53.5 | 46.5 | 120.9 | 1.146 | 56.2 | 43.8 | 382.7 | 1.239 | 94.9 | 5.09 | 315.9 | 1.515 | 97.9 | 2.1 |
| CNC | | | | | | | | | | | | | | | | |
| 0 | NP | 0.554 | 0 | 100 | 3.60 | 0.576 | 0.064 | 99.9 | 6.250 | 0.632 | 3.45 | 96.6 | 40.3 | 1.651 | 81.2 | 18.8 |
| 0.1 | NP | 0.553 | 0 | 100 | 3.60 | 0.578 | 0.051 | 99.9 | 8.078 | 0.621 | 4.40 | 95.6 | 74.3 | 1.517 | 90.3 | 9.7 |
| 0.5 | NP | 0.546 | 0.083 | 99.9 | 3.60 | 0.608 | 0.320 | 99.7 | 7.289 | 0.614 | 3.63 | 96.4 | 70.4 | 1.512 | 77.5 | 22.5 |
| 1.0 | 3.598 | 0.556 | 0.163 | 99.8 | 9.56 | 0.625 | 3.057 | 96.9 | 7.672 | 0.620 | 3.97 | 96.0 | 82.4 | 1.421 | 84.0 | 16.0 |
| 2.0 | 3.607 | 0.565 | 0.114 | 99.9 | 4.13 | 0.635 | 0.717 | 99.3 | 6.659 | 0.677 | 3.96 | 96.0 | 78.1 | 1.399 | 82.9 | 17.1 |
| 3.0 | 3.659 | 0.612 | 0.311 | 99.7 | 3.60 | 0.630 | 0.211 | 99.8 | 7.415 | 0.685 | 4.34 | 95.7 | 76.0 | 1.339 | 82.4 | 17.6 |
| Cellulose | | | | | | | | | | | | | | | | |
| 1.0 | 66.68 | 0.7446 | 84.4 | 15.5 | 68.3 | 0.739 | 84.1 | 15.8 | 68.5 | 0.772 | 85.8 | 14.2 | 87.1 | 1.581 | 92.2 | 7.76 |

[a]NP represents no particles in this region.

Table 4.2. Parameters for the curves of apparent viscosity (η) at 20 $s^{-1}$ versus nanocellulose concentration (C) fitted by Power law model (log η = a + blog C) (as shown by Fig 4.4)

| Fiber | Phase | Fitting | | | | |
|---|---|---|---|---|---|---|
| | | Concentration range (w/w) | | Parameters | | |
| | | Low | High | a | b | Adj. $R^2$ |
| CNF | Initial | 0.23% | 2.34% | 4.316 | 2.341 | 0.9999 |
| | Salivary | 0.18% | 1.81% | 3.928 | 2.135 | 0.9980 |
| | Gastric | 0.13% | 1.25% | 3.557 | 1.981 | 0.9945 |
| | Intestine | 0.10% | 1.00% | 3.232 | 1.860 | 0.9775 |
| TEMPO-CNF | Initial | 0.12% | 0.85% | 6.914 | 2.997 | 0.9798 |
| | Salivary | 0.09% | 0.65% | 5.731 | 2.563 | 0.9811 |
| | Gastric | 0.06% | 0.13% | 0.576 | 0.917 | -- |
| | | 0.13% | 0.45% | 7.072 | 3.155 | 0.9998 |
| | Intestine | 0.05% | 0.10% | -0.261 | 0.708 | -- |
| | | 0.10% | 0.36% | 3.672 | 2.020 | 0.9957 |
| CNC | Initial | 0.23% | 1.17% | -2.324 | 0.161 | |
| | | 1.17% | 7.04% | -0.184 | 1.295 | 0.8395 |
| | Salivary | 0.18% | 0.91% | -2.554 | 0.075 | |
| | | 0.91% | 5.45% | -1.280 | 0.714 | 0.7530 |
| | Gastric | 0.13% | 0.63% | 1.234 | 1.253 | -- |
| | | 0.63% | 3.75% | 2.790 | 1.910 | 0.9967 |
| | Intestine | 0.10% | 0.50% | 0.173 | 0.923 | -- |
| | | 0.50% | 3.00% | 3.500 | 2.430 | 0.9738 |

Table 4.3 Cholesterol adsorption capacity of CNF or cellulose

| Fiber | Cholesterol adsorption (%) | Cholesterol adsorption capacity (mg/g) |
|---|---|---|
| Cellulose | 84%±12% | 7.1±0.7 |
| CNF | 99.99%±19% | 8.5±0.7 |

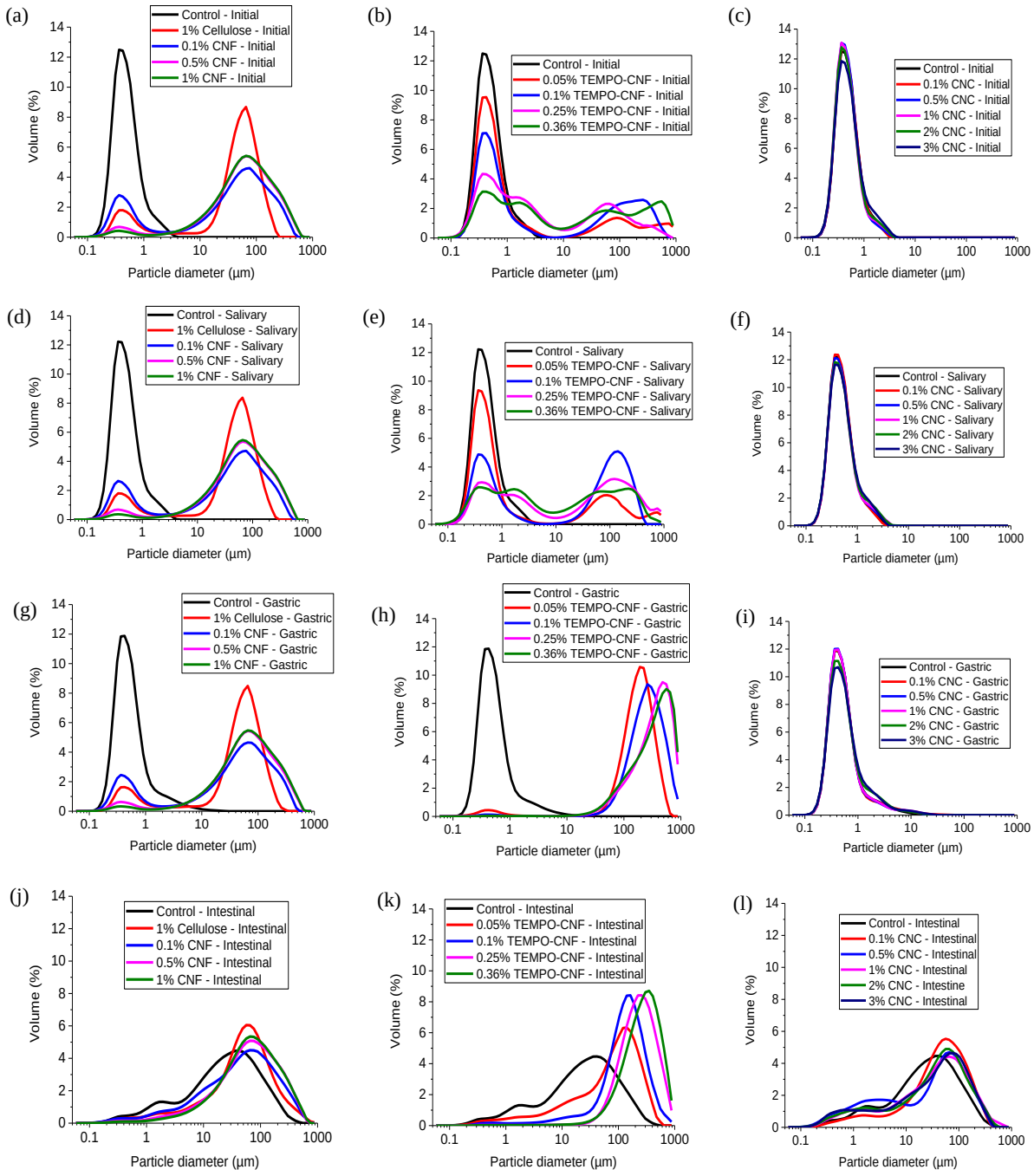


Fig 4.1. Particle size distribution of lipid emulsions after each digestion phase, with the addition of (a), (d), (g), (j) CNF/cellulose; (b), (e), (h), (k) TEMPO-CNF and (c), (f), (i), (l) CNC.

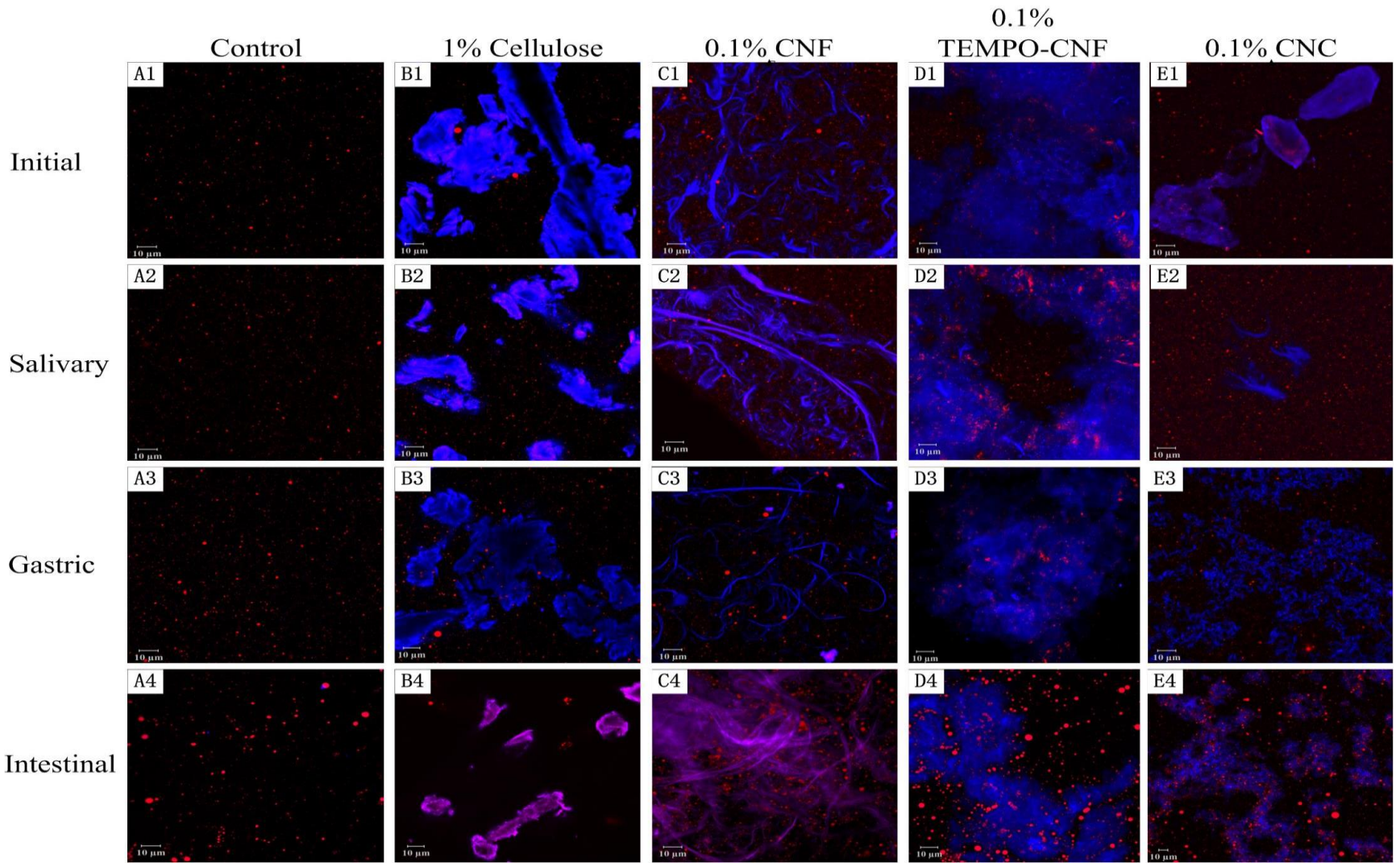


Fig 4.2. Confocal microscopy images showing microstructure of lipid emulsions containing nanocellulose/cellulose after exposure to each *in vitro* digestion phase

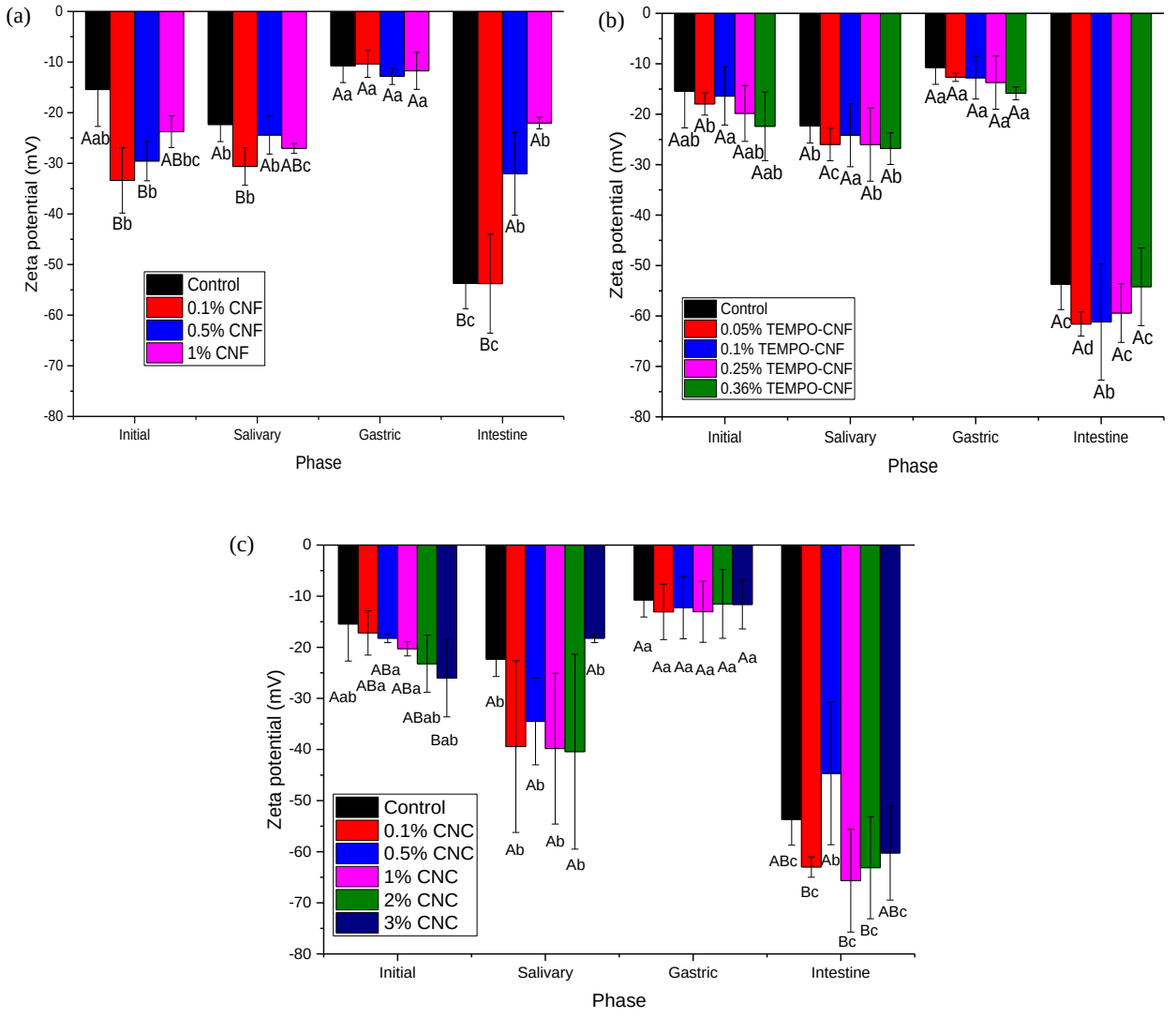


Fig 4.3. Surface charge (zeta-potential) of lipid emulsions containing nanocellulose after each *in vitro* digestion phase: (a) CNF; (b) TEMPO-CNF and (c) CNC. Samples designated with upper case letters were significantly different (Duncan, $p < 0.05$) when compared among different concentrations (at the same digestion phase); samples designated with lower case letters were significantly different (Duncan, $p < 0.05$) when compared among different digestion phases (at the same fiber concentration).

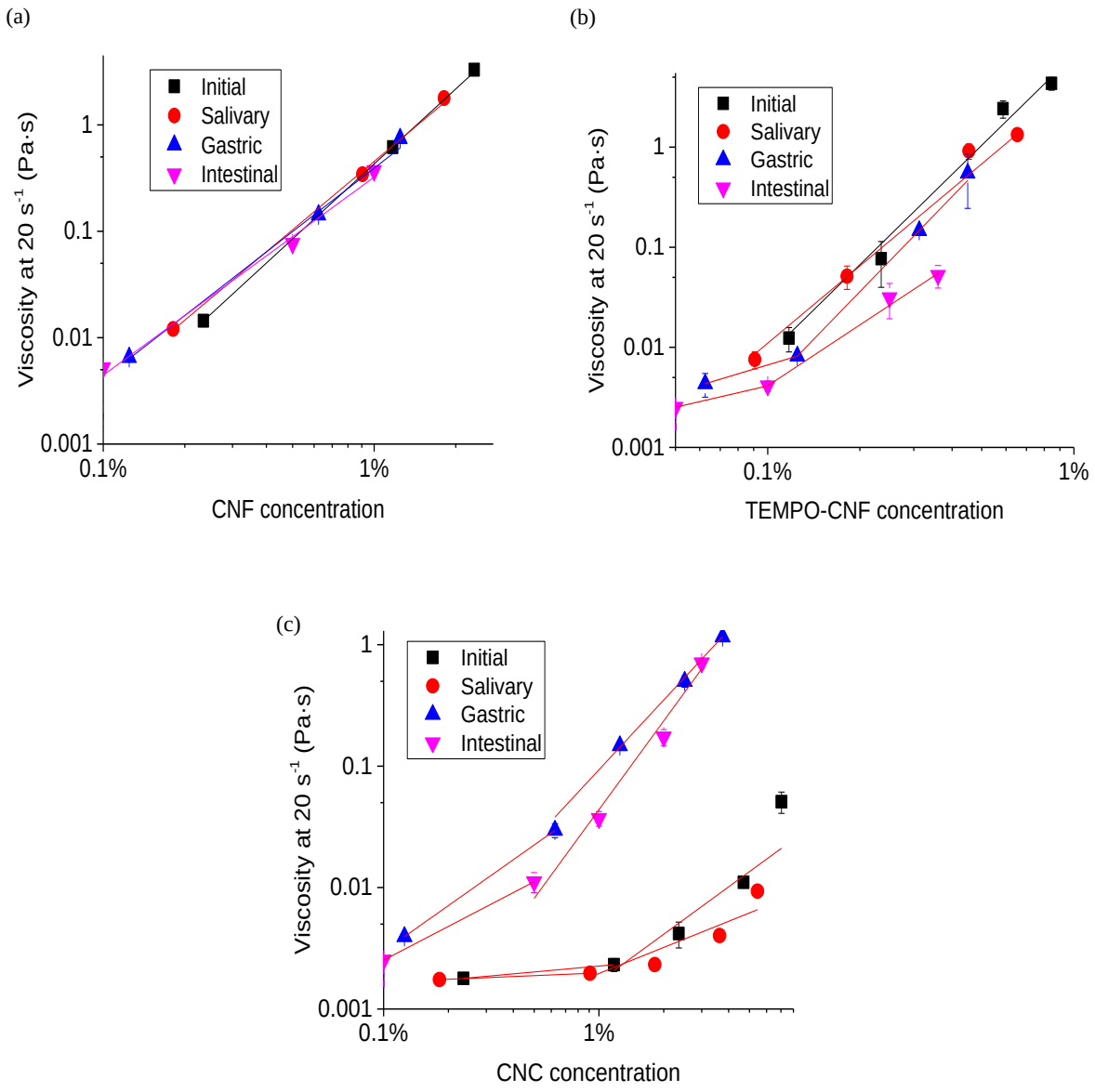


Fig 4.4. Apparent viscosity of lipid emulsions at 20 $s^{-1}$ after each digestion phase with different concentrations of nanocellulose: (a) CNF; (b) TEMPO-CNF and (c) CNC.

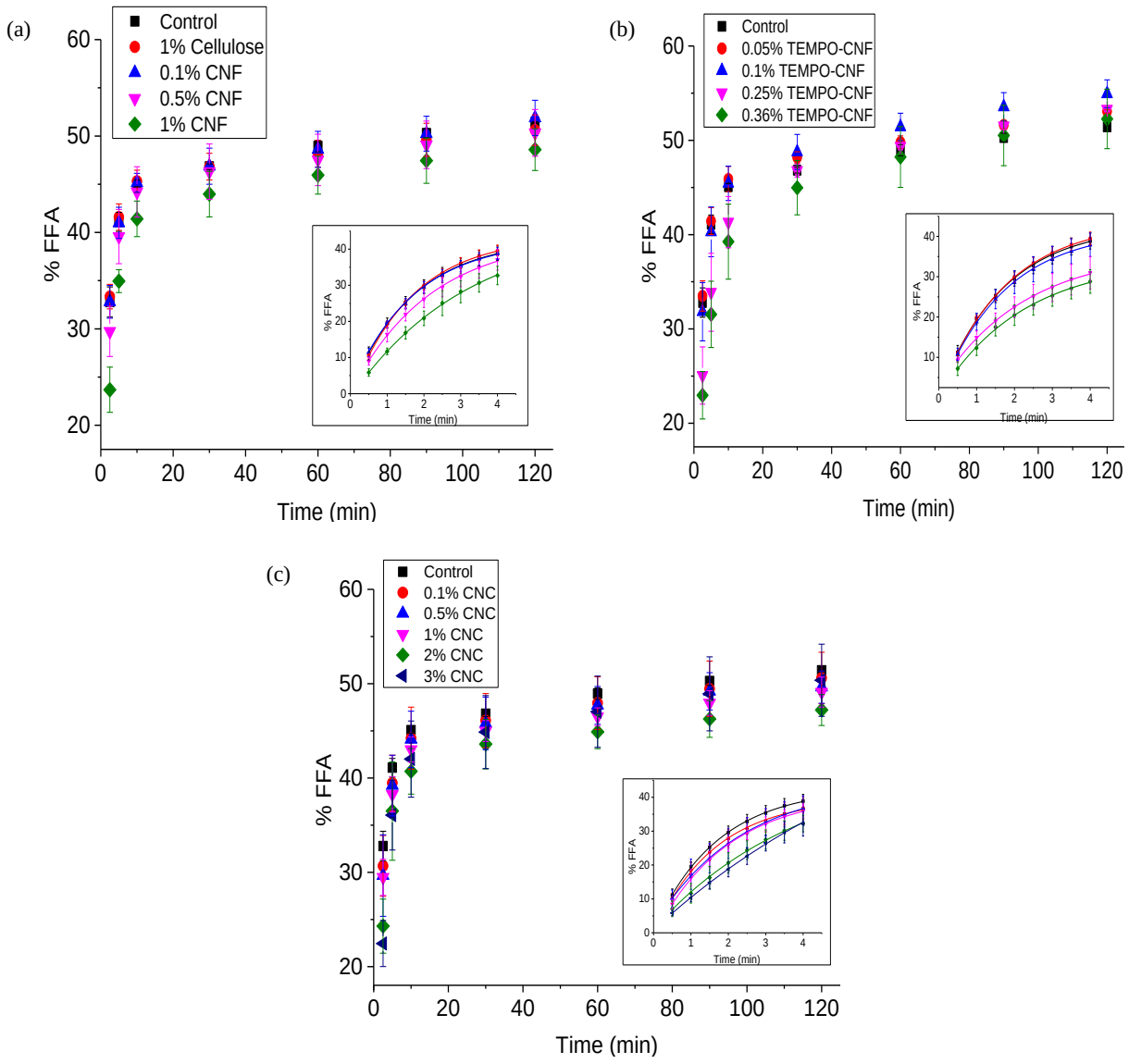


Fig 4.5. Free fatty acid release profiles from lipid emulsions containing (a) CNF/cellulose; (b) TEMPO-CNF; (c) CNC during pH-stat *in vitro* digestion

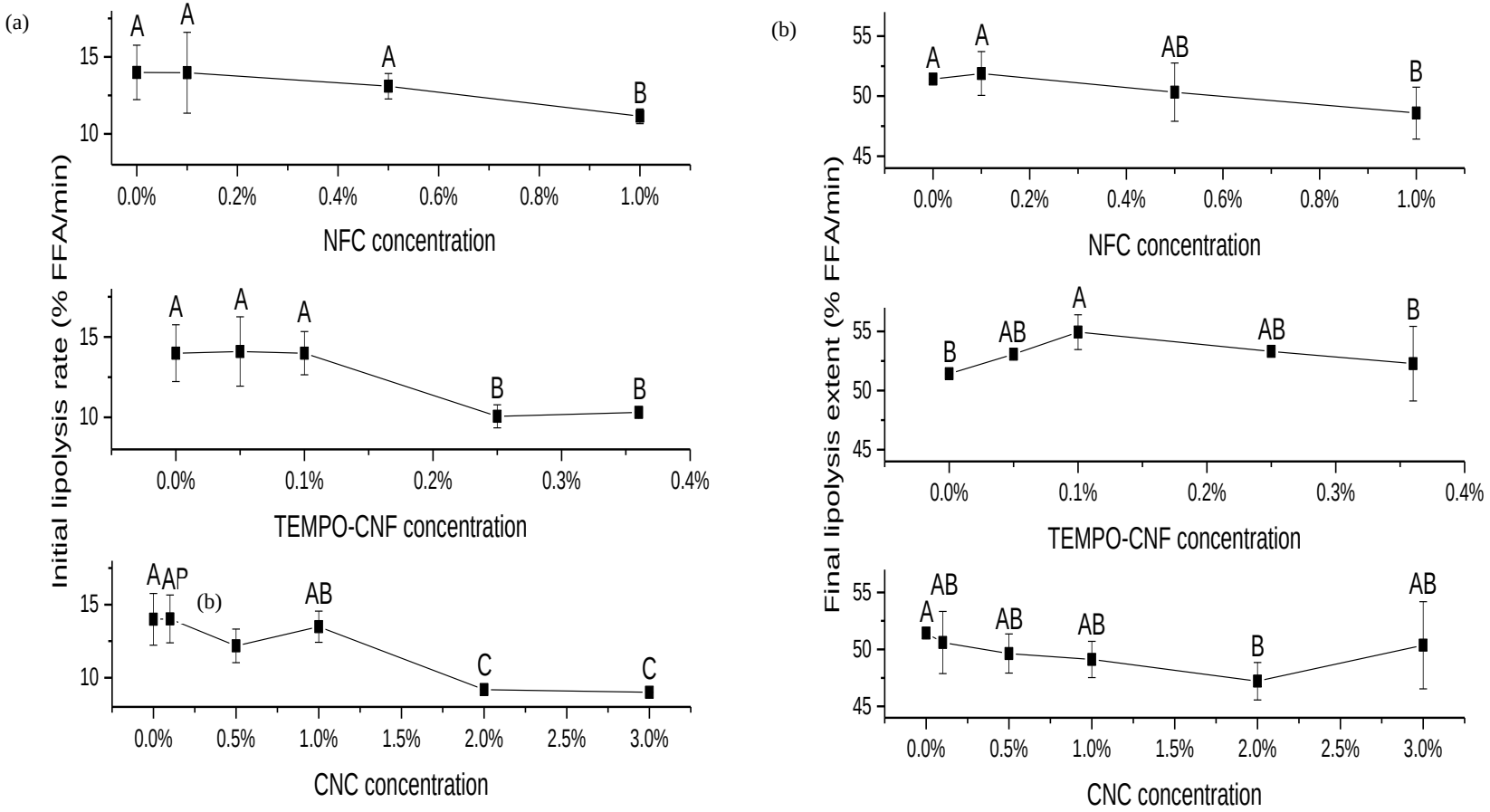


Fig 4.6. Influence of three types of nanocellulose on (a) initial lipolysis rate and (b) final lipolysis extent of Tween 80 stabilized emulsions during pH-stat *in vitro* digestion. Samples denoted with different letters were significantly different (Duncan, $p < 0.05$) when compared among different concentrations of the same nanocellulose.

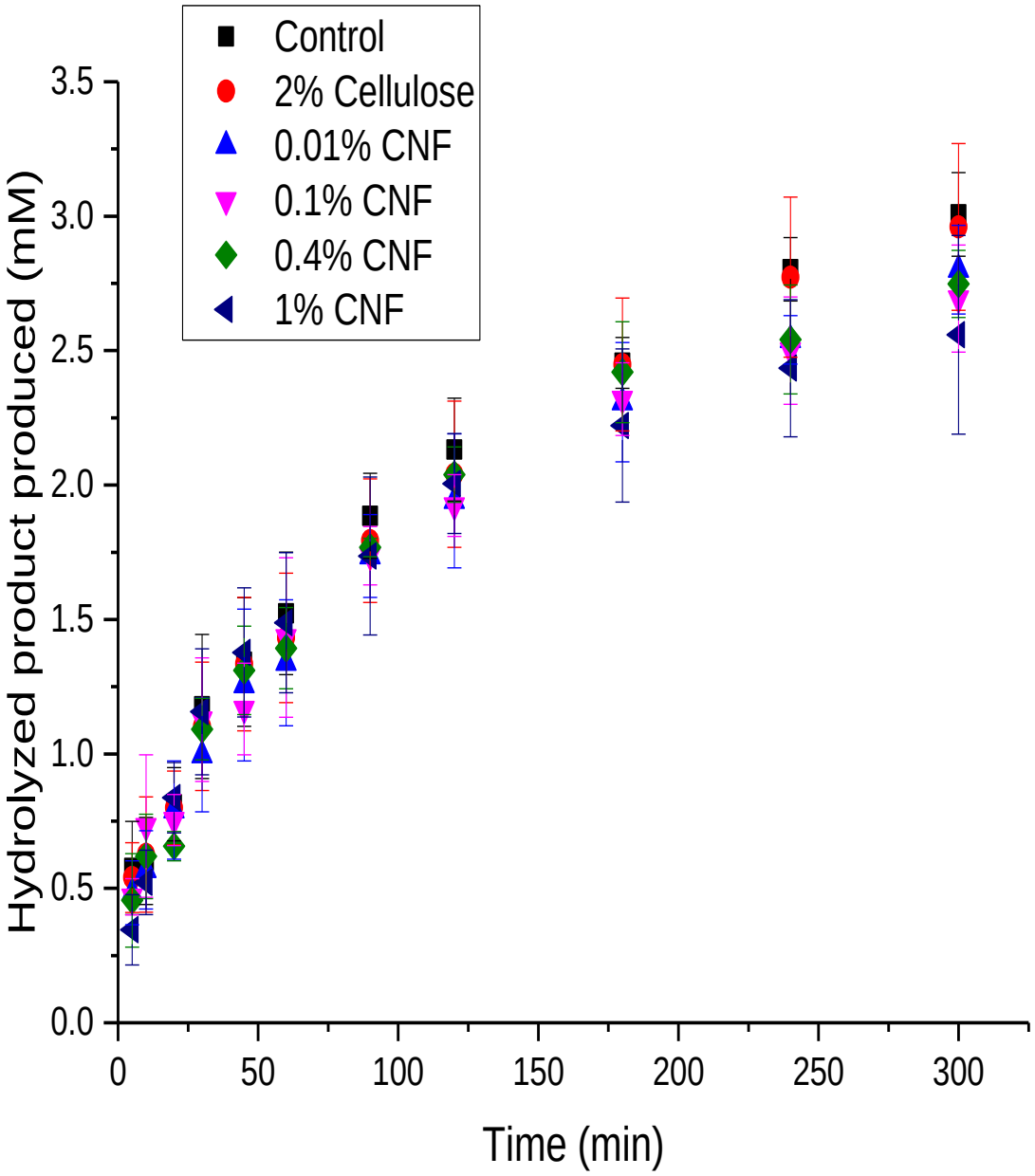


Fig 4.7 Effect of CNF or cellulose on lipase activity

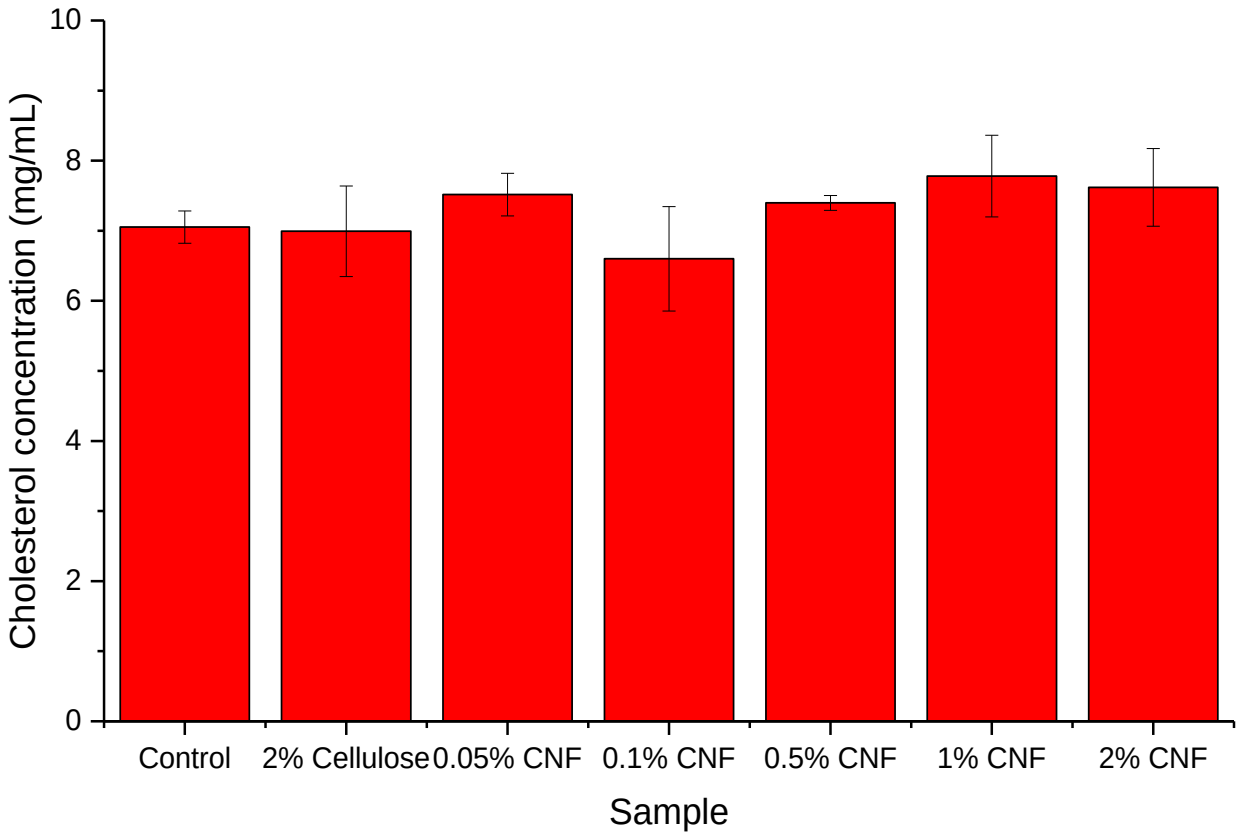


Fig 4.8 Micellar solubility of cholesterol in samples containing CNF or cellulose

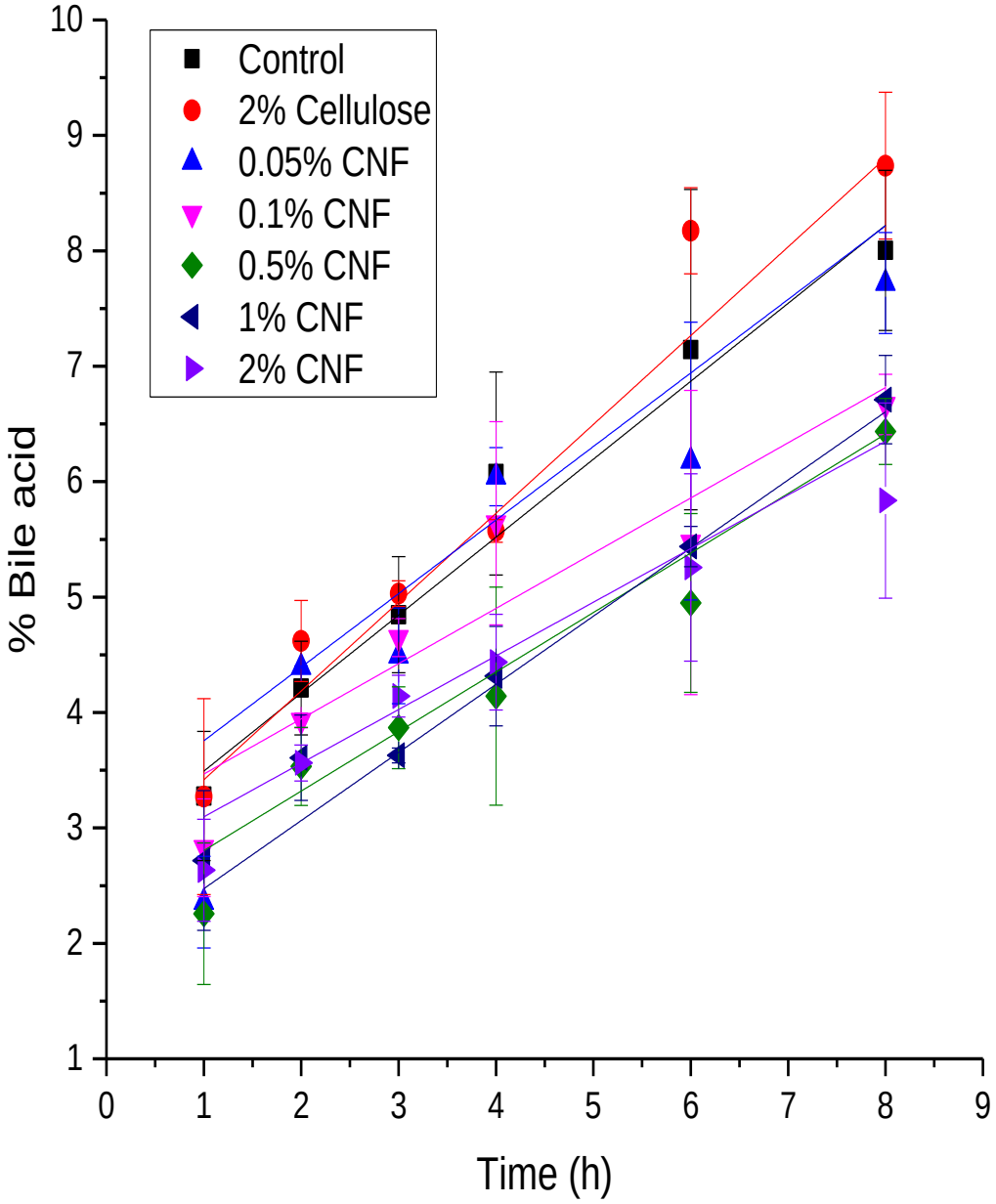


Fig 4.9 Effect of CNF or cellulose on bile acid diffusion

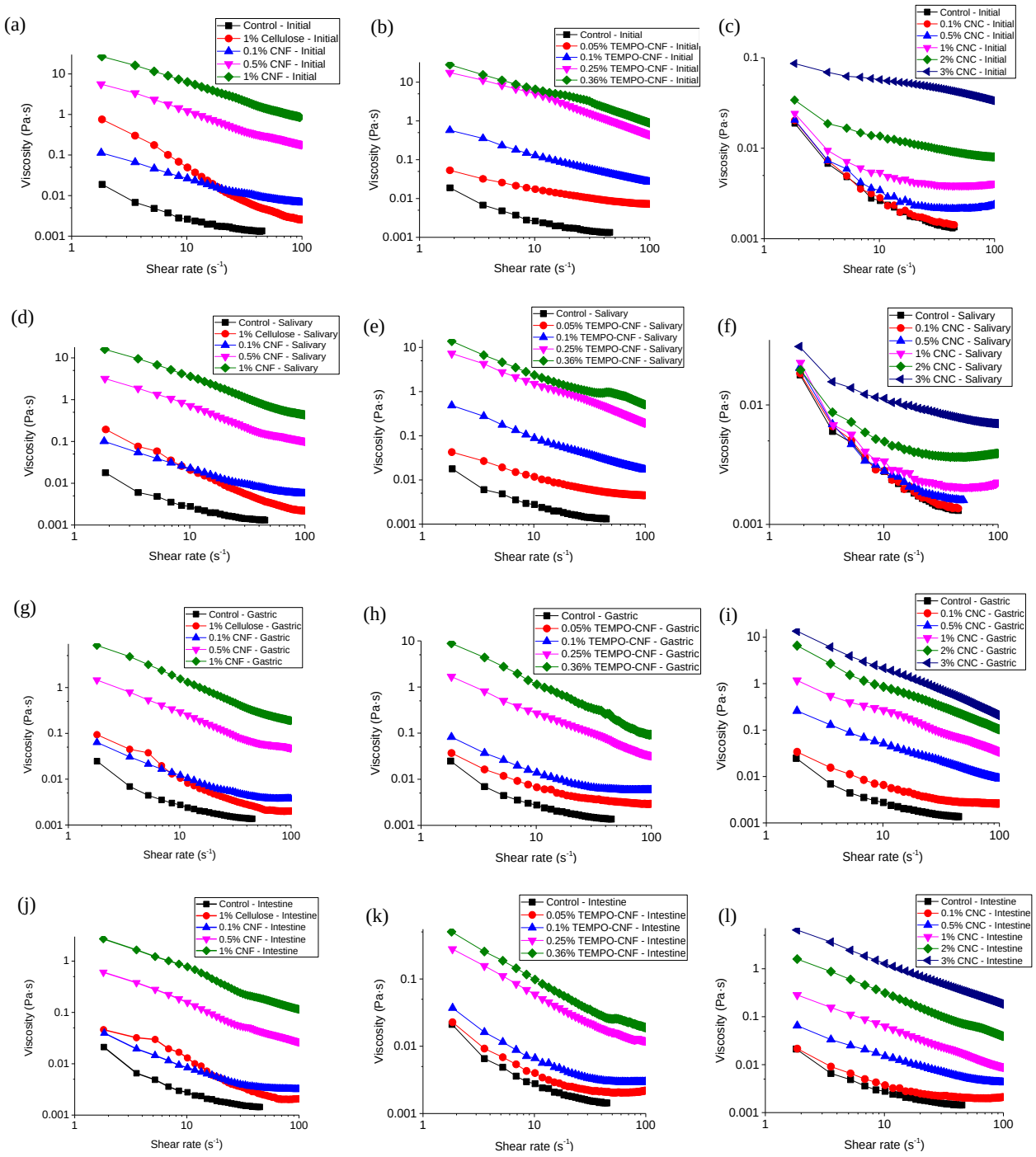


Fig S4.1. Viscosity of lipid emulsions after each *in vitro* digestion phase with different concentrations of fiber: (a), (d), (g), (j) CNF/cellulose; (b), (e), (h), (k) TEMPO-CNF and (c), (f), (i), (l) CNC.

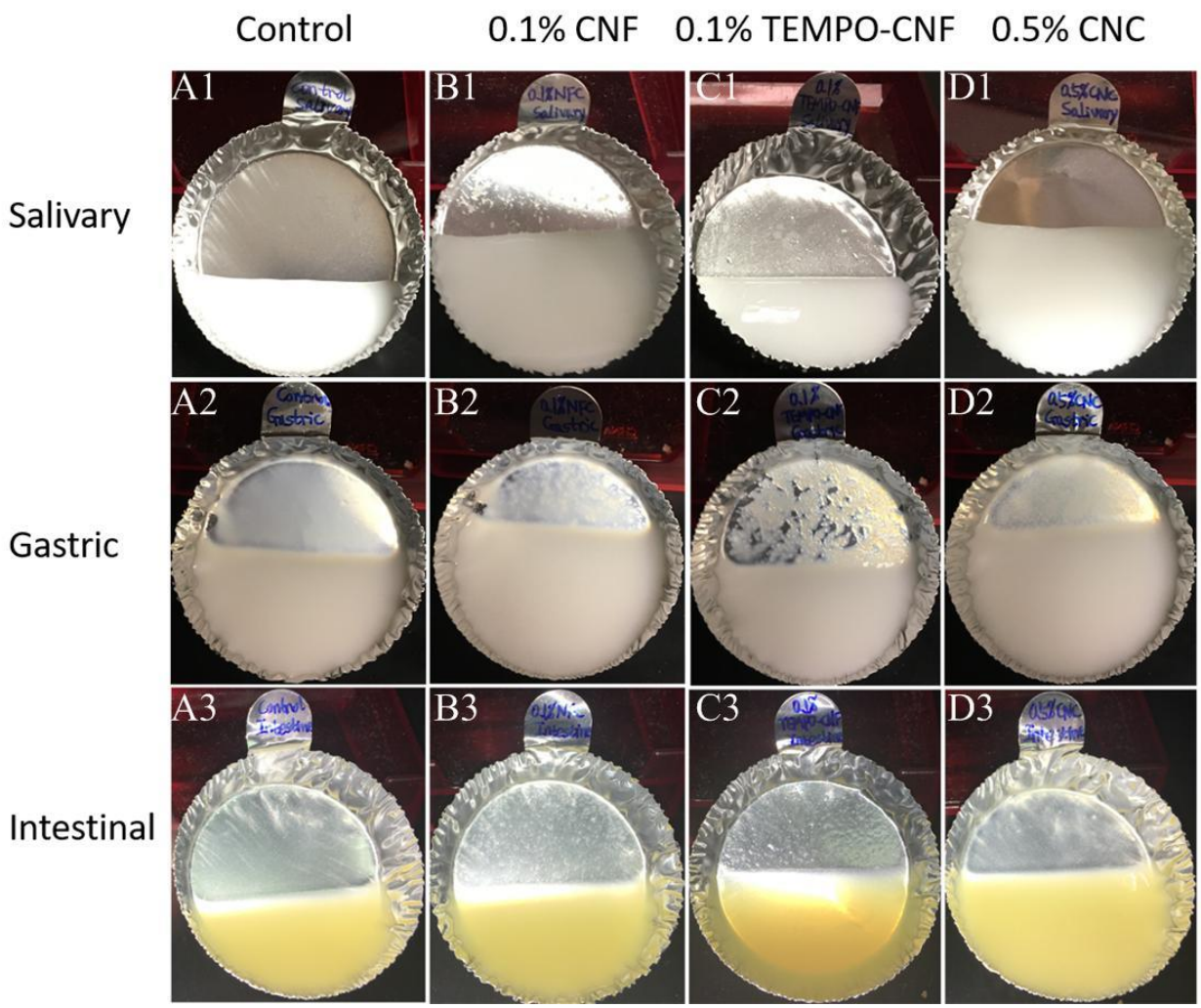


Fig S4.2. Macroscopic observation of lipid emulsions containing nanocellulose/cellulose after each *in vitro* digestion phase: (A) Control (without fiber addition); (B) CNF; (C) TEMPO-CNF and (D) CNC.

# CHAPTER 5

# INFLUENCE OF NANO-CELLULOSE ON *IN VITRO* DIGESTION OF PROTEIN[3]

[3] Liu L, Kong F. Influence of nanocellulose on *in vitro* digestion of whey protein isolate. To be submitted to *Carbohydrate Polymers*.

**Abstract:**

Three types of nanocellulose (NC), namely cellulose nano-fibrils (CNF), TEMPO-oxidized CNF and cellulose nanocrystals (CNC), were studied in terms of their effects on whey protein isolate (WPI) *in vitro* digestion. The behavior of NC itself during simulated gastrointestinal (GI) digestion was monitored by several measurements (including particle size, confocal microscopy imaging, viscosity, and zeta potential) performed in addition to its effect on percent free amino nitrogen (FAN) release and diffusion. It was shown that CNF and CNC significantly retarded nitrogen diffusion at high fiber concentrations due to high viscosity. Specifically, 23% and 50% reductions in FAN diffusion were achieved by 1% (w/w) CNF and 4% (w/w) CNC respectively. TEMPO-CNF was shown to be the least effective at reducing the amount of FAN diffusion. In addition, 4% (w/w) CNC significantly reduced % N release during intestinal digestion, though all other samples did not. It was found that anionic NC (TEMPO-CNF and CNC) bounded with WPI causing less aggregation of protein at the gastric phase. Moreover, the presence of WPI caused reductions on both mean particle size and viscosity in systems containing TEMPO-CNF or CNC at the initial and gastric phase. However, cellulose and CNF did not bind with WPI, thus WPI addition had no impact to the morphology, particle size, or viscosity of digesta containing cellulose/CNF. The findings from this study lay a foundation for future applications of nanocellulose for delaying gastric emptying and promoting satiety.

**Keywords**: Cellulose nano-fibrils; TEMPO-oxidized cellulose nano-fibrils; cellulose nanocrystals; viscosity; fluorescence

## 5.1 Introduction

Nanocellulose (NC) is a nanomaterial of increasing interest in recent years due to its special characteristics, including viscous property and large specific surface area. NC is a family of cellulosic materials that at least have one dimension less than 100 nm. As a special type of fiber, NC is insoluble but possesses gelling behavior. The viscous property together with large specific area, negligible toxicity, low density, biodegradability, and biocompatibility have rendered the applications of NC in fields including textile, pharmaceutics, cosmetics, and packaging (Ioelovich & Figovsky, 2008; Jorfi & Foster, 2015; Kolakovic, Laaksonen, Peltonen, Laukkanen, & Hirvonen, 2012; Lin & Dufresne, 2014; Minko et al., 2016; Sun et al., 2018). Nano-fibrillated cellulose (NFC, also called cellulose nano-fibrils (CNF)), TEMPO (2,2,6,6-tetramethylpiperidine-1-oxyl radical) oxidized CNF (TEMPO-CNF), and nano-crystalline cellulose (NCC, also called cellulose nano-crystals (CNC)), which vary in fiber length, diameter, surface charge and rheological properties, are amongst the most studied nanocellulose materials.

NC was effective at increasing digesta viscosity according to our previous studies (Liu, Kerr, Kong, Dee, & Lin, 2018). Increased digesta viscosity was reported to be related to delayed gastric emptying, slowed transit time along the GI tract, as well as enhanced satiety (Borreani et al., 2016). In addition, our previous studies have investigated the effects of nanocellulose on starch and lipid digestion where results showed that all three types of nanocellulose (CNF, TEMPO-CNF and CNC) at high concentrations are effective at hampering glucose diffusion and delayed initial lipid digestion (Liu et al., 2018 and unpublished results). However, very few studies have been carried out on the effects of varieties of nanocellulose on protein digestion and nitrogen absorption. Among the limited studies, the focus of their research is generally towards the effects of CNC or

carboxylated CNC on protein-stabilized lipid emulsions (Sarkar, Li, Cray, & Boxall, 2018; Sarkar et al., 2017).

Protein, as a major component in the human diet, has been shown to be a more effective contributor to satiety than carbohydrates and fats (Anderson & Moore, 2004; Borreani, Llorca, Larrea, & Hernando, 2016). Whey protein isolate (WPI), a group of serum proteins in milk byproducts, is often incorporated in research studies (Gbassi et al., 2012; Sarkar, Zhang, Murray, Russell, & Boxal, 2017). Whey protein isolate is comprised of small portions of bovine serum albumin (BSA), α-lactalbumin (α-la) and large portions (60~70%) of β-lactoglobulin (β-Lg). Specifically, native β-Lg (a globular protein) is resistant to gastric digestion while BSA and α-la can be easily degraded in the gastric digestion (Kitabatake & Kinekawa, 1998). Dietary fibers, especially viscous soluble fibers, have been shown to decrease protein digestibility as well as increase pancreatic-bile excretion and fecal nitrogen content (Hughes, Acevedo, Bressani, & Swanson, 1996; Ikegami et al., 1990). Research has shown that the addition of anionic polysaccharides (including xanthan gum, pectin and carrageenan) to the protein (soy protein isolate, whey or casein) solution can cause increased digesta viscosity, delayed proteolysis, slower gastric emptying and induced satiety (Zhang & Vardhanabhuti, 2014; Zhang, Zhang, & Vardhanabhuti, 2014). Furthermore, an increase in fiber (including apple pectin, holocellulose, lignin, predigested wheat bran and predigested great northern bean) to protein ratio resulted in decreased protein digestibility *in vitro* (Acton, Breyer, & Satterlee, 1982).

As a nanoscale fiber, it is of interest to investigate if nanocellulose possesses similar effects as dietary fiber in protein digestion and nitrogen absorption. Thus the objective of this study was to compare the effects of various types of nanocellulose on protein digestion and nitrogen absorption using a simulated *in vitro* digestion model, and characterize the behaviors of

nanocellulose during gastrointestinal (GI) digestion. To our knowledge, this is the first study to investigate the inter-influence of protein diet and nanocellulose during GI digestion. The results could be used to develop new applications of nanocellulose in the food industry aiming to delay digestion and control satiety.

## 5.2 Materials and methods

### 5.2.1. Materials

The BiPRO® whey protein isolate powder used in this study was kindly provided by Davisco Foods International (Agropur Ingredients, Eden Prairie, MN). The cellulose nano-fibrils (3 wt%) was purchased from the Process Development Center at the University of Maine (Orono, ME). Samples of TEMPO-based cellulose nano-fibrils (1.1 wt% in water, 1.5 mmol-COONa/g dry CNF) and cellulose nanocrystals (10.8 wt% in water, 0.94 wt% sulfur on dry CNC, sodium form) were both obtained from the USDA's Forest Products Laboratory. The nominal sizes of the three nanocellulose materials were: CNF (~50 nm width and length up to several hundred microns); CNC (~ 5 nm width and 150 nm length); TEMPO-CNF (~ 20 nm width and length up to 2 μm).

Digestive components including α-amylase from porcine pancreas (A3176, 12 U/mg), pepsin from porcine gastric mucosa (P7000, 479 U/mg), bile extract porcine (B8631), lipase from porcine pancreas (Type II, L3126), pancreatin from porcine pancreas (P1750), and mucin from porcine stomach (Type II, M2378, bound sialic acid 0.4%) were purchased from Sigma-Aldrich Chemical Co. (St. Louis, MO). According to the manufacturer, the pancreatin could digest no less than 25 times its weight of casein in 60 minutes at pH 7.5 at 40°C. Other chemicals were purchased from either Fisher Scientific (Pittsburgh, PA) or Sigma-Aldrich.

5.2.2. *In vitro* digestion of whey protein isolate

WPI solutions (30% (w/w)) were prepared by dissolving whey protein isolate (WPI) powder in DI water with stirring until fully dispersed. Different concentrations of nanocellulose (NC) solution were prepared by diluting the stock NC with DI water. The initial fiber-protein systems included 6.67% WPI (w/w) and several concentrations of CNF (0.23%, 1.17% and 2.33% (w/w)); TEMPO-CNF (0.12%, 0.23% and 0.84% (w/w)); or CNC (0.23%, 2.33% and 9.33% (w/w)). In addition, 2.33% cellulose suspensions were prepared to determine the differences between nanocellulose and conventional cellulose on protein digestion. These concentrations were selected based on calculations of the final fiber concentration after intestinal digestion as shown below. Moreover, the final fiber concentrations were chosen based on the original NC stock concentration as well as the viscosity of the NC solution.

*In vitro* digestion of WPI with or without the addition of fiber was performed based on a modified method from Liu et al. (2018). Specifically, 21 mL of fiber solution was mixed well with 6 mL of the WPI stock solution. The mixture was held at 37 °C in a shaking water bath (Model 290400S, Boekel Scientific, USA) prior to the *in vitro* digestion. A control sample was also prepared that contained no added fiber. The digestion trial was initiated by the addition of 6 mL of 'salivary juice' to the samples with pH quickly adjusted to 6.8 ± 0.2, followed by incubation at 37°C with a shaking speed of 100 rpm for 5 min. The process of gastric digestion was simulated following the salivary phase via the addition of 'gastric juices' (12 mL) with the pH adjusted to 3.0 ± 0.1 and incubated for 2 hrs. After gastric digestion, aliquots were taken with NaOH addition to inactivate the enzymes, followed by centrifugation at 5000 *g* for 15 min (AccuSpin Micro 17, ThermoFisher Scientific, Germany). The amount of free amino nitrogen in the supernatant was determined by using the o-phthaldialdehyde/N-acetyl-l-cysteine (NOPA) method (Dukes &

Butzke, 1998). Following the gastric phase, intestinal digestion was initiated by the addition of duodenal juice (12 mL) and the supernatant of pre-centrifuged (5000 *g* for 5 min (Hermle Z200A, Labnet International, Inc.) to remove large debris) bile juice (6 mL), with pH adjusted to 7.0 ± 0.1. To study the effects of fiber on protein digestion and nitrogen absorption separately, the simulated intestinal digestion process was performed both with and without a dialysis membrane. For the experiments with dialysis, digesta was placed inside a dialysis tubing (1 KDa, Spectra/Por 6 Dialysis tubing, Spectrum Laboratories, Los Angeles, CA) against 0.1 M PBS (pH 7.4) (with an outside volume of 500 mL). Aliquots were collected from outside the tubing and results were presented based on the amount of FAN diffusion. For experiments carried out without dialysis, aliquots were taken, inactivated, then centrifuged, and % N release was determined using the same methods as mentioned above.

In order to determine the independent behavior of fiber during digestion, fiber-only specific controls were also performed by replacing WPI solution with DI water. Due to the addition of digestive juices, the final nanocellulose concentrations were lower than initial values. During intestinal digestion, the corrected concentrations for each were: CNF (0.1%, 0.5% and 1% (w/w)), TEMPO-CNF (0.05%, 0.1% and 0.36% (w/w)), CNC (0.1%, 1% and 4% (w/w)) and cellulose (1% (w/w)). Results were then reported with respect to the final concentration of each fiber.

5.2.3. Determination of particle size

The particle size distribution of fiber-protein and fiber-only systems during digestion was measured using a laser diffraction device (Mastersizer S, Malvern Instruments Ltd., Worcestershire, United Kingdom) with a detection range of 0.05 ~ 900 μm. Samples were added to the detection chamber until the obscuration reached between approximately 10% and 20%. A dispersion rate of 2000 rpm was applied inside the chamber to disperse the samples and ensure

homogeneity. A polydisperse model and a standard-wet (3OHD) presentation were chosen for the analysis. A relative particle refractive index of 1.15 was chosen as the refractive indexes of WPI and cellulose/cellulose were 1.52 and 1.47~1.54, respectively, while the refractive index of water is 1.33. Results of particle size were reported as distribution profiles (showing volume fraction (%) versus particle diameter (μm)) as well as mean particle size ($D_{43}$). Due to the opalescency of digesta systems containing high concentrations of CNC (1% ~ 4% (w/w)) (Ren, Sun, Lei, & Wu, 2014), artificial peaks which were present at particle sizes larger than 200 μm were removed from the generated distribution profiles (Sabin, 2011) and $D_{43}$ as well as distribution profiles were calculated using an in-house MATLAB script (MATLAB R2018b).

5.2.4. Microstructural characterization

The microstructure of fiber-protein systems containing nanocellulose/cellulose during each digestion phase was characterized by a Zeiss LSM 710 confocal microscope system, using a Zeiss AXIO Observer Z1 inverted microscope stand with transmitted (HAL), UV (HBO) and laser illumination sources. A 63x (oil) objective lens was used to capture images. Solutions of the fluorescent dye fast green (0.1% (w/v) and fluorescent brightener 28 (0.1% (w/v) dissolved in water were prepared and used for staining of protein molecules and nanocellulose/cellulose, respectively. Control samples, as well as samples containing 1% cellulose, 0.1% CNF, 0.1% TEMPO-CNF and 0.1% CNC during each digestion phase were stained with the fluorescent dyes at a volume ratio of 200:1:1, followed by vortexing for ~5 s to ensure homogeneous staining. A small aliquot of the stained samples (5 μl) was added to a glass slide and covered with a cover slip. The samples were illuminated at the excitation wavelengths of 633 nm and 405 nm corresponding to the fast green and fluorescent brightener 28, respectively. The emission spectra were collected

at 698 nm and 441 nm for both dyes, respectively. Images were analyzed with the instrument software ZEN 2.3 SP1.

5.2.5. Determination of surface charge (zeta potential)

The surface charge of fiber-protein and fiber-only systems during digestion was measured by electrophoretic light scattering with a NanoBrook 90Plus Zeta instrument (NanoBrook 90Plus Zeta instrument, Brookhaven Instruments Corporation, New York, USA). Prior to analysis, samples were diluted with buffer solution to a concentration range between 0.25% (w/v) and 2% (w/v). 1 mM PBS (pH 7.0) was used for dilution for initial and salivary samples, while 1 mM citric buffer (pH 3.0) and 0.01 mM PBS (pH 7.0) were used for gastric and intestinal samples, respectively. The choices of the sample concentration for measurement depended on the ratio between sample and reference count rate as well as the conductance of the samples. Specifically, higher sample concentrations (2% (w/v)) was used for fiber-only systems at the initial and salivary phases, while lower sample concentrations (0.25% (w/v) were used for fiber-protein systems at the gastric and intestinal phases. Measurements were performed with 10 continuous runs at 25°C and results were reported using the averaged values.

5.2.6 Rheological measurement

The viscosity of fiber-protein and fiber-only systems during digestion was measured by a 4-blade rotor vane (42 mm in length and 28 mm in diameter) geometry within a Discovery HR-2 rheometer (TA instruments, Newcastle, DE). The viscosity of samples was measured at 37°C with a pre-shear rate of 40 $s^{-1}$ for 2 min, followed by the flow ramp test over a shear rate range of 1–100 $s^{-1}$. A pre-shear step was performed in order to obtain well-mixed and homogeneous samples before rheological test, due to the phase separation of some samples (including digesta containing

TEMPO-CNF at the gastric/intestinal phase and cellulose at all phases). The flow ramp test was performed over a 180 s period with a sampling interval of 3 s/pt.

5.2.7. Statistical analysis

Triplicate measurements were performed for all parameters and significant analysis was performed by Duncan's multiple comparison tests with SAS/STAT software (SAS Institute Inc., Cary, NC). Regression models generated in the graphs were done using Origin data analysis and graphing software.

**5.3 Results and discussion**

5.3.1 Particle size measurement of fiber-protein and fiber-only systems

Particle size distribution curves of fiber-protein and fiber-only systems during digestion were plotted in Fig 5.1 and Fig 5.2. The mean particle size ($D_{43}$) of these digesta systems is shown in Table 1. The size of CNF itself did not change during digestion (with a $D_{43}$ of ~100 μm), neither in the fiber-protein or fiber-only systems. In addition, the addition of WPI resulted in slightly smaller $D_{43}$ of digesta containing CNF, TEMPO-CNF or CNC at the gastric phase except for 4% CNC. In the fiber-only systems at the initial phase, CNF at all concentrations tested showed the same particle size distribution, and CNC showed similar distribution patterns. However, TEMPO-CNF showed different distribution curves at various concentrations.

The particle sizes of WPI at the initial, gastric, and intestinal phase had trimodal distributions, though the peak positions varied at each digestion phase. WPI was partially degraded at the gastric phase, as shown by its slight decrease in $D_{43}$. The degradation of WPI at the gastric phase was also shown in Borreani et al. (2016), where the authors observed similar patterns of particle size distribution of WPI after gastric digestion. At the intestinal phase, WPI was further degraded and the increase in $D_{43}$ may be due to the presence of some digestive components (e.g.,

bile and pancreatin) or the aggregates of digestion products. As shown by Sarkar et al. (2018), large floc formation occurred in the WPI or CNC-WPI stabilized oil-in-water emulsions in the presence of bile salts and pancreatin.

Cellulose-WPI had both a major peak and minor peak at the initial, gastric and intestinal phases. CNF-WPI had only one peak at the initial, gastric and intestinal phases except that of 0.1% (w/w) CNF-WPI which had two peaks after gastric digestion. For the CNF containing systems, the addition of WPI did not cause changes in $D_{43}$ of the digesta except at the gastric phase. That is, $D_{43}$ of CNF-WPI systems was slightly smaller than that of CNF-only systems at the gastric phase. This may be because the addition of WPI caused slight shifts of the volume distribution curve of digesta systems containing CNF, even though the mean particle size of CNF (~100 μm) is much larger than that of WPI (~23 μm).

The mean particle size increased as a function of higher TEMPO-CNF concentrations at the initial phase in the fiber-only systems. This may be a direct consequence of the effective dispersion of TEMPO-CNF at low concentrations while the opposite occurs at higher concentrations due to the formation of gels. In order to show as a comparison for all TEMPO-CNF concentrations at other digestion phases, the size data at the initial phases are shown (Fig 5.2(b)). For TEMPO-WPI, the mean particle size at the initial phase was around 135 ~ 295 μm, and the size changed slightly after gastric and intestinal digestion. Compared with TEMPO-only systems, WPI addition caused reductions in the mean particle size of TEMPO-CNF at the gastric phase for all the concentrations studied.

For CNC-WPI systems, the mean particle size at the initial phase was around 54 ~ 103 μm, which was larger than the size of CNC-only systems. However, at the gastric phase, WPI addition caused reductions in the size of 0.1%~1% (w/w) CNC except 4% (w/w) CNC. Similar to the

decreased size in WPI after moving from initial phase to the gastric phase, CNC-WPI systems also showed a decrease in size following the same process. However, for CNC-only systems, at low concentrations (0.1% ~ 1% (w/w) CNC), an increase in $D_{43}$was observed after moving from the initial phase to the gastric phase. The combination between the effects of size decrease as a result of WPI degradation and size increase due to the addition of gastric juices (together with mucin and low pH) contributed to the size change of CNC-WPI systems. For a concentration of 4% (w/w) CNC, a larger $D_{43}$ was observed in the CNC-WPI systems than CNC-only systems at the gastric phase, which appears to be due to the strong electrostatic attractions between CNC and WPI. This is similar to the large aggregates formed between whey protein and other anionic fibers (alginate or carrageenan) at the gastric phase (Borreani et al., 2016; Zhang et al., 2014). At the intestinal phase, similar particle size distribution patterns were observed between CNC-WPI and CNC-only systems, which may indicate that WPI was digested and had limited contribution on the particle size distribution patterns of CNC containing digesta systems. In addition, a higher volume percentage in the peak of a smaller size was observed at higher CNC concentrations at the intestinal phase for both CNC-WPI and CNC-only systems. It could thus be concluded that after digestion of WPI, the volume proportion of CNC was more pronounced in the volume distribution curve of the digesta samples. The size of CNC-WPI or CNC-only systems at the intestinal phase decreased compared to those at the gastric phase except for 0.1% (w/w) CNC-WPI (which had large standard errors). The particle size results of CNC with WPI were similar to those reported by Sarkar et al. (2017, 2018). Specifically, the authors found that CNC-WPI systems had a large proportion of particles within the size range of 10-100 μm after gastric digestion (Sarkar et al., 2017). However, it was noted that the particle size distribution patterns shifted after intestinal digestion, and smaller

peaks in the size range of 100-1000 μm were only observed at low CNC concentrations (Sarkar et al., 2018).

5.3.2 Microstructural characterization of fiber-protein systems

Fig 5.3 shows confocal imaging of WPI (pink color) and nanocellulose/cellulose (blue color). At initial and salivary phases, WPI itself was very stable and no aggregation was observed (Fig 5.3 A1-A2). However, WPI formed aggregates at the gastric phase (Fig 5.3 A3) even though the aggregates were dissociated/digested at the intestinal phase (Fig 5.3 A4) and only small particles were observed. At the gastric phase (pH 3), WPI formed aggregates, which is similar to that reported in literature (Borreani et al., 2016). Aggregation of WPI is influenced by pH, ionic strength, temperature, nature of co-solute and solvent as well as concentrations of protein (Unterhaslberger, Schmitt, Sanchez, Appolonia-Nouzille, & Raemy, 2006). The aggregation of native β-lg was reported to be favored by the presence of salt, and this effect was reported to be more pronounced at pH 4.0 than pH 7.0 (Nicolai, Britten, & Schmitt, 2011). The presence of ions in the systems can reduce the repulsion forces due to charge shielding. It was also found that larger aggregates formed at less net charge of β-Lg (Macierzanka et al., 2012). However, the particle size results in Table 1 showed slight decreases in the mean particle size of WPI at the gastric phase but increase in size after intestinal digestion. This may be because that other components (like mucin or digestive enzymes or bile) also contributed to the particle size measured in Table 1, but these unstained particles were not visible in the confocal imaging.

In the systems containing nanocellulose/cellulose at the initial phase, WPI seemed to be either randomly distributed in the fiber systems containing cellulose/CNF/TEMPO-CNF (Fig 5.3 B1-D2), or co-localized with fiber in systems containing CNC (Fig 5.3 E1-E2). Each fiber shows different morphology during gastrointestinal digestion. As shown in Fig 5.3 B1-C4, cellulose and

CNF did not show morphological changes at any digestion phases. However, TEMPO-CNF bound with WPI and formed individual discrete gels at the gastric phase (Fig 5.3 D3), and the gel network resumed at the intestinal phase (Fig 5.3 D4). In terms of CNC, it bound with WPI at the initial, salivary, and gastric phases (Fig 5.3 E1-E3), though a larger network was formed at the intestinal phase (Fig 5.3 E4).

Slight changes were observed during the movement of digesta from the initial to salivary phases for systems containing TEMPO-CNF. Results suggested that WPI was embedded in the TEMPO-CNF gel network for both phases, but the gel network seems to have discontinued during gastric digestion (Fig 5.3 D3). This may be due to de-swelling of TEMPO-CNF which would result in phase separation at increased ionic strength and low pH (Fukuzumi, Tanaka, Saito, & Isogai, 2014; Mendoza, Batchelor, Tabor, & Garnier, 2018). Even though the binding between WPI and TEMPO-CNF may also play a role, it is possible that the complexes formed between WPI and TEMPO-CNF could be dissociated by calcium ions, since a tight junction could form between carboxyl groups of fiber and calcium ions (Zhao, Li, Carvajal, & Harris, 2009). Similarly, Zhao et al. (2009) found that the complexes formed between BSA and alginate could be dissociated by calcium ions without much change in protein structure.

Results suggest that the presence of TEMPO-CNF or CNC reduced the aggregate formation of WPI at the gastric phase, since smaller sizes of WPI were observed in TEMPO-WPI (Fig 5.3 D3) or CNC-WPI (Fig 5.3 E3) when compared to control (Fig 5.3 A3). This together with the particle size results in Table 1 may show some evidence of the interaction between WPI and anionic NC. Electrostatic interaction is reported to occur between positively charged WPI and negatively charged anionic NC at the gastric phase (Sarkar et al., 2017). Our observations are similar to those reported by Mouécoucou, Villaume, Sanchez, & Méjean (2004) that gum arabic,

low methylated pectin, and xylan could bind with β-lg and resulted in less aggregation of the protein. However, results in this study are different to those reported by Borreani et al. (2016), who found that anionic fiber (e.g., alginate) formed larger aggregates with dairy protein than neutral charge fiber (e.g., konjac glucomannan) and the former was less degraded during gastric digestion. The difference in fiber and protein interaction as well as the compatibility/solubility of their complex depended on pH, ionic strength, processing conditions (temperature, shearing and time), the charge density of fiber and protein, as well as their ratios (Ye, 2008). After moving to the intestinal phase, the surface charge of WPI switches from positive to negative. The strong electrostatic interaction occurred under gastric conditions diminished, and was left only with weak local electrostatic or non-electrostatic interactions (hydrophobic, H-bonding) (Mouécoucou et al., 2004). This would explain the phenomenon that no differences were observed in the sizes of protein or protein hydrolysis products at the intestinal phase in samples containing nanocellulose/cellulose (Fig 5.3 B4-E4) as compared to that of control (WPI).

In systems containing CNC, the gel network was observed to increase from the initial phase (Fig 5.3 E1) to the intestinal phase (Fig 5.3 E4). This can be related to the increased ionic strength of the digesta following successive digestion phases. It is reported in literature that increased ionic strength caused an increase in CNC viscosity, which corresponds to larger gel network (Bertsch, Isabettini, & Fischer, 2017). At the gastric phase, the binding between positively charged WPI and negatively charged CNC resulted in less exposed surface charges of CNC to the environment, which also caused less hydrogel network formation among CNC macromolecules. In the intestinal phase, electrostatic repulsion or weak electrostatic attraction between negatively charged WPI and anionic CNC rendered CNC with more surface charge to form a hydrogel network. This may

explain the larger gel network formed in the CNC-WPI systems in the intestinal phase when compared to that in the gastric phase.

5.3.3 Surface charge (zeta-potential) of fiber-protein and fiber-only systems

The surface charge of fiber-protein and fiber-only systems during each digestion phase is shown in Fig 5.4. The surface charge of fiber-protein systems have been used in literature as a means to study the interactions between fiber and protein under certain conditions (Harnsilawat, Pongsawatmanit, & McClements, 2006; Jones, Lesmes, Dubin, & McClements, 2010). Furthermore, the surface charge of a colloidal system is also influenced by the fiber itself as well as condition changes (e.g., pH and ionic strength). In the fiber-protein systems, positive surface charge ($\zeta$) was observed at the gastric phase for all samples, while negative surface charge was observed at the other digestion phases. The $\zeta$ of digesta containing 4% (w/w) CNC was significantly different from that of control based on statistical analysis among different sample groups (each fiber type and its concentration are treated as an individual group). In the fiber-only systems, negative $\zeta$ values were observed at all digestion phases for all NC types.

In the fiber-only systems, TEMPO-CNF carried the most negative surface charges when compared to CNF and CNC. Slight changes occurred in surface charge when moving the digesta from initial to salivary phases, though CNC was shown to be slightly more negative. When moving to the gastric phase, CNC showed concentration dependent surface charges, with significantly more negative charges at higher CNC concentration. CNF and TEMPO-CNF showed similar surface charges to that of control. Thus it can be concluded that CNC is more dissociated at gastric conditions while the opposite is true for TEMPO-CNF. When moving the digesta to the intestinal phase, control showed more negative values when compared to the other digestion phases, which may be due to the contribution of negative charges from bile salt and pancreatin present in the

intestinal juice (Sarkar et al., 2018). CNF addition resulted in significantly less negative values than that of control at the intestinal phase. Similarly, TEMPO-CNF addition also caused less negative values, with 0.36% (w/w) TEMPO-CNF significantly different from that of control. The less negative values with CNF or TEMPO-CNF addition can indicate some interaction between CNF and other digestive components (e.g., bile salt). As shown by DeLoid et al. (2018), CNF could sequester bile salts and cause reduced lipid digestion as well as absorption of protein-stabilized oil-in-water emulsions. Similarly, other dietary fibers have been shown to possess bile acid sequestering effects as well (Vahouny, Tombes, Cassidy, Kritchevsky, & Gallo, 1980). However, CNC showed more negative charges at higher CNC concentrations, though no significant differences were observed. As shown by Sarkar et al. (2018), CNC-WPI mixture had more negative charges in the intestinal buffer (pH 6.8), but less negative charges in the bile salt solution (with or without pancreatin) as compared to that of WPI only. It was shown by the authors that CNC could reduce the negative charge of bile salt by sequestering effects, but CNC itself was also protonated under intestinal conditions and contributed to more negative charges (Sarkar et al., 2018). Thus the surface charge of CNC-WPI mixture at the intestinal phase is a combination of the effects of intestinal juice as well as bile salt and/or pancreatin on the CNC-WPI mixture.

In the fiber-protein systems, nanocellulose concentration did not cause significant differences in $\zeta$. Addition of either type of NC at any concentration did not cause significant differences in $\zeta$ at the initial phase. When moving the digesta to salivary phase, slight but no significant changes occurred for all the samples. When moving the digesta to the gastric phase, addition of CNF caused significantly lower $\zeta$ values, while the addition of TEMPO-CNF or CNC caused slightly higher but not significant differences. Thus, it can be concluded that there exists strong binding between WPI and TEMPO-CNF/CNC but not CNF at the gastric phase.

Specifically, CNF is unmodified and contained large quantities of hydroxyl groups, though negative ζ values were shown. TEMPO-CNF and CNC contained carboxyl groups and sulfate ester groups respectively, which tended to dissociate at pH values away from their isoelectric points. This also corresponded to the microstructural results in Fig 5.3 where TEMPO-CNF and CNC bound with WPI while CNF did not. As shown by Sarkar et al. (2017), the addition of 3% (w/w) CNC to 1% (w/w) WPI caused significant ζ changes both before and after digestion when compared to WPI control. However, in our study, we did not see any significant differences in ζ values among different CNC concentrations in CNC-WPI systems as shown in Fig 5.4(c). Combining the zeta potential results of Fig 5.4(f) with Fig 5.4(c), it is possible that the amount of CNC in our study was not enough to cover all the surfaces of WPI molecules at the gastric phase.

At the intestinal phase in the fiber-protein systems, similar to that of fiber-only systems, CNF addition caused significantly less negative values though no significant differences were observed. It can be shown that there were little to no interactions between CNF and WPI under intestinal conditions, but it can also emphasize the interaction between CNF and digestive components. For TEMPO-CNF, more negative values were observed with TEMPO-CNF addition, though no significant differences occurred. Similarly, the addition of CNC resulted in more negative values at higher CNC concentrations with no significant differences. The opposite trend occurs for surface charges in TEMPO-WPI and TEMPO-only systems at the intestinal phase, indicating that there may exist some interaction between TEMPO-CNF and WPI or its digestion products. Existence of non-specific interactions, including non-electrostatic and weak local electrostatic interactions have been reported in the mixtures of protein and polysaccharide at or close to neutral pHs. Specifically, non-electrostatic interactions include hydrophobic and hydrogen bonding, while weak local electrostatic interaction can occur between positively-charged regions

on protein (so-called "patches") and anionic polysaccharides or positively charged protein digestion products (e.g., peptides containing lysine and arginine) and polysaccharides (Mouécoucou, Villaume, Sanchez, & Méjean, 2004). It was also shown that amino acids zwitterions could adsorb on carboxyls of oxidized cellulose surface and formed multilayers (Zimnitsky, Yurkshtovich, & Bychkovsky, 2005). However, for CNC, similar surface charges with and without the presence of WPI showed that there existed weak or no interaction between CNC and WPI or its digestion products at the intestinal phase. It was reported that individual amino acids did not bind with CNC (Lombardo et al., 2017). Thus by comparing the different trends between TEMPO-CNF and CNC in the fiber-protein systems, it seemed that the interaction between amino acids and anionic fibers may contribute to the surface charge of the fiber-protein mixture at the intestinal phase.

5.3.4 Rheological measurement of fiber-protein and fiber-only systems

Results in Fig S5.1 and S5.2 (in supporting information) illustrated that all fibers showed dose-dependent viscosity and most of the digestive viscosity decreased following successive digestion phases, except CNC at the gastric phase. The apparent viscosity at 20 $s^{-1}$ ($\eta_{20}$) of the digesta systems is shown in Fig 5.5 as a function of fiber concentration. It was found that the presence of higher fiber concentrations (specifically 1% (w/w) CNF, 1% (w/w) cellulose, 0.36% (w/w) TEMPO-CNF or 4% (w/w) CNC) resulted in significantly higher digesta viscosity than that of control or lower fiber concentrations at any digestion phases for either fiber-protein or fiber-only systems. Furthermore, digestion phases also played an important role in the digesta viscosity. Specifically, for cellulose, CNF or TEMPO-CNF at any concentrations tested, the viscosity at the initial phase was significantly higher than those at the gastric or intestinal digestion phases for either fiber-protein or fiber-only systems. For 0.1%~1% (w/w) CNC-WPI systems, the viscosity

at the gastric phase was significantly higher than those at the other digestion phases. In the 4% (w/w) CNC-WPI systems, the viscosity at the intestinal phase was the highest, followed by that at the initial phase, and with the gastric phase being the lowest.

For digesta systems containing CNF, it was found that the presence of WPI had little or no impact on its viscosity. Specifically, the apparent viscosity at 20 $s^{-1}$ of both CNF-only and CNF-WPI digesta systems was a power law function of CNF concentrations, as shown in Fig 5.5(a), with slight differences in the power law indexes and intercepts. As an example, the power law indexes of CNF-only and CNF-WPI systems at the gastric phase were 2.00 and 1.86, respectively. In addition, the presence of digestive components (including enzymes, mucin and bile) or changes in digesta pH seemed to show little influence on the digesta viscosity, since the power law index decreased slightly over successive digestion phases. Specifically, the power law indexes of CNF-WPI systems varied from 2.20 at the initial phase to 1.72 at the intestinal phase. Similarly, the power law indexes of CNF-only systems varied from 2.23 at the initial phase to 1.85 at the intestinal phase.

For TEMPO-CNF, the addition of WPI caused a reduction in viscosity at the initial and gastric phases. This may be explained by the microscopy results shown in Fig 5.3 that TEMPO-CNF bound with WPI at the initial and gastric phase, and the particle size results in Table 1 showed that the presence of WPI caused smaller mean particle size at the gastric phase. At the intestinal phase, it was found that similar viscosity was achieved between fiber-WPI and fiber-only systems for either type of fiber. This can be due to the fact that WPI was digested after the intestinal phase as shown in the confocal imaging results (Fig 5.3), and limited effects were exerted on the digesta systems containing either type of fiber.

In terms of CNC containing systems, it was found that WPI addition had a slight impact on viscosity for CNC concentrations between 0.1~1% (w/w), but caused a reduction in that of 4% (w/w) CNC at the gastric phase. That is, the viscosity of 4% (w/w) CNC-only was higher than that of 4% CNC-WPI at the gastric phase. This also correlates to the particle size results in Table 1 that WPI addition caused reductions in the mean particle size of 0.1%~1% (w/w) CNC but not 4% CNC at the gastric phase. However, after intestinal digestion, the viscosity of 4% (w/w) CNC-only and 4% (w/w) CNC-WPI was nearly the same. It is possible that upon the addition of WPI, the positively charged WPI bound with anionic CNC at the gastric phase, which rendered CNC with less negatively charged groups, and caused a reduction in CNC viscosity at the gastric phase. It can also be concluded that in the presence of WPI, a concentration of 0.1~1% (w/w) CNC was not enough to fully cover the surface of WPI at the gastric phase, and even though small changes occurred in the system between CNC and WPI as well as between CNC and ionic environment, these changes were not detectable from the rheological measurement (on the macroscopic scale). However, in the presence of 4% (w/w) CNC, stronger interactions between CNC and WPI caused changes in both mean particle size as well as rheological measurement. Thus the differences were only observed in samples with 4% (w/w) CNC addition. The impact of ratios between CNC and WPI was also shown in other studies. Specifically, it has been reported by Liu et al. (2018) and Sarkar et al. (2018) that CNC can bind with WPI or BSA at pH 3 and there exists an optimum ratio for the binding between CNC and protein (WPI/BSA). A much denser network surround WPI interface at higher CNC concentrations (e.g., 3 wt%) than lower (e.g., 1 wt%) was reported by Sarkar et al. (2017). The interaction between CNC and WPI was reported to involve van der Waals forces, hydrogen bonding and capillary forces (Sarkar et al., 2018). The increase in digesta viscosity at the gastric phase after addition of CNC was also shown in other studies. Specifically,

the addition of 3% (w/w) CNC was reported to cause around 40 times increase in the interfacial shear viscosity of protein film at the gastric phase (Sarkar et al., 2017; Sarkar et al., 2018). In our study, it was found that the addition of 1.4% and 5.6% (w/w) CNC (the concentration at the gastric phase, which corresponded to 1% and 4% (w/w) CNC at the intestinal phase) resulted in a viscosity that was ~39 and 230 folds higher than that of WPI only at the gastric phase.

5.3.5 Percent free amino nitrogen release during *in vitro* digestion of protein solution

The effects of nanocellulose/cellulose on percent FAN release of WPI during gastric and intestinal digestion is shown in Fig 5.6. No significant differences were observed in % N release during gastric digestion for all samples, but significantly lower amount of % N release was observed in samples with 4% (w/w) CNC addition during intestinal digestion. Specifically, the % N release of WPI after gastric and intestinal digestion was ~10% and 34%, while the % N release in digesta containing 4% (w/w) CNC was ~29%. The dialysis process showed significantly lower amounts of % N in the dialysate for samples containing 1% (w/w) cellulose, 0.5%~1% (w/w) CNF, 0.1% (w/w) TEMPO-CNF and 1%~4% (w/w) CNC. In addition, it was found that higher CNF or CNC viscosity (that is, higher NC concentrations) correspond to lower initial FAN diffusion rate, as shown in Fig 5.7.

During gastric digestion, major products of proteolysis are peptides (large polypeptides and small oligopeptides), while only small amounts of free amino acids are released (Erickson & Kim, 1990). The digestion products of protein in the intestinal phase include free amino acids and oligopeptides (2-6 amino acids) (Erickson & Kim, 1990). Similar to those reported in literature (Acton et al., 1982), fiber types and concentrations play a role in protein digestion and nitrogen release/retention. Specifically, cellulose and CNF did not show any effects on % N release during gastric and intestinal digestion. Based on the results of particle size measurement, confocal

imaging and viscosity data, weak or no binding was observed between WPI and CNF/cellulose. This is similar to other results reported in literature regarding the effects of neutral polysaccharides on protein digestion. Specifically, guar and locust bean gum as well as holo-cellulose (containing cellulose and semi-cellulose) were shown to have negligible effects on casein digestibility *in vitro* (Acton et al., 1982). Anionic fibers have been shown to affect proteolysis at the gastric phase mainly due to the electrostatic attraction between positively charged protein and anionic fibers at the gastric pH, even though non-electrostatic interaction (including hydrogen bonding) may also play a role in the complexes formed between protein and polysaccharides (Mouécoucou et al., 2004). Studies have shown that some anionic polysaccharides (e.g., alginate) decreased dairy protein digestibility during gastric digestion due to their capability of forming aggregates with protein substrate (Borreani et al., 2016). However, other polysaccharides (like gum arabic, low methylated pectin or xylan) caused an increase in nitrogen release during gastric digestion of protein (e.g., β-lg) due to the formation of fiber-protein complex that reduced the aggregation of protein, even though fibers caused inhibition in pepsin activity (Mouécoucou et al., 2004). In the case of TEMPO-CNF or CNC addition, binding existed between anionic NC and the protein substrate. However, the complex formation or increase in digesta viscosity did not show any significant differences in the amount of free amino nitrogen produced. As shown by Sarkar et al. (2017), based on SDS-PAGE patterns, 3% (w/w) CNC could cause 60% intact protein bands remaining after gastric digestion, and 3% (w/w) CNC was more capable at reducing WPI digestibility than 1% (w/w) CNC. Thus it is possible that the addition of anionic NC may cause some changes in peptide products, which may require further investigation.

In our study, 4% (w/w) CNC significantly reduced the %N release during intestinal digestion, while no significant differences were observed at lower CNC concentrations. This

mechanism for reduced protein digestibility can be due to the inhibition of digestive enzymes and/or interaction with protein substrates or its digestion products (Harmuth-Hoene & Schwerdtfeger, 1979; Mouécoucou et al., 2004). Specifically, partially inhibited apparent trypsin activity was shown upon the addition of 10% (w/w) carrageenan in the rat diets, as shown by Harmuth-Hoene & Schwerdtfeger (1979). CNC possesses sulfate ester groups in its polymer chain, which is similar to the structure of carrageenan, thus it's possible that CNC may inhibit protease activity. The effect of CNC on inhibition of digestive enzyme activity has been reported by Ji, Liu, Li, Sun, & Xiong (2018), where the authors found that CNC could inhibit a-amylase activity and result in reduced starch hydrolysis.

At the intestinal phase, negatively charged polysaccharides (such as xanthan gum and carrageenan) were shown to have little interaction with protein at neutral pH due to the repulsion between them (Zhang et al., 2014). Similarly, it was reported that negatively charged nanocellulose (either sulfated or carboxylated) or pure cellulose showed little or no binding to negatively charged BSA (Lavenson, Tozzi, McCarthy, Powell, & Jeoh, 2011; Lombardo et al., 2017). Thus it is possible that anionic NC had little or no binding with WPI at the intestinal phase. However, interactions could exist between anionic NC and protein digestion products, which may show more pronounced effects on % N diffusion. According to Mouécoucou et al. (2004), gum arabic and xylan reduced peanut protein isolate (PPI) hydrolysis via interaction with some proteins and high molecular weight (MW) peptides, while LM pectin did not impact PPI hydrolysis but affect nitrogen diffusion via interaction with protein hydrolysis products (low MW peptides and amino acids). Moreover, these fibers only significantly reduced protein digestibility when using a dialysis membrane of MWCO 1 KDa while no significant effects were observed with a MWCO of 8 KDa (Mouécoucou et al., 2004).

In the digestion experiments with the dialysis process, linear trends were observed in the first 120 min. for all the samples, as shown in the inserted figures of Fig 5.6(d)-(f). Significantly lower amount of % N in the dialysate was observed in samples with higher fiber concentration. Specifically, the % N diffusion in WPI was 18.9%, while the % N diffusion was 13.82%, 14.54%, 15.38% and 9.41% in the presence of 1% (w/w) cellulose, 1% (w/w) CNF, 0.1% (w/w) TEMPO-CNF and 4% (w/w) CNC, respectively. The initial diffusion rates (% N release per min) of control, 1% (w/w) CNF, 0.1% (w/w) TEMPO-CNF and 4% (w/w) CNC were 0.00087, 0.00060, 0.00081 and 0.00031, respectively. A correlation between initial N diffusion rate and viscosity of digesta containing NC (CNF or CNC) was also found, as shown in Fig 5.7. No correlations were found in the TEMPO-CNF systems, since TEMPO-CNF had phase separation and formed discrete individual gels in the suspension, as shown in Fig 5.3. The effects of CNF concentration on N diffusion was similar to the results reported in Liu et al. (2018), where it was shown that higher CNF concentration resulted in lower glucose diffusion rate and lower amount of glucose diffused. Similarly, for CNC-WPI systems, the increased digesta viscosity also played a role in N diffusion. Furthermore, small peptides (with seven amino acids) were shown to be efficiently bound to CNC with a binding constant of $\sim 10^5\ M^{-1}$ (Guo et al., 2013), though no interactions occurred between individual amino acids and CNC (Lombardo et al., 2017).

**5.4 Conclusions**

Results from our study showed that among the three types of nanocellulose (CNF, TEMPO-CNF and CNC), CNC was the most effective at reducing the release and diffusion of free amino nitrogen during proteolysis of WPI in a simulated static digestion model. Specifically, concentrations of 4% (w/w) CNC could significantly reduce the amount of free amino nitrogen release during the intestinal digestion, though no significant effects of CNC on WPI hydrolysis

during gastric digestion were observed. Higher CNC concentrations resulted in a lower initial diffusion rate of free amino nitrogen (FAN) as well as less amounts of FAN diffused out. In particular, around 50% of FAN diffusion was reduced in the presence of 4% (w/w) CNC during intestinal digestion. CNF was the second most effective towards reducing the diffusion of FAN during intestinal digestion, even though CNF at concentrations up to 1% (w/w) did not show any significant effects towards the amount of FAN release. CNF also showed concentration dependent effects on FAN diffusion. Specifically, the concentration of CNF was proportional to its viscosity which at higher levels, resulted in lower initial diffusion rate as well as less amounts of FAN diffused. With the presence of 1% (w/w) CNF, the FAN diffusion was reduced by 23% at the end of digestion. However, TEMPO-CNF was the least effective at reducing FAN diffusion during intestinal digestion. Even though 0.1% (w/w) TEMPO-CNF caused slight but significant reduction in the amount of FAN diffusion, higher TEMPO-CNF concentration at 0.36% (w/w) did not cause any significant differences. In addition, no correlations were found between TEMPO-CNF concentration and its initial diffusion rate. Furthermore, TEMPO-CNF did not show any significant effects at the amount of FAN release either at the gastric or intestinal digestion.

It was concluded that cellulose and CNF were very stable during *in vitro* digestion and they did not bind with WPI. Thus, WPI addition did not impact the morphology, particle size, or viscosity of digesta containing cellulose and CNF. However, anionic NC (TEMPO-CNF and CNC) bound with WPI, and the presence of WPI caused some changes in the mean particle size, microstructure as well as viscosity of digesta. Specifically, the presence of WPI resulted in reductions in both mean particle size and viscosity for digesta containing TEMPO-CNF at the initial and gastric phase. Reductions only in particle size occurred for digesta containing CNC concentrations of 0.1%~1% (w/w) while digesta containing concentrations of 4% (w/w) CNC only

saw reductions in viscosity at the gastric phase. Results from our study also showed that all three types of nanocellulose (especially CNC) are effective in increasing digesta viscosity. These findings suggested that all three types of NC may be applicable for delaying gastric emptying and promoting satiety.

## 5.5 Supporting Information

Viscosity of fiber-protein and fiber-only systems with different concentrations of fibers as a function of shear rate (1~100 $s^{-1}$) after each *in vitro* digestion phase was shown in Fig S5.1 and S5.2, respectively.

## 5.6 Acknowledgements

This work was supported by the USDA National Institute of Food and Agriculture [grant no. 2016-67021-24994/project accession no. 1009090].

## 5.7 References

Acton, J., Breyer, L., & Satterlee, L. (1982). Effect of dietary fiber constituents on the in vitro digestibility of casein. *Journal of Food Science,* 47(2), 556-560.

Anderson, G. H., & Moore, S. E. (2004). Dietary proteins in the regulation of food intake and body weight in humans. *The Journal of nutrition,* 134(4), 974S-979S.

Bertsch, P., Isabettini, S., & Fischer, P. (2017). Ion-Induced Hydrogel Formation and Nematic Ordering of Nanocrystalline Cellulose Suspensions. *Biomacromolecules,* 18(12), 4060-4066.

Borreani, J., Llorca, E., Larrea, V., & Hernando, I. (2016). Adding neutral or anionic hydrocolloids to dairy proteins under in vitro gastric digestion conditions. *Food Hydrocolloids,* 57, 169-177.

DeLoid, G. M., Sohal, I. S., Lorente, L. R., Molina, R. M., Pyrgiotakis, G., Stevanovic, A., . . . Bousfield, D. W. (2018). Reducing Intestinal Digestion and Absorption of Fat Using a Nature-Derived Biopolymer: Interference of Triglyceride Hydrolysis by Nanocellulose. *ACS nano*, 12 (7), 6469–6479.

Dukes, B. C., & Butzke, C. E. (1998). Rapid determination of primary amino acids in grape juice using an o-phthaldialdehyde/N-acetyl-L-cysteine spectrophotometric assay. *American Journal of Enology and Viticulture,* 49(2), 125-134.

Erickson, R. H., & Kim, Y. S. (1990). Digestion and absorption of dietary protein. *Annual review of medicine,* 41(1), 133-139.

Fukuzumi, H., Tanaka, R., Saito, T., & Isogai, A. (2014). Dispersion stability and aggregation behavior of TEMPO-oxidized cellulose nanofibrils in water as a function of salt addition. *Cellulose,* 21(3), 1553-1559.

Gbassi, G., Yolou, F., Sarr, S., Atheba, P., Amin, C. N., & Ake, M. (2012). Whey proteins analysis in aqueous medium and in artificial gastric and intestinal fluids. *International Journal of Biological and Chemical Sciences,* 6(4), 1828-1837.

Guo, J., Catchmark, J. M., Mohamed, M. N. A., Benesi, A. J., Tien, M., Kao, T.-h., . . . Kubicki, J. D. (2013). Identification and characterization of a cellulose binding heptapeptide revealed by phage display. *Biomacromolecules,* 14(6), 1795-1805.

Harmuth-Hoene, A.-E., & Schwerdtfeger, E. (1979). Effect of indigestible polysaccharides on protein digestibility and nitrogen retention in growing rats. *Annals of Nutrition & Metabolism,* 23(5), 399-407.

Harnsilawat, T., Pongsawatmanit, R., & McClements, D. (2006). Characterization of β-lactoglobulin–sodium alginate interactions in aqueous solutions: a calorimetry, light scattering, electrophoretic mobility and solubility study. *Food Hydrocolloids,* 20(5), 577-585.

Hughes, J. S., Acevedo, E., Bressani, R., & Swanson, B. G. (1996). Effects of dietary fiber and tannins on protein utilization in dry beans (Phaseolus vulgaris). *Food Research International,* 29(3-4), 331-338.

Ikegami, S., Tsuchihashi, F., Harada, H., Tsuchihashi, N., Nishide, E., & Innami, S. (1990). Effect of viscous indigestible polysaccharides on pancreatic-biliary secretion and digestive organs in rats. *The Journal of nutrition,* 120(4), 353-360.

Ioelovich, M., & Figovsky, O. (2008). Nano-cellulose as promising biocarrier. *Advanced Materials Research* (Vol. 47, pp. 1286-1289): Trans Tech Publ.

Ji, N., Liu, C., Li, M., Sun, Q., & Xiong, L. (2018). Interaction of cellulose nanocrystals and amylase: Its influence on enzyme activity and resistant starch content. *Food chemistry,* 245, 481-487.

Jones, O. G., Lesmes, U., Dubin, P., & McClements, D. J. (2010). Effect of polysaccharide charge on formation and properties of biopolymer nanoparticles created by heat treatment of β-lactoglobulin–pectin complexes. *Food Hydrocolloids,* 24(4), 374-383.

Jorfi, M., & Foster, E. J. (2015). Recent advances in nanocellulose for biomedical applications. *Journal of Applied Polymer Science,* 132(14).

Kitabatake, N., & Kinekawa, Y.-I. (1998). Digestibility of bovine milk whey protein and β-lactoglobulin in vitro and in vivo. *Journal of Agricultural & Food Chemistry,* 46(12), 4917-4923.

Kolakovic, R., Laaksonen, T., Peltonen, L., Laukkanen, A., & Hirvonen, J. (2012). Spray-dried nanofibrillar cellulose microparticles for sustained drug release. *International journal of pharmaceutics,* 430(1-2), 47-55.

Lavenson, D. M., Tozzi, E. J., McCarthy, M. J., Powell, R. L., & Jeoh, T. (2011). Investigating adsorption of bovine serum albumin on cellulosic substrates using magnetic resonance imaging. *Cellulose,* 18(6), 1543-1554.

Lin, N., & Dufresne, A. (2014). Nanocellulose in biomedicine: Current status and future prospect. *European Polymer Journal,* 59, 302-325.

Liu, F., Zheng, J., Huang, C.-H., Tang, C.-H., & Ou, S.-Y. (2018). Pickering high internal phase emulsions stabilized by protein-covered cellulose nanocrystals. *Food Hydrocolloids,* 82, 96-105.

Liu, L., Kerr, W. L., Kong, F., Dee, D. R., & Lin, M. (2018). Influence of nano-fibrillated cellulose (NFC) on starch digestion and glucose absorption. *Carbohydrate polymers,* 196, 146-153.

Lombardo, S., Eyley, S., Schütz, C., Van Gorp, H., Rosenfeldt, S., Van den Mooter, G., & Thielemans, W. (2017). Thermodynamic study of the interaction of bovine serum albumin and amino acids with cellulose nanocrystals. *Langmuir,* 33(22), 5473-5481.

Macierzanka, A., Böttger, F., Lansonneur, L., Groizard, R., Jean, A.-S., Rigby, N. M., . . . Mackie, A. R. (2012). The effect of gel structure on the kinetics of simulated gastrointestinal digestion of bovine β-lactoglobulin. *Food chemistry,* 134(4), 2156-2163.

Mendoza, L., Batchelor, W., Tabor, R. F., & Garnier, G. (2018). Gelation mechanism of cellulose nanofibre gels: A colloids and interfacial perspective. *Journal of colloid and interface science,* 509, 39-46.

Minko, S., Sharma, S., Hardin, I., Luzinov, I., Daubenmire, S. W., Zakharchenko, A., . . . Kim, Y. S. (2016). Textile dyeing using nanocellulosic fibers. Google Patents.

Mouécoucou, J., Villaume, C., Sanchez, C., & Méjean, L. (2004). Effects of gum arabic, low methoxy pectin and xylan on in vitro digestibility of peanut protein. *Food Research International,* 37(8), 777-783.

Mouécoucou, J., Villaume, C., Sanchez, C., & Méjean, L. (2004). β-Lactoglobulin/polysaccharide interactions during in vitro gastric and pancreatic hydrolysis assessed in dialysis bags of different molecular weight cut-offs. *Biochimica et Biophysica Acta (BBA)-General Subjects,* 1670(2), 105-112.

Nicolai, T., Britten, M., & Schmitt, C. (2011). β-Lactoglobulin and WPI aggregates: formation, structure and applications. *Food Hydrocolloids,* 25(8), 1945-1962.

Ren, S., Sun, X., Lei, T., & Wu, Q. (2014). The effect of chemical and high-pressure homogenization treatment conditions on the morphology of cellulose nanoparticles. *Journal of Nanomaterials,* 2014, 168.

Sabin, A. (2011). Problems in particle size: laser diffraction observations. *Journal of GXP Compliance,* 15(4), 35-44.

Sarkar, A., Li, H., Cray, D., & Boxall, S. (2018). Composite whey protein–cellulose nanocrystals at oil-water interface: Towards delaying lipid digestion. *Food Hydrocolloids,* 77, 436-444.

Sarkar, A., Zhang, S., Murray, B., Russell, J. A., & Boxal, S. (2017). Modulating in vitro gastric digestion of emulsions using composite whey protein-cellulose nanocrystal interfaces. *Colloids & Surfaces B: Biointerfaces,* 158, 137-146.

Sun, X., Wu, Q., Zhang, X., Ren, S., Lei, T., Li, W., . . . Zhang, Q. (2018). Nanocellulose films with combined cellulose nanofibers and nanocrystals: tailored thermal, optical and mechanical properties. *Cellulose,* 25(2), 1103-1115.

Unterhaslberger, G., Schmitt, C., Sanchez, C., Appolonia-Nouzille, C., & Raemy, A. (2006). Heat denaturation and aggregation of β-lactoglobulin enriched WPI in the presence of arginine HCl, NaCl and guanidinium HCl at pH 4.0 and 7.0. *Food Hydrocolloids,* 20(7), 1006-1019.

Vahouny, G. V., Tombes, R., Cassidy, M. M., Kritchevsky, D., & Gallo, L. L. (1980). Dietary fibers: V. Binding of bile salts, phospholipids and cholesterol from mixed micelles by bile acid sequestrants and dietary fibers. *Lipids,* 15(12), 1012-1018.

Ye, A. (2008). Complexation between milk proteins and polysaccharides via electrostatic interaction: principles and applications–a review. *International journal of food science & technology,* 43(3), 406-415.

Zhang, S., & Vardhanabhuti, B. (2014). Intragastric gelation of whey protein–pectin alters the digestibility of whey protein during in vitro pepsin digestion. *Food & function*, 5(1), 102-110.

Zhang, S., Zhang, Z., & Vardhanabhuti, B. (2014). Effect of charge density of polysaccharides on self-assembled intragastric gelation of whey protein/polysaccharide under simulated gastric conditions. *Food & function*, 5(8), 1829-1838.

Zhao, Y., Li, F., Carvajal, M. T., & Harris, M. T. (2009). Interactions between bovine serum albumin and alginate: an evaluation of alginate as protein carrier. *Journal of Colloid & Interface Science*, 332(2), 345-353.

Zimnitsky, D. S., Yurkshtovich, T. L., & Bychkovsky, P. M. (2005). Multilayer adsorption of amino acids on oxidized cellulose. *Journal of Colloid & Interface Science*, 285(2), 502-508.

Table 5.1. Mean particle size ($D_{43}$) of fiber-protein and fiber-only systems during digestion

| | Fiber concentration (wt%) | Fiber-WPI-Initial | Fiber-WPI-Gastric | Fiber-WPI-Intestinal | Fiber-only-Initial | Fiber-only-Gastric | Fiber-only-Intestinal |
|---|---|---|---|---|---|---|---|
| CNF | 0.00 | 23±8 | 18±5 | 52±8 | | 30±6 | 18±14 |
| | 0.10 | 92±5 | 83±7 | 102±3 | 101±1 | 103±4 | 105±3 |
| | 0.50 | 102±2 | 98±2 | 103±1 | 105.8 | 109±3 | 105±3 |
| | 1.00 | 100±2 | 99±2 | 102±4 | 101.1 | 106±1 | 104±1 |
| TEMPO-CNF | 0.00 | 23±8 | 18±5 | 52±8 | | 30±6 | 18±14 |
| | 0.05 | 175±30 | 238±70 | 230±39 | 125±25 | 260±19 | 222±46 |
| | 0.10 | 295±30 | 176±10 | 282±41 | 187±52 | 383±35 | 240±37 |
| | 0.36 | 135±30 | 177±39 | 293±30 | 291±13 | 361±52 | 360±19 |
| CNC | 0.00 | 23.5 | 18±5 | 52±8 | | 30±6 | 18±14 |
| | 0.10 | 54±7 | 14±4 | 43±29 | 9±4 | 71±18 | 71±39 |
| | 1.00 | 55±10 | 29±10 | 21±3 | 6.9±0.2 | 34±8 | 9±3 |
| | 4.00 | 103±38 | 33±2 | 11±5 | 16±6 | 11±6 | 6.3±5.8 |

Table 5.2. Parameters for the curves of apparent viscosity of fiber-only or fiber-WPI systems (η) at 20 $s^{-1}$ versus nanocellulose concentration (C) fitted by Power law model ($\log \eta = a + b \log C$) (as shown by Fig 5.5)

| Fiber | Phase | Fitting | | | | | | | |
|---|---|---|---|---|---|---|---|---|---|
| | | Concentration range (wt%) | | Fiber only | | | Fiber-WPI | | |
| | | | | Parameters | | | Parameters | | |
| | | Low | High | a | b | Adj. $R^2$ | a | b | Adj. $R^2$ |
| CNF | Initial | 0.23 | 2.33 | 4.04 | 2.23 | 0.9984 | 4.11 | 2.2 | 0.9989 |
| | Gastric | 0.14 | 1.40 | 3.47 | 2.00 | 0.9721 | 3.25 | 1.86 | 0.9956 |
| | Intestinal | 0.10 | 1.00 | 3.16 | 1.85 | 0.9766 | 2.8 | 1.72 | 0.9906 |
| TEMPO-CNF | Initial | 0.12 | 0.84 | 5.45 | 2.42 | 0.9971 | 5.83 | 2.71 | 0.9991 |
| | Gastric | 0.07 | 0.14 | 2.21 | 1.46 | -- | 0.37 | 0.91 | -- |
| | | 0.14 | 0.50 | 6.66 | 3.02 | -- | 6.86 | 3.19 | -- |
| | Intestinal | 0.05 | 0.10 | 0.04 | 0.78 | -- | -0.46 | 0.63 | -- |
| | | 0.10 | 0.36 | 4.21 | 2.17 | -- | 4.67 | 2.34 | -- |
| CNC | Initial | 0.23 | 2.33 | -1.81 | 0.35 | -- | -1.86 | 0.32 | -- |
| | | 2.33 | 9.33 | 3.91 | 3.86 | -- | 3.83 | 3.8 | -- |
| | Gastric | 0.14 | 5.60 | 2.74 | 1.81 | 0.9993 | 1.24 | 1.29 | 0.99999 |
| | Intestinal | 0.10 | 1.00 | 0.59 | 1.06 | -- | 0.41 | 1.00 | -- |
| | | 1.00 | 4.00 | 4.25 | 2.89 | -- | 4.03 | 2.81 | -- |

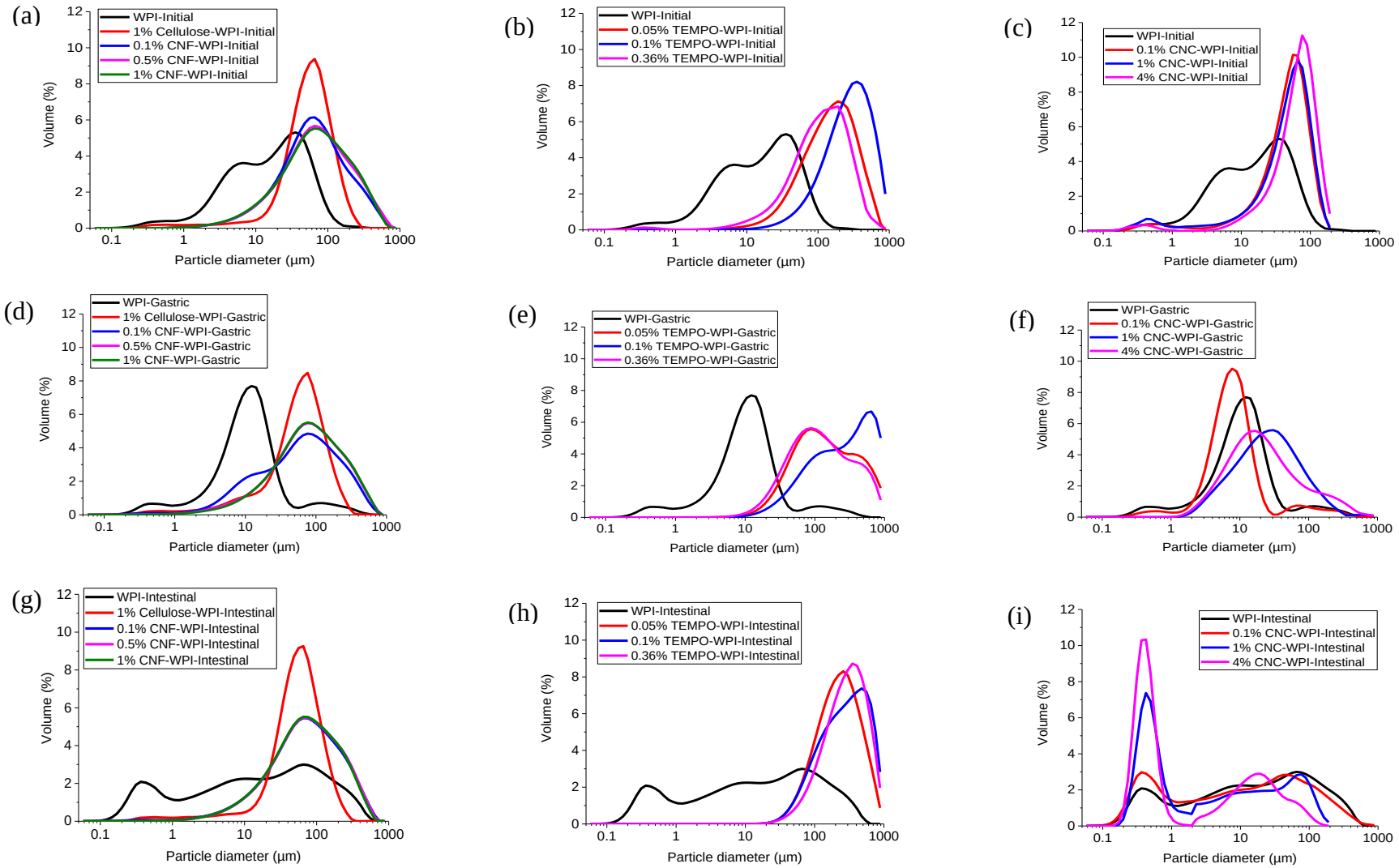


Fig 5.1. Particle size distribution of fiber-protein systems after each digestion phase, with the addition of (a), (d), (g) CNF/cellulose; (b), (e), (h) TEMPO-CNF and (c), (f), (i) CNC

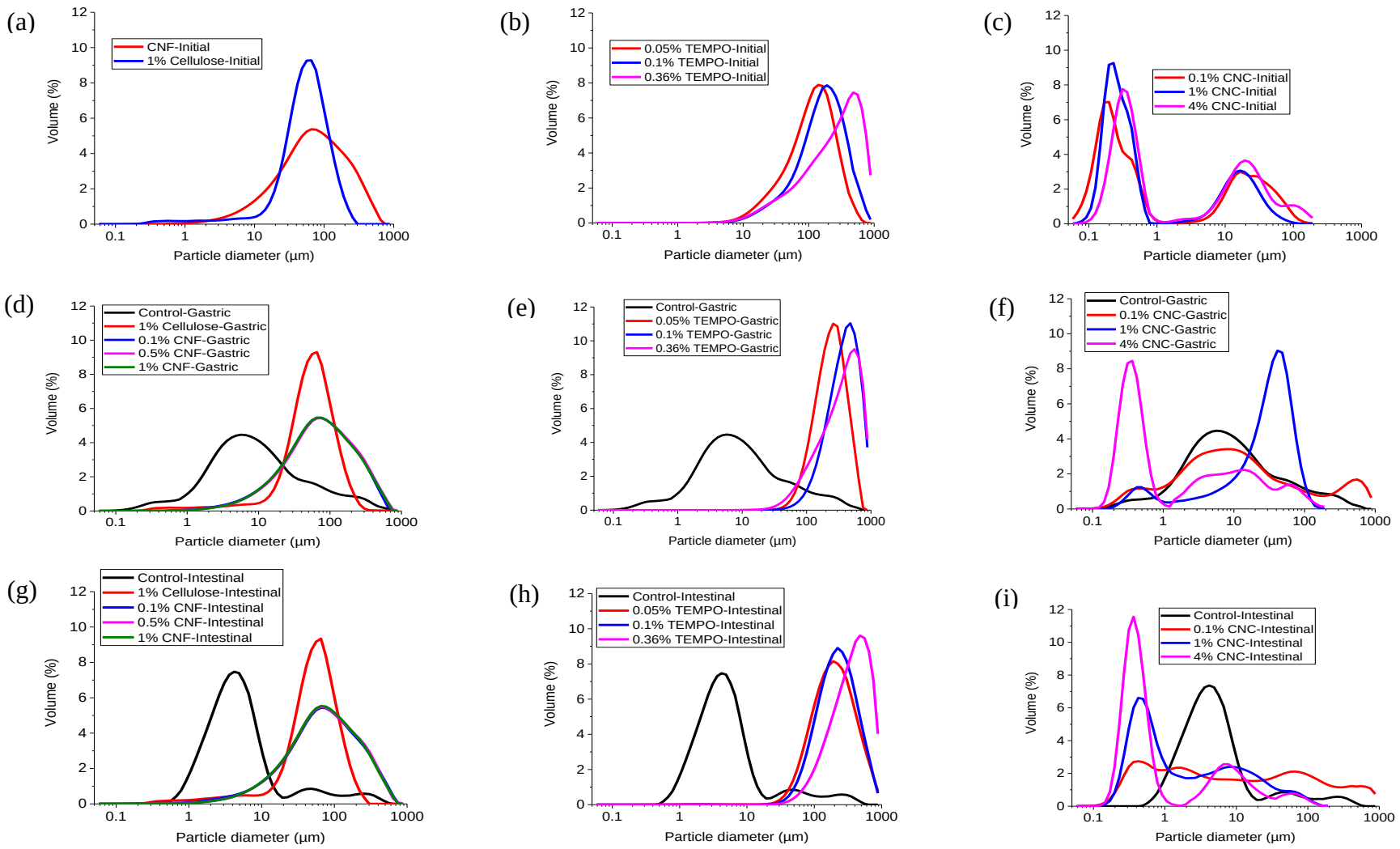


Fig 5.2. Particle size distribution of fiber-only systems after each digestion phase, with the addition of (a), (d), (g) CNF/cellulose; (b), (e), (h) TEMPO-CNF and (c), (f), (i) CNC.

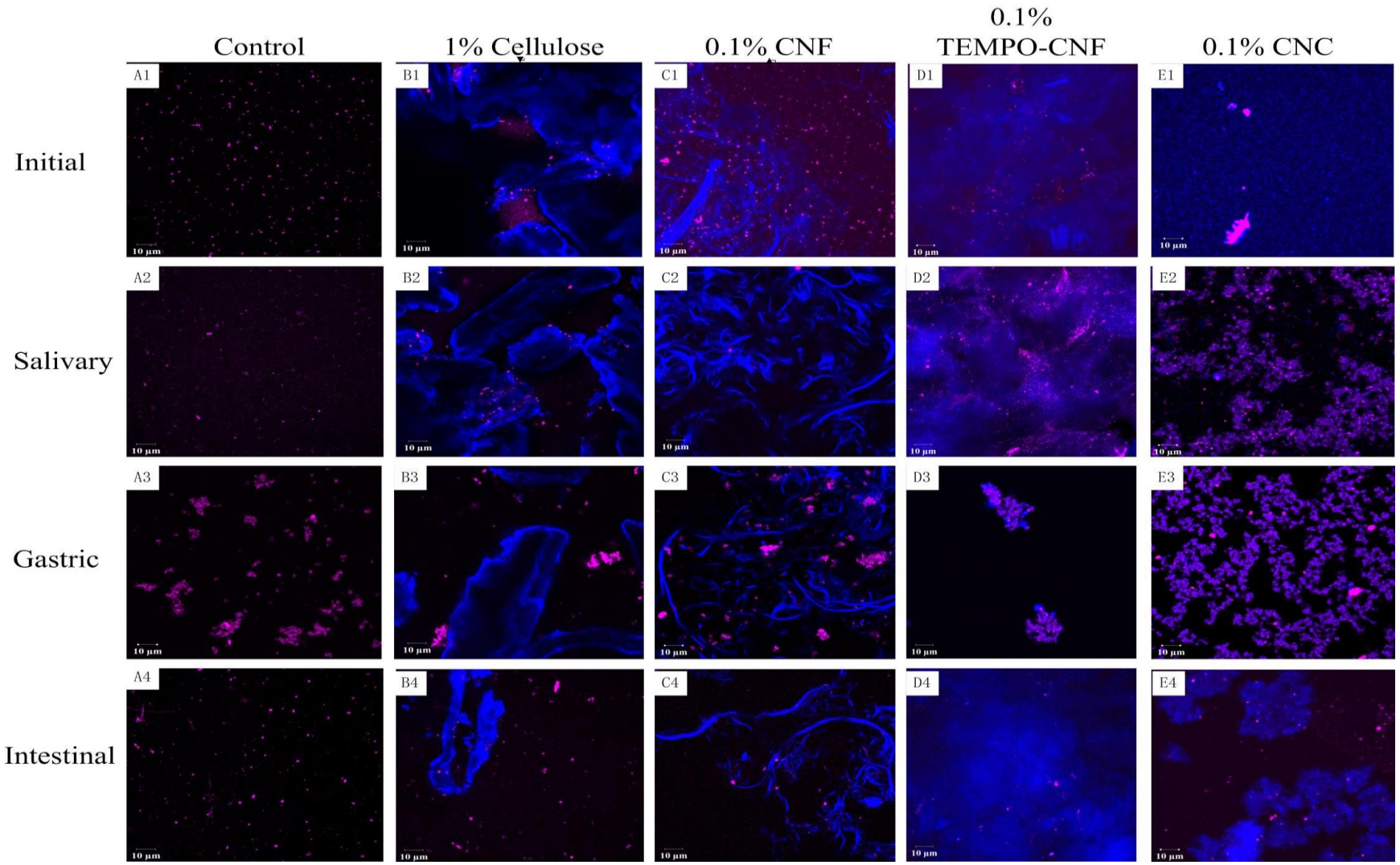


Fig 5.3. Confocal microscopy images showing microstructure of whey protein isolate (WPI) containing nanocellulose/cellulose after exposure to each *in vitro* digestion phase

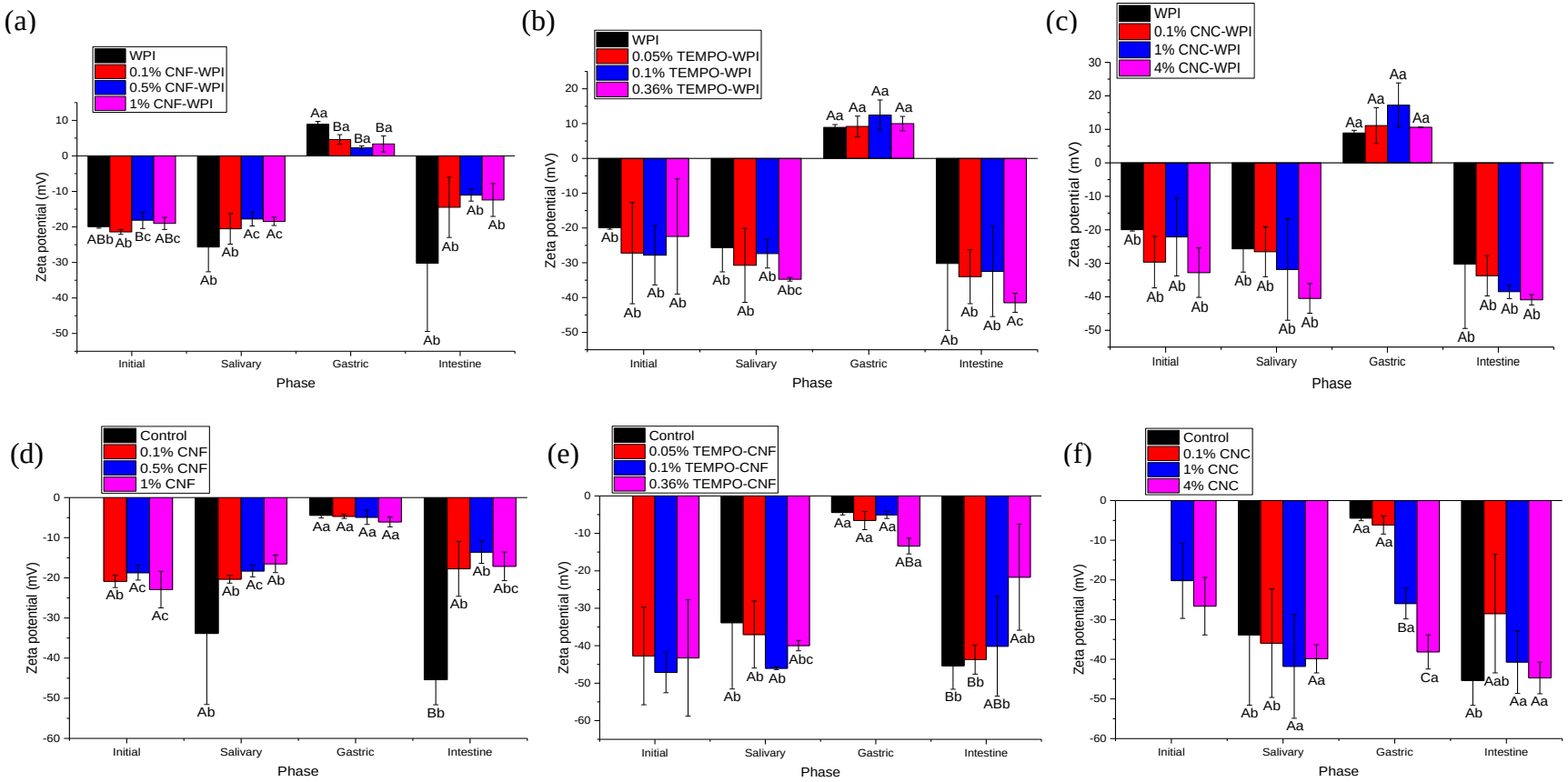


Fig 5.4. Surface charge (zeta-potential) of nanocellulose-whey protein isolate (WPI) systems or nanocellulose-only systems after each *in vitro* digestion phase: (a) CNF with WPI; (b) TEMPO-CNF with WPI; (c) CNC with WPI; (d) CNF without WPI; (e) TEMPO-CNF without WPI and (f) CNC without WPI. Samples designated with upper case letters were significantly different (Duncan, $p < 0.05$) when compared among different concentrations (at the same digestion phase); samples designated with lower case letters were significantly different (Duncan, $p < 0.05$) when compared among different digestion phases (at the same fiber concentration).

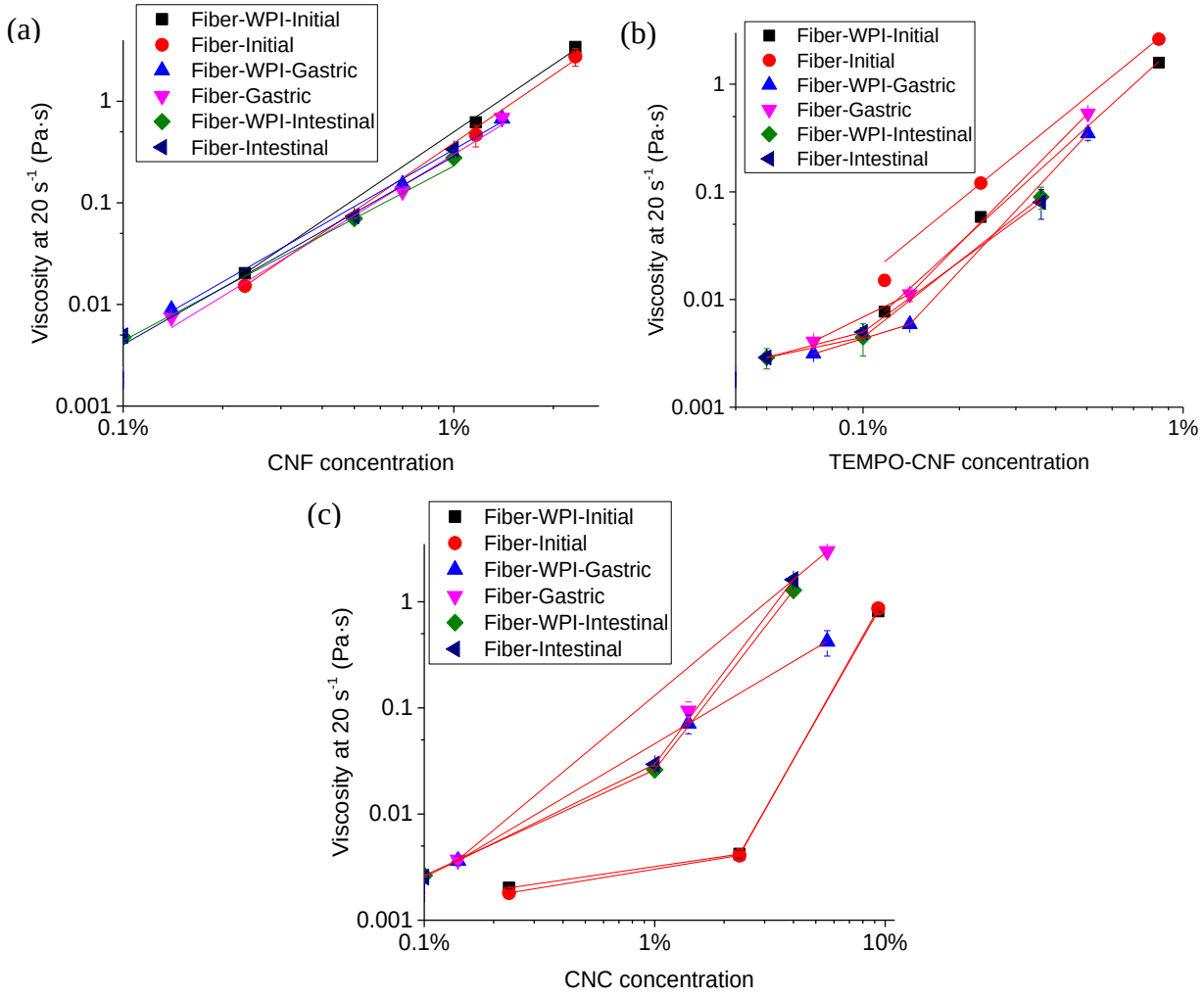


Fig 5.5. Apparent viscosity of whey protein isolate (WPI) at 20 $s^{-1}$ after each digestion phase with and without different concentrations of nanocellulose: (a) CNF; (b) TEMPO-CNF and (c) CNC.

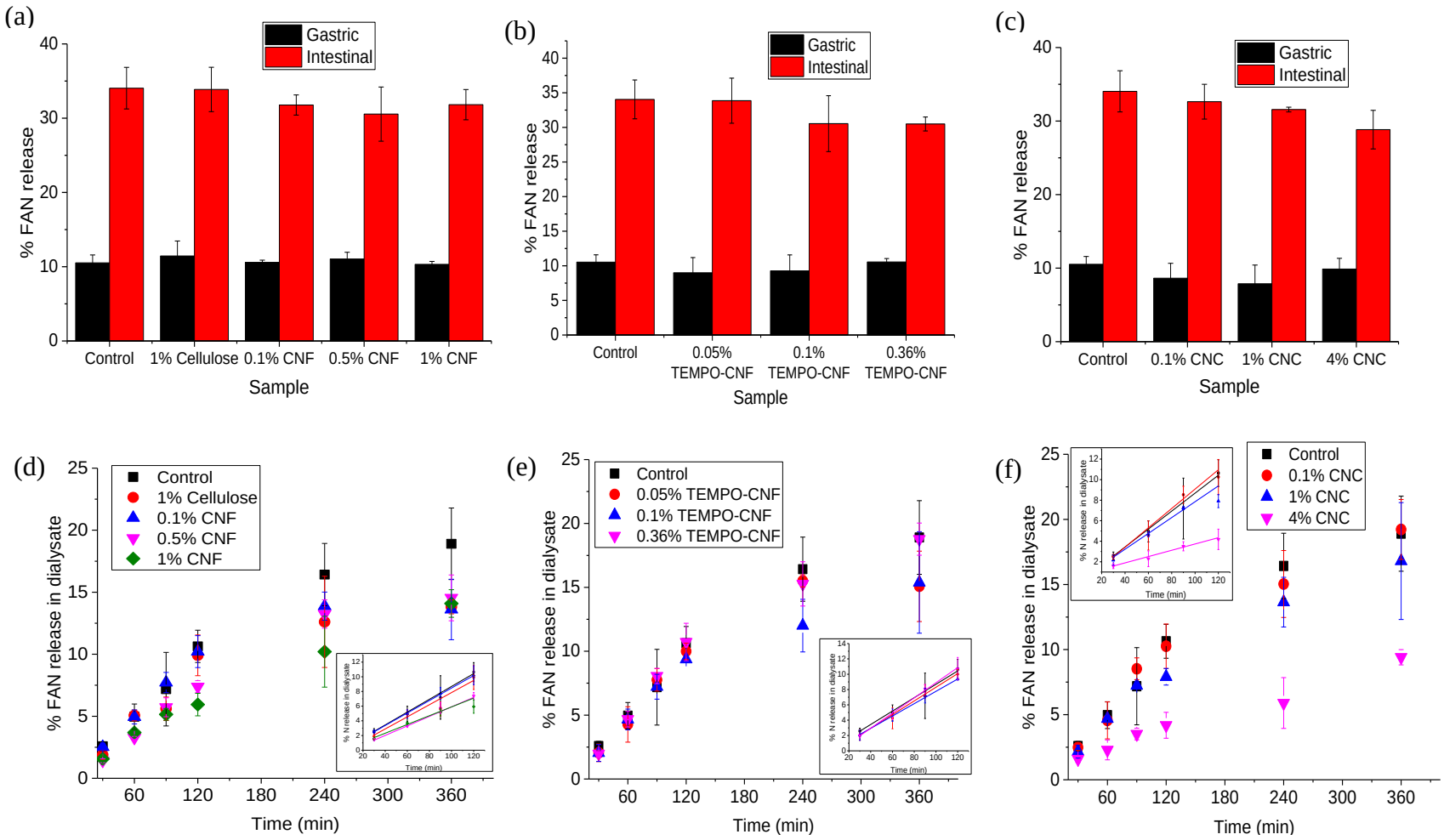


Fig 5.6. Percent free amino nitrogen (FAN) release of whey protein isolate (WPI) with and without addition of fiber after gastric and intestinal digestion: (a) CNF, (b) TEMPO-CNF; (c) CNC; and percent FAN diffusion in the dialysate for (d) CNF, (e) TEMPO-CNF and (f) CNC.

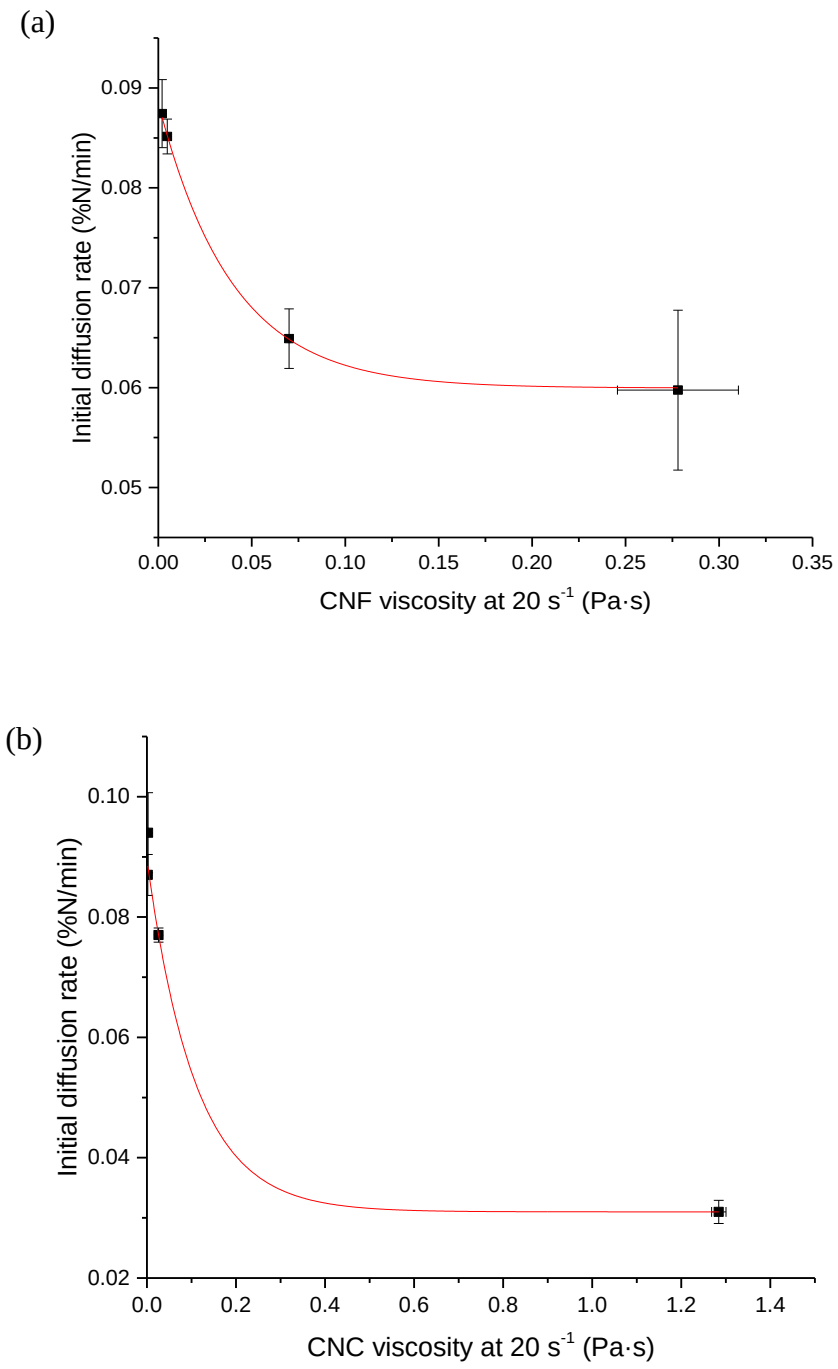


Fig 5.7. Initial diffusion rate of % N diffusion versus digesta viscosity containing nanocellulose in the fiber-protein systems: (a) CNF; (b) CNC

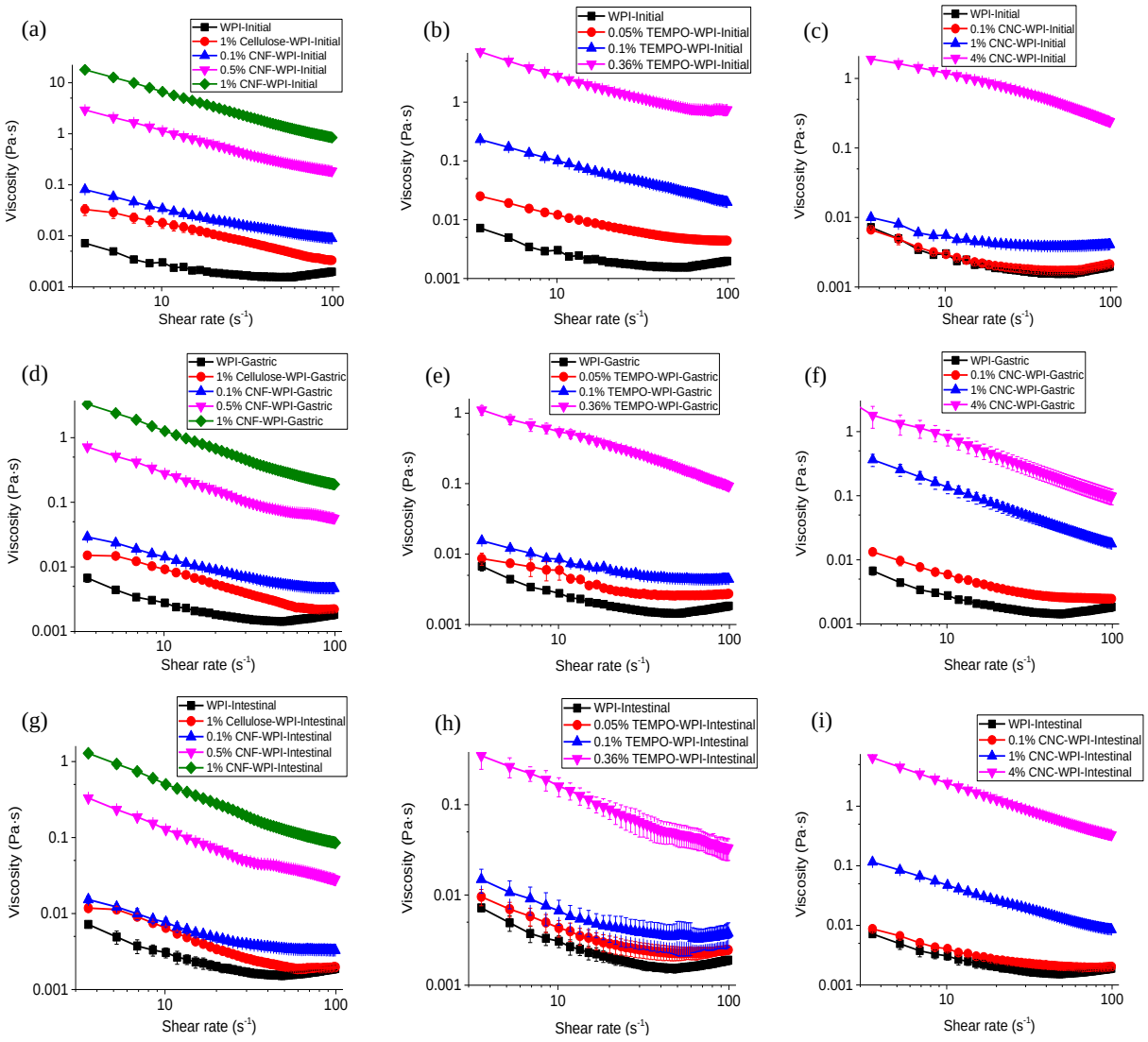


Fig S5.1. Viscosity of fiber-protein systems after each *in vitro* digestion phase with different concentrations of fiber: (a), (d), (g) CNF/cellulose; (b), (e), (h) TEMPO-CNF and (c), (f), (i) CNC.

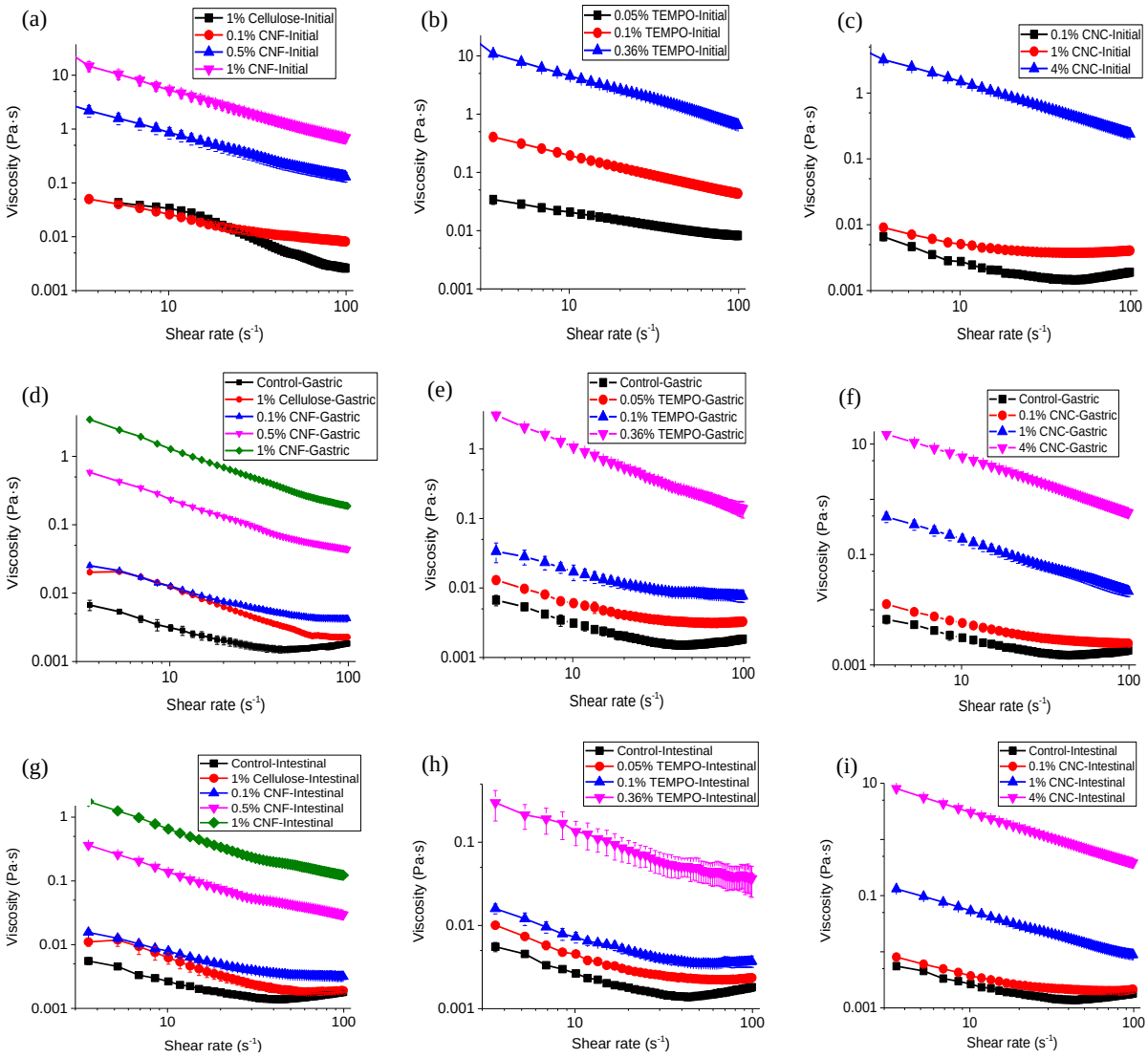


Fig S5.2. Viscosity of fiber-only systems after each *in vitro* digestion phase with different concentrations of fiber: (a), (d), (g) CNF/cellulose; (b), (e), (h) TEMPO-CNF and (c), (f), (i) CNC.

# CHAPTER 6

# SUMMARY AND RECOMMENDATIONS

## 6.1. Summary

Our study showed that all 3 types of nanocellulose at high concentrations (1% (w/w) CNF, 0.36% (w/w) TEMPO-CNF and 2~4% (w/w) CNC) exerted hypoglycemic potential in addition to delayed lipid digestion and free amino nitrogen absorption. At lower concentrations, no significant effects were observed. Nanocellulose itself could go through various changes during digestion. Specifically, CNF and cellulose were morphologically stable during *in vitro* digestion, while TEMPO-CNF aggregated, causing phase separation at the gastric phase with lower viscosity, while CNC formed hydrogels at the gastric phase with higher viscosity.

CNF did not show any significant effects on α-amylase and α-glucosidase enzyme activities but significantly reduced lipase activity. In terms of starch *in vitro* digestion, all three types of NC did not exert significant effects on the amount of glucose produced. During *in vitro* digestion of Tween 80 stabilized oil-in-water emulsions, all three types of NC significantly delayed the initial release of free fatty acids (FFA) at high concentrations (1% (w/w) CNF, 0.25~0.36% (w/w) TEMPO-CNF or 2~3% (w/w) CNC), but not on the final lipolysis extent, and this delaying effect was mainly due to higher viscosity found at higher NC concentrations. Furthermore, all types of NC observed did not exert any significant effects on the amount of free amino nitrogen (FAN) released during gastric or intestinal digestion of whey protein isolate (WPI), except for 4% (w/w) CNC.

Specific interactions can occur between NC and certain food products. TEMPO-CNF was found to bind with WPI at the initial and gastric phases, resulting in lower viscosity compared with TEMPO-alone systems. High concentrations of CNC (4% (w/w)) bound with WPI at the gastric phase and caused reductions in viscosity. Lower concentrations of CNC (0.1~1% (w/w)) showed less binding with WPI and no changes were observed in viscosity except for smaller mean particle sizes. Cellulose and CNF did not bind with WPI while all three forms of NC did not bind with Tween 80 stabilized anionic lipid emulsions.

All three types of nanocellulose were shown to exert non-specific interactions towards digestion products (including glucose and free amino nitrogen) as well as cholesterol and bile acid. These non-specific interactions ascribed to adsorption properties as well as gel entrapment by NC due to higher viscosity at higher concentrations. Specifically, CNF exerted higher glucose and cholesterol adsorption capacity as well as higher bile acid retardation effects when compared to conventional cellulose. In addition, higher concentrations of NC (0.5~1% (w/w) CNF, 0.36% (w/w) TEMPO-CNF and 2~4% (w/w) CNC) significantly retarded glucose diffusion. Similarly, significant retardation of free amino nitrogen diffusion was achieved at higher NC concentrations (0.5~1% (w/w) CNF, 0.1% (w/w) TEMPO-CNF and 1~4% (w/w) CNC).

### 6.2. Recommendations

This study has shown the influence of three types of nanocellulose on food digestion and nutrient absorption as well as the behavior of nanocellulose itself during digestion under a simulated static *in vitro* digestion model. Further *in vivo* studies are recommended to validate these results. Furthermore, since nanocellulose is an insoluble fiber and its fermentation can occur in the large intestine, the effects of nanocellulose on microbiota growth as well as short-chain fatty acid release may also need future investigation. The particle sizes of three types of nanocellulose

showed different changes during each digestion phase as well as in the presence of different types of food. Thus, the transit of nanocellulose along the GI tract may also need further *in vivo* or cell culture studies. Overall, this study suggests the potential applications of nanocellulose in the food industry as a fiber source to control nutrient absorption and promote satiety, but additional research is still needed before these applications can truly be realized.

# APPENDIX

## INFLUENCE OF NANO-CELLULOSE ON *IN VITRO* DIGESTION OF MILK

## 1 Objective

To study the influence of three types of nanocellulose on *in vitro* digestion of a model food (milk).

## 2 Materials and methods

### 2.1 *In vitro* digestion of milk

Whole milk was purchased from a local grocery store. The fiber materials and digestive components were the same as described in Chapter 5. Specifically, different types of nanocellulose solution were prepared by diluting the stock nanocellulose with DI water. The initial fiber-milk systems included 6 mL of milk and 21 mL of nanocellulose solution (0.70% (w/w) CNF, TEMPO-CNF or CNC). In addition, 0.70% (w/w) cellulose suspension was studied as a comparison. A control sample was also prepared that contained no added fiber. The mixture was held at 37 °C in a shaking water bath (Model 290400S, Boekel Scientific, USA) prior to the *in vitro* digestion.

*In vitro* digestion of milk with or without the addition of fiber was performed based on a modified method from Liu et al. (2018). The digestion trial was initiated by the addition of 6 mL of 'salivary juice' to the samples with pH quickly adjusted to 6.8 ± 0.2, followed by incubation at 37°C with a shaking speed of 100 rpm for 5 min. The process of gastric digestion was simulated following the salivary phase via the addition of 'gastric juices' (12 mL) with the pH adjusted to 3.0 ± 0.1 and incubated for 2 hrs. Following the gastric phase, duodenal (12 mL) and bile juice (6 mL) were added, pH adjusted to 7.0 ± 0.2, then the digesta was placed inside a dialysis tubing (8 KDa, Spectra/Por 6 Dialysis tubing, Spectrum Laboratories, Los Angeles, CA) against 0.1 M PBS (pH 7.4) (with an inside and outside volume ratio of 1:12.5), and incubated for 2 hrs. Aliquots (4 mL) were collected from outside the tubing and the amount of free amino nitrogen in aliquots was determined by using the o-phthaldialdehyde/N-acetyl-l-cysteine (NOPA) method (Dukes & Butzke, 1998). During intestinal digestion, the concentration for all fibers (CNF, TEMPO-CNF,

CNC and cellulose) was 0.30% (w/w). Results were presented based on the amount of free amino nitrogen diffusion with respect to the final concentration of each fiber.

### 2.2 Statistical analysis

Triplicate measurements were performed for all parameters and significant analysis was performed by Duncan's multiple comparison tests with SAS/STAT software (SAS Institute Inc., Cary, NC). Regression models generated in the graphs were done using Origin data analysis and graphing software.

## 3 Results and discussion

The effect of different types of nanocellulose or cellulose on free amino nitrogen (FAN) release was plotted in Fig A1. Results showed that 0.3% (w/w) CNC addition caused significant lower amount of FAN diffusion during intestinal digestion, while the addition of the other fibers (cellulose, CNF or TEMPO-CNF) did not cause any significant differences from control. The result shown here was similar to that reported in Chapter 5, where the addition of CNC caused significant lower amount of FAN diffusion during intestinal digestion. The mechanisms behind were thought to be similar to those discussed in Chapter 5. Thus it can be concluded that CNC could interact with protein and delay free amino nitrogen diffusion.

## 4 Conclusions

CNC with a concentration of 0.3% (w/w) was able to interact with milk protein and delay diffusion of free amino nitrogen during intestinal digestion, while the other fibers (cellulose, CNF or TEMPO-CNF) at the same concentration showed no effects.

## 5 References

Liu, L., Kerr, W. L., Kong, F., Dee, D. R., & Lin, M. (2018). Influence of nano-fibrillated cellulose (NFC) on starch digestion and glucose absorption. *Carbohydrate Polymers,* 196, 146-153.

Dukes, B. C., & Butzke, C. E. (1998). Rapid determination of primary amino acids in grape juice using an o-phthaldialdehyde/N-acetyl-L-cysteine spectrophotometric assay. *American Journal of Enology and Viticulture*, 49(2), 125-134.

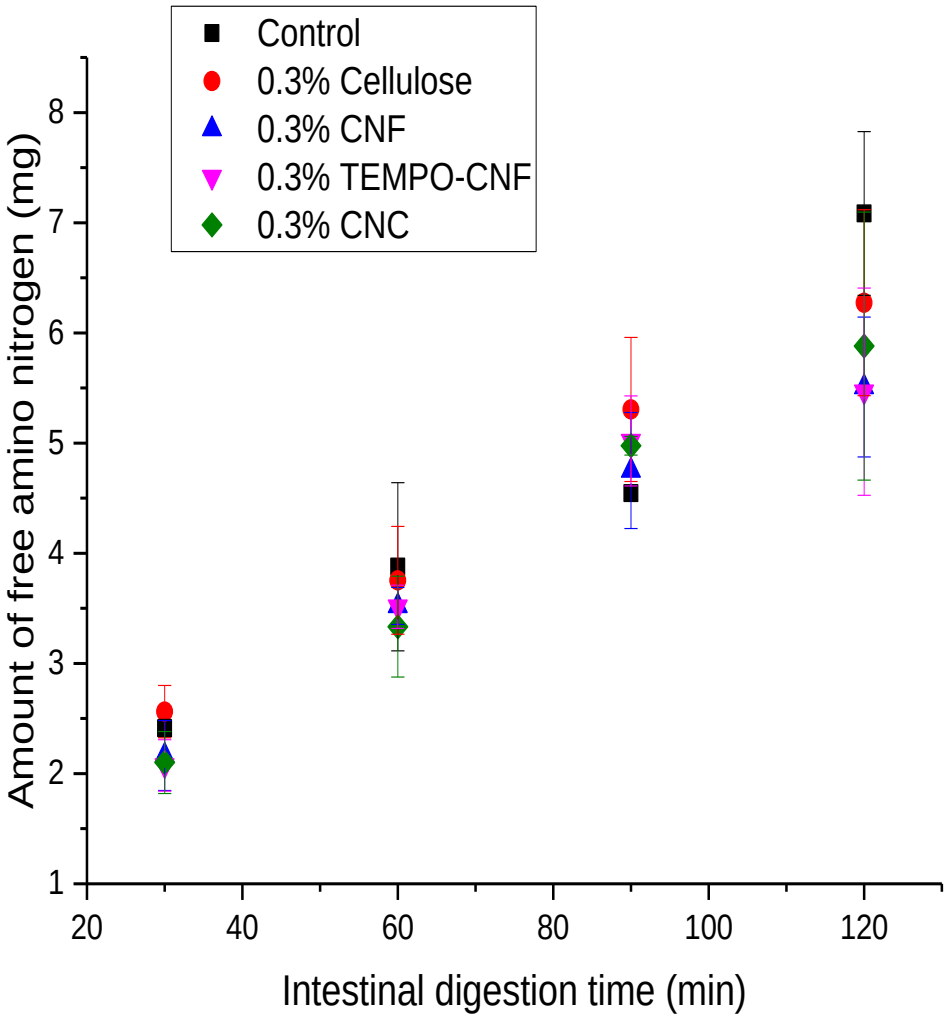


Fig A1. The amount of free amino nitrogen release with and without addition of nanocellulose/cellulose during intestinal digestion.